On the hydro-mechanical behavior of ancient railway flatforms in term of reinforcement by soil-mixing

Trong Vinh Duong

▶ To cite this version:

HAL Id: pastel-00945680

https://pastel.hal.science/pastel-00945680

Submitted on 12 Feb 2014

UNIVERSITÉ PARIS-EST

Thèse présentée pour obtenir le grade de

Docteur de l'Université Paris-Est

Spécialité : Géotechnique

par

Trong Vinh DUONG

Ecole Doctorale : SCIENCES, INGENIERIE ET ENVIRONNEMENT

Etude du comportement hydromécanique des plateformes ferroviaires anciennes en vue du renforcement par « soil-mixing »

Thèse soutenue le 25 Novembre 2013

JURY

Prof. Erol Tutumluer	Rapporteur	University of Illinois at Urbana-Champaign
Prof. Pierre Breul	Rapporteur	Université Blaise Pascal - Clermont II
Prof. Antonio Gomes Correia	Examinateur	University of Minho
Dr. Anh Minh Tang	Examinateur	Ecole des Ponts ParisTech
M. Nicolas Calon	Examinateur	Société Nationale des Chemins de fer Français
Prof. Yu-Jun Cui	Directeur de thèse	Ecole des Ponts ParisTech

Invités :
  Dr. Jean Canou (ENPC), M. Alain Robinet (SNCF), M. Jean François Mosser (Soletanche-Bachy)

UNIVERSITÉ PARIS-EST

Dissertation presented for the degree of

Doctor of Philosophy of Université Paris-Est

Specialty: Geotechnical Engineering

by

Trong Vinh DUONG

Doctoral School: SCIENCE, ENGINEERING AND ENVIRONMENT

Investigation of the hydro-mechanical behavior of ancient railway platforms in scope to reinforcement by soil-mixing

PhD Defense Day: 25 November 2013

REVIEWERS

Prof. Erol Tutumluer	Reporter	University of Illinois at Urbana-Champaign
Prof. Pierre Breul	Reporter	Université Blaise Pascal - Clermont II
Prof. Antonio Gomes Correia	Examiner	University of Minho
Dr. Anh Minh Tang	Examiner	Ecole des Ponts ParisTech
M. Nicolas Calon	Examiner	Société Nationale des Chemins de fer Français
Prof. Yu-Jun Cui	Supervisor	Ecole des Ponts ParisTech

Invited :
Dr. Jean Canou (ENPC), M. Alain Robinet (SNCF), M. Jean François Mosser (Soletanche-Bachy)

To my parents

Con luôn biết ơn bố mẹ đã sinh ra con

cho con dòng máu, tinh thần

và luôn dõi theo con lặng lẽ

…

« Dans le monde de chaos, la science est la seule lumière qui ne me trahit jamais »

DƯƠNG Trọng Vĩnh - 2013

Merci beaucoup à ma famille au Vietnam qui m'a donné un soutien permanent et une source d'énergie éternelle.

En fin, je m'adresse à ma femme, une personne qui compte beaucoup pour moi, qui dégage du charme de l'amour et de l'intelligence. Avec toi, j'ai bravement passé les bémols et les dièses de la vie pleine de jolies couleurs...Merci Tâm.

...et encore merci...

Abstract

The present work deals with the behavior of ancient railway sub-structure in France. A statistical study was firstly undertaken on problems occurred in the whole ancient French railway network. The analysis evidenced the particular importance of sub-grade quality for the performance of the sub-structure and the track geometry. Afterwards, an ancient railway line in the West of France was investigated. The analysis showed that the degradation speed of this line was correlated with different parameters such as the nature of sub-grades and the thickness of different layers. An increase trend of degradation speed with the increase in interlayer thickness was identified.

The interlayer has a positive impact since it reduces the train-induced stress applied to the sub-grade. The hydro-mechanical behavior of interlayer soil under different conditions (water content, fines content, stress, number of cycles) was investigated. A set of triaxial tests and infiltration tests were performed for this purpose. By analyzing the shear strength properties, the permanent axial strain and the resilient modulus of interlayer soil, we found that the water content and the fines content must be considered together. Adding more fines into the interlayer presents a positive impact under unsaturated conditions thanks to the suction effect, but a negative impact under saturated conditions. The infiltration column tests with drying/wetting cycles showed that the hydraulic conductivity of interlayer soil is governed by fines fraction but did not change significantly with fines content.

In order to study the mechanism of interlayer creation and mud pumping, a physical model of 550 mm inner diameter was developed. Soil samples representing the ancient French railway substructure with a ballast layer overlying an artificial silt layer (mixture of crushed sand and kaolin were tested. The effects of monotonic and cyclic loadings, water content and dry unit mass of sub-soil were investigated. It was found that the pore water pressure developed in the sub-soil and the sub-soil stiffness are the key factors for the migration of fine particles or the creation of interlayer/mud pumping. Water is the necessary condition, but it is the soil compressibility that governs the phenomenon to occur.

Keywords: railway substructure; degradation speed; interlayer; mud pumping; water content; fines content; hydro-mechanical behavior; physical model.

Résumé

Le présent travail porte sur le comportement des plateformes ferroviaires anciennes en France. Tout d'abord, une étude statistique a été menée sur les problèmes survenus dans l'ensemble du réseau ferroviaire français. L'analyse montre l'importance particulière de la qualité du sol support pour la performance de la sous-structure et pour la tenue géométrique des voies. Ensuite, une ligne ferroviaire ancienne située à l'Ouest de la France a été étudiée spécifiquement. Les analyses montrent que la vitesse de dégradation de cette ligne est en corrélation avec les différents paramètres tels que la nature de sol support, l'épaisseur des couches de la sous-structure. Une tendance d'augmentation de la vitesse de dégradation avec la diminution de l'épaisseur de la couche intermédiaire est identifiée. Cette couche as un impact positif puisqu'elle réduit les contraintes appliquées au sol support.

Le comportement hydromécanique du sol de la couche intermédiaire dans des conditions différentes (teneur en eau, teneur en particules fines, charge, nombre de cycles) a été étudié. Des essais triaxiaux et des essais de colonne d'infiltration ont été réalisés à cette fin. En analysant les propriétés de résistance au cisaillement, la déformation axiale permanente et le module réversible, on a constaté que les effets de la teneur en eau et de la teneur en fines doivent être pris en compte ensemble. Une augmentation de teneur en fines dans la couche intermédiaire présente un impact positif à l'état non saturé grâce à l'effet de la succion, mais un impact négatif à l'état saturé. Les essais de colonne d'infiltration avec des cycles de séchage/humidification ont montré que la conductivité hydraulique du sol est gouvernée par la fraction de fines et qu'elle ne change pas significativement avec la teneur en fines.

Afin d'étudier les mécanismes de la création de la couche intermédiaire et de remontée boueuse, un modèle physique de 550 mm de diamètre intérieur a été développé. Des échantillons de sol qui représentent la sous-structure ferroviaire ancienne avec une couche de ballast posée sur une couche de limon artificielle (mélange de sable concassé et du kaolin) ont été testés. Les effets des charges monotones et cycliques, de la teneur en eau et de la masse volumique sèche du sol support ont été étudiés. Il a été constaté que la pression interstitielle développée dans le sol support et la rigidité du sol support sont des facteurs clés pour la migration des particules fines ou la création de la couche intermédiaire/la remontée boueuse. L'eau est la condition nécessaire, mais c'est la compressibilité du sol support qui gouverne le phénomène à se produire.

Mot clés: Plate-forme ferroviaire; vitesse de dégradation; couche intermédiaire; remontée boueuse; teneur en eau; teneur en fines; comportement hydromécanique; modèle physique.

Publications

Journal papers

1 **Duong T.V.**, Trinh V.N., Cui Y.J., Tang A.M., Calon N. 2013. Development of a large-scale infiltration column for studying the hydraulic behavior of fouled ballast. *Geotechnical Testing Journal*, Vol. 36, No. 1, 54-63.

2 **Duong T.V.**, Tang A.M., Cui Y.J., Trinh V.N., Dupla J.C., Calon N., Canou J., Robinet A. 2013. Effects of fines and water contents on the mechanical behavior of interlayer soil in ancient railway sub-structure. *Soils and Foundations*, Vol. 53, No. 6, 868-878.

3 **Duong T.V.**, Cui Y.J., Tang A.M., Dupla J.C., Calon N. 2013. Effect of fine particles on the hydraulic behavior of interlayer soil in railway sub-structure. *Canadian Geotechnical Journal (under review).*

4 **Duong T.V.**, Cui Y.J., Tang A.M., Dupla J.C., Canou J., Calon N., Robinet A. 2013. Effects of water and fines contents on the resilient modulus of the interlayer soil of railway sub-structure. *Acta Geotechnica (under review).*

5 **Duong T.V.**, Cui Y.J., Tang A.M., Calon N., Robinet A. 2013. Assessment of ancient French railway sub-structure: a case study. *Bulletin of Engineering Geology and the Environment (under review).*

6 **Duong T.V.**, Cui Y.J., Tang A.M., Dupla J.C., Canou J., Calon N., Robinet A., Chabot B., De Laure E. 2013. A physical model for studying the migration of fine particles in railway sub-structure. *Geotechnical Testing Journal (under review).*

7 **Duong T.V.**, Tang A.M., Cui Y.J., Dupla J.C., Canou J., Calon N., Robinet A. 2013. Investigating the mud pumping and interlayer creation phenomena in railway sub-structure. *Engineering Geology (accepted for a publication).*

8 Cui Y.J., **Duong T.V.**, Tang A.M., Dupla J.C., Calon N., Robinet A. 2013. Investigation of the hydro-mechanical behavior of fouled ballast. *Journal of Zhejiang University-Science A (Applied physics and Engineering)*, Vol. 14, No. 4, 244-255.

Conference papers

1 Trinh, V.N., Tang A.M., Cui Y.J., **Duong, T.V.**, Dupla J.C., Canou J., Calon N., Robinet A. 2012. Water effect on the cyclic mechanical behavior of blanket layer soil of old railway in France. The First International Conference on Railway Technology: Research, Development and Maintenance, 18-20 April 2012. Las Palmas de Gran Canaria, Spain.

2   **Duong, T.V.**, Cui, Y.J., Tang, A.M., Trinh, V.N., Calon N., Robinet A., Dupla J.C, Canou J. 2012. Unsaturated hydraulic properties of fine particles of a blanket layer material from an old railway trackbeds. The 2nd European Conference on Unsaturated Soils, 20-22 June 2012. Naples, Italy.

3   **Duong, T.V.**, Cui, Y.J., Tang, A.M., Calon N., Robinet A., Dupla J.C, Canou J. 2013. Hydro-mechanical behavior of interlayer of railway sub-structure. The 2nd International Conference CIGOS. 4th & 5th April 2013, Lyon, France.

4   **Duong, T.V.**, Tang, A.M., Cui, Y.J., Trinh, V.N., Dupla J.C, Calon N., Canou J., Robinet A. 2014. Investigation of the mechanical behavior of interlayer soil in ancient railway sub-structure under different conditions. The Second International Conference on Railway Technology: Research, Development and Maintenance. Ajaccio, Corsica, France.

5   **Duong, T.V.**, Cui, Y.J., Tang, A.M., Calon N., Robinet A., Dupla J.C, Canou J. 2011. Hydro-mechanical behavior of old railway trackbeds. The 1st Sino-French PhD Students Seminar on Sustainable Transportation. 22-24 November 2011, Champs sur Marne, France.

6   **Duong, T.V.**, Cui, Y.J., Tang, A.M., Calon N., Robinet A., Dupla J.C, Canou J. 2012. Hydro-mechanical behavior of ancient railway platforms. French-Portuguese workshop, Railway track: Diagnostic&Characterization. 12th & 13th July 2012. Paris, France.

7   **Duong, T.V.**, Cui, Y.J., Tang, A.M., Calon N., Robinet A., Dupla J.C, Canou J. 2013. The interaction between ballast and underlying layer in railway sub-structure. Railway track science & Engineering International workshop. Ballast: Issues and Challenges. 5th & 6th December 2013. UIC Paris, France.

CONTENTS

INTRODUCTION

The French railway network started to be constructed in 1850s. Nowadays, railway has become one of the important transportation means and plays an important role in the economy of the country. The French national railway company (SNCF) operates a total of about 30000 km lines. To satisfy the increasing social and economic demand, the train speed, axle load or traffic need to be increased constantly. Obviously, this would have significant impact on the sub-structure of tracks. Indeed, problems related to tracks have been frequently recorded, and in order to ensure normal train circulations, a huge number of maintenance and improvement activities have been regularly conducted, especially for the ancient lines that represent 94% of the French railway network. However, as the railway consists of various parts (upper-structure, granular layers, sub-grade), the maintenance activities are not always of easy tasks. The experience in France showed that there are a large number of cases where the causes are not explicitly figured out and very often, problems still persist even after costly maintenance campaigns. In order to optimize the maintenance and make this task efficient, the behavior of the whole railway sub-structure in general and of each layer in particular must be investigated in-depth.

The ancient railway sub-structures in France were constructed with a ballast layer directly overlying the sub-grade. Recently in a maintenance campaign (Calon et al., 2010; Trinh, 2011; Trinh et al., 2012), it was found that in such sub-structures there is a layer namely interlayer that was naturally created mainly by the interpenetration of ballast and sub-grade soils. Thanks to its high mechanical performance related to its high dry unit mass ρ_d (2.4 Mg/m^3 at the site of Sénissiat near Lyon, France, according to Trinh, 2011), it was decided to keep this layer as part of the sub-structure during the renewal of tracks. However, as this layer was naturally created, it can contain a large variety of fines which are in general sensitive to changes in water content. Therefore, it is necessary to investigate its hydro-mechanical behavior under different conditions (fines content, water content, stress, etc.).

The migration of fine particles can sometimes lead to mud pumping. This extremely detrimental mode corresponds to the situation where sub-soil fine particles are pumped up to the surface of ballast layer, thereby fouling the ballast layer. However, up to now, the real mechanism of this phenomenon has not been revealed and the driving factors are still unknown. From a practical point of view, in order to conduct efficient maintenance activities and to choose suitable improvement

methods, several questions can be raised: Why is there mud pumping? How was the interlayer created? What are the corresponding driving factors? How do the fine content and water content affect the hydro-mechanical behavior of interlayer soil? How does the interlayer influence the overall behavior of sub-structure? Responding to these questions constitutes the main objectives of this PhD work.

The work conducted is part of the French national research project namely RUFEX (Reuse and reinforcement of ancient railway sub-structure and existing foundations). This project gathers three industrial partners - French National Railway Company (SNCF), Soletanche Bachy and Terrasol, and three academic partners - ENPC (Ecole des Ponts ParisTech), INSA Lyon (Institut National des Sciences Appliquées) and IFSTTAR (Institut Français des Sciences et Technologies des Transports, de l'Aménagement et des Réseaux). This project deals with reinforcement of ancient railway and building foundations using the soil-mixing technique. This PhD work is related to the part of reinforcement of railway sub-structure where interlayer is involved. The soil mixing column is used when sub-grade needs to be reinforced to meet the requirement in terms of mechanical performance. In this case, the interlayer is considered as the transmission layer for the train-induced stress: the stress is transmitted from the ballast layer to the soil-mixing columns through the interlayer. On the other hand, the interaction between interlayer and the subgrade reinforced by soil mixing column depends strongly on the hydro-mechanical behavior of interlayer soil. As the behavior of interlayer soil changes with changes in fines content and water content, in order to ensure the good mechanical performance of the whole interlayer - soil-mixing columns system, the effects of fines content and water content must be investigated in-depth. This constitutes the main objective of this study. The results obtained will be helpful in assessing the behavior of tracks by considering the interaction between the interlayer and the soil mixing columns.

The study presented in this dissertation covers a large spectrum: from a national scale (French railway network) to a local scale (specific study on one ancient railway line); from the identification tests (hydro-mechanical behavior of the interlayer soil) to the physical model of interlayer creation and mud pumping. The results have been subjected to several journal papers, either published or submitted or under review. The first paper on the development of a large-scale infiltration column was published in *Geotechnical Testing Journal*. The second paper on the effect of fines and water contents on the mechanical behavior of interlayer soil was published by *Soils and Foundations*. The third paper on the hydraulic behavior of interlayer soil is under the second review for *Canadian Geotechnical Journal*; the forth on the assessment of the ancient railway network in France is under the second review for *Bulletin of Engineering Geology and the Environment*. A new

physical model for testing degradation of sub-structure (mud-pumping and interlayer creation) was presented in the fifth paper submitted to ***Geotechnical Testing Journal***. The analysis on the mechanisms of interlayer creation and mud-pumping are presented in the sixth paper accepted for a publication in ***Engineering Geology***. The seventh paper on the effect of fines and water content on the resilient modulus of interlayer soil was submitted to ***Acta Geotechnica***. The dissertation is presented in the form of papers/manuscripts, each chapter being composed of a short introduction and the corresponding papers/manuscripts.

In the first chapter, a statistical study was firstly undertaken. Problems related to the circulation of train in the whole French railway network during a period of more than one year were analyzed. Emphasis was put on the relation between the track degradation speed and various parameters such as the geological information, UIC group, maintenance policy of SNCF, number of problems per month, distribution of problems as a function of territory and infra-poles. The analysis evidenced the particular importance of sub-grade quality for the performance of the whole track. After this general analysis, an ancient railway line in the West of France was investigated in-depth. The degradation speed of this track was correlated with different factors such as the nature of sub-grades involved along the line and the thickness of different layers. The results showed that the degradation speed is correlated with the layer thicknesses. Furthermore, it was observed that the interlayer plays an important role in the performance of track: it corresponds to a transition layer to reduce train-induced stress applied to the sub-grade. The results of this chapter are presented in an article submitted to ***Bulletin of Engineering Geology and the Environment***.

The second chapter investigates the mechanical behavior of interlayer soil by carrying out a number of large-scale monotonic and cyclic triaxial tests. Interlayer soils having different fines contents were tested. The results of monotonic triaxial tests showed the significant influence of fines content and water content on changes in shear strength parameters (friction angle and cohesion). The cyclic triaxial tests were performed at various deviator stress levels and three water contents ($w = 4\%$; 6% and 12%). The results of these cyclic tests allowed drawing a global picture of the variations of the permanent axial strain and the resilient modulus of interlayer soil with changes of parameters such as water content, fines content, deviator stress and number of cycles. It was found that the effects of water content and fines content are linked and should not be separated when analyzing the behavior of interlayer soils. The results on the permanent axial strain were presented in a paper published in ***Soils and Foundations***. The results on resilient modulus were presented in a paper submitted to ***Acta Geotechnica***.

The third chapter depicts the results on the hydraulic behavior of interlayer soil, presented in two papers. The first, published in ***Geotechnical Testing Journal***, presents a large-scale infiltration column (H = 600 mm and D = 300 mm) developed for testing the hydraulic behavior of interlayer soil. The hydraulic properties of interlayer soil were also presented in this paper. The second paper, submitted to ***Canadian Geotechnical Journal*** presents the study on the influence of fines content on the hydraulic properties of interlayer soil through two comparisons of hydraulic properties: 1) between natural interlayer soil and natural interlayer soil with addition of 10% sub-soil (ITL_{10}); 2) between ITL_{10} and the fine particles fraction (< 2 mm) of ITL_{10}.

The fourth chapter consists of two papers, and focuses on the mechanisms of the interlayer creation and mud-pumping phenomena. The first paper, submitted to ***Geotechnical Testing Journal***, depicts a physical model developed to investigate mud pumping and interlayer creation. It involves a transparent cylindrical cell (H = 600 mm and D = 550 mm) that allows simulating the degradation process of ancient railway sub-structure with a 220 mm thick sub-grade layer underlying a 160 mm thick ballast layer. The second paper presents the key factors for the interlayer creation and the mud-pumping phenomenon. The study evidenced the important role of pore water pressure, dry unit mass of sub-grade soil in the behavior of the ballast/sub-grade interface. This paper was accepted for a publication in ***Engineering Geology***.

The fifth and last chapter is devoted to the recommendations. The main results obtained in the previous chapters were synthesized and further analyzed. Some recommendations are then proposed for optimization of the maintenance policy and improvement of the sub-structure quality.

CHAPTER I

Assessment of ancient railway network in France

Railway track consists of several components (rail, fastening system, sleeper, different granular material layers, sub-grade, etc.) ensuring different functions and normal conditions for train circulation. Several valuable studies were reported in the literature focusing on different components such as ballast (Indraratna et al., 1997; Indraratna and Salim, 2005; Karraz, 2008; Aursudkij et al., 2009; Indraratna et al., 2011) and sub-soils (Li and Selig, 1996; Miller et al., 2000; Adam et al. 2007; Liu and Xiao, 2010). However, once problem occurs and the train rate has to be reduced, it is not always obvious to determine the corresponding failed component.

In order to define a suitable investigation method, it appears necessary to start by a global analysis on the whole railway network to identify the problems, and then to focus on the zone where problems occur. Following this approach, the study conducted here starts by an analysis of the problems recorded over the whole French railway network; then a case study was done on a representative ancient line. In this chapter, the importance of railway sub-structure, in particular the interlayer and sub-grade was assessed.

The results are presented in a paper submitted to ***Bulletin of Engineering Geology and the Environment***. The corresponding manuscript is presented in this chapter.

Assessment of ancient French railway sub-structure: a case study

Trong Vinh Duong[1], Yu-Jun Cui[1], Anh Minh Tang[1], Nicolas Calon[2], Alain Robinet[2]

Abstract: A statistical study was firstly undertaken on problems occurred in a period of more than one year and related to the circulation of train in the whole ancient French railway network. Emphasis was put on the degradation of track components. The analysis evidenced the particular importance of sub-grade quality in the performance of the whole track. After this general analysis, an ancient railway line in the West of France was investigated. In the sub-structure of this line, an interlayer was identified that has been created mainly by interpenetration of ballast and sub-grade. In the analysis, the degradation rate of this line was correlated with different parameters such as the nature of sub-grades involved along the line, the thickness of different layers. The results showed that the degradation rate is correlated to the thickness of various layers. Furthermore, it was observed that the interlayer plays an important role in the performance of tracks as it represents a transition layer before any train-induced stress is applied to the sub-grade.

Keywords: French railway network; interlayer; sub-grade; degradation rate; NL; layer thickness.

Introduction

Ballasted tracks are composed of two parts: super-structure (rail, fastening system and sleeper) and sub-structure (ballast, sub-ballast and platform). To ensure the good performance of tracks and thus the normal circulation of train, both super-structure and sub-structure need to be regularly examined and maintained (Burrow et al. 2007). Normally, problems related to super-structure can be visually determined and thus rapidly solved. It is however not the case for those related to sub-structure. Once problems occur in the sub-structure, it is often difficult to explicitly identify and expensive to remediate. Previous studies showed that the cost related to the maintenance of sub-structure often represents a huge budget (Ebrahimi 2011; Indraratna et al. 2011). The experiences in France showed that after the track remedial work to decrease rail deformations, the problems persist and the phenomenon as mud pumping (fine particles of sub grade are pumped up to ballast surface), defects of bearing capacity occurs locally. These observations suggest that problems are highly related to the behavior of sub-structure. From a practical point of view, if the main mechanisms of the occurring problems are not understood, the origin of the problems may remain even though expensive remedial works have been undertaken (Brough et al. 2003; 2006). The variability of sub-

---

[1]: Ecole des Ponts ParisTech, U.R. Navier/CERMES
[2]: French Railway Company (SNCF)

grade soils along a line often represents the major difficulty or challenge for both the fundamental investigation and the practical operations.

An appropriate thickness of sub-structure layers is important for adequately distributing the train-induced stress. If the track-bed layers do not have the required thickness, significant stress can be transmitted to the sub-grade soils and important deformations can take place, leading to the degradation of tracks. It is worth noting that the designed thickness of track-bed layers is not the same, depending on types of lines (for high rate train or normal train), on countries and also on the construction times (Li and Selig 1998a; 1998b; Burrow et al. 2011). In France, the ancient railway lines were constructed long time ago in 1850s, and the design in that time did not follow the current standards (Trinh 2011) in terms of super-structure composition, sub-structure mechanical behavior and exploitation. This inevitably leads to stability-related problems to the tracks in case of increasing load, traffic and rate of train. In particular, for the ancient railway tracks, as the ballast was mainly installed directly onto the sub-grade during construction, a layer namely interlayer was created mainly by the interpenetration of ballast and sub-grade soils (Calon et al. 2010; Trinh 2011; Trinh et al. 2011; 2012; Cui et al. 2013; Duong et al. 2013; Duong et al. 2013). The thickness and the hydro-mechanical behavior of this interlayer can strongly affect the performance of the whole tracks.

This paper aims to assess the performance of track sub-structure of ancient French railway network. Firstly, a statistical study on the French railway network was conducted. Problems related to train circulation in the period from January 2010 to May 2011 were collected and analyzed. It was concluded that it is important to conduct a global investigation followed by an in-depth sub-structure one. In particular, the analysis showed that there is a good correlation between the train circulation problems and the presence of fine particles in the sub-structure. After this global analysis, an in-depth analysis was undertaken on one line with problems identified. The increase rate of the rail geometrical degradation was studied. This increase rate was then correlated with other parameters such as the natures of sub-grade involved along the line and the thicknesses of different layers.

Assessment of the French railway network

The problems related to train circulation (for instance, forced rate reduction in order to ensure the comfort of passengers) were recorded in the French railway network from January 2010 to May 2011. A total of 1705 cases was involved (Calon 2010). It was found that the causes can come from

every track components (steel rail, fastening system, sleeper, ballast, sub-ballast and sub-grade). Four main groups can be defined as presented in Fig. 1, in relation to super-structure; sub-structure; rate reduction due to maintenance/engineering works and "no information" meaning that the cause has not been explicitly found out, respectively.
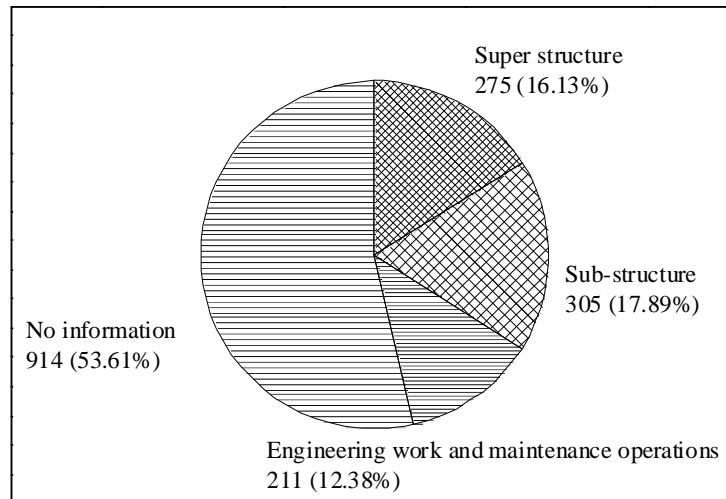
Fig. 1: Cause of the problems for the deceleration of train

Among 1705 cases, those related to the super-structure represent 16.13% (275 cases), to the sub-structure represent 17.89% (304 cases), to the maintenance and engineering works represent 12.38% (211 cases), and 53.61% corresponds to "no information" (914 cases). The huge number of "no information" cases is mainly due to the complexity of the track composition; it is often difficult to determine the cause of a problem. On the other hand, this huge number confirms that railway structures is a complex issue that needs extensive investigations in order to reveal the real mechanisms involved in the problems. It is also worth noting that the part of problems related to the sub-structure (17.89%) is a little higher than that related to the super-structure (16.13%). This implies significant maintenance works involving the sub-structure. Note that in the past, most attention has been paid to the super-structure and the consideration given to the sub-structure is not enough to reveal all problems. Among the sub-structure-related problems, there are 186 cases where clayey sub-grade was recorded and very often mud pumping was observed. These zones are henceforth referred to as sensitive zones.

In order to enable the assessment of the French network in terms of economic indicators, the railway lines are classified in different groups according to the nature and the importance of traffic (SNCF 1989). The classification, called UIC groups, is based on the fictive traffic T_{f2} calculated as follows:

$$T_{f2} = S \times T_{f1} \tag{1}$$

where S is the coefficient of the line quality, and it is equal to 1 for the lines without passenger train or local traffic, to 1.1 for the lines with passenger train at a rate lower than 120 km/h, to 1.2 for the lines with passenger train at a rate from 120 km/h to 140 km/h, to 1.25 for the line with passenger train at a rate higher than 140 km/h. T_{f1} is the fictive weight calculated by:

$$T_{f1} = T_v + K_m T_m + K_t T_t \tag{2}$$

where T_v is the weight of passenger train (ton/day), T_m is the weight of freight train (ton/day), T_t is the weight of locomotive (ton/day), K_m is a coefficient (1.15 in normal case, 1.3 in the case of 20 ton axle load), K_t is a constant which is equal to 1.4.

According to the value of T_{f2}, the corresponding UIC group can be defined and presented in Table 1. The order in this table follows the decreasing traffic and loading. In France, on the RFF (French Department of Industry) network, there is no line within group 1. Based on the amplitude of fictive traffic, the maintenance policy of SNCF (French Railway Company) was set up accordingly: maintenance activities are undertaken more frequently for the first six groups and less for the other groups.

As the total length of each group is not the same (Table 1), it appears necessary to normalize the number of problems with respect to the length. The number of recorded problems per 1000 km of each UIC group was then determined and the result is presented in Fig. 2. The first category corresponds to the whole data recorded involving the problems related to all track components; the second category corresponds to the sub-structure-related problems. The third category involves the sensitive zones. It is observed that in the first category, the number of problems is indeed larger for the groups 2 to 4. It is group 4 that gathered the most part of problems.

When only the data related to sub-structure was taken into account, the configuration became different and the greatest value was recorded for group 7 (passenger train). The same observation can be made with the data related to the sensitive zones. This finding suggests that the maintenance policy should be changed when referring to the sub-structure and more attention should be paid to the track bed within group 7.

Table 1: Classification of group UIC

Group UIC	Characteristic T_{f2} Value	Length (km)
Group 1	$T_{f2} > 120000$	0
Group 2	$120000 \geq T_{f2} > 85000$	2385
Group 3	$85000 \geq T_{f2} > 50000$	8968
Group 4	$50000 \geq T_{f2} > 28000$	12218
Group 5	$28000 \geq T_{f2} > 14000$	6807
Group 6	$14000 \geq T_{f2} > 7000$	7381
Group 7 Passenger train and Freight train	$7000 \geq T_{f2} > 3500$	4149 (Pass. Train) and 292 (Frei. Train)
Group 8 Passenger train and Freight train	$3500 \geq T_{f2} > 1500$	7607 (Pass. Train) and 1291 (Frei. Train)
Group 9 Passenger train and Freight train	$1500 \geq T_{f2}$	6288 (Pass. Train) and 7942 (Frei. Train)
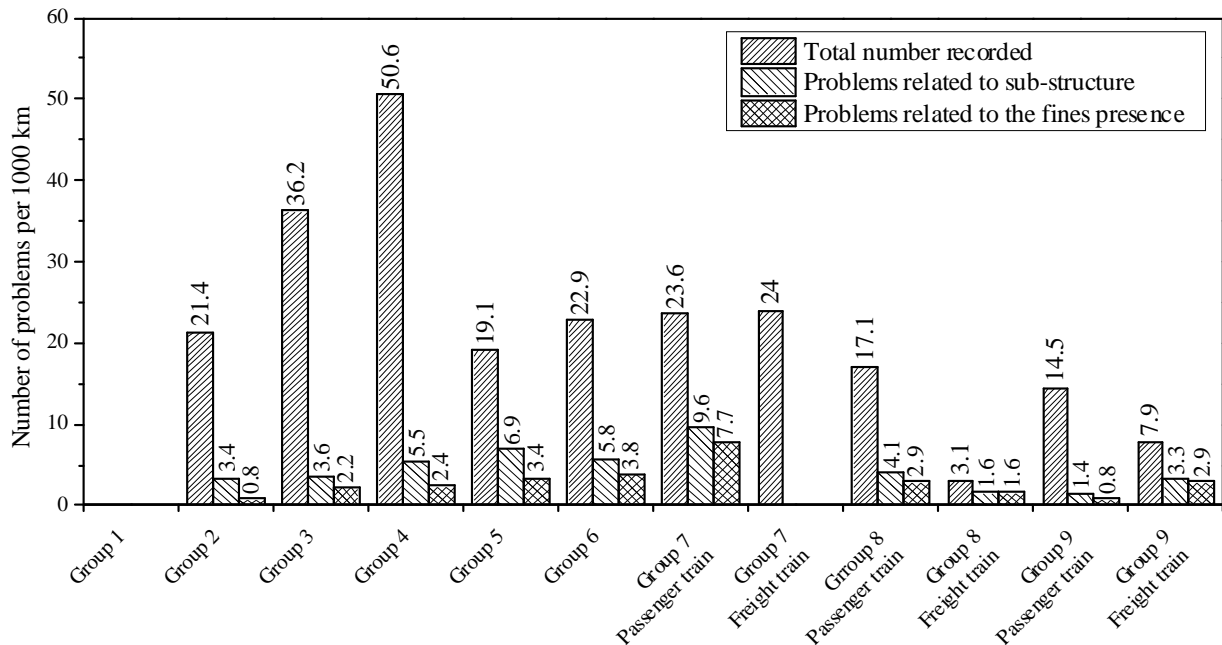
Fig. 2: Number of problems versus group UIC

Problems occurred over a year are presented in Fig. 3a for the sub-structure and in Fig. 3b specifically for the clayey sub-soils (sensitive zones). Very often, the mud pumping phenomenon occurs in the sensitive zones where the fine particles are pumped from sub-grade up to ballast surface and the whole ballast layer becomes fouled and loses all its performance (Selig and Waters 1994; Indraratna et al. 2011). A similar configuration can be observed in two figures. There is a peak around the months of February, March and April. In 2010, for the sensitive zones, the numbers of cases for these three months are 28, 48 and 13, respectively; while those of other months are all lower than 10. It is worth noting that the period from February to April corresponds to late winter and early summer. In the literature, research studies reported that ballast can be fouled after one winter due to freeze/thaw (Raymond 1999).
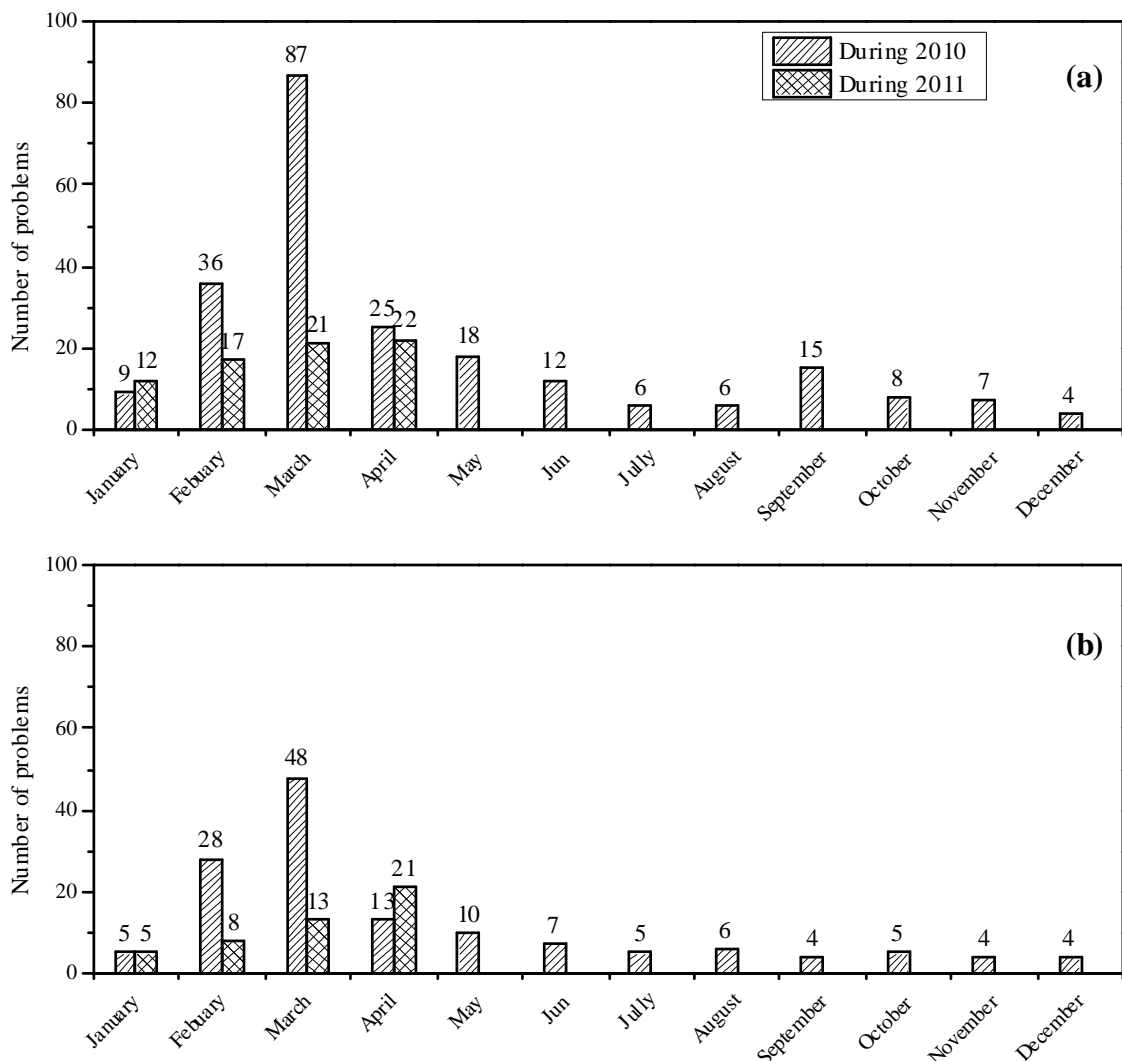
Fig. 3: Problems occurring over one year. a) Problems related to the substructure and b) problems related to the sensitive zones

11

Fig. 4 presents the data recorded versus the type tracks. Track 1 corresponds to the down line, Track 2 corresponds to the up line and "Other" corresponds to the single track line or secondary tracks. In the case of sub-structure-related problems, the number for Track 1 (110 cases) is equal to that for Track 2 (109 cases), while in the case of sensitive zones-related problems, the number for Track 1 (71 cases) is clearly larger than that for Track 2 (51 cases). Note that the drainage condition and the traffic for the Track 1 and Track 2 are not always the same.
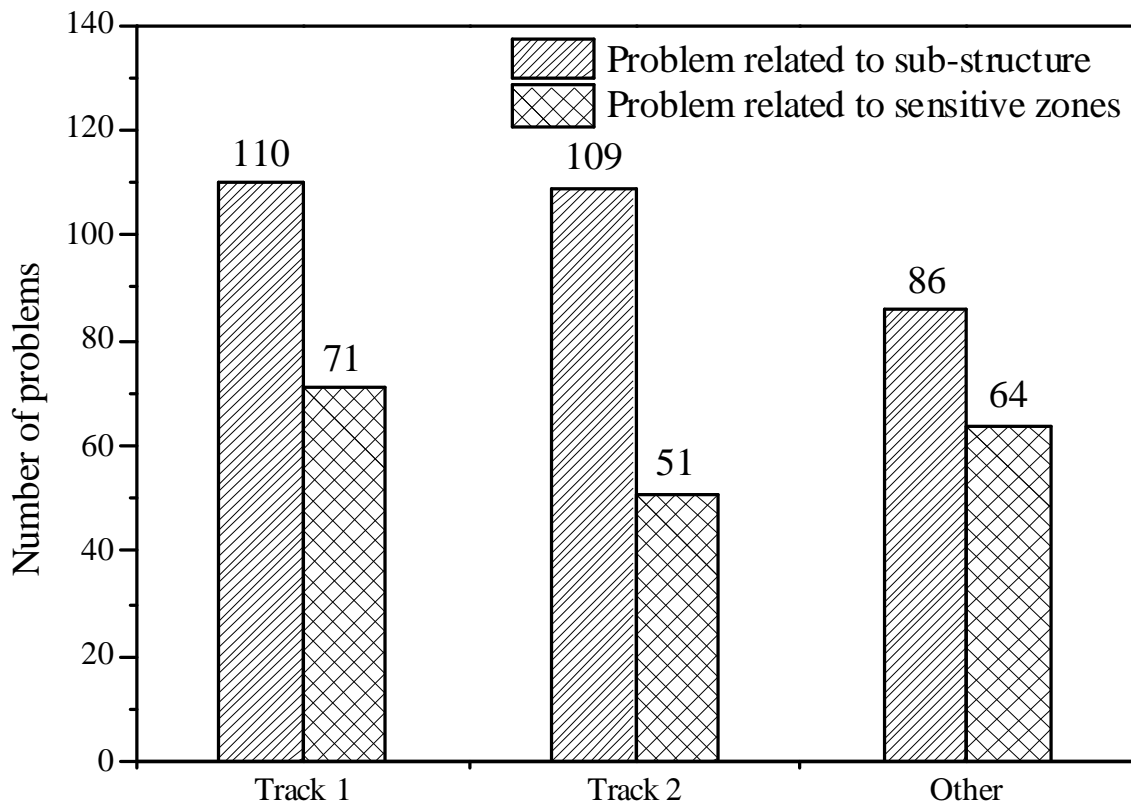
Fig. 4: Problems recorded versus type of track

Fig. 5 depicts the problems according to the territory. Note that the French railway network is divided into three territories, each consisting of various infra-poles (sub-territory). It can be seen that *Atlantique* is the territory where there is the largest number of problems. This observation is clearer if only the sub-structure is accounted for (Fig. 5b). When considering the configuration in terms of sensitive zones (Fig. 5c), the contrast is even higher: the percentage of problems in *Atlantique* is 60% against 22% in *South-East* and 18% in *North East Normandy*. Note that *Atlantique* is the territory with a long coast of Atlantic Ocean and a large number of harbors with high frequency trading activities. However, *Atlantique* is also the territory having the highest total line length, hence a possible higher problem number.

North East - Normandy
500 (29.33%)

South East
458 (26.86%)

Atlantique
747 (43.81%)

(a)

North East - Normandy
62 (20.33%)

South East
75 (24.59%)

Atlantique
168 (55.08%)

(b)

North East - Normandy
34 (18.28%)

South East
40 (21.51%)

Atlantique
112 (60.22%)

(c)
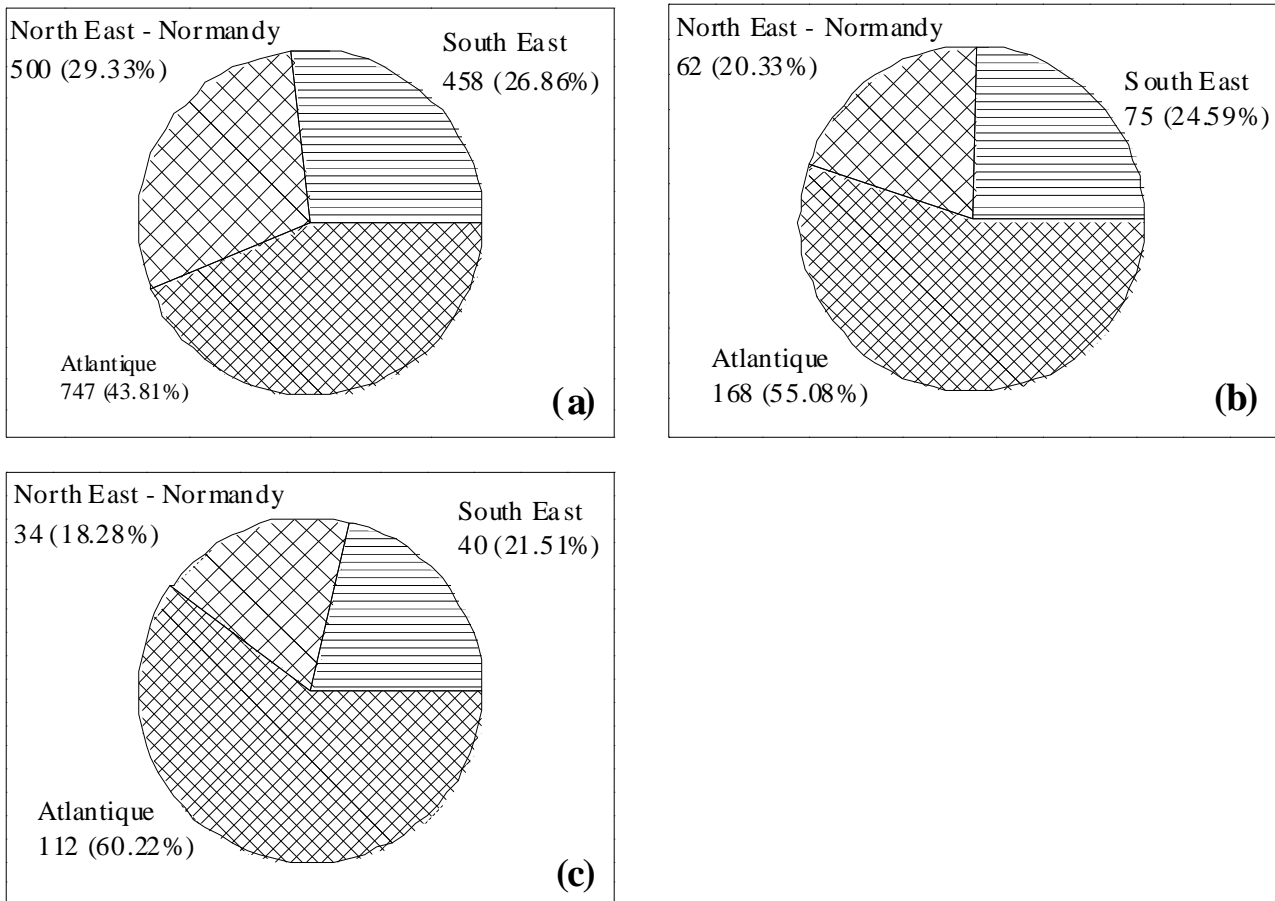
Fig. 5: Classification of problems according to the territory. a) All problems; b) Problems related to sub-structure and c) sensitive zones

Fig. 6 shows the distribution of problems in different infra-poles (problems related to sub-structure in Fig. 6a and problems related to sensitive zone in Fig. 6b). It can be observed that the problems occurred almost everywhere in France; however, most cases appeared in the infra-poles of "Ouest Parisien" (West Paris) and Poitou Charentes. Based on this observation, one line situated in the infra-pole of Poitou Charentes was selected for further in-depth investigation.
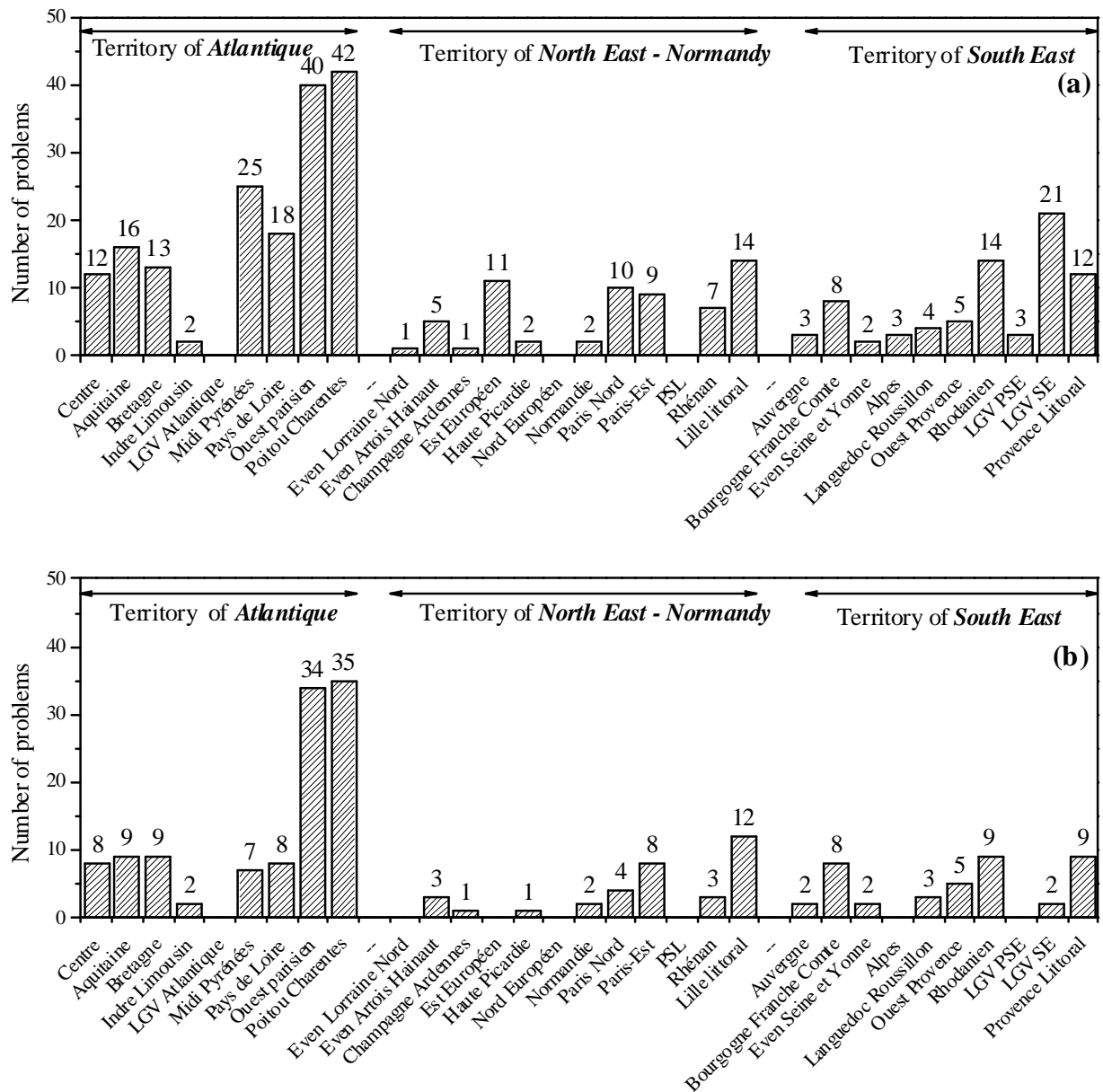
Fig. 6: Classification of problems according to the Infrapole. a) Problems related to sub-structure and b) problems related to sensitive zone

Assessment of a line in the infra-pole of Poitou Charentes

Evaluated line

A studied segment from kilometer 72 to 140 was selected. Information about the thicknesses of different layers should be estimated based on the data from core samples and from Panda investigation (dynamic cone penetrometer test) coupled with geo-endoscope observation.

This railway line was constructed in 1860s. It is classified in group 6 of UIC (see Table 1). As mentioned before, like other ancient lines, this line was constructed with ballast directly overlying the sub-grade. After years of circulations and operation, an interlayer was created as a result of the interpenetration of ballast and fine particles of sub-grade soils (Trinh 2011; Cui et al. 2013; Duong et al. 2013).

Geological situation

Fig. 7 presents the geological map of the studied line with the kilometer point (PK) and the geological information. The sub-grade includes five soil types. The first one at the very first kilometer of the line (from PK 74 to 75) consists of hard limestone and marl. The second (from 75 to 76) involves argillaceous limestone, marl, and to a lesser extent fine alluvial deposit and peat. The third consists of marl mainly (from 76 to 79). The fourth (from 80 to 102) corresponds to white argillaceous limestone and marl. The fifth type involves marl, white chalky limestone and limestone sub-lithographic. This complex geological situation should be correlated to the large number of problems recorded. In the literature, the importance of geological situation for the track performance was also reported by Bednarik et al. (2010) and Li and Selig (1994).
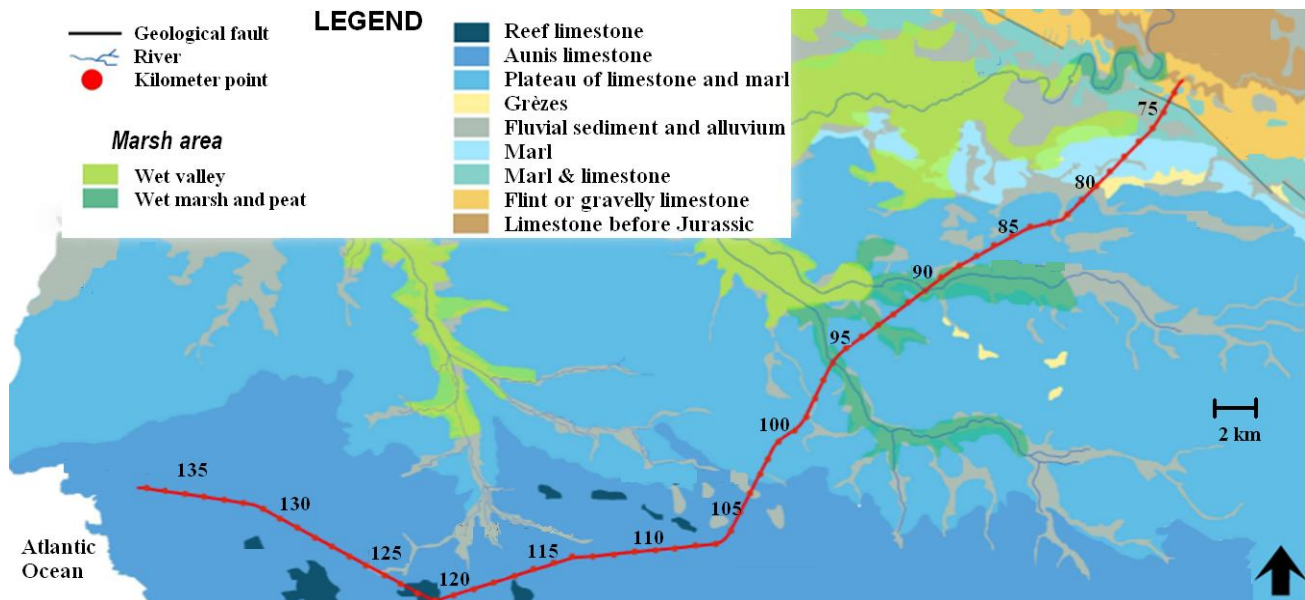
Fig. 7: Geological map of the studied line

Longitudinal Leveling - NL

For a smooth train circulation, rails/wheel contact must present a satisfactory leveling which is defined referring to UIC group. In other words, leveling of rail is an indicator of track quality. Note

15

that the geometrical degradation of tracks that induces changes in leveling can be due to problems related to super-structure, granular materials and platform (Guerin 1996). In the French railway network, the term of longitudinal leveling *NL* (*Nivellement longitudinal* in French) is used to assess the geometrical state of tracks. A large value of *NL* implies a bad state of railway line. Beyond a certain threshold of *NL*, maintenance is required in order to bring *NL* back to an admissible value (ballast tamping, stone blowing and ballast renewal).

NL is calculated from the difference between the local leveling of each rail and the average profile of the line. The principle is to calculate the difference between the represent Euler and Lagrange of the wheel ordinate (Rhayma 2010). From Fig. 8, this difference *N* is calculated as follows:

$$
\begin{aligned}
N &= z_D - \left(z_{D'} - h \right) \\
&= z_D - \frac{1}{\alpha + \beta} \left(\beta z_M + \alpha z_N \right) + h \\
&= z_D - \frac{1}{4(\alpha + \beta)} \left[\beta \left(z_A + z_B + z_C + z_D \right) + \alpha \left(z_E + z_F + z_G + z_H \right) \right]
\end{aligned}
\tag{3}
$$

NL is the standard deviation of the recorded measurements with a mean value *μ* and for a distance of 200 m:

$$
NL = \sqrt{\frac{1}{M} \sum_{i=1}^{M} \left(N_i - \mu \right)^2}
\tag{4}
$$

Fig 8a: Mauzin train
(*http://lapassiondutrain.blogspot.f*)
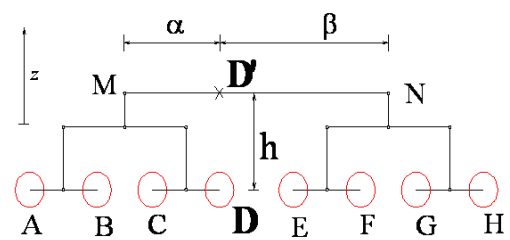
Fig. 8b: Parameters used to calculate NL

Fig. 9 presents the variations of *NL* at kilometer 70.3 of Track 2 from 1997 to 2013. It can be observed that the value of *NL* decreased sharply after maintenance (in the year of 2001, 2003, 2007 and 2012). However, after the maintenance, the value of *NL* continued to increase at almost the same rate: a linear increase trend of *NL* over time can be identified. It is worth noting that the slope represents the increase rate of NL or the degradation rate of tracks. The increase trend of *NL* persisted after maintenance, suggesting that ballast replacement did not resolve the problem, and the track degradation was rather related to the sub-structure.
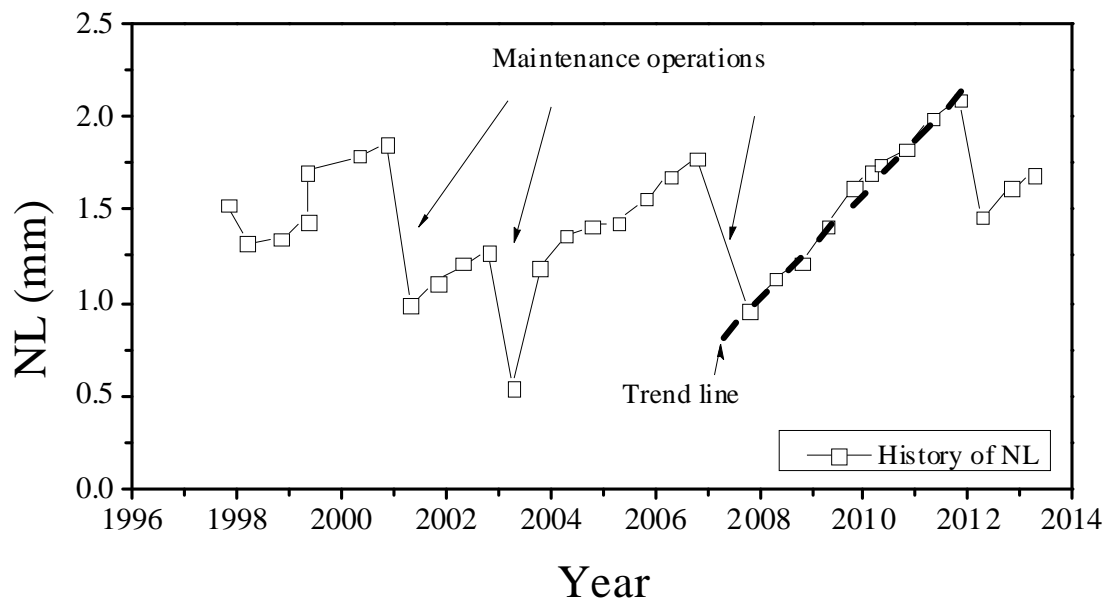
Fig. 9: History of NL variations for a given kilometer, with maintenance operation

Core sampler train

The core sampler train is a special train which has the function as indicated by its name (SNCF 2011). The train was equipped with drilling equipment. Sample tubes are driven dynamically into track-bed to obtain a continuous core sample composed of ballast and underlying formations (Fig. 10). A digital camera is used taking photographs of the sample. From the photograph (see Fig. 10), the thickness of each layer is analyzed and recorded. It can be seen that a typical track-bed consists of a clean ballast layer underlying fouled ballast layer and/or interlayer and sub-grade soil. The sample tube allows core sample to be taken till a depth of about 1.50 m. This depth is enough for identifying the different layers in the ancient railway track-beds. This investigation method was also reported in Brough et al. (2003; 2006).

Fig. 10: Core sample from typical ancient railway sub-structure

Panda cone penetrometer and endoscope

The first Panda penetrometer was presented in 1991 in France (Langton 1999) and it is nowadays widely used thanks to its light weight and easy usage. Panda works following the principle of a dynamic cone penetrometer that uses a manual hammer for driving a standard cone into the soil. The dynamic cone resistance (q_d) is then calculated and plotted versus the corresponding depth, giving the profile of q_d (Langton 1999; Quezada 2012). The cone penetrometer is a useful tool for track-bed investigation and for obtaining information about the in-situ characteristic of ballast and underlying sub-grade material.
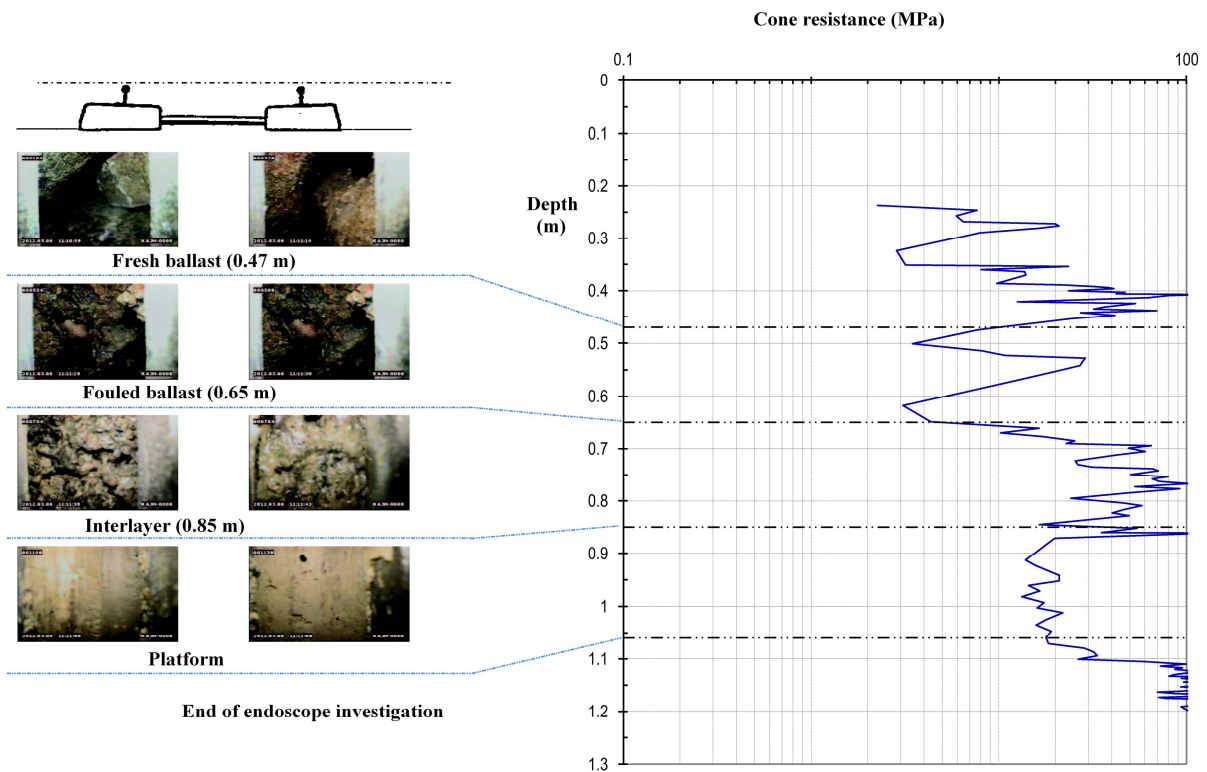
Fig. 11: Typical result from Panda and Endoscope

Once the Panda test is performed, the rod is removed, leaving a small hole having the rod dimension. This allows an endoscope, a very small digital camera, to be introduced into this hole to take photographs of the materials involved. This provides a visual observation allowing the track-bed components to be distinguished.

The Panda tests and endoscope observation were conducted along the studied line according to the SNCF standard (SNCF 2011). The obtained results allowed the thicknesses of different sub-structure layers to be estimated. Fig. 11 presents typical results from Panda test and Endoscope observation at PK 126.7 of Track 1. The correlation between the image of endoscope and the Panda results allowed the identification of a layer of fresh ballast of 0.25 m, a fouled ballast layer of 0.2 m, an interlayer of 0.3 m and the top of sub-grade at 0.95 m depth. As it is very difficult to distinguish fouled ballast layer and interlayer, the summary of thickness of these two layers is accounted for in the following analysis.

Result and interpretation

Fig. 12 depicts the degradation rate (the increase of NL per year which was calculated from the slope as presented in Fig. 9) versus the kilometer point for Track 1 and Track 2. On the whole, there

is an agreement between the data of two tracks; the peaks of Track 1 appeared almost at the same kilometer points as the peaks of Track 2.
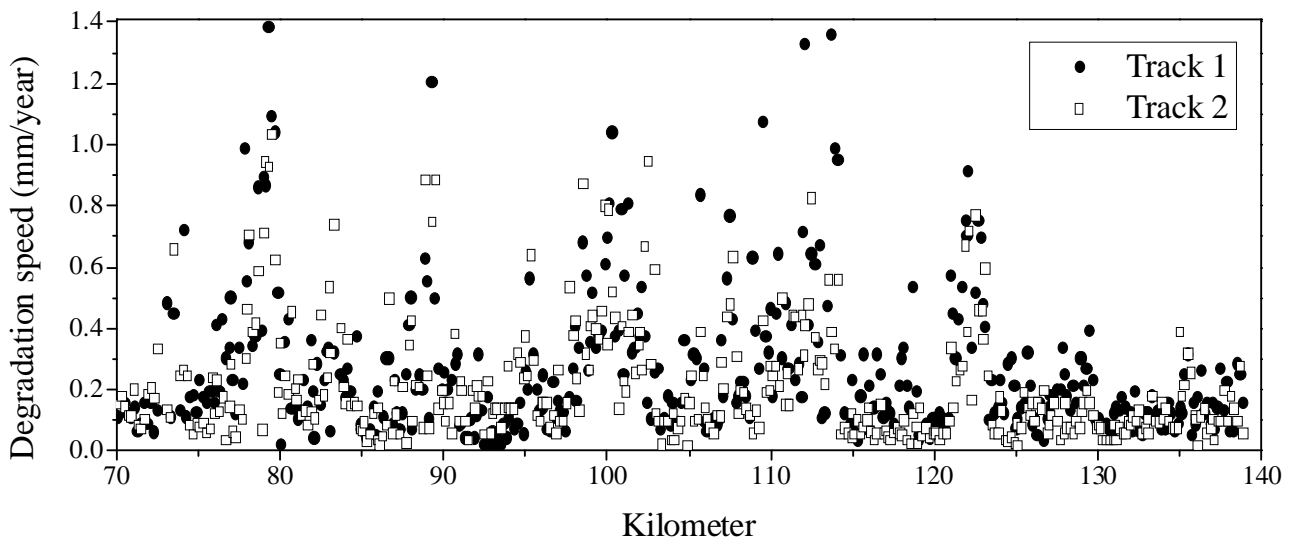
Fig. 12: Degradation rate along the studied line

Fig. 13 and Fig. 14 present the degradation rates according to the year of rail (Fig. a) and the year of sleeper (Fig. b) for Track 1 and Track 2, respectively. From these figures, it can be seen that there is no correlation between the year of super-structure (rail or sleeper) and the increase rate of *NL*, even though theoretically in the calculation of *NL*, the super-structure can have an influence on the value of *NL*. It is worth noting that these data correspond to the year of the current super-structure, and that in past the types of rail and sleeper could be different. Thus, it is not possible to exclude the contribution of the super-structure to the degradation of tracks identified. However, as shown in Fig. 9, after the remedial work of tamping, the value of *NL* continued to increase. This suggests that the rail or sleeper type did not clearly influence the evolution of *NL* identified. Furthermore, admitting that the traffic, train load and rate and the type of sleeper in two tracks are not necessary identical, the coincidence between the degradation rates of Track 1 and Track 2 (Fig. 12) confirms that the general cause of the increase of *NL* came from the sub-structure. Based on this observation, the following analysis focuses on the sub-structure.
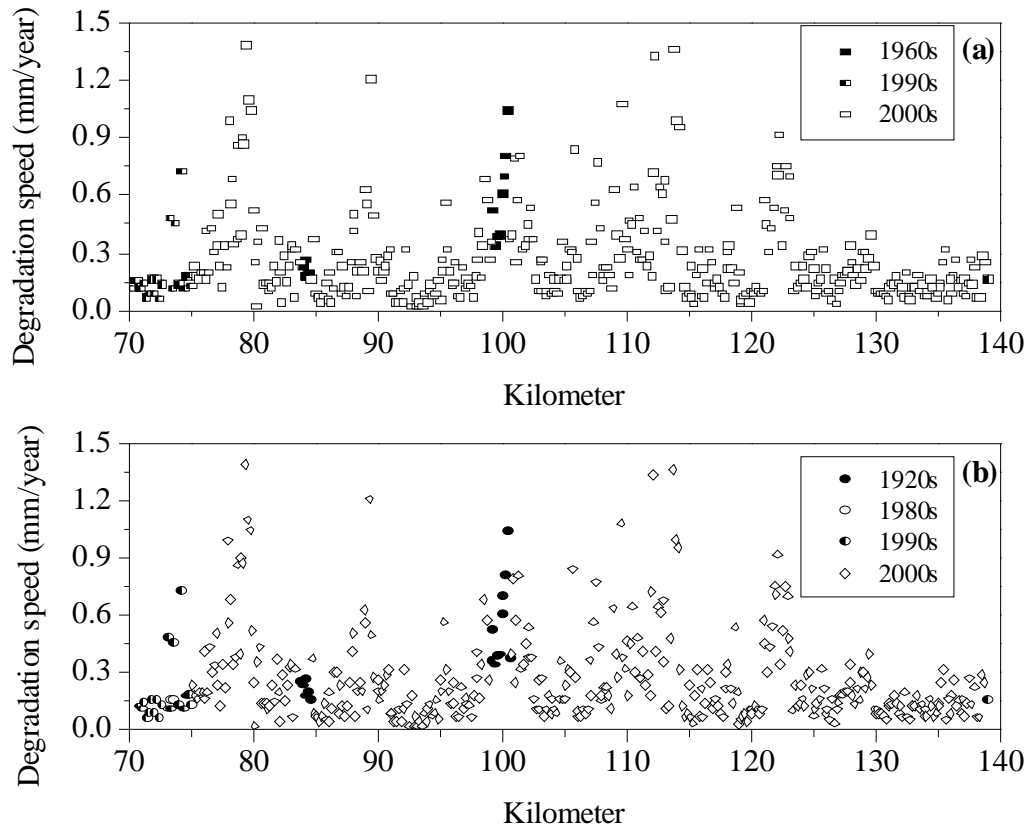
Fig. 13: Degradation rate of Track 1 according to (a) year of rail and (b) year of sleeper
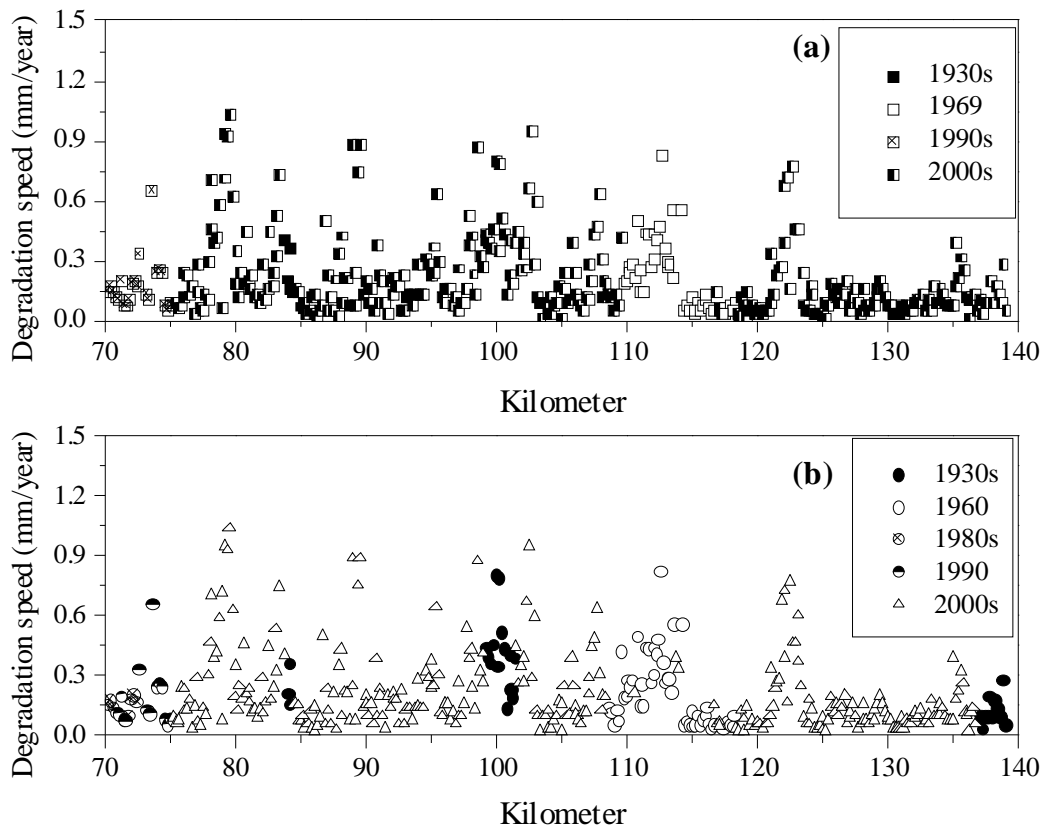
Fig. 14: Degradation rate of Track 2 according to (a) year of rail and (b) year of sleeper

From Fig. 12, the zones with high degradation rates can be identified. They are around PK 73, 79, 88, from 99 to 103, from 106 to 114 and 122. Referring to the geological information, it can be concluded that these kilometer points correspond to the zones where sub-grades contains large fraction of fine particles. Around PK 73, the sub-grade is rather argillaceous limestone and marl. Around PK 79, the sub-grade is fine alluvial deposits and peat. From PK 88 to 89, it is the alluvial deposits overlying the argillaceous limestone or marl or peat. From PK 98-103, the sub-grade involves argillaceous limestone, marl and fine limestone. Around PK 113, the sub-grade contains sometimes colluviums. It is important to note that these soils are sensitive to the changes of water content and train solicitations. Soils like peat, alluvial deposit and colluviums are very compressible and do not have the required mechanical properties for sustaining the train-induced loading. This can explain the high increase rate of *NL* in these zones. From PK 123 to the end of the line, the increase rate of *NL* became low along the line, indicating a good performance of the tracks. This can be also explained by the sub-grade nature: hard limestone is involved along this section. For the first part of the line (up to PK 103), the sub-grade soils are quite variable. These changes in soil natures are also detrimental to the track performance.

From the analysis above, it can be seen that the sub-grade has a significant influence on the performance of railway structure. From a practical point of view, the zones with a sub-grade of low mechanical properties are not apt to become the foundation of railway sub-structure. If it is inevitable, improvement must be conducted in order to meet the requirements, such as a good drainage system, or some soil improvements.

Fig. 15 presents the correlation between the degradation rates of Track 1 and Track 2. It is observed that the *NL* of Track 1 increased more quickly than that of Track 2, because more data fall below the equality line. This is in agreement with the finding in the first part of work where the number of sub-structure related problems were recorded (Fig. 4). It is normally admitted that the train heading to the center (up line) carrying more freights and passengers than the train leaving the center (down line). More studies are needed to clarify this observation.
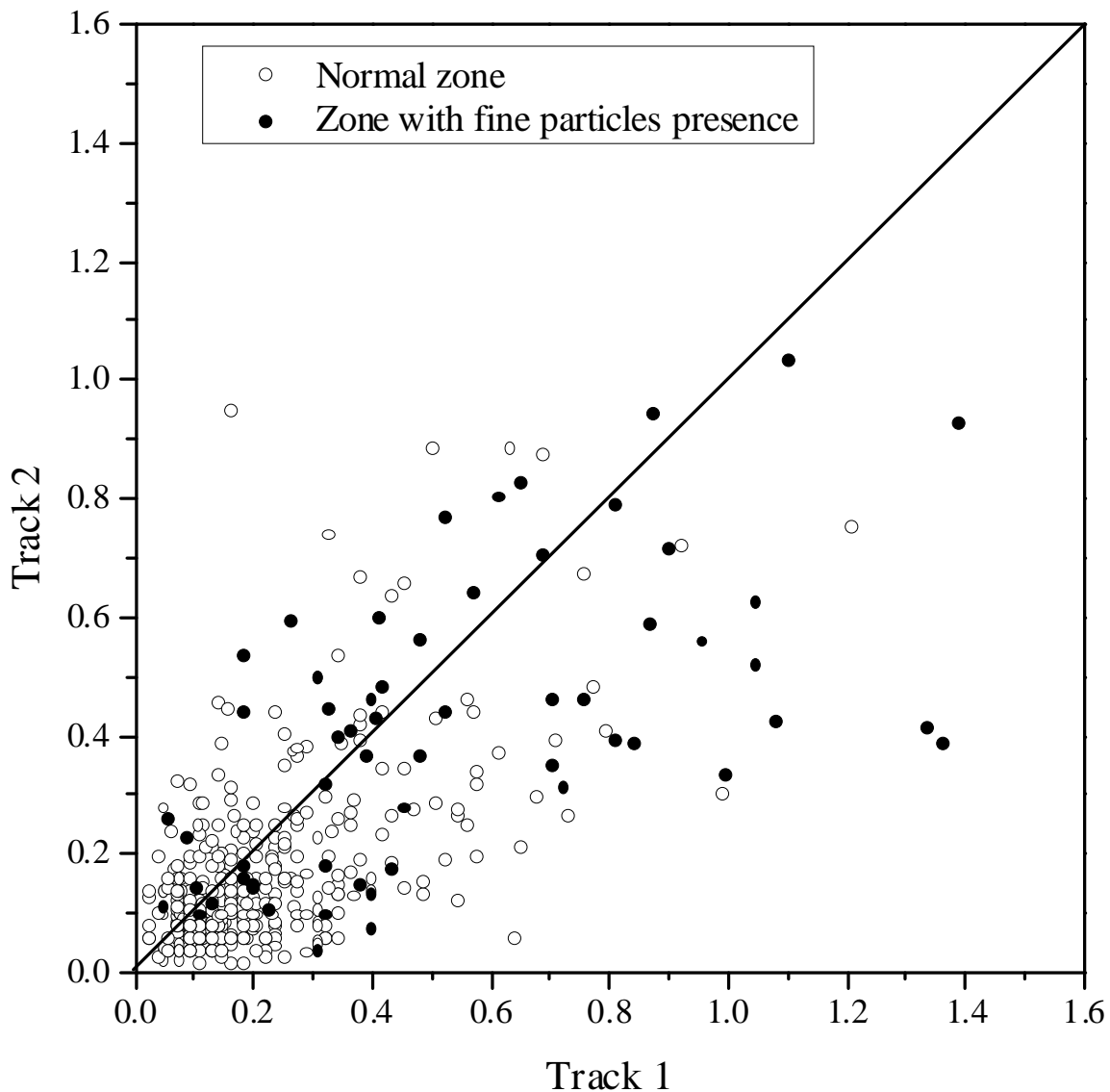
Fig. 15: Correlation between degradation rate of Track 1 and Track 2

During the assessment of the whole line, the zones where fine particles were found on the ballast layer surface were identified. The degradation rates of these zones are presented in Fig. 15 with the black symbols. It can be seen that most of the zones with the presence of fine particles correspond to the zones with high increase rate of *NL*. These fine particles came probably from the sub-grade when mud pumping occurred. This implies that the sub-grade containing large fraction of fine particles is detrimental to the performance of sub-structure. Indeed, for this kind of sub-grade soils, a decrease of mechanical performance can be expected when the moisture content rises. It appears thereby important to further investigate the effect of water content of sub-soil having large fine particles fraction and also the mud-pumping phenomenon.
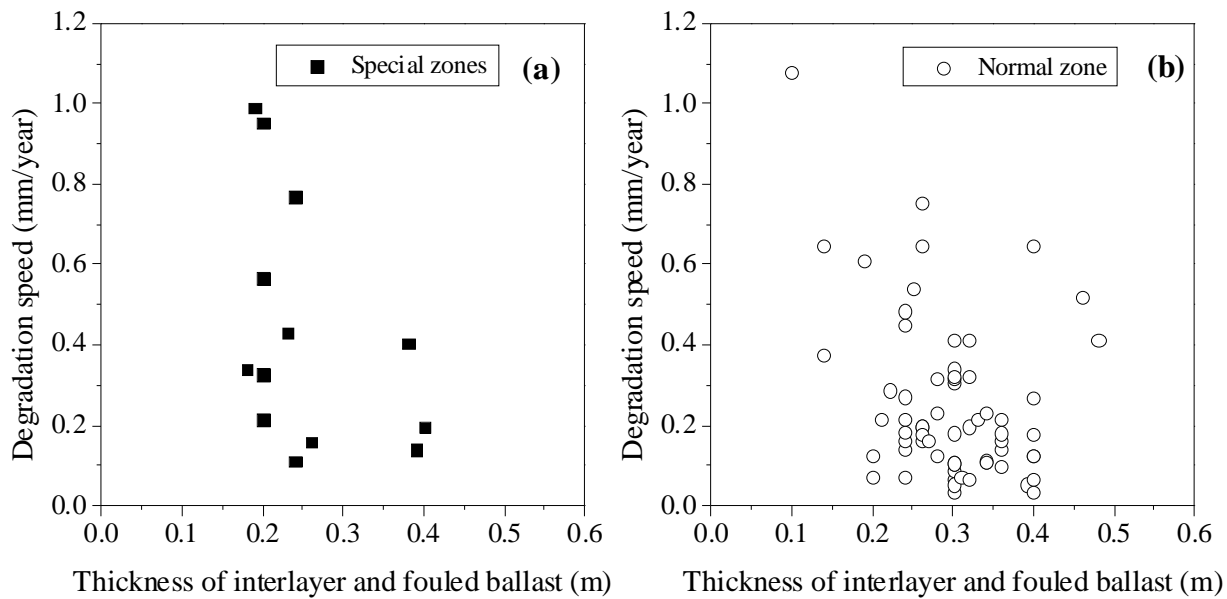
Fig. 16: Correlation of the degradation rate to the thickness of interlayer and fouled ballast for Track 1- Data from coring train. a) special zones and b) normal zone

Fig. 16 presents the correlation between the thickness of fouled ballast and interlayer (*e*) and the increase rate of *NL* for special zones (Fig. a) and normal zones (Fig. b), for Track 1. The same correlation is presented in Fig. 17 for Track 2. The special zones correspond to the zone of stations, the zones with bridges or viaducts. The other zones are referred to normal zones. For the special zones, Track 1 (Fig. 16a) presents a sharp decrease trend of degradation speed with the increase of *e*, while this trend is not observed for Track 2 (Fig. 17a). For the normal zones, despite the data scatter that can be explained by the presence of fouled ballast taken into account in the study, both Track 1 (Fig. 16a) and Track 2 (Fig. 17a) present a decrease of degradation rate as the layers thickness increases. As mentioned before, in the sub-structure of new lines for high rate train, there are a number of layers protecting more or less the sub-grade. On the contrary, in the sub-structure of ancient lines with the absence of an appropriate transition layer such as the sub-ballast layer, significant stress can be exerted to sub-grade soils, leading to significant deformation of tracks or degradation of tracks. The presence of interlayer somehow plays the role of a transition layer to reduce the stress applied to sub-grade. This explains the decrease trend of the degradation rate with the increase of *e*.
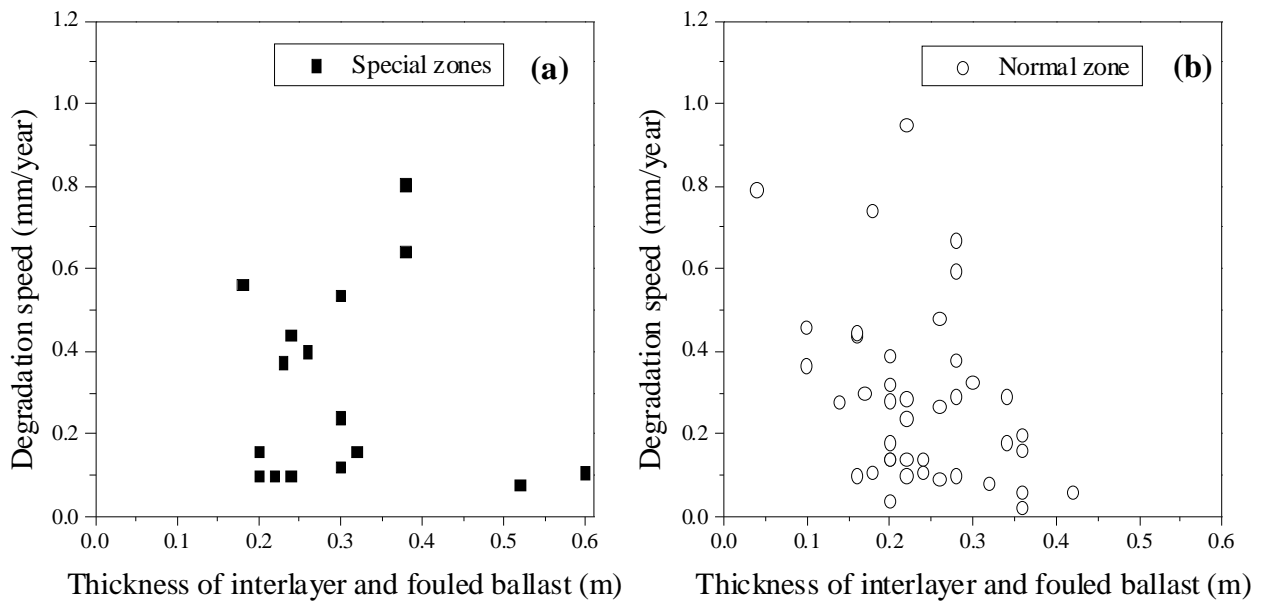
Fig. 17: Correlation of the degradation rate to the thickness of interlayer and fouled ballast for Track 2- Data from coring train. a) Special zones and b) normal zone
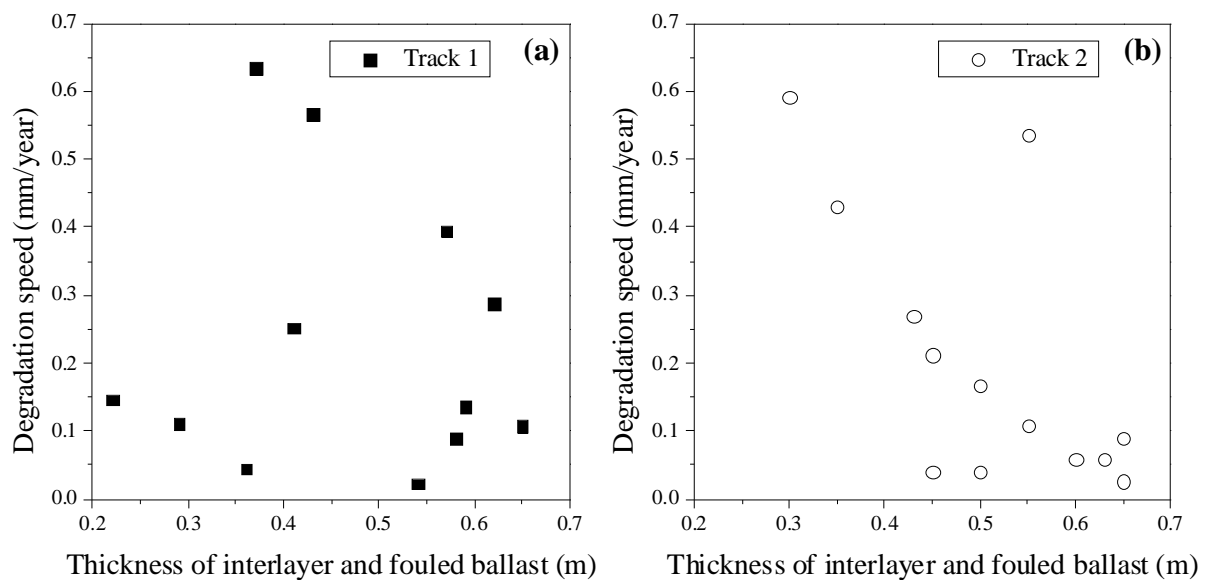
Fig. 18: Correlation of the degradation rate to the thickness of interlayer and fouled ballast - Data from Panda and Endoscope. a) Track 1 and b) Track 2

This trend is also observed in Fig. 18 where the layer thickness deduced from Panda penetrometer tests and endoscope observation is used. The trend is not clear for Track 1 but very clear for Track 2. This confirms the positive impact of interlayer in reducing the degradation of tracks with the increase of interlayer thickness. Note that in other countries, the presence of some layers such as capping layer or blanket layer that can protect sub-grade was also reported by Selig and Waters (1994); Radampola et al. (2008) and Burrow (2011).

Conclusions

25

This paper presents a statistical study on the problems related to the train circulation in the French railway network, followed by an in-depth analysis of an ancient railway line in the West of France. The conducted analyses and observations allow the following conclusions to be drawn:

- The maintenance of sub-structure is as important as that of super structure since the number of problems identified in the whole French railway network for sub-structure was slightly larger than that for super structure. In addition, because the problems related to sub-structure cannot be identified as quickly as those related to super structure, it is recommended to pay more attention to sub-structure part.

- The sub-grade quality controls the degradation rate of tracks. The peak values of degradation rate correspond to the zones where sub-grade is not mechanically stable, i.e., soils with large fraction of fine particles. Moreover, frequent changes of sub-grade along a line are also detrimental to the performance of tracks.

- Comparison between the two tracks of the studied line shows that Track 1 (up line) was degraded faster than Track 2 (down line). More studies are needed to clarify this observation.

- There is a reasonable correlation between the degradation rate and the thickness of fouled ballast layer and interlayer, suggesting a positive role of interlayer in reducing the degradation of tracks.

Acknowledgements

References:

Bednarik M, Magulová B, Matys M, Marschalko M (2010) Landslide susceptibility assessment of the kralovany–liptovsky mikuláš railway case study. Physics and Chemistry of the Earth 35:162–171.

Brough M, Ghataora G, Stirling A, Madelin K, Rogers C, Chapman D (2003) Investigation of railway track subgrade. Part 1: In-situ assessment. Proceedings of the Institution of Civil Engineers - Transport 156(3):145–154.

Brough M, Ghataora G, Stirling A, Madelin K, Rogers C, Chapman D (2006) Investigation of railway track subgrade. Part 2: Case study. Proceedings of the Institution of Civil Engineers - Transport 159(2):83–92.

Burrow M, Bowness D, Ghataora G (2007) A comparison of railway track foundation design methods. Proceedings of the Institution of Mechanical Engineers, Part F: Journal of Rail and Rapid Transit 221(1):1–12.

Burrow M, Ghataora G, Evdorides H (2011) Railway foundation design principles. Journal of Civil Engineering and Architecture 5(3):224–232.

Calon N, (2010) Etude de recommandation en vue d'assurer de façon pérenne le RVL 220 sur *une ligne classique.* Technical report, SNCF. (In French)

Calon N, Trinh VN, Tang AM, Cui YJ, Dupla JC, Canou J, Lambert L, Robinet A, Schoen O (2010) Caractérisation hydromécanique des matériaux constitutifs de plateformes ferroviaires anciennes. Conférence JNGG2010, Grenoble, France, pp. 787–794. (In French)

Cui YJ, Duong TV, Tang AM, Dupla JC, Calon N, Robinet A (2013) Investigation of the hydro-mechanical behavior of fouled ballast. Journal of Zhejiang University- Science 144(4):244–255.

Duong TV, Trinh VN, Cui YJ, Tang AM, Nicolas C (2013) Development of a large-scale infiltration column for studying the hydraulic conductivity of unsaturated fouled ballast. Geotechnical Testing Journal 36(1):54–63.

Duong TV, Tang AM, Cui YJ, Trinh VN, Dupla J, Calon N, Canou J, Robinet A (2014) Effects of fines and water contents on the mechanical behavior of interlayer soil in ancient railway sub-structure. Soil and Foundations. (Accepted for publications).

Ebrahimi A (2011) Behavior or fouled ballast. Railway Track and Structures 107(8):25–31.

Guerin N (1996) Approche expérimentale et numériques du comportement du ballast des voies ferrées. PhD Dissertation, Ecole Nationale des Ponts et Chaussées. (In French)

Langton DD (1999) The panda lightweight penetrometer for soil investigation and monitoring material compaction. Ground Engineering 1999, September.

Indraratna B, Salim W, Rujikiatkamjorn C (2011) Advanced Rail Geotechnology - Ballasted Track. CRC Press.

Li D, Selig ET (1994) Resilient modulus for fine-grained subgrade soils. Journal of geotechnical engineering 120(6):939–957.

Li D, Selig ET (1998a) Method for railroad track foundation design. I: Development. Journal of Geotechnical and Geoenvironmental Engineering 124(4):316–322.

Li D, Selig ET (1998b) Method for railroad track foundation design. II: Applications. Journal of Geotechnical and Geoenvironmental Engineering 124(4):323–329.

Quezada JC (2012) Mécanismes de tassement du ballast et sa variabilité. PhD dissertation, Université Montpellier 2. (In French)

Radampola SS, Gurung N, McSweeney T, Dhanasekar M (2008) Evaluation of the properties of railway capping layer soil. Computers and Geotechnics 35(5):719–728.

Raymond GP (1999) Railway rehabilitation geotextiles. Geotextiles and Geomembranes 17(4):213–230.

Rhayma N (2010) Contribution à l'évolution des méthodologies de caractérisation et d'amélioration des voies ferrées. PhD Dissertation, Université Blaise Pascal - Clermont II. (In French)

Selig ET, Waters JM (1994). Track geotechnology and substructure management. Thomas Telford.

SNCF (1989) Armement, ballastage et entretien de la voie généralités classement des lignes en groupes au point de vue de la maintenance de la voie- ef2a1n°1. Technical report. (In French)

SNCF (2011) Référentiel Infrastructure – Procédure IN4103. (In French).

Trinh VN (2011) Comportement hydromécanique des matériaux constitutifs de plateformes ferroviaires anciennes. PhD Dissertation, Ecole Nationales des Ponts et Chaussées - Université Paris - Est. (In French)

Trinh VN, Tang AM, Cui YJ, Dupla JC, Canou J, Calon N, Lambert L, Robinet A, Schoen O (2012) Mechanical characterization of the fouled ballast in ancient railway track substructure by large-scale triaxial tests. Soils and Foundations 52(3):511-523.

Trinh VN, Tang AM, Cui YJ, Canou J, Dupla JC, Calon N, Lambert L, Robinet A, Schoen O (2011) Caractérisation des matériaux constitutifs de plate-forme ferroviaire ancienne. Revue Française de Géotechnique (134-135):65–74. (In French).

CHAPTER II

Mechanical behavior of interlayer soil

The first chapter showed that interlayer can strongly influence the quality of sub-structure. This chapter deals with the mechanical behavior of interlayer soil.

Because the field conditions can change and the components of interlayer can vary from one site to another, it is then important to test the interlayer under different conditions. For this purpose, the fines content of interlayer soil was varied by adding (+5%; +10%) or removing (-10%) sub-soil fractions. The interlayer soils with different fines contents were subjected to a series of monotonic and cyclic triaxial tests to investigate their mechanical behavior in terms of shear strength, permanent axial strain and resilient modulus under different conditions (fines content, water content, stress and number of cycles).

The results are presented in two papers that constitute this chapter. The first one depicts the monotonic triaxial tests and the variations of permanent axial strain, and was published in *Soils and Foundations*. The second paper deals with the variations of the resilient modulus of interlayer, and was submitted to *Acta Geotechnica*.

Effects of fines and water contents on the mechanical behavior of interlayer soil in ancient railway sub-structure

Trong Vinh Duong[1], Anh Minh Tang[1], Yu-Jun Cui[1], Viet Nam Trinh[1], Jean-Claude Dupla[1], Nicolas Calon[2], Jean Canou[1] , Alain Robinet[2]

Abstract: In the ancient railway sub-structure in France, after years of operation, the inter-penetration of fine particles of sub-grade and ballast has created a new layer namely interlayer. As it was naturally formed, its state presents a large variability in terms of fines content and water content. This study deals with the effects of fines and water contents on the mechanical behavior of interlayer soil, by carrying out large-scale monotonic and cyclic triaxial tests. The results of monotonic triaxial tests show that adding more fines in the interlayer soil does not significantly change the shear strength in dry condition (water content $w = 4\%$ and 6%), but drastically decreases the shear strength parameters (friction angle and cohesion) in the nearly saturated condition ($w = 12\%$). The cyclic triaxial tests were performed at various deviator stress levels. By considering the permanent axial strain at the end of application of each stress level, we observe that in the nearly saturated condition ($w = 12\%$), the higher the fines content the larger the permanent axial strain. In the case of lower water contents ($w = 4\%$ and 6%), an opposite trend is identified: adding fines decreases the permanent axial strain.

Keywords: railway sub-structure; interlayer; fine particles; water content; triaxial test; permanent strain

Introduction

In France, even though some new railway lines for high speed train have been constructed since 1970s, ancient lines (most of which were constructed in the 1800s) still represent 94% of the 30 000 km total network. If the new railway sub-structures are composed of several layers (ballast, sub-ballast, capping layer, etc.) whose characteristics and functions are well defined, it is not the case for the ancient ones that consist mainly of ballast emplaced directly on natural sub-grade at the moment of construction. Under train action over years, the inter-penetration between ballast and fine particles of sub-grade created a new layer namely interlayer (Calon et al., 2010; Trinh et al., 2011, Duong et al., 2013).

The presence of fines inside ballast is known as one of the main causes of fouling (Ayres, 1986; Selig and Waters, 1994; Alobaidi and Hoare, 1998a; 1998b; 1999; Indraratna and Salim, 2002;

---

[1] Ecole des Ponts Paris Tech (ENPC), Laboratoire Navier/CERMES
[2] French Railway Company (SNCF)

Voottipruex and Roongthanee, 2003; Ghataora et al., 2006; Mayoraz et al.*,* 2006; Zeghal, 2009; Giannakos, 2010; Lieberenz and Piereder, 2011; Indraratna et al., 2011a; 2011b; Bailey et al.*,* 2011; Read et al.*,* 2011; Sussmann et al., 2012). Fouled ballast is usually considered as detriment to the sub-structures and needs to be replaced in practice. However, the interlayer can be maintained during the renewal of ancient tracks mainly due to its good bearing capacity. As the interlayer is naturally formed, it can present a large variability in terms of fines nature and fines content. In addition, its water content can change significantly depending on the weather conditions. From a practical point of view, it is important to assess the effect of fines content and water content on the permanent strain of interlayer under cyclic loading.

Various studies evidenced the important role of water content in the mechanical behavior of sub-structures: when water is entrapped in the sub-structure, pore pressure can increase significantly under train's action; as a result, the shear strength and stiffness of sub-structures decrease (Alobaidi and Hoare, 1994; 1996; Huang et al., 2009; Indraratna et al., 2011b; Trinh et al., 2012). Various studies also showed the significant influence of fines content: increasing the quantity of fines significantly affect the mechanical behavior of coarse-grained materials (Babic et al., 2000; LCPC and SETRA, 2000; Pedro, 2004; Naeini and Baziar, 2004; Kim et al., 2005; Verdugo and Hoz, 2007; Cabalar, 2008, 2011; Seif El Dine et al., 2010; Ebrahimi, 2011; Anbazhagan et al., 2011). It has been observed that if the fines content reaches a critical value, the soil behavior changes completely. However, it seems that there is no any unique threshold of fines content for all kinds of soil, suggesting that the influence of fines content depends on the soil nature.

On the whole, for the railway sub-structures, the combined effect of water content and fines content has been scarcely studied. In this study, the effects of water content and fines content are investigated by performing large-scale monotonic and cyclic triaxial tests on interlayer soil specimens prepared by compaction at three water contents and four fines contents. The mechanical properties such as friction angle, cohesion and permanent axial strain are analyzed.

Materials

Interlayer soil was taken from the site of Sénissiat, near Lyon, France. The interlayer has a thickness of about 0.3 m. The grain size distribution curves of the interlayer soil (ITL_0) and the sub-grade (SG) are presented in Fig. 1. Mineralogical analysis showed that the interlayer soil is a mixture of materials that came from the construction of the track, the maintenance (broken stones, gravel, sand, etc.), the aging process of track components and the sub-grade. The density of soil

particles smaller than 2 mm is $\rho_s = 2.67$ Mg/m^3. For the soil particles larger than 2 mm and those greater than 20 mm, the value is $\rho_s = 2.68$ Mg/m^3. More details about the characterization of this soil can be found in Trinh (2011) and Trinh et al. (2010a; 2010b; 2011a; 2011b). According to the USCS, these interlayer soils are classified as gravel poorly graded with clay and sand.
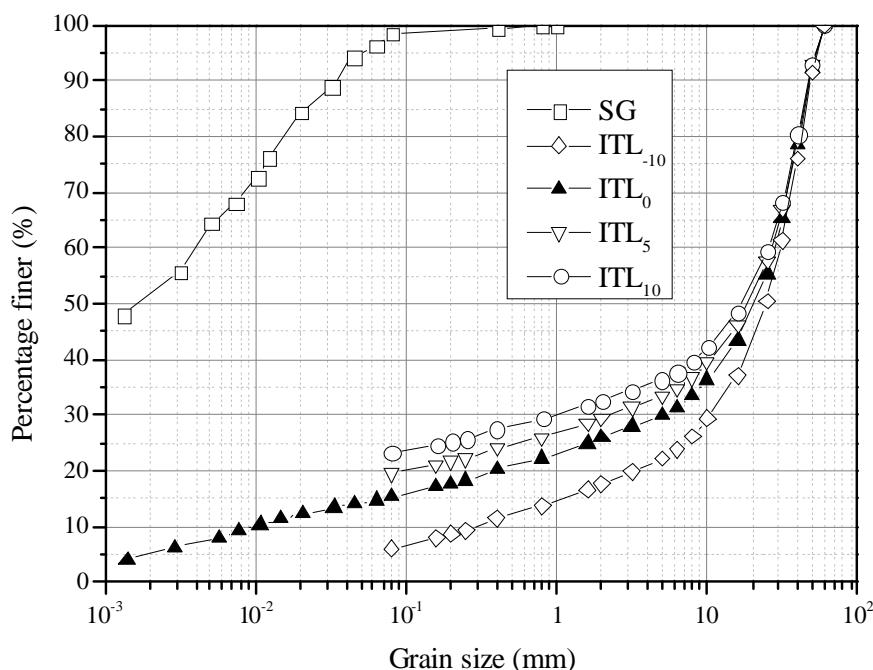
Fig. 1: Grains size distribution of the studied soils

In order to study the influence of fines content on the mechanical behavior of interlayer soil, the fines content was varied by decreasing or increasing the sub-grade fraction: -10% (*ITL$_{-10}$*), +5% (*ITL$_5$*) and +10% (*ITL$_{10}$*) by dry mass (dry mass of sub-grade/dry mass of interlayer soil). Note that unlike in the case of fouled ballast where fouling material is defined as the portion passing through 9.5 mm sieve (Selig and Waters, 1994), as the interlayer was created mainly by the interpenetration of ballast and sub-grade, the sub-grade was considered as fines in the interlayer when changing the fines contents. As the sub-grade consists mainly of fine particles smaller than 80 μm (see Fig. 1), *ITL$_{-10}$* was prepared by removing a certain quantity of particles smaller than 80 μm from the natural interlayer soil by sieving. *ITL$_5$* and *ITL$_{10}$* were prepared simply by adding the mass of sub-grade required. The grain size distribution curves of *ITL$_{-10}$*, *ITL$_5$* and *ITL$_{10}$* are also shown in Fig. 1. According to the AASHTO, *ITL$_0$*; *ITL$_5$* and *ITL$_{10}$* are classified into the group A1b and *ITL$_{-10}$* is classified into the group A1a.

Basically, the effect of fines on the mechanical behavior of interlayer soil is similar to that on fouled ballast; thereby, some parameters used to characterize the fouling state of ballast can be adopted for the interlayer soil. Selig and Waters (1994) proposed the fouling index (*FI*) to describe the ballast fouling based on the gradation obtained from representative specimens in North-America, as follows:

$$FI = P_4 + P_{200} \tag{1}$$

where P_4 and P_{200} are percentages of ballast particles passing through sieve N° 4 (4.75 mm) and N° 200 (0.075 mm), respectively.

The Relative Fouling Ratio (R_{b-f}), proposed by Indraratna et al. (2011)b, describes the weighted ratio of the dry mass of fouling particles M_f (passing through 9.5-mm sieve) to the dry mass of ballast M_b (particles retained in 9.5-mm sieve):

$$R_{b-f} = \frac{M_f \times \dfrac{G_{s-b}}{G_{s-f}}}{M_b} \times 100\% \tag{2}$$

where G_{s-f}, G_{s-b} are specific densities of fouling materials and ballast, respectively.

Using these two parameters, the fouling states of *ITL$_{-10}$*, *ITL$_0$*, *ITL$_5$* and *ITL$_{10}$* can be evaluated and the results are presented in Table 1. It can be seen that only *ITL$_{-10}$* is in the category of "*fouled*" while the other three materials fall in the category of "*highly fouled*". Note that the values divided these two categories are 39 for *FI* and 50 for R_{b-f}.

Table 1: Fouling state of the materials studied

Soil	Fouling Index FI (-)	Relative Fouling Ratio R_{b-f} (%)	Fouling category
ITL$_{-10}$	35	40	*Fouled*
ITL$_0$	45	56	*Highly fouled*
ITL$_5$	52	64	*Highly fouled*
ITL$_{10}$	59	72	*Highly fouled*

Experimental procedure

All soil specimens were prepared before subjected to triaxial tests. For the specimens preparation, after the soil was oven-dried for 24 h, water were added using a large mixer to reach the target water contents. The wet materials were then stored in hermetic containers for at least 24 h for moisture homogenization. Compaction was performed using a vibrating hammer. This procedure of sample preparation follows the French standard (AFNOR 2005) and was used by Trinh et al. (2012). All the tested specimens were prepared at a dry unit mass of 2.01 Mg/m³. This is the maximum dry density which can be reached in the adopted condition. To test this interlayer soil with the largest particles whose diameter can reach 60 mm, a large-scale triaxial device developed by Dupla et al. (2007) was used allowing testing specimens of 300 mm in diameter and 600 mm in height. A schematic view of the triaxial apparatus was presented in Fig. 2. A vertical displacement was integrated in the hydraulic actuator giving the axial deformation. A second external hydraulic actuator generates the confining water pressure σ_3. The change of water volume allows the volumetric strain ε_v to be determined.
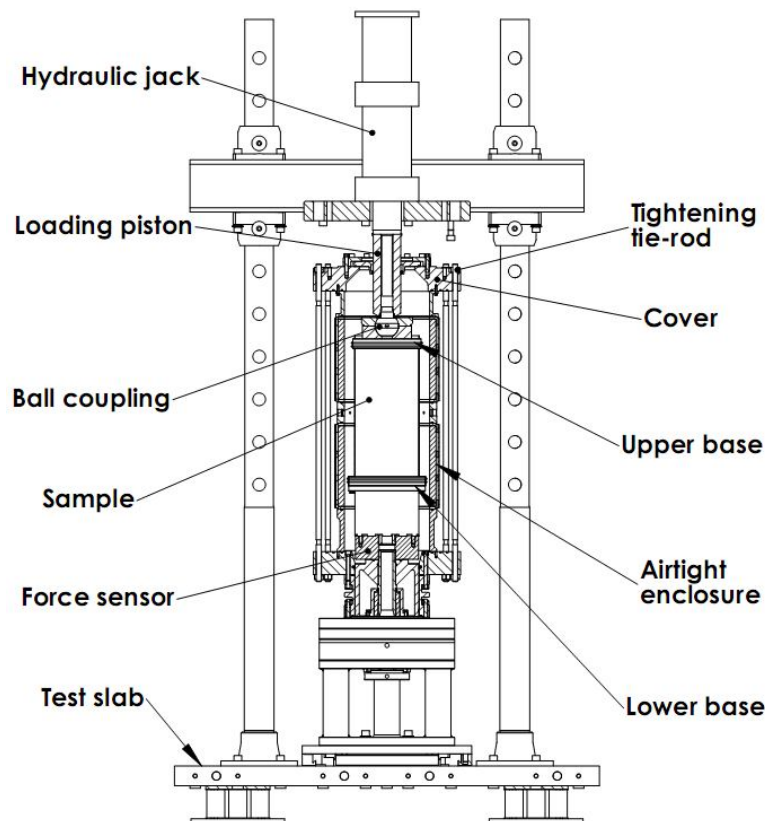
Fig. 2: Schematic view of the large triaxial apparatus (Trinh et al. 2012)

Both monotonic and cyclic triaxial tests can be carried out. In the case of cyclic tests, large number of cycles (up to several millions) at a frequency of several tens of Hertz (depending on the displacement amplitude) can be applied.

In order to determine the shear strength parameters of interlayer soil (friction angle and cohesion), monotonic drained triaxial tests were first performed on ITL_0 and ITL_{10} at two different water contents and under different confining pressures. Some studies with triaxial tests on other similar materials under different confining pressures were performed by Taheri and Tatsuoka (2012) and Vilhar et al. (2013). To investigate the permanent strain development under cyclic loading, cyclic triaxial tests were conducted on all soils at three different water contents. The experimental program is presented in Table 2 for the monotonic triaxial tests and in Table 3 for the cyclic triaxial tests. The tests are named according to the material (ITL_{-10}, ITL_0, ITL_5, ITL_{10}), water content and confining pressure. For instance, ITL_0w4s30 means a monotonic triaxial test on ITL_0 at 4% water content and 30 kPa confining pressure; ITL_0w4C means a cyclic triaxial test on ITL_0 at 4% water content.

Table 2: Program of monotonic triaxial tests

Water content	Confining pressure (kPa)	Soil	
		ITL_0	ITL_{10}
	30	ITL_0w4s30	$ITL_{10}w4s30$
$w = 4\ \%$	100	$ITL_0w4s100$	$ITL_{10}w4s100$
	200	$ITL_0w4s200$	$ITL_{10}w4s200$
	400	$ITL_0w4s400$	-
	100	$ITL_0w12s100$	$ITL_{10}w12s100$
$w = 12\ \%$	200	-	$ITL_{10}w12s200$
	400	$ITL_0w12s400$	-

Table 3: Program of cyclic triaxial tests

Water content	Soil			
	ITL_{-10}	ITL_0	ITL_5	ITL_{10}
$w = 4\%$	$ITL_{-10}w4C$	ITL_0w4C	-	$ITL_{10}w4C$
$w = 6\%$	$ITL_{-10}w6C$	ITL_0w6C	ITL_5w6C	$ITL_{10}w6C$
$w = 12\%$	$ITL_{-10}w12C$	ITL_0w12C	-	$ITL_{10}w12C$

For the cyclic triaxial tests, the multi-step loading procedure proposed by Gidel et al. (2001) was adopted. This procedure allows several stress levels to be applied before the soil specimen reaches failure state, reducing thus the number of tests and avoiding the variability of soil specimens. After the specimen installation, a confining pressure $\sigma_3 = 30$ kPa was applied. The choice of the stress levels was based on the stress distribution in the railway platform as well as the envelope of shear strength determined from the monotonic triaxial tests. Note that the stress distribution within the interlayer depends on the wheel load, dimensions of sleeper, thickness of ballast layer. In the case of France, the wheel load applied by train is about 16 - 22 tons per axle (Alias, 1984); the thickness of ballast and interlayer varies from 250 mm to 600 mm and the distance between two sleepers is 0.6 m. Based on the elasticity theory, the vertical stress at the top of interlayer can be calculated: 40 – 90 kPa. This range is similar to that observed for Indian railways (Jain and Keshav, 1999) and American railways (Selig and Waters, 1994; Yang et al., 2009). Considering a Poisson's ratio of 0.3- 0.4 as proposed by Selig and Waters (1994), an average value of 30 kPa can be estimated for the horizontal stress. Note however that in other countries where heavier wagons are used the wheel load may reach 30 tons per axle (Alias, 1984), corresponding to a vertical stress of 120 - 140 kPa on the interlayer (Li and Selig, 1998; Jain and Keshav, 1999; Grabe and Clayton, 2009). In this study, a maximum vertical stress of 200 kPa was applied in the cyclic triaxial tests.

During the cyclic tests, the maximum deviator stress (q_{max}) was increased in steps (from 0 to various desired values) while the confining pressure was kept constant. The specimens were loaded to 30000 cycles at a frequency of 5 Hz for each maximum deviator stress level. The frequency considered is the dominant one among a number of frequencies generated in the French ancient sub-structures at a train speed of 100 km/h (SNCF, 2009). For ITL_{-10}, ITL_0 and ITL_{10}, the specimens were loaded at three water contents ($w = 4\%$; 6% and 12%), corresponding to three initial degrees of saturation ($S_{ri} = 32\%$; 49% and 100%). In the case of ITL_5, because of lack of material, only one cyclic test at a water content of $w = 6\%$ was conducted.

Results and discussion

Monotonic triaxial test

The results of monotonic triaxial tests on ITL_0 and ITL_{10} at two water contents ($w = 4\%$ and 12%) and under different confining pressures are presented in Fig. 3 to Fig. 6. Dilation is considered as

negative and compression is positive. On the whole, the higher the confining pressure the higher the peak deviator stress and the more significant the contractive behavior as expected.
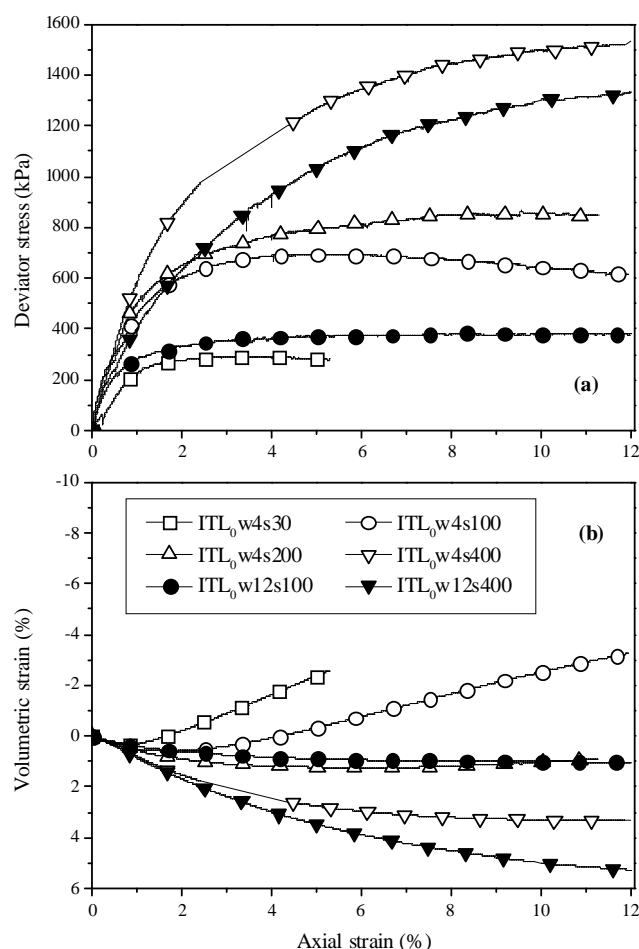
Fig. 3: Results from monotonic triaxial tests on *ITL$_0$* – effect of water content

For *ITL$_0$*, under 400 kPa confining pressure, the behavior is merely contractive (Fig. 3b) and no peak deviator stress is observed till 12% of axial deformation (Fig. 3a) in the cases of water content $w = 4\%$ and 12%. However, it is possible that peak deviator stress appear at a larger axial strain. Indeed, previous studies on ballast shear behavior showed that the peak value can be recorded at an axial strain beyond 12% (Indraratna et al. 1998). Under 100 kPa confining pressure and at $w = 4\%$, a peak deviator stress is recorded, and the volume change behavior is first contractive then dilative. On the contrary, at saturated state ($w = 12\%$) peak deviator stress was not recorded and the behavior is solely contractive. As mentioned before, it is possible that peak deviator stress appear at a larger axial strain. This effect of water content on the ductility/fragility was also identified by Cui and Delage (1996) for a compacted unsaturated silt.
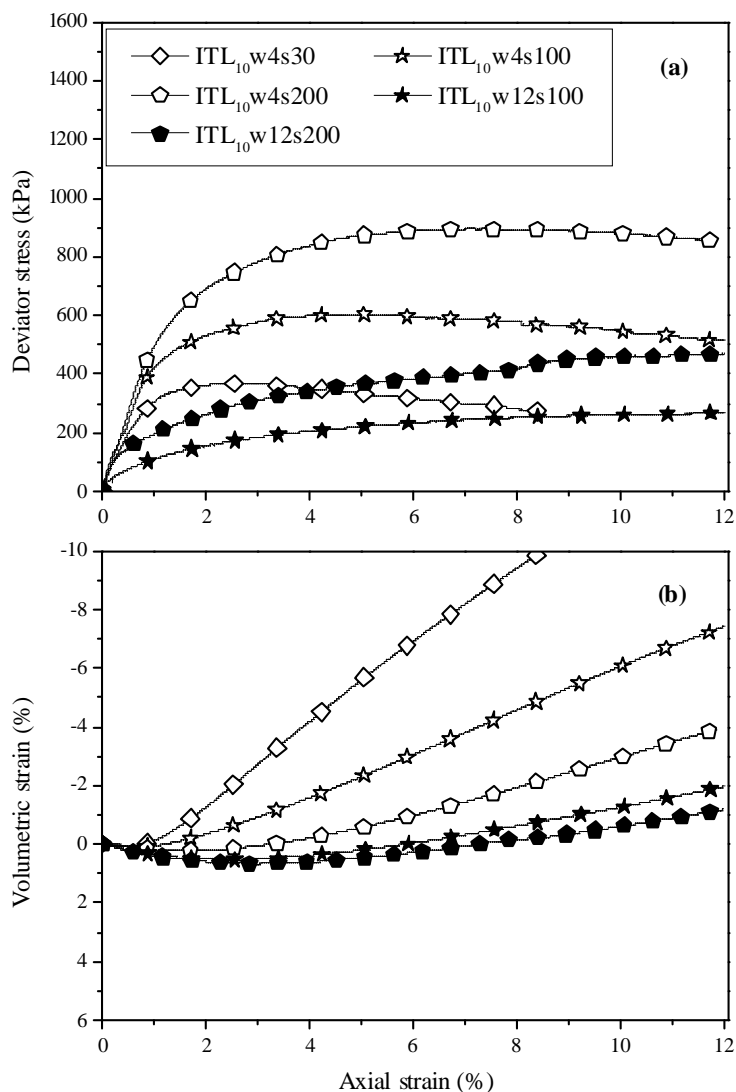
Fig. 4: Results from monotonic triaxial tests on *ITL$_{10}$* – effect of water content

For *ITL$_{10}$* (Fig. 4), whatever the water content and the confining pressure, the volume change behavior is clearly characterized by contraction followed by dilatancy. However, increasing water content from $w = 4\%$ to 12% favorites the compression behavior (Fig. 4b). In Fig. 4a, peak deviators are recorded at $w = 4\%$ but not at $w = 12\%$, showing again the effect of water content on the ductility/fragility of soil.

The effect of fines content can be appreciated in Fig.5 and Fig. 6 for $w = 4\%$ and 12%, respectively. Under unsaturated condition ($w = 4\%$), adding more fines increases the deviator stress or shear strength in the test with $\sigma_3 = 30$ kPa and 200 kPa but decreases in the test with $\sigma_3 = 100$ kPa (Fig. 5a). The decrease under 100 kPa confining pressure is difficult to explain and further study is needed to clarify this point. Note that this particularity does not affect the overall interpretation thanks to the data with other three confining pressures (30, 200 and 400 kPa). On the volumetric

strain, the increase of fines content makes the compression more pronounced (Fig. 5b). This phenomenon can be explained as follows: the fine particles are normally more compressible than the big solid grains. The compression of specimen becomes more significant when the big particles were replaced by fine particles.
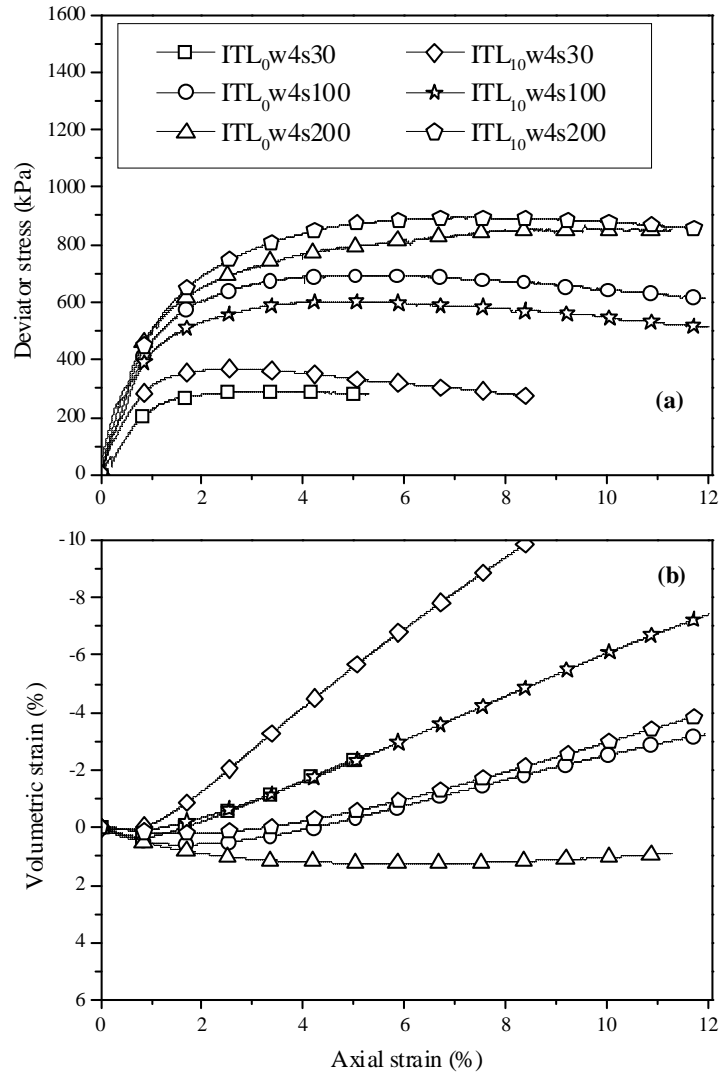
Fig. 5: Results from monotonic triaxial tests on *ITL₀* and *ITL₁₀* at *w* = 4% - effect of fine particles content

At nearly saturated state ($w = 12\%$), adding fines makes the volume change more dilative (Fig. 6a). In Fig. 6a, the curve of ITL_0 is always above the curve of ITL_{10}, showing that addition fines decreases the shear strength. The different effect of fines content on shear strength between ITL_0 and ITL_{10} can be explained by both suction and fines effects. In unsaturated state, for the same water content, increasing fines content makes the suction higher, thus strengthening the soil. On the contrary, in saturated state, suction becomes zero and the shear strength decreases accordingly.
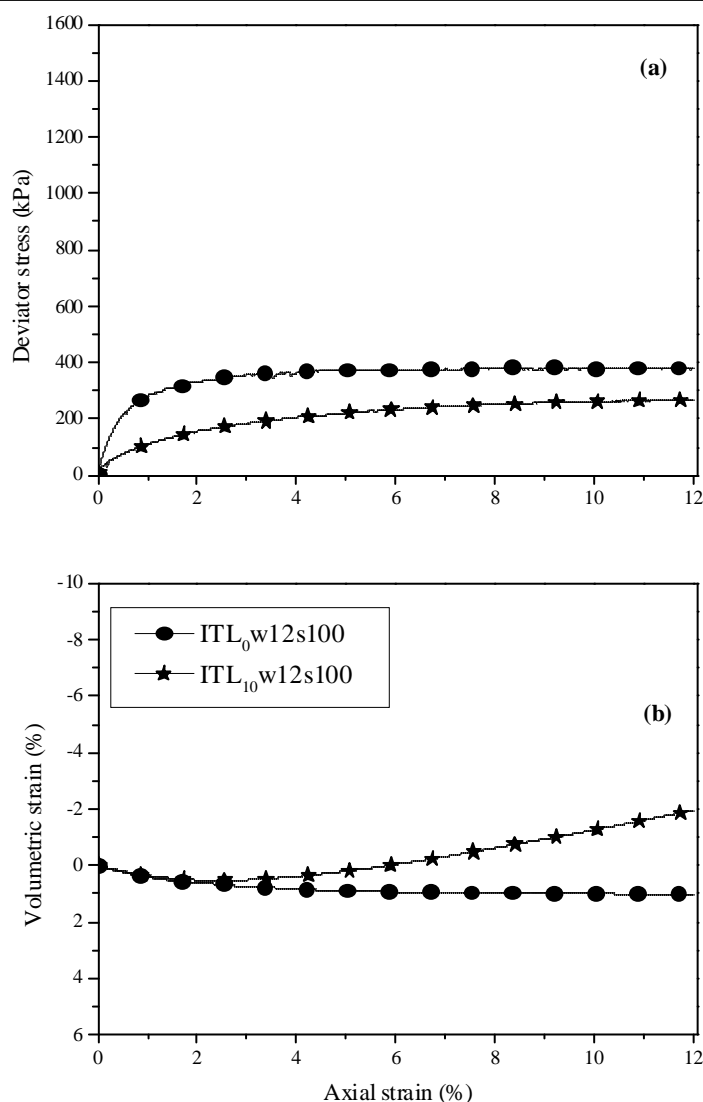
Fig. 6: Results from monotonic triaxial tests on *ITL_0* and *ITL_10* at *w* = 12% - effect of fines content

Fig. 7 shows the pseudo-elastic modulus determined in the range from 0 to 0.1% of axial strain. It can be observed that increasing confining pressure leads to an increase in Pseudo-elastic modulus, the increasing rate being larger in the lower range of confining pressure (smaller than 200 kPa).

The values of internal friction angle and cohesion are determined and presented in Table 4. It can be observed that when water content increases from 4% to 12%, the values of friction angle and cohesion decrease for both *ITL_0* and *ITL_10* - the internal friction angle changes from 39° to 37° for *ITL_0* and from 37° to 29° for *ITL_10* while the cohesion decreases significantly from 42 kPa to 16 kPa for *ITL_0* and from 48 kPa to 21 kPa for *ITL_10*. Similar observation about the decrease of internal friction angle when increasing water content was made by Seif El Dine et al. (2010), Indraratna et al. (2011b), Selig and Waters (1994), Fortunato et al. (2010) and Ebrahimi (2011).
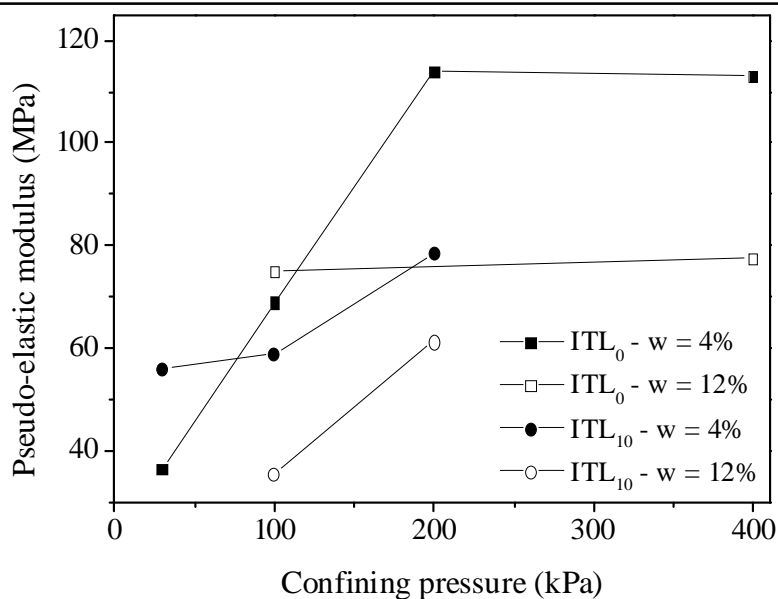
Fig. 7: Pseudo-elastic modulus versus confining pressure for *ITL₀* and *ITL₁₀* at *w* = 4% and 12%

Table 4: Internal friction angle and cohesion of studied materials

Water content (%)	Soil	Internal friction angle φ (°)	Cohesion c (kPa)
$w = 12$	ITL_0	37	16
	ITL_{10}	29	21
$w = 4$	ITL_0	39	42
	ITL_{10}	37	48

The effect of fines content on shear strength can also be analyzed by fixing a water content value. In dry conditions (w = 4%), adding 10% of fines does not significantly change the shear strength parameters: 39° against 37° (friction angle) and 42 kPa against 48 kPa (cohesion) for ITL_0 and ITL_{10}, respectively. But in nearly saturated conditions (w = 12%), there is a large difference between two soils: adding fines decreases the internal friction angle from 37° to 29° and increases the cohesion from 16 kPa to 21 kPa. The test results show that the fines content has a more pronounced effect when the soil is close to saturation. Similar observations were made by Ebrahimi (2011), Kim et al. (2005); Huang et al. (2009) on fouled ballast: the effects of water content and fines content are strongly related and should not be considered separately - increasing water content negatively boosts the effect of fines content on shear strength parameters. The reason for the shear strength decline can be explained by the sensitivity of fines to changes of water content. In dry conditions, at given water content, thanks to the effect of suction, adding fines does not significantly change the

behavior of soil. Upon water content increase, soil suction decreases, leading to a decrease in interlayer soil strength. Note that similar suction effect was identified by Inam et al. (2012) and Wang et al. (2013).

Cyclic triaxial tests

The results of test *ITL$_0$w4C* (for *ITL$_0$* at 4% water content) are presented in Fig. 8 for the first ten cycles. The deviator stress, q, varies following a sinusoidal function between 0 and the maximum value, q_{max} = 45 kPa (Fig. 8a). In Fig. 8b, two distinct parts can be identified on the axial strain curve: a reversible part, ε_1^r, and an irreversible part, ε_1^p. The reversible strain remains fairly constant, while the irreversible strain (permanent strain) increases with loading cycles, at a rate that tends to decrease with increasing number of cycles. After the stage of q_{max} = 45 kPa, the deviator stress q_{max} is then increased to 90 kPa, 140 kPa and 200 kPa. For each value of q_{max}, 30 000 cycles are in general applied. This number of cycles is applied for almost all loading stages except the last one in order to be able to compare the results.
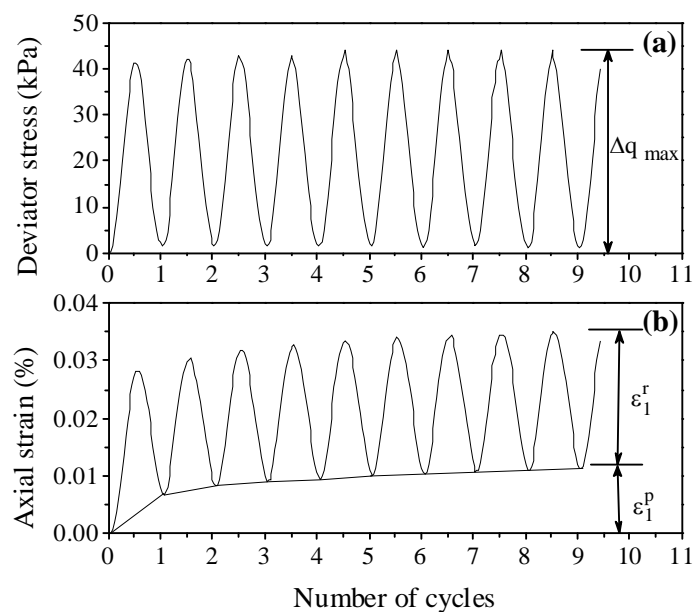
Fig. 8: First cycles of cyclic triaxial test on *ITL$_0$* at *w* = 4% (test *ITL$_0$w4C*) - (a) Deviator stress; (b) Axial strain

In Fig. 9a, the results of test *ITL$_0$w4C* are shown in terms of permanent axial strain versus number of cycles. For all deviator stress levels, the permanent axial strain increases quickly during the first cycles. It stabilizes then after 30 000 cycles at 2.19×10^{-2} % and 9.20×10^{-2} % for q_{max} = 45 kPa and 90 kPa, respectively. At the end of stage 3 (q_{max} = 140 kPa), the permanent axial strain is not stable after 30000 cycles. At the last deviator stress level (q_{max} = 200 kPa), some data was lost for the first

cycles, but the test was continued until 180 000 cycles. No stabilization is observed even at this large number of cycles. In Fig. 9b and Fig. 9c, the results of tests ITL_0w6C and ITL_0w12C are presented, respectively. The trend for test ITL_0w6C (for ITL_0 at 6% of water content) is similar to that for ITL_0w4C. For test ITL_0w12C (near saturated state), failure is observed at $q_{max} = 200$ kPa after just some limited cycles.

Fig. 9: Permanent axial strain versus number of cycles for ITL_0 – (a) 4% water content; (b) 6% water content; (c) 12% water content

The variations of permanent axial strains with number of cycles for tests ITL_{-10}, ITL_5 and ITL_{10} are shown in Fig. 10, Fig. 11 and Fig. 12, respectively. For ITL_{-10}, three tests were performed at three water contents (4%; 6% and 12%). In each test, the deviator stress was increased in steps: 23, 45, 71, 90, 140 and 200 kPa. At low stress levels (up to 90 kPa deviator stress), the permanent axial

43

strain reaches stabilization at the end of each loading stage (30 000 cycles). By contrast, for higher stress levels (140 and 200 kPa deviator stress), the permanent axial strain continues to increase even after 30 000 cycles. For the test in near saturated state at 200 kPa deviator stress (Fig. 10c), failure is observed after some limited cycles.
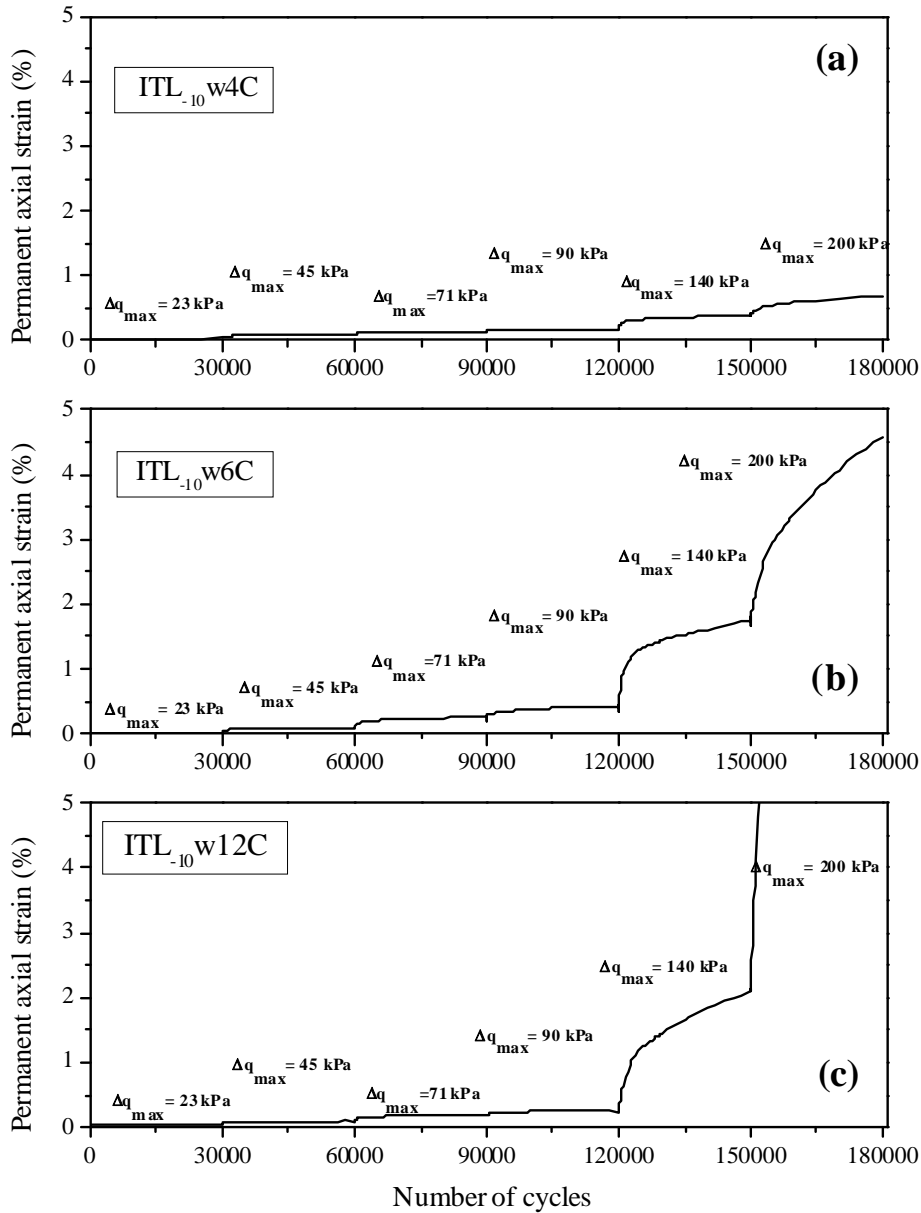
Fig.10: Permanent axial strain versus number of cycles for *ITL$_{-10}$* – (a) 4% water content; (b) 6% water content; (c) 12% water content

For *ITL$_5$* (Fig. 11), due to the limited quantity of material only one test was performed for 6% of water content. Four deviator stress levels were applied (45, 90, 140 and 200 kPa). For all the stress levels, the permanent axial strain reaches stabilization at the end of loading cycles (30 000 cycles).

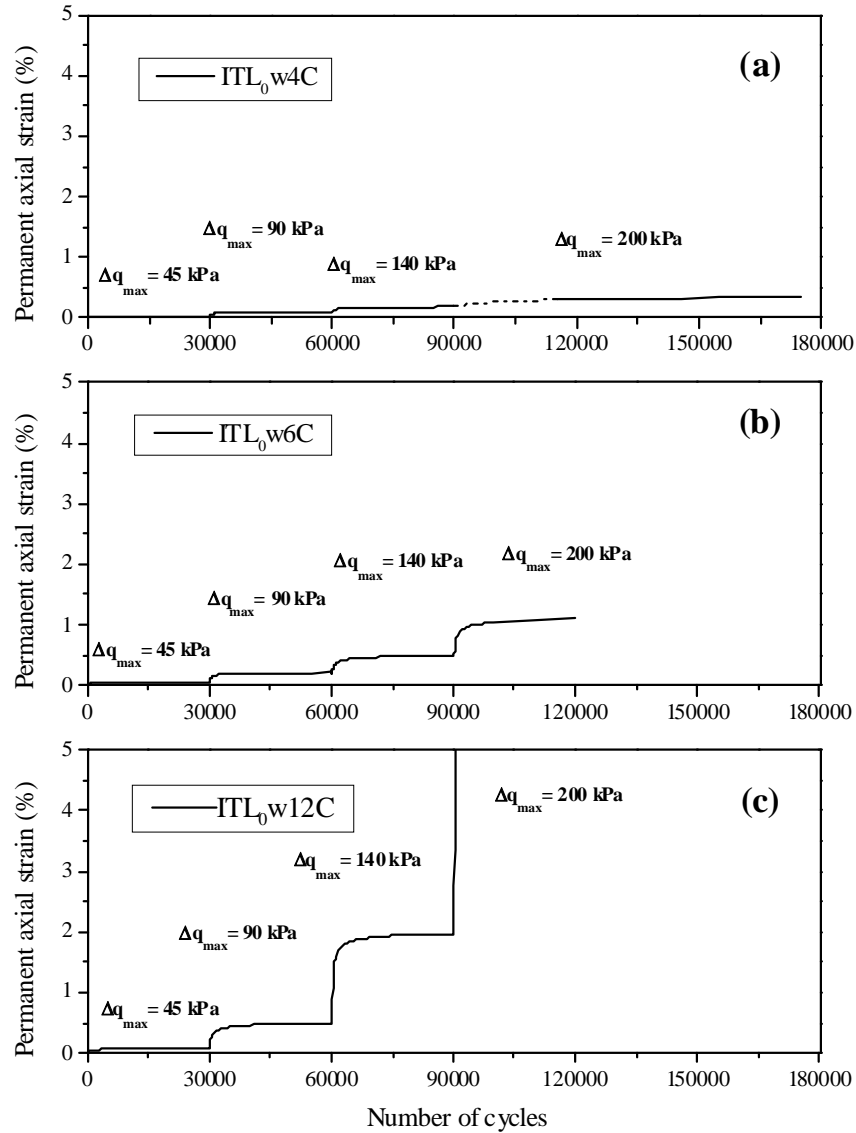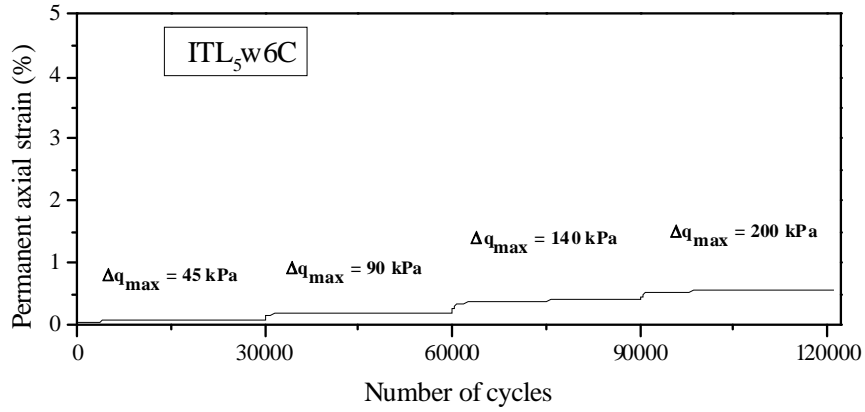**Fig. 11: Permanent axial strain versus number of cycles for *ITL₅* at 6% water content**
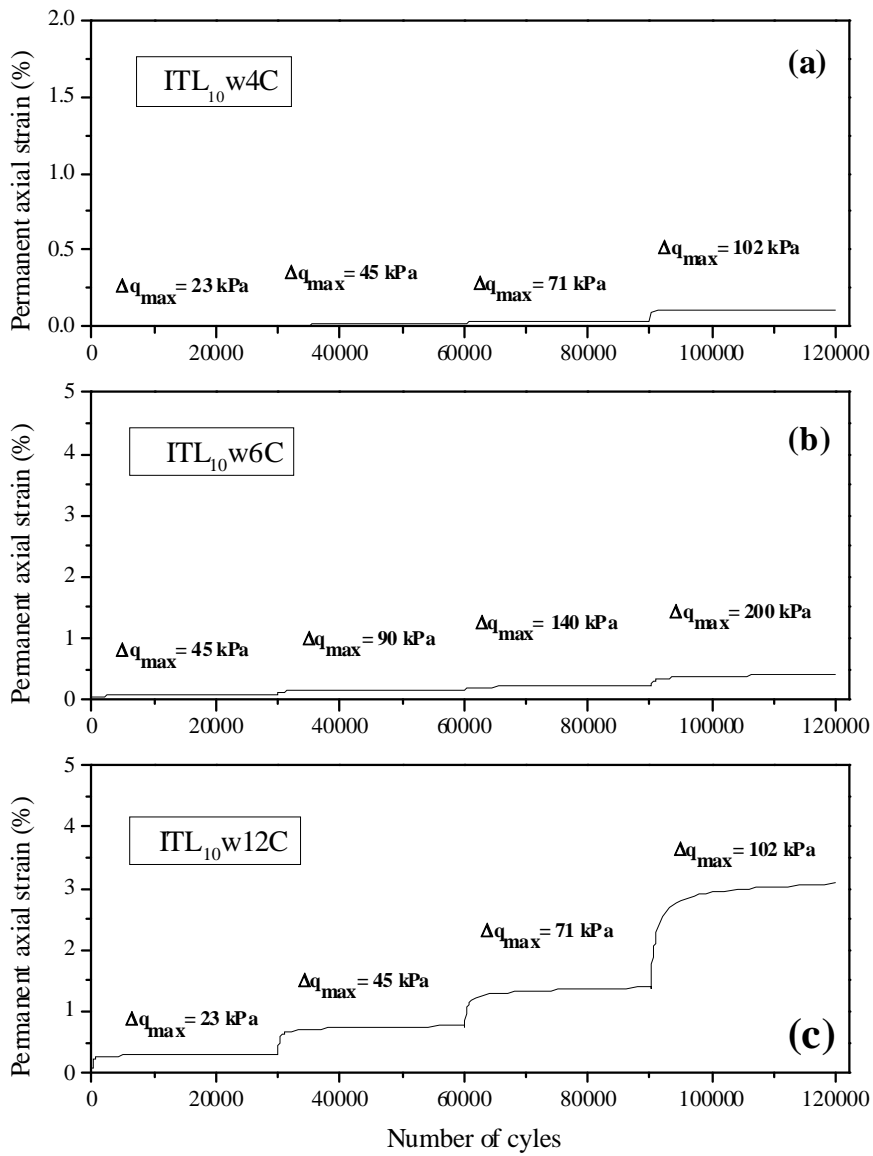
Fig. 12: Permanent axial strain versus number of cycles for *ITL₁₀* – (a) 4% water content; (b) 6% water content; (c) 12% water content

45

For ITL_{10} (Fig. 12), four maximum deviator stress levels of 23, 45, 71, and 102 kPa were applied for 4% and 12% of water contents. For the test of $w = 6\%$ (Fig. 12b), the deviator stress was increased in steps from 0 to 45, to 90, 140, and 200 kPa. It can be observed that in all tests the permanent axial strain reaches stabilization at the end of loading cycles. In other words, failure did not take place.
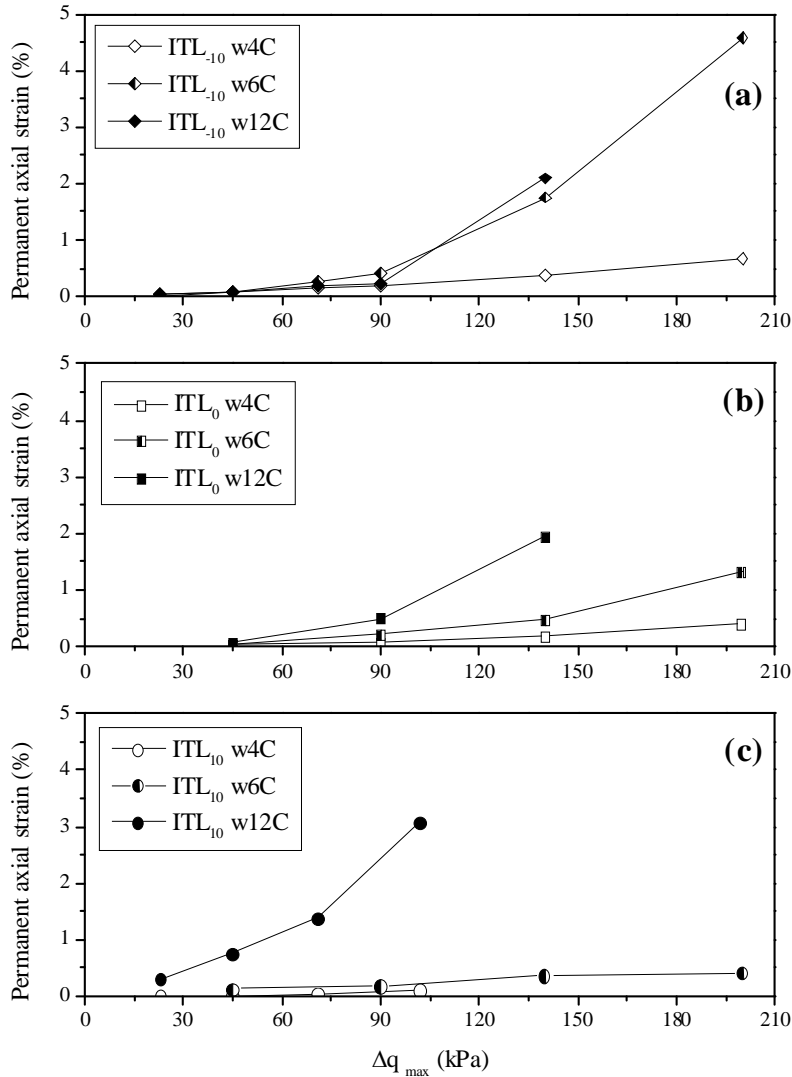
Fig. 13: Effect of water content on the end-stage permanent axial strain for ITL_{-10}, ITL_0 and ITL_{10}

Fig. 13 presents the permanent axial strains obtained at the end of each loading step (same number of cycles) versus the corresponding q_{max} for each soil at three different water contents, allowing analyzing the effects of stress level and water content on the permanent axial strain. For ITL_{-10} (Fig. 13a), the curves are similar up to 90 kPa deviator stress. Beyond 90 kPa, the permanent axial strain of $ITL_{-10}w4C$ is smaller than that of $ITL_{-10}w6C$ and $ITL_{-10}w12C$. Note that failure occurred for the nearly saturated specimen ($w = 12\%$) when $\Delta q_{max} = 200$ kPa. For ITL_0 (Fig. 13b), three curves are

well separated. At all stress levels, the higher the water content, the larger the permanent axial strain. Failure was also observed for the nearly saturated specimen at $\Delta q_{max} = 200$ kPa. For ITL_{10} (Fig. 13c), the curve of the specimens at $w = 4$ and 6% are similar, while for the nearly saturated specimen ($ITL_{10}w12C$), the permanent axial strain is much larger. The effect of water content depends not only on the soil nature but also on the variation range of water content. Changing water content from 4% to 6% does not significantly affect the permanent axial strain of ITL_{10} which has the highest fines content but induces significant changes in the case of lower fines content (ITL_{-10} and ITL_0). On the contrary, increasing water content from 6% to 12% induces a significant change in the permanent axial strain for ITL_{10} (having the highest fines content), but not for ITL_{-10} (having the lowest fines content) when the stress is lower than 140 kPa.
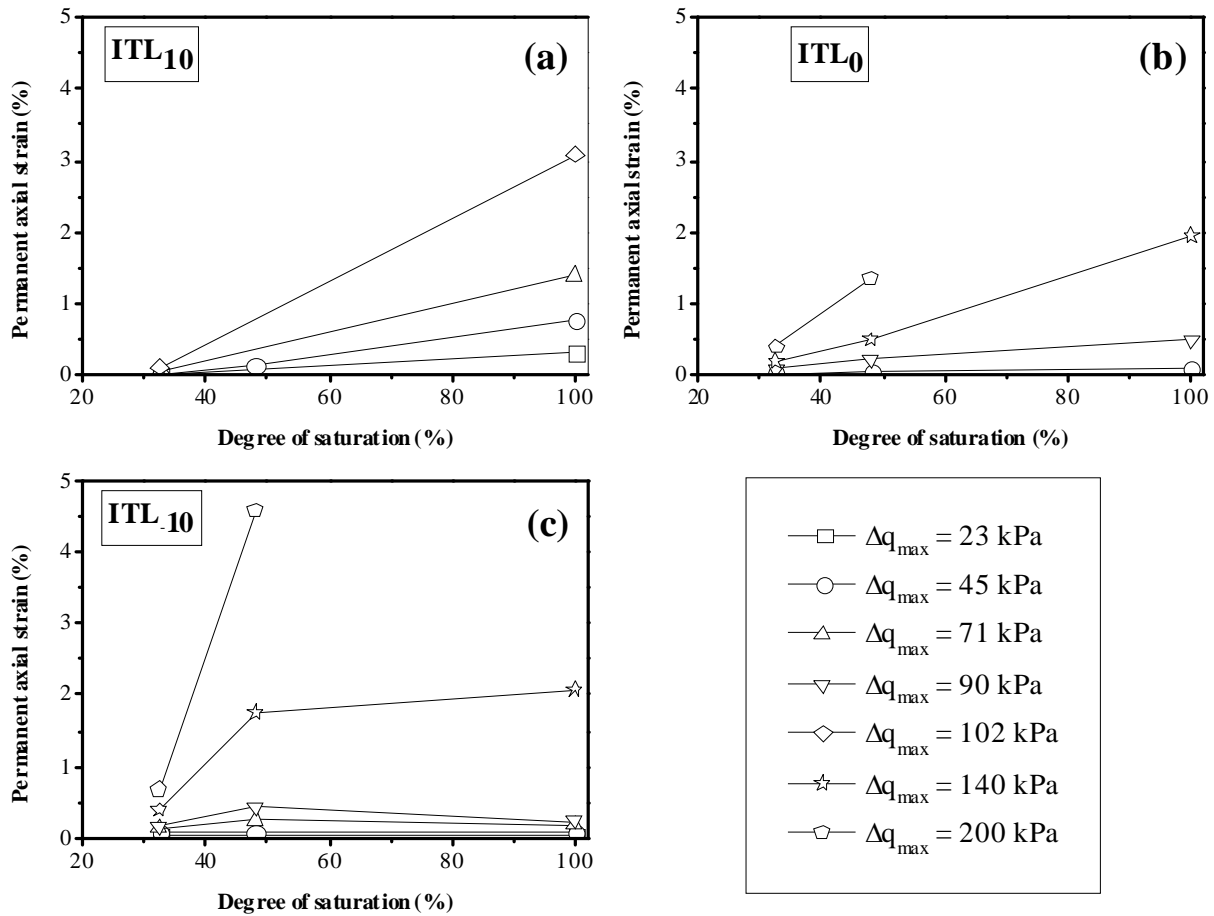
Fig. 14: Water effect with different stress value a) *ITL₁₀*; b) *ITL₀*; c) *ITL₋₁₀*

At a given stress level, increasing water content results in an increase in permanent axial strain. These permanent axial strains are presented in Fig. 14 showing the influence of degree of saturation

under difference applied deviator stresses. The influence of water content can be then depicted more clearly. In the case of ITL_{10} (Fig. 14c), when the deviator stress is lower than 90 kPa, a small decrease trend is observed within a small axial strain range ($< 5 \times 10\text{-}3$) when the degree of saturation increases from 49% (6% water content) to 100% (12% water content). When the applied stress becomes higher, the axial strain increases with the increase of degree of saturation (water content) as in other cases (Fig. 14a and Fig. 14b).

Fig. 15 shows the permanent axial strains obtained at the end of each loading step versus the corresponding q_{max} for each water content value, allowing analyzing the effect of fines content on the permanent axial strain. In the case of $w = 4\%$ and 6% (Fig. 15a and Fig. 15b, respectively), the permanent axial strain for test *ITL$_{-10}$w4C* and *ITL$_{-10}$w6C* is significantly higher than for others, suggesting that the lower the fines content, the larger the permanent axial strain. In nearly saturated state (Fig. 15c), the effect of fines content is inversed: the soil having the highest fines content (*ITL$_{10}$*) exhibits the largest permanent axial strain.

Uthus et al. (2005) and Uthus (2007) also observed that the effect of water content on the permanent axial strain depends on the fines content. This phenomenon can be explained as follows: in unsaturated state, water is mainly trapped by fine particles. At the same density and water content, if the fines content is higher, the soil suction must be higher. As a result, the soil is mechanically more resistant. On the other hand, fine particles are well known to be very sensitive to changes in water content, and when the water content is 12%, the soil becomes saturated and its suction approaches zero leading to a decrease in fine particles strength and further the overall mechanical behavior of soil. Similar observations were reported by Fortunato et al. (2010), Seif El Dine et al. (2010) and Huang et al. *(*2009).

On the whole, at a given water content in dry condition, adding more fines has a positive effect on the mechanical behavior of interlayer soil (the permanent axial strain is reduced), while in nearly saturated condition, adding more fines boosts the axial strain. This means that in the railway context, during the assessment and exploitation of the interlayer soil, the effect of water content and fines content must be taken into account together. The interlayer soil containing a larger quantity of fine particles have to be protected from water infiltration in order to avoid any increase of water content that would decrease its mechanical performance.
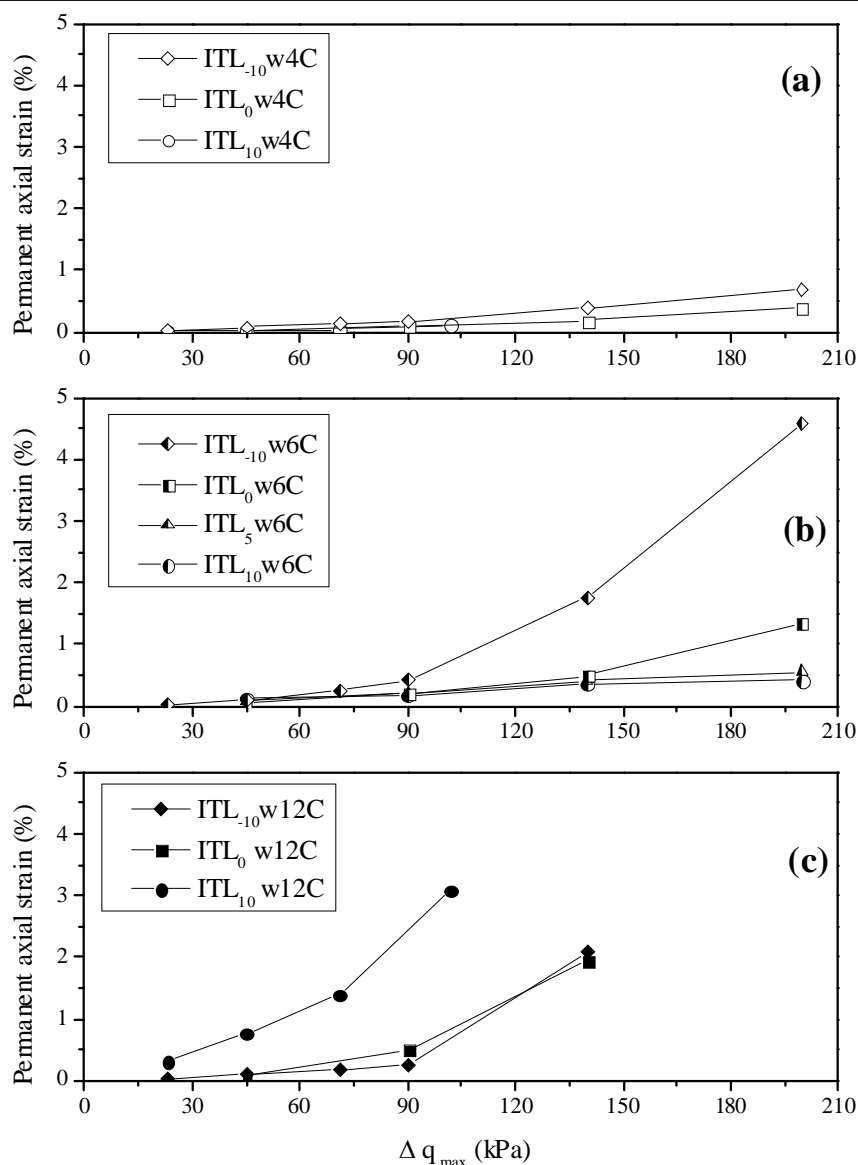
Fig. 15: Effect of fines content on the end-stage permanent axial strain at various water contents

Conclusion

The present work investigates the effects of water content and fines content on the mechanical behavior of interlayer soil. The quantity of fine particles in soil was modified by adding/removing fines. Four materials having different fines contents were tested using a large-scale triaxial cell. Monotonic triaxial tests were first performed to study the variation of internal friction angle and cohesion and to help define the deviator stress levels in cyclic triaxial tests. Cyclic triaxial tests were conducted at different water contents and deviator stress levels. The permanent axial strain was investigated to analyze the effects of water and of fine particle contents.

49

The monotonic triaxial tests showed that increasing water content decreases the shear strength of interlayer soil at two fines contents corresponding to two fouling indices (*FI* = 45 and 59). In addition, the effect of water content is more pronounced in the case of higher fine content. Adding more fine particles does not result in a clear change in mechanical properties (friction angle and cohesion) in unsaturated condition (*w* = 4%) but results in significant decrease in nearly saturated condition.

Adding more fine particles affects the cyclic behavior of interlayer soil in different fashions. In dry condition (*w*= 4% and 6%), adding fines decreases the permanent axial strain due to the suction effect. On the contrary, in nearly saturated condition (*w* = 12%), the higher the fines content the higher the axial permanent strain. This is because that the interlayer soil in weakened mechanically due to the sensitivity of fine particles to water content changes in nearly saturated condition.

From a practical point of view, the increase of fines content on the mechanical behavior of interlayer can still meet some requirements in case of lower water content (dry state). But in case of high water content (nearly saturated state), the interlayer with high fines content needs to be protected from water infiltration. Otherwise, significant decrease in mechanical performance can be expected.

Acknowledgements

References

AFNOR, 2005. XP CEN ISO/TS 17892-9 : Geotechnical investigation and testing, Laboratory testing of soil – Part 9: Consolidated triaxial compression tests on water-saturated soils.

Alias, J., 1984. La voie ferrée. Techniques de construction et d'entretien, 2nd Ed., Eyrolles. (In French).

Alobaidi, I., Hoare, D., 1994. Factors affecting the pumping of fines at the sub-grade- subbase interface of highway pavements. A laboratory study. Geosynthetics International. 1(2), 221–259.

Alobaidi, I., Hoare, D., 1996. The development of pore water pressure at the sub-grade-subbase interface of a highway pavement and its effect on pumping of fines. Geotextiles and Geomembranes. 14, 111-135.

Alobaidi, I., Hoare, D., 1998a. The role of geotextile reinforcement in the control of pumping at the sub-grade-subbase interface of highway pavements. Geosynthetics International. 5(6), 619–636.

Alobaidi, I., Hoare, D., 1998b. Quantitative criteria for anti-pumping geocomposites. Geotextiles and Geomembranes. 16, 221-245.

Alobaidi, I., Hoare, D., 1999. Mechanisms of pumping at the subgrade-subbase interface of highway pavements. Geosynthetics International. 6(4), 241-259.

Anbazhagan, P., Lijun, S., Buddhima, I., Cholachat, R., 2011. Model track studies on fouled ballast using ground penetrating radar and multichannel analysis of surface wave. Journal of Applied Geophysics. 74(4), 175–184.

Ayres, D., 1986. Geotextiles or geomembranes in track? British railways' experience. Geotextiles and Geomembranes. 3(2-3), 129–142.

Babic, B., Prager, A., Rukavina, T., 2000. Effect of fine particles on some characteristics of granular base courses. Materials and Structures. 33(7), 419–424.

Bailey, B., Hutchinson, D., Gordon, D., Siemens, G., Ruel, M., 2011. Field and laboratory procedures for investigating the fouling process within railway track ballast. Proceeding of the 2011 Pan-Am CGS Geotechnical Conference, 8p.

Cabalar, A., 2008. Effect of fines content on the behavior of mixed specimens of a sand. Electronic Journal of Geotechnical Engineering. 13(D), 1-11.

Cabalar, A., 2011. The effects of fines on the behaviour of a sand mixture. Geotechnical and Geological Engineering. 29(1), 91–100.

Calon, N., Trinh, V., Tang, A., Cui, Y., Dupla, J., Canou, J., Lambert, L., Robinet, A., Schoen, O., 2010. Caractérisation hydromécanique des matériaux constitutifs de plateformes ferroviaires anciennes. Proceeding of the Conference JNGG2010, Grenoble, France, pp. 787–794. (In French).

Cui, Y. J., Delage, P., 1996. Yielding and plastic behaviour of an unsaturated compacted silt. Géotechnique. 46 (2), 291-311.

Dupla, J.-C., Pedro, L.S., Canou, J., Dormieux, L., 2007. Mechanical behaviour of coarse grained soils reference. Bulletin de Liaison des Laboratoires des Ponts et Chaussées. (268-269), 31-58.

Duong, T.V., Trinh, V.N., Cui, Y.J., Tang, A.M., Calon, N., 2013. Development of a large-scale infiltration column for studying the hydraulic conductivity of unsaturated fouled ballast. Geotechnical Testing Journal. 36(1):1-10. [doi:10.1520/GTJ20120099]

Ebrahimi, A., 2011. Behavior or fouled ballast. Railway Track and Structures. 107(8), 25–31.

Fortunato, E., Pinelo, A., Matos Fernandes, M., 2010. Characterization of the fouled ballast layer in the sub-structure of a 19th century railway track under renewal. Soils and foundations. 50(1), 55–62.

Ghataora, G., Burns, B., Burrow, M., Evdorides, H., 2006. Development of an index test for assessing anti-pumping materials in railway track foundations. Proceeding of the First International Conference on Railway Foundations. pp. 355–366.

Giannakos, K., 2010. Loads on track, ballast fouling, and life cycle under dynamic loading in railways. Journal of Transportation Engineering. 136(12), 1075–1084.

Gidel, G., Hornych, P., Chauvin, J.J., Breysse, D., Denis, A., 2001. A new approach for investigating the permanent deformation behavior of unbound granular material using the Repeated Load Triaxial Apparatus. Bulletin de Liaison des Laboratoires des Ponts et Chaussées. 233, 5-21.

Grabe, P., Clayton, C., 2009. Effects of principal stress rotation on permanent deformation in rail track foundations. Journal of Geotechnical and Geoenvironmental Engineering. 135(4), 555–565.

Huang, H., Tutumluer, E., Dombrow, W., 2009. Laboratory characterization of fouled railroad ballast behavior. Journal of the Transportation Research Board. 2117(1), 93–101.

Inam, A., Ishikawa, T., Miura, S., 2012. Effect of principal stress axis rotation on cyclic plastic deformation characteristics of unsaturated base course material. Soils and Foundations, 52(3), 465-480.

Indraratna, B., Ionescu, D., Christie, H.D., 1998. Shear behavior of railway ballast based on large-scale triaxial tests. Journal of Geotechnical and Geoenvironmental Engineering. 124(5), 439–449.

Indraratna, B., Salim, W., 2002. Modelling of particles breakage of coarse aggregates incorporating strength and dilatancy. Proceedings of the ICE - Geotechnical Engineering. 155(4), 243–252.

Indraratna, B., Su, L., Rujikiatkamjorn, C., 2011a. A new parameter for classification and evaluation of railway ballast fouling. Canadian Geotechnical Journal. 48(2), 322–326.

Indraratna, B., Salim, W., Rujikiatkamjorn, C., 2011b. Advanced Rail Geotechnology - Ballasted Track. CRC Press. 413p.

Jain, V., Keshav, K., 1999. Stress distribution in railway formation–a simulated study. Proceeding og the 2nd International Symposium on Pre-Failure Deformation Characteristics of Geomaterials–IS Torino. pp. 653–658.

Kim, D., Sagong, M., Lee, Y., 2005. Effects of fine aggregate content on the mechanical properties of the compacted decomposed granitic soils. Construction and Building Materials. 19(3), 189–196.

LCPC, SETRA, 2000. Technical Guidelines on Embankment and Capping Layers Construction (GTR).

Li, D., Selig, E., 1998. Method for railroad track foundation design. I. Development. Journal of Geotechnical and Geoenvironmental Engineering. 124(4), 316–322.

Lieberenz, K., Piereder, F., 2011. Track sub-structure improvements to increase load-bearing strength. Rail Engineering International. 40(4), 6–10.

Mayoraz, F., Vulliet, L., Laloui, L., 2006. Attrition and particle breakage under monotonic and cyclic loading. Comptes Rendus Mécanique. 334(1), 1–7.

Naeini, S., Baziar, M., 2004. Effect of fines content on steady-state strength of mixed and layered specimens of a sand. Soil Dynamics and Earthquake Engineering. 24(3), 181–187.

Pedro, L., 2004. De l'étude du comportement mécanique de sols hétérogènes modèles à son application au cas des sols naturels, PhD disertation, Ecole Nationale des Ponts et Chaussées, France. (In French).

Read, D., Hyslip, J., McDaniel, J., 2011. Heavy axle load revenue service mud-fouled ballast investigation, Technical report. Federal railroad administration, U.S. Departement of Transportation.

Seif El Dine, S., Dupla, J., Frank, R., Canou, J., Kazan, Y., 2010. Mechanical characterization of matrix coarse-grained soils with a large-sized triaxial device. Canadian Geotechnical Journal. 47(4), 425–438.

Selig, E., Waters, J., 1994. Track geotechnology and sub-structure management. Thomas Telford, 450p.

SNCF., 2009. Sollicitations mécaniques dans la plate-forme. Mesures d'accélérations verticales dans la plate-forme. Technical report R2520-2009-01. (In French)

Sussmann, T. R.; Ruel, M., Christmer, S., 2012. Sources, influence, and criteria for ballast fouling condition assessment. Proceeding of the 91st Annual Meeting of the Transportation Research Board. 11p.

Taheri, A., Tatsuoka F., 2012. Stress-strain relations of cement-mixed gravelly soil from multiple-step triaxial compression test results. Soils and Foundations. 52(4), 748-766.

Trinh, V.N., Tang, A.M., Cui, Y.J., Dupla, J.C., Canou, J., Calon, N., Lambert, L., Robinet, A., Schoen, O., 2010a. Calibration of smart irrigation sensor (sis-ums) for the blanket layer soil from old railway lines. Proceeding of the Conference UNSAT2010, Barcelone, Espagne. Pp. 739–744.

Trinh, V.N., Tang, A.M., Cui, Y.J., Dupla, J.C., Canou, J., Calon, N., Lambert, L., Robinet, A.,Schoen, O., 2010b. Unsaturated hydraulic properties of fines-grained soil from the blanket

layer of old railway lines in France. Proceeding of the Conference UNSAT2010, Barcelone, Espagne. pp 501–507.

Trinh, V., 2011. Comportement hydromécanique des matériaux constitutifs de plateformes ferroviaires anciennes. PhD disertation, Ecole Nationale des Ponts et Chaussées - Université Paris – Est, France. (In French).

Trinh, V.N., Tang, A.M., Cui, Y.J., Dupla, J.C., Canou, J., Calon, N., Lambert, L., Robinet, A., Schoen, O., 2011a. Caractérisation des matériaux constitutifs de plate-forme ferroviaire ancienne. Revue Française de Géotechnique. 134-135, 65–74. (In French).

Trinh, V.N., Tang, A.M., Cui, Y.J., Dupla, J.C., Canou, J., Calon, N., Lambert, L., Robinet, A., Schoen, O., 2011b. Caractérisation hydromécanique des matériaux constitutifs de plateformes ferroviaires anciennes. Proceeding of the International Symposium Georail 2011, Paris, France. pp. 377–387. (In French).

Trinh, V.N., Tang, A.M., Cui, Y.J., Dupla, J.C., Canou, J., Calon, N., Lambert, L., Robinet, A., Schoen, O., 2012. Mechanical characterisation of the fouled ballast in ancient railway track sub-structure by large-scale triaxial tests, Soils and Foundations. 52 (3), 511-523.

Uthus, L., 2007. Deformation Properties of Unbound Granular Aggregat. PhD disertation, Norwegian University of Science and Technology, Norway.

Uthus, L., Hoff, I., Horvli, I., 2005. A study on the influence of water and fines on the deformation properties of unbound aggregates. Proceeding of the 7th International Conference on the Bearing Capacity of Roads, Railways and Airfields. Trondheim, Norway, pp. 1-13.

Verdugo, R., Hoz, K., 2007. Strength and stiffness of coarse granular soils. Solid Mechanics and Its Application. 146(3), 243–252.

Voottipruex, P.,Roongthanee, J., 2003. Prevention of mud pumping in railway embankment, a case study from Baeng pra-pitsanuloke, Thailand, The Journal of KMITB, 13(1), 20–25.

Vilhar, G., Jovicic, V., Coop, M.R., 2013. The role of particle breakage in the mechanics of a non-plastic silty sand. Soils and Foundations. 53(1), 91-104.

Wang, Q., Tang, A.M., Cui, Y.J., Delage, P., Barnichon, J.D., Ye, W.M., 2013. The effects of technological voids on the hydro-mechanical behaviour of compacted bentonite-sand mixture. Soils and Foundations. 53(2), Pages 232-245.

Yang, L., Powrie, W., Priest, J., 2009. Dynamic stress analysis of a ballasted railway track bed during train passage. Journal of Geotechnical and Geoenvironmental Engineering. 135(5), 680–689.

Zeghal, M., 2009. The impact of grain crushing on road performance. Geotechnical and Geological Engineering. 27(4), 549–558.

Effects of water and fines contents on the resilient modulus of the interlayer soil of railway sub-structure

Trong Vinh Duong[1], Yu-Jun Cui[1], Anh Minh Tang[1], Jean-Claude Dupla[1], Jean Canou[1], Nicolas Calon[2], Alain Robinet[2]

Abstract: This paper deals with the resilient behavior of the interlayer soil which is created mainly by the interpenetration of ballast and sub-grade soils. The interlayer soil studied was taken from a site in the South-East of France. Large-scale cyclic triaxial tests were carried out at three water contents (w = 4, 6 and 12%) and three fines contents corresponding to 5% sub-grade added to the natural interlayer soil, 10% sub-grade added to the natural interlayer soil and 10% fine particles (< 80 μm) removed from the natural interlayer soil. Soil specimens underwent various deviator stresses, and for each deviator stress a large number of cycles were applied. The effects of deviator stress, number of cycles, water content and fines content on the resilient modulus (M_r) were analyzed. It appears that the effects of water content and fines content must be analyzed in a global fashion because the two effects are closely linked. Under unsaturated conditions, the soil containing high fines content has higher resilient modulus due to the contribution of suction. When the soil approaches the saturated state, it loses its mechanical performance with a sharp decrease in resilient modulus.

Keywords: railway sub-structure; interlayer soil; resilient modulus; fines content; water content; large-scale cyclic triaxial test.

Introduction

The soils in the sub-structures of highway and railway are subjected to a huge number of traffic loading cycles. In this context, the resilient modulus of sub-structure soils is an important parameter to be considered when designing new tracks or when maintaining under-operation tracks. Indeed, several authors (Selig and Waters 1994, ASSHTO 1993 and Basudhar et al. 2010) reported that the resilient modulus of sub-grade can strongly influence the mechanical behaviour of sub-structure.

For the French ancient railway tracks constructed in the 1880s, as ballast was placed directly on the sub-grade during the construction without any separation layers, an interlayer was naturally created over time mainly by the interpenetration of ballast and sub-soil under the traffic effect (Trinh 2011, Cui et al. 2013, Duong et al. 2013*a* and 2013*b*). This interlayer has been kept as part of the sub-structure considering its high mechanical performance related to its high unit mass (Trinh et al.

2011). As the interlayer is a "component" of the sub-structure overlying the sub-grade, its mechanical behavior appears to be of primary importance for the overall behavior of sub-structure even the overall track structure. However, because this material has been formed naturally, it can present large variability in terms of fines natures and fines contents. Moreover, under the effect of climatic conditions, soil water content changes also constantly. These changes in fines content, fines nature and water content can greatly affect soil mechanical behavior such as soil resilient modulus.

The notion of resilient behavior appeared for the first time in the middle of the 20th century (Heveen and Carmany 1948, Hveem 1955). In the railway context, the resilient modulus (M_r) is defined as the secant slope of the curve of deviator stress versus axial strain obtained from cyclic triaxial tests (Stewart 1982, Selig and Water 1994, Lim 2004, Werkmeister 2003, Radampola 2006, Kim and Kim 2007). Previous studies showed that there are several factors that affect the resilient modulus of unbound granular materials, in particular the stress level (Stewart 1982, Hicks and Monismith 1971, Kolisoja 1997, Lekarp et al. 2000, Lim 2004). The increase in moisture content appears to decrease the resilient modulus (Hicks and Monismith 1971, Ekblad 2007, Ekblad and Isacsson 2006). For the effect of loading cycles, a large disagreement exists in terms of number of cycles required to reach the stabilization of resilient modulus (Stewart 1982, Lekarp et al. 2000, Uthus et al. 2005, Lackenby 2006, Uthus 2007). As far as the effect of fines content is concerned, there is no conclusive observation as mentioned by Lekarp et al. (2000). Thom and Brown (1987) and Kamal et al. (1993) reported that the resilient modulus generally decreases when the fines content increases. However, Jorenby and Hicks (1986) observed that the stiffness of crushed aggregate has an initially increase trend followed by a considerable reduction when clayey fines content increased.

All these factors (moisture content, fines content, number of cycles) influence the resilient response of materials. However, to the authors' knowledge, their combined effect has rarely investigated especially for the interlayer soil. In the present work, large-scale cyclic triaxial tests were carried out to study the variations of M_r of an interlayer soil under the combined effects of stress level, water content, fines content and cyclic loadings.

Materials and methods

The studied interlayer soil was taken from Sénissiat, near Lyon, France. The grain size distribution curves of the natural interlayer soil (*ITL$_0$*) and the sub-grade soil (SG) are presented in Fig. 1. It can be observed that the interlayer soil has a large fines content (16% of particles are smaller than 80 μm), and its grain size distribution curve is well graded from ballast size (60 mm) to clay size (< 2

µm). Its physical properties (density, plasticity index, blue methylene value and standard Proctor curve) of this material were reported by Trinh et al. (2011, 2012). For the SG, almost all soil particles are smaller than 80 µm.
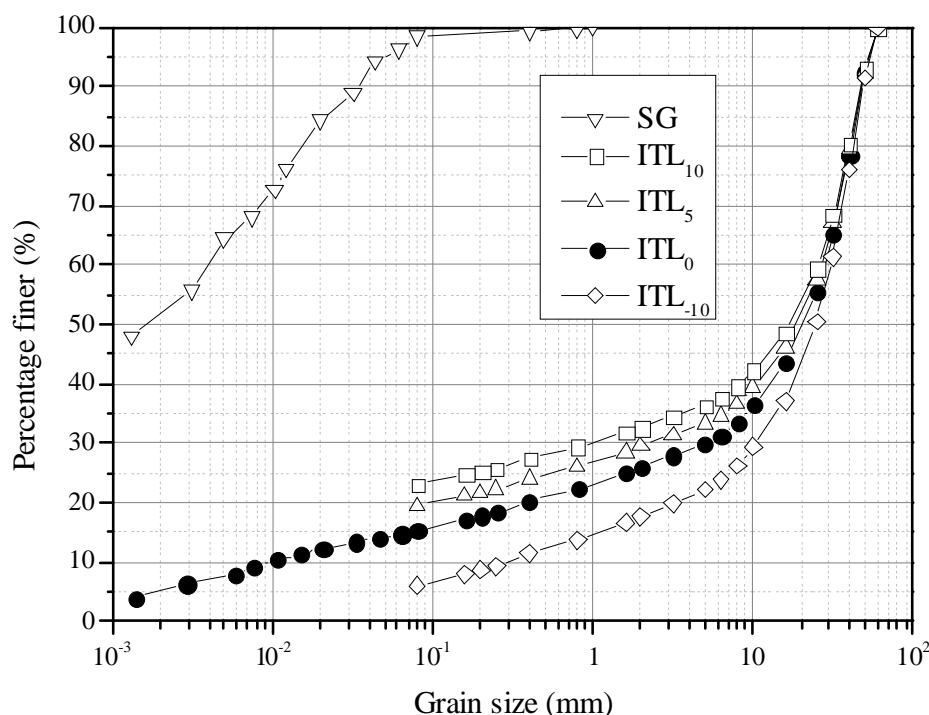
Fig. 1: Grain size distribution of the studied materials

In order to study the influence of fines content, the fines content of the soil was varied by either removing fine particles smaller than 80 µm from the interlayer soil (-10% for *ITL$_{-10}$*) or adding sub-grade soil into the interlayer soil (+5% for *ITL$_5$* and +10% for *ITL$_{10}$*). The percentages refer to the ratio of dry mass of fine particles to dry mass of interlayer soil. The removal of fine particles for the preparation of *ITL$_{-10}$* was done by sieving. The grain size distribution curves of *ITL$_{-10}$*, *ITL$_5$* and *ITL$_{10}$* are also shown in Fig. 1.

For the specimen preparation, water were first added and mixed with the material using a large mixer to reach the target water content. After mixing, the wet materials were stored in hermetic containers for at least 24 h for moisture homogenization. Compaction was performed in 6 layers of 0.1 m thick each using a vibratory hammer to a dry unit mass of 2.01 Mg/m^3. This is the maximum dry unit mass which can be reached in the adopted conditions without breaking ballast particles.

Because large particles were involved, a large-scale triaxial apparatus developed by Dupla et al. (2007) was used, enabling specimens of 300 mm in diameter and 600 mm in height to be tested.

This apparatus can apply large number of loading cycles (up to several millions) at a frequency up to several tens of Hertz.

The program of tests is presented in Table 1. All the four soils were tested at three water contents (w = 4%; 6% and 12%) corresponding to three initial degrees of saturation (S_{ri} = 32%; 49% and 100%), except ITL_5 on which only one test at a water content of w = 6% was conducted owing to lack of material. The tests are named according to the material (ITL_{-10}, ITL_0, ITL_5, ITL_{10}) and water content. For instance, ITL_0w4 corresponds to the test on ITL_0 at 4% water content. To overcome the problem related to the limited material quantity, the multi-step loading procedure proposed by Gidel et al. (2001) was adopted. This procedure enables several deviator stress levels to be applied before the soil specimen reaches the failure state, thereby reducing the number of tests on one hand and avoiding the effect of variability of soil specimens on the other hand.

Table 1: Test program

Soil	Water content - w (%)		
	4 %	6 %	12 %
ITL_{10}	$ITL_{10}w4$	$ITL_{10}w6$	$ITL_{10}w12$
ITL_5	-	ITL_5w6	-
ITL_0	ITL_0w4	ITL_0w6	ITL_0w12
ITL_{-10}	$ITL_{-10}w4$	$ITL_{-10}w6$	$ITL_{-10}w12$

The cyclic triaxial tests were performed under a constant confining pressure σ_3 = 30 kPa. This value was chosen by referring to the wheel load generated by train (Alias, 1984), the depth of the interlayer (from 250 mm to 600 mm), the Poisson's ratio (0.3 - 0.4 as proposed by Selig and Waters, 1994). The vertical stress at the top of interlayer was found to be 40 to 90 kPa. These values correspond to the Indian railways as reported by Jain and Keshav (1999) and American railways as reported by Selig and Waters (1994) and Yang et al. (2009). In other countries where heavier wagons are used, the wheel load may reach 30 tons per axle (Alias, 1984), leading to a vertical stress of 120 to 140 kPa on the interlayer (Li and Selig 1998, Jain and Keshav 1999, Grabe and Clayton 2009). In this study, a maximum deviator stress of 200 kPa was applied. For the loading frequency, a value of 5 Hz was chosen because this is the dominant one among a number of frequencies generated in the French ancient sub-structures at a train speed of 100 km/h (SNCF 2009). During the tests, the deviator stress was increased in steps from 0 to various target values; in each step, 30 000 cycles were applied and the variations of axial strain were recorded.

Results

Fig. 2 presents typical curves of deviator stress versus axial strain for the first cycles in test *ITL5w6*. It also shows the definition of permanent axial strain (ε_p), the resilient axial strain (ε_r) through the first cycle. It can be observed that the minimum deviator stress did not totally reach zero for all cycles. This was probably due to the high loading/unloading speed (frequency of 5 Hz) that caused a delay between the target signal and the real signal. However, it is believed that this problem does not affect the resilient modulus (M_r) that corresponds to the secant slope of curves (see Fig. 2).
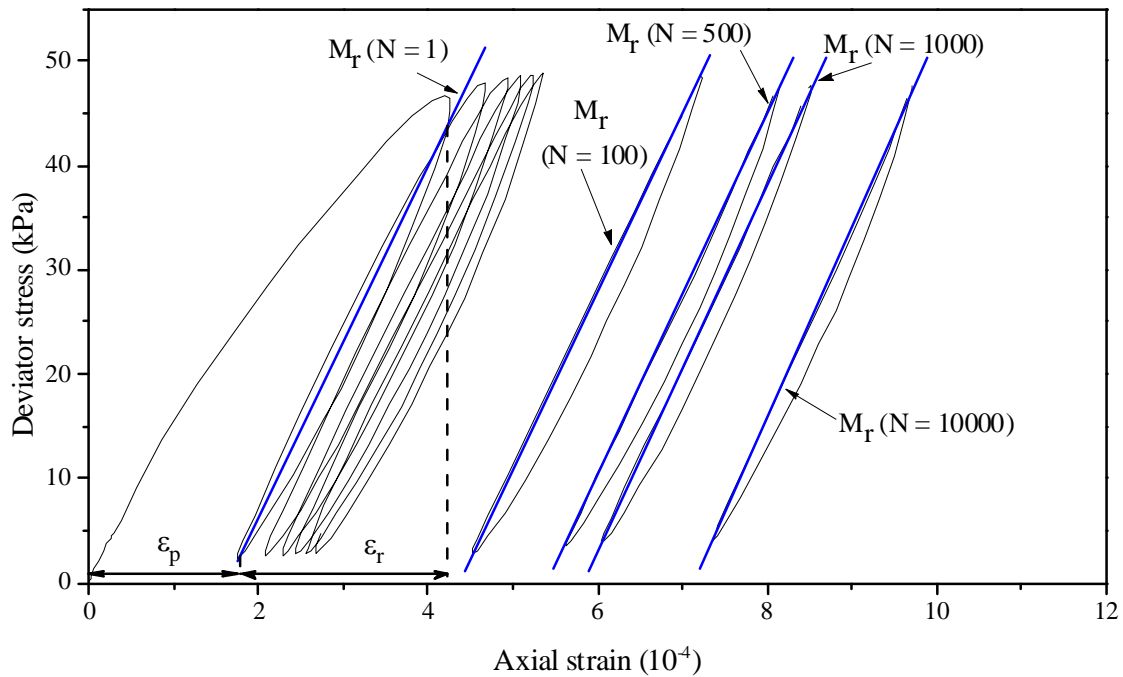
Fig. 2: Deviator stress versus axial strain for test *ITL5w6* - Determination of resilient modulus

Fig. 3 plots the deviator stress versus the axial strain for the moments where the values of Δq_{max} were increased: during the first 8 cycles ($N = 8$) under $\Delta q_{max} = 45$ kPa (Fig. 3a), from $\Delta q_{max} = 45$ kPa ($N = 30\ 000$) to $\Delta q_{max} = 90$ kPa ($N = 30\ 001 \div 30\ 0004$) (Fig. 3b), from $\Delta q_{max} = 90$ kPa ($N = 60\ 000$) to $\Delta q_{max} = 145$ kPa ($N = 60\ 001 \div 60\ 0004$) (Fig. 3c) and from $\Delta q_{max} = 145$ kPa ($N = 90\ 000$) to $\Delta q_{max} = 20$ kPa ($N = 90\ 001 \div 90\ 0004$) (Fig. 3d). It can be observed that when a new deviator stress was applied, the axial strain increased accordingly. During the very first cycles under each stress level, the loading and unloading paths did not form close cycles, suggesting that significant permanent axial strain developed. In this case, the resilient modulus was determined based on the unloading path of a cycle and the loading path of the next cycle. The hysteresis loop was large in the first cycles, and with the increase of number of cycles, this hysteresis became less

and less significant. At large number of cycles by the end of each loading level, the material behaved almost in a purely elastic fashion. Werkmeister et al. (2004) reported that the change in the loop shape provides information about the different deformation mechanisms. In the beginning, there was probably particles rotation and rearrangement producing the plastic strain. Over time, these particles movements became limited and a purely resilient state is reached where strain is due to the deformation at the contacts of particles. Note that the shape of loading/unloading loops is related to the slope adopted for the determination of the resilient modulus. When two paths formed a close cycle, the straight line between the lowest and highest point of the loading/unloading cycle was used in the determination.
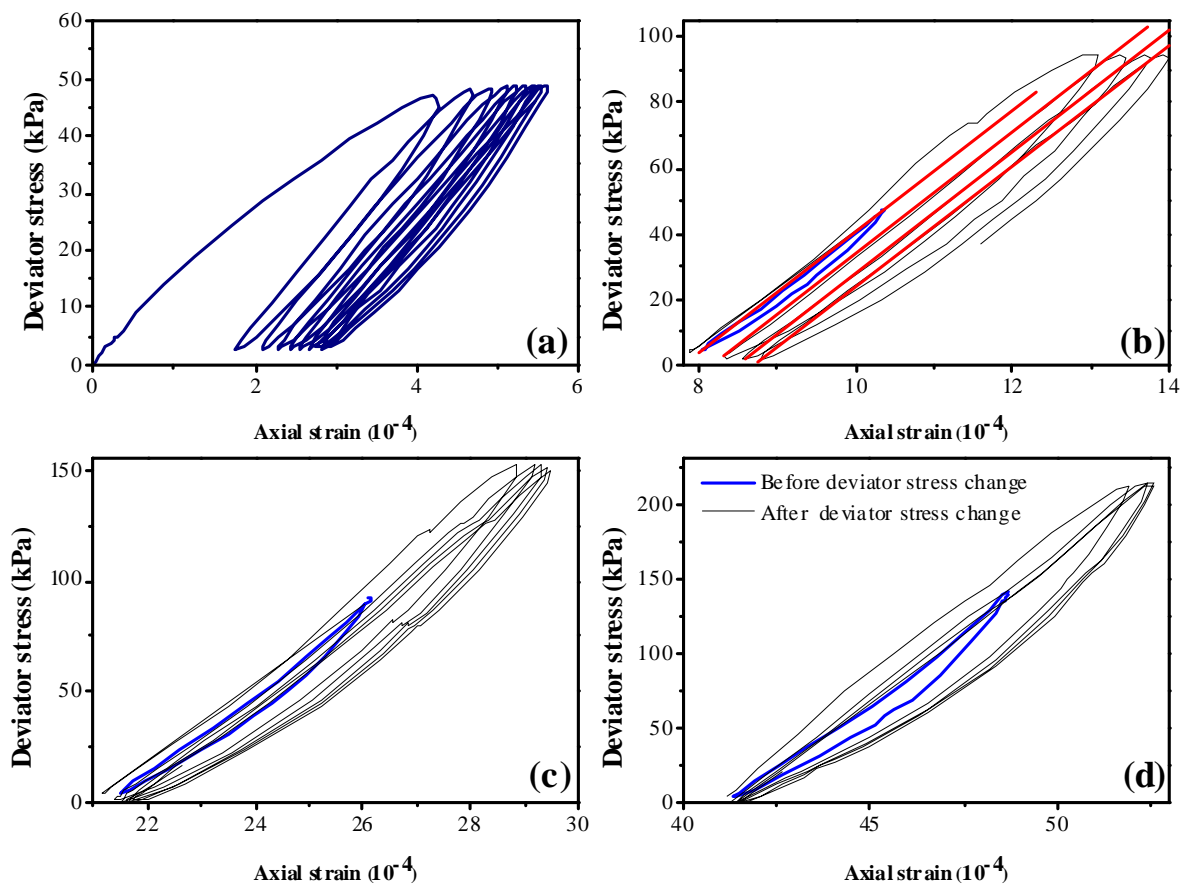
Fig. 3: Deviator stress versus axial strain for test *ITL$_5$w6*. a) N = 1-8 (Δq_{max} = 45 kPa); b) from Δq_{max} = 45 kPa (N = 30 000) to Δq_{max} = 90 kPa (N = 30 001 ÷ 30 0004); c) from Δq_{max} = 90 kPa (N = 60 000) to Δq_{max} = 145 kPa (N = 60 001 ÷ 60 0004); d) from Δq_{max} = 145 kPa (N = 90 000) to Δq_{max} =20 kPa (N = 90 001 ÷ 90 0004)

Fig. 4 depicts the evolution of resilient strain with number of cycles for test *ITL$_{10}$w12*. When the deviator stress increased, the resilient strain increased sharply during the first cycles of each stress level, and decreased afterwards to reach stabilization. The resilient strain was larger under higher deviator stress.
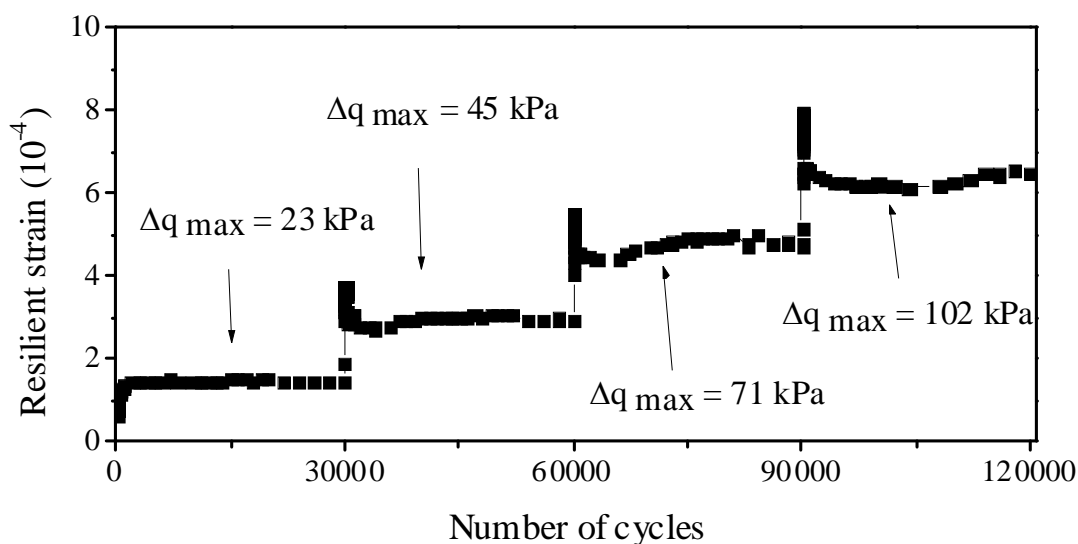
Fig. 4: Resilient strain versus number of cycles in test *ITL$_{10}$w12*

Fig. 5 depicts the variations of M_r with the number of cycles (N) at three water contents and various deviators stress levels for *ITL$_{10}$*. In the case of *ITL$_{10}$w4* (Fig. 5a) at Δq_{max} = 23 kPa, the data of resilient modulus shows some scatter, but in general an increase trend can be identified. Because of the data scatter, it is difficult to determine the number of cycles at which the stabilization of resilient modulus started. The values in other stress levels are more or less constant around 250 MPa. For *ITL$_{10}$w6* (Fig. 5b), the resilient modulus for all stress levels are found to increase significantly in the beginning and then stabilize after around 15 000 cycles. When Δq_{max} was increased from 45 kPa to 90 kPa, the resilient modulus rose up sharply. By contrast, an opposite trend was observed when Δq_{max} was increased from 90 to 140 kPa. It can be seen from Fig. 5c that for each deviator stress level, the resilient modulus decreased during the first cycles. For instance, it decreased from 168 MPa to 144 MPa from cycle 1 to cycle 7. However, this decreasing trend came very quickly to its end and was replaced by an increasing one. Afterwards, the increase rate slowed down and the resilient modulus value tended to stabilize after about 5000 loading cycles. Referring to Fig. 4, the significant variations of resilient modulus in Fig. 5 correspond to the phase characterized by quick development of resilient axial strain just after the change of stress level, and the stabilization states of resilient modulus corresponds to the stabilization of resilient axial strain.

60
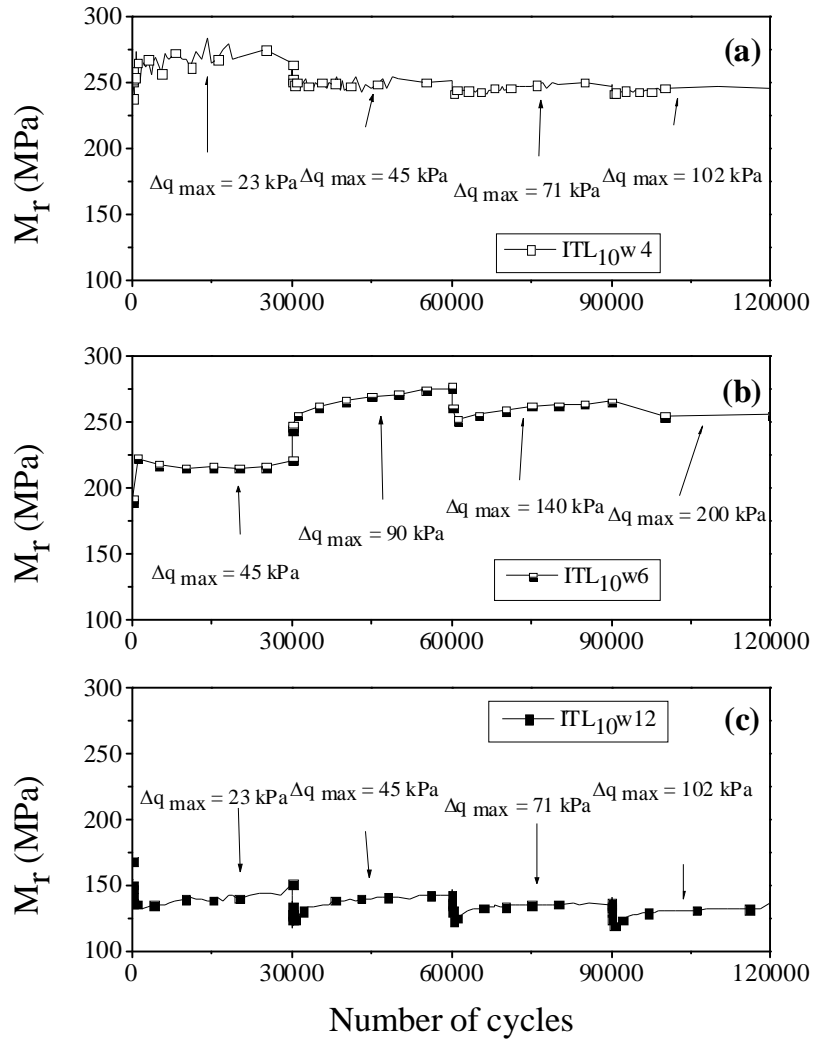
Fig. 5: Resilient modulus versus number of cycles for *ITL₁₀*. a) *w* = 4%; b) *w* = 6%; c) *w* = 12%
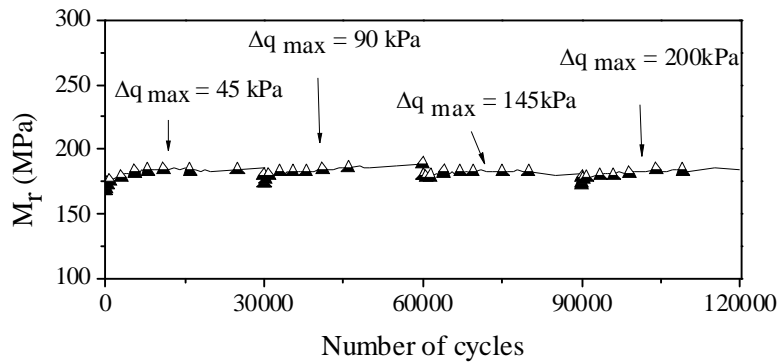
Fig. 6: Resilient modulus versus number of cycles for *ITL₅w6*

These observations are confirmed in the case of *ITL₅w6* (see Fig. 6). For all stress levels, the resilient modulus increased with the number of cycles during the first cycles. At Δq_{max} = 45 kPa, about 10 000 cycles were needed for the resilient modulus to become stable while at Δq_{max} = 140

61

kPa and 200 kPa, about 5000 cycles were needed. The variation range of M_r at all stress levels is about ±10 MPa. On the whole, the effect of deviator stress is not as clear as in the case of $ITL_{10}w6$.
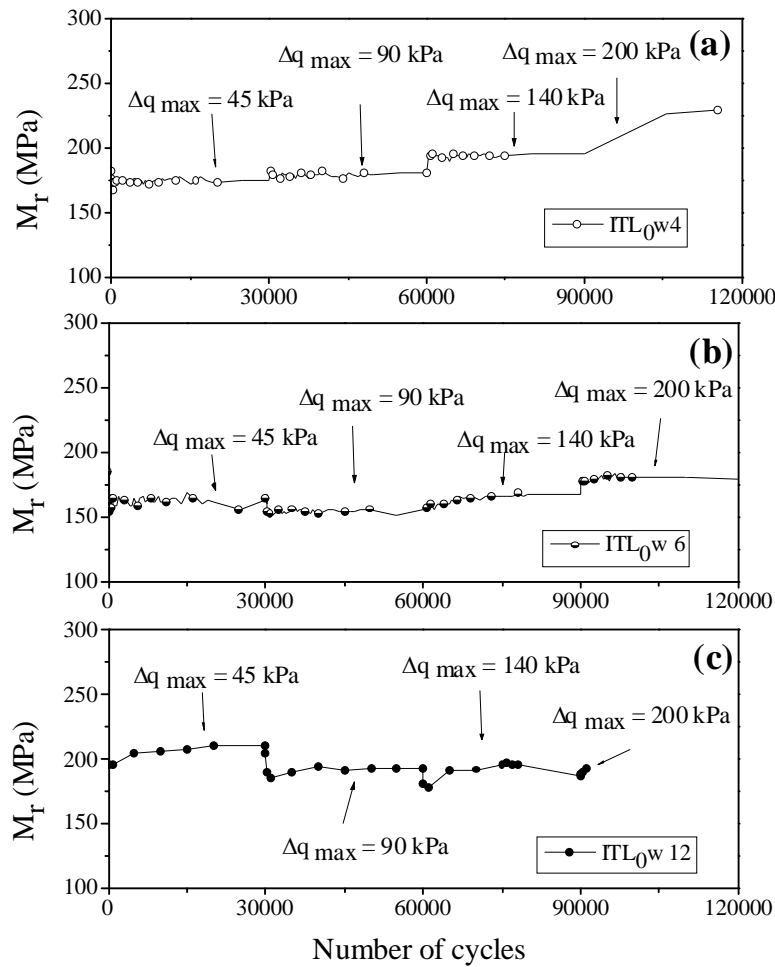
Fig. 7: Resilient modulus versus number of cycles for *ITL_0*. a) *w* = 4%; b) *w* = 6%; c) *w* = 12%

The results of ITL_0 are presented in Fig. 7. The variation of M_r with N is more pronounced in the case of ITL_0w12 (Fig. 7c) than in the cases of ITL_0w4 (Fig. 7a) and ITL_0w6 (Fig. 7b). After the first variations when the deviator stress Δq_{max} changed, the resilient modulus increased with the number of cycles in the case of ITL_0w12, while the changes in the two other cases are not clear.

As regards ITL_{-10}, the results with three different water contents are presented in Fig. 8. In the two cases of $w = 4\%$ and 12%, the resilient modulus did not vary much for the deviator stress up to 90 kPa, suggesting an insignificant influence of the number of cycles. Also, the influence of Δq_{max} is insignificant because albeit the variation of Δq_{max}, the resilient modulus remained at a steady value: about 230 MPa for $ITL_{-10}w12$ and 250 MPa for $ITL_{-10}w4$. In the case of $w = 6\%$ (Fig. 8b), the variation is clearer as the results show a slight increasing trend of M_r with the number of cycles and

Δq_{max}. At the stress level of 140 kPa, there was a sharp decrease of M_r, regardless of the water content: for the three tests, when Δq_{max} was increased from 90 kPa to 140 kPa, a reduction of M_r of about 50 kPa was produced. Afterwards, the variations of resilient modulus with the number of cycles became much more pronounced than in the cases of other deviator stress levels.
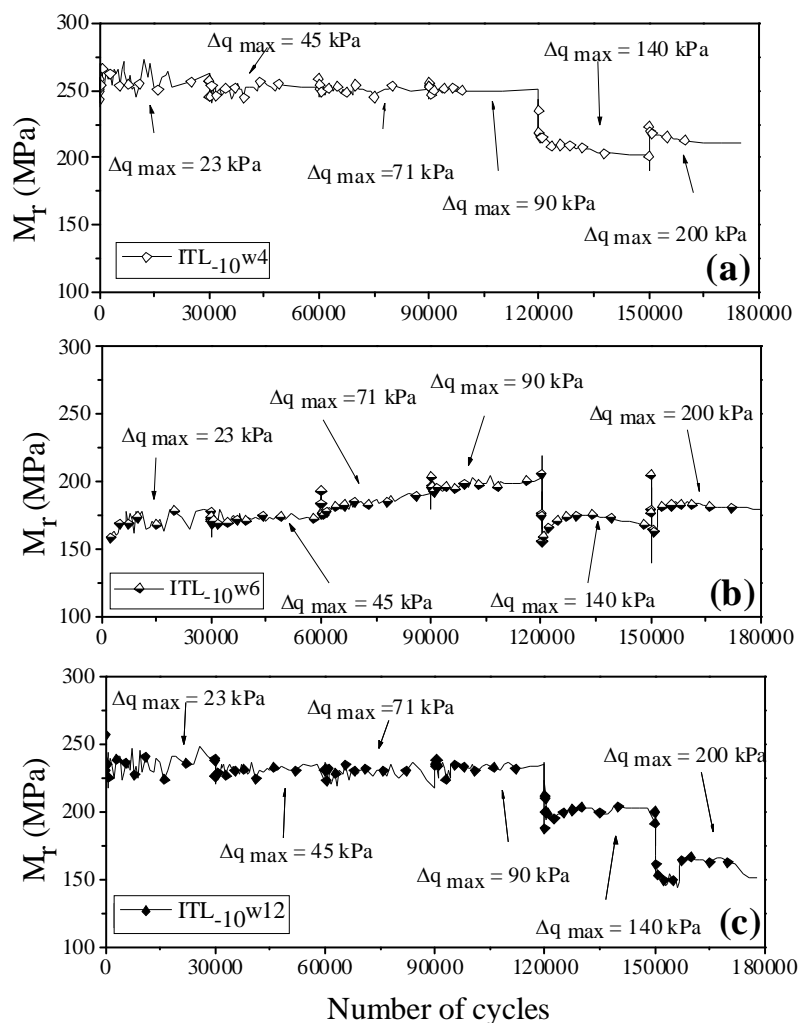
Fig. 8: Resilient modulus versus number of cycles for *ITL$_{-10}$*. a) *w* = 4%; b) *w* = 6%; c) *w* = 12%

Discussions

From the test results, it was observed that after a few scattered results at the beginning of each stress level, the resilient modulus became stable with the number of cycles. However, the variations were different for different soils and different water contents. The variations were clear in the case of *ITL$_{10}$* (Fig. 5b and c), insignificant in the first part of test *ITL$_0$w4* (Fig. 7a) and *ITL$_{-10}$w4* (Fig. 8a). The stabilization value was reached right after the first cycles in test *ITL$_0$w4* (see Fig. 7a) and after 15 000 cycles in test *ITL$_{10}$w6* (see Fig. 5b). Therefore, it can be stated that the number of cycles

needed for M_r to reach stabilization depends on the stress level, water content, and fines content. This can explain the disagreement found in literature regarding the number of cycles required to attain a stable resilient state: Stewart (1982) studied the ballast behavior and reported a stabilization after 1000 cycles while Hicks and Monismith (1971) and Allen and Thompson (1974) (cited by Lekarp et al. 2000 and Lackenby 2006) observed that 50 – 100 cycles are needed for the stabilization for granular materials.

The variations of resilient modulus during the scattered phase at the beginning of each Δq_{max} were observed in all tests. This phase corresponds to the stage where the permanent axial strain developed quickly and the loading/unloading path did not form a close cycle in the deviator stress – axial strain plane. This can be explained as follows: when Δq_{max} was increased, the soil behavior became elasto-plastic; thus irreversible strain was produced. However, this phenomenon occurred during the first loading. Afterwards, the cyclic loading led to a progressive stabilization of the particles arrangement, thereby a negligible plastic strain.

For a better analysis on the effects of deviator stress and water content, the end-level resilient modulus values (after 30 000 cycles for each deviator stress level) are plotted versus deviator stress in Fig. 9. For ITL_{10} (Fig. 9a), the results at 4% and 12 % water contents present a slight decrease of resilient modulus when the deviator stress was increased from 23 to 102 kPa. On the contrary, in the case of 6% water content, the resilient modulus increased and then reached stabilization. The values of 4% and 6% water contents fall in the same range, around 250 MPa and clearly higher than the values of 12% water content. For ITL_0 (Fig. 9b), at 4% and 6% water content, the resilient modulus increased with the deviator stress and the values of 4% are higher than those of 6%. The values of ITL_0 in near saturated state ($w = 12\%$) are, as opposed to the case of ITL_{10}, higher than those of 4% water content. In the case of ITL_{-10} (Fig. 9c), the curves have almost the same shape: a stage of slight variations up to 90 kPa of deviator stress followed by a stage of decrease, the decrease being more pronounced in the case of $ITL_{-10}w12$.
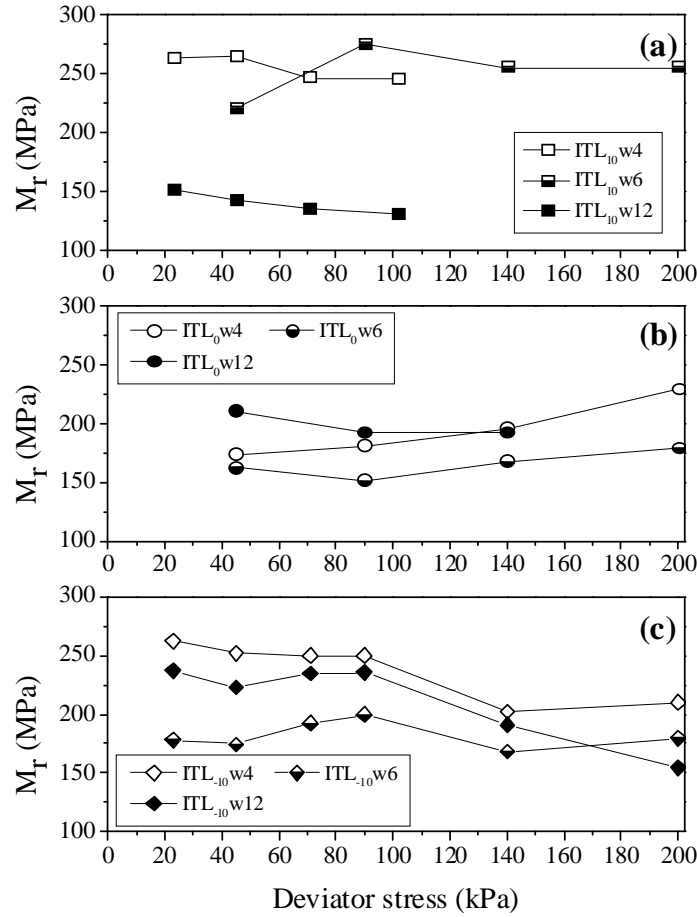
Fig. 9: End-stage resilient modulus versus deviator stress - Effect of water content. a) *ITL$_{10}$*; **b)** *ITL$_0$*; **c)** *ITL$_{-10}$*

In terms of water content effect, the value of *ITL$_{-10}$* at 4% water content is the highest; the values of 12% water content are lower than those of 4% water content but higher than those of 6% water content. The relative positions of these curves show that the water content effect is not the same for the three materials. It appears that the increase of water content brings a negative effect to the resilient modulus of the soil that has the highest fines content (*ITL$_{10}$*). However, for *ITL$_0$* and *ITL$_{-10}$*, the resilient modulus decreased when water content changed from 4% to 6% but increased when water content was increased to 12%. Note that only a decreasing trend of resilient modulus with growing saturation level for granular material was observed by Lekarp (2000). More studies are required to clarify this issue.

For *ITL$_{-10}$*, a deviator stress of 90 kPa appears to be the critical value for the variations of resilient modulus: all tests showed a decrease of resilient modulus at this stress level, suggesting a significant change in soil behavior. As mentioned previously, after a certain number of cycles, the resilient behavior was mainly governed by the contacts of soil particles. When the imposed deviator stress increased, the stress applied at the inter-particles contact exceeds its limit and particle

breakage may occur. As a result, a sharp decrease of M_r is produced. This could be the case for *ITL$_{-10}$* that has the lowest fines content. For *ITL$_0$* and *ITL$_{10}$*, this phenomenon of particle breakage was probably attenuated, leading to much smaller decrease of M_r.

As far as the effect of water content is concerned, the results show that the relative positions of the curves of three different water contents are not the same for the three materials. This suggests that the soil composition can strongly influence the material resilient modulus. Fig. 10 presents the results according to the water content: 4%; 6% and 12% in Fig a, b and c, respectively. The effect of fines content can be observed clearly. In the case of $w = 4\%$, the results of *ITL$_{-10}$* and *ITL$_{10}$* are almost identical for the deviator stress up to 100 kPa. But much lower values are observed for *ITL$_0$* for the deviator stress up to 140 kPa. Beyond 140 kPa deviator stress, the values become almost the same for *ITL$_{-10}$* and *ITL$_0$*. At 6% water content, the resilient modulus of *ITL$_0$* is also the smallest, showing that when decreasing the fines content (from *ITL$_{10}$* to *ITL$_0$*), a reduction of resilient modulus is produced. However, when the fines content is decreased to a level as low as *ITL$_{-10}$*, the resilient modulus starts to increase. Under the near saturation conditions ($w = 12\%$ in Fig. 10c), it is observed that the greater the fines content, the lower the resilient modulus.

To identify the mechanisms of these phenomena, it appears necessary to consider the combined effects of the fines content and the water content which is linked to the soil suction. It is well known that for unsaturated soils, suction contributes to the soils shear strength, especially for the fine-grained soils. This explains why fine particles show a positive effect on the resilient modulus under unsaturated conditions, but a negative effect under saturated conditions. This implies that in unsaturated conditions, due to the suction effect the interlayer soil containing high fines content has a better mechanical performance, while in near saturation conditions, higher fines contents leads to a significant degradation of mechanical performance. This is in agreement with the observations of Huang et al. (2009), Ebrahimi (2011) and Duong et al. (2013b). From a practical point of view, these findings are important for the maintenance of railway tracks. If the soil containing high fines content can satisfy the requirements in terms of resilient modulus under unsaturated conditions, measures must be taken to protect it from water infiltration. Very often, it is a good drainage system that should be set up for this purpose.
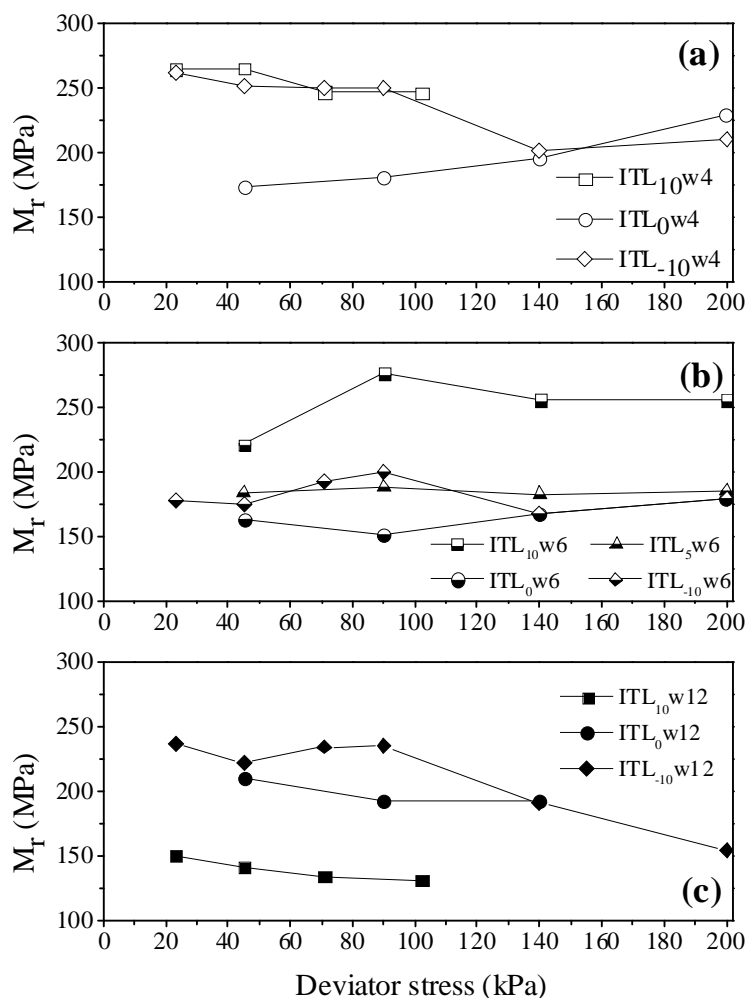
Fig. 10: End-stage resilient modulus versus deviator stress - Effect of fines content. a) *w* = 4%; b) *w* = 6% and c) *w* = 12%

Conclusions

The resilient behavior of an interlayer soil taken in a railway sub-structure in France was studied in the laboratory. The effects of deviator stress level, number of cycles, water content and fine content were investigated by performing large-scale cyclic triaxial tests. Four fines contents and 3 water contents were considered.

At each deviator stress level, after the first scattered results due to the plastic behavior of soil, the resilient modulus tended to stabilize with the number of cycles. It was found that the number of cycles needed to reach stabilization depends on the material nature, water content and stress level.

The effects of water content and of fines content are linked, and it appeared impossible to distinguish the two effects. Indeed, in unsaturated conditions, due to the suction effect, the soil

having high fines content showed higher resilient modulus. On the contrary, when the soil approached the saturated conditions, the fine particles provided a negative effect. This suggests that drainage measures must be taken to protect the interlayer soil when its mechanical performance appears satisfactory under unsaturated conditions but unsatisfactory under saturated conditions.

Acknowledgements

References

ASSHTO. (1993). "Guide for design of pavement structures".

Alias, J. (1984). "La voie ferrée. Techniques de construction et d'entretien." 2nd Ed., Eyrolles (In French).

Allen, J. J., and Thompson, M. R. (1974). "Resilient response of granular materials subjected to time dependent lateral stresses." Transportation Research Record, 510, 1-13.

Basudhar, P. K., Ghosh, P., Dey, A., Valsa, S., and Nainegali, L. S. (2010). "Reinforced earth design of embankment and cuts in railway." Research Designs and Standards Organization, Department of Civil Engineering, Indian Institute of Technology Kanpur.

Cui, Y. J., Duong, T. V., Tang, A. M., Dupla, J., Calon, N., and Robinet, A. (2013). "Investigation of the hydro-mechanical behaviour of fouled ballast." Journal of Zhejiang University- Science A, 14(4), 244-255.

Duong, T. V., Trinh, V. N., Cui, Y. J., Tang, A. M., and Calon, N. (2013a). "Development of a large-scale infiltration column for studying the hydraulic conductivity of unsaturated fouled ballast." Geotechnical Testing Journal, 36(1), 1-10.

Duong, T. V., Tang, A. M., Cui,Y. J., Trinh, V. N., Dupla, J.C., Calon, N., Canou, J., and Robinet, A. (2013b). "Effects of fines and water contents on the mechanical behavior of interlayer soil in ancient railway sub-structure." Soils and Foundations (accepted for publications).

Dupla, J. C., Pedro, L. S., Canou, J., and Dormieux, L. (2007). "Mechanical behaviour of coarse grained soils reference." Bulletin de Liaison des Laboratoires des Ponts et Chaussées, (268-269), 31-58.

Ebrahimi, A. (2011). "Behavior or fouled ballast." Railway Track and Structures, 107(8), 25–31.

Ekblad, J., and Isacsson, U. (2008). "Influence of water and mica content on resilient properties of coarse granular materials." International Journal of Pavement Engineering, 9(3), 215–227.

Ekblad, J. (2007). "Influence of water on coarse granular road materials properties." PhD dissertation, Royal Institute of Technology KTH, Stockholm, Sweden.

Gidel, G., Hornych, P., Chauvin, J. J., Breysse, D., and Denis, A. (2011). "A new approach for investigating the permanent deformation behavior of unbound granular material using the repeated load triaxial apparatus." Bulletin de Liaison des Laboratoires des Ponts et Chaussées, 233, 5-21.

Grabe, P., and Clayton, C. (2009). "Effects of principal stress rotation on permanent deformation in rail track foundations." Journal of Geotechnical and Geoenvironmental Engineering, 135(4), 555–565.

Hicks, R. G., and Monismith, C. L. (1971). "Factors influencing the resilient response of granular materials." Highway Research Record, 345, 15–31.

Huang, H., Tutumluer, E., and Dombrow, W. (2009). "Laboratory characterization of fouled railroad ballast behavior." Journal of the Transportation Research Board, 2117(1), 93–101. http://dx.doi.org/10.3141/2117-12.

Hveem, F. N. (1955). "Pavement deflections and fatigue failures." In Highway research board bulletin, Highway Research Board, 114, 43–87.

Hveem, F. N., and Carmany, R. M. (1948). "The factors underlying the rational design of pavements." In Highway Research Board Proceedings, 28, 101–136.

Jain, V., and Keshav, K. (1999). "Stress distribution in railway formation–a simulated study." Proceeding of the 2nd International Symposium on Pre-Failure Deformation Characteristics of Geomaterials–IS Torino, 653–658.

Jorenby, B. N., and Hicks, R. G. (1986). "Base course contamination limits." Transportation Research Record, 1095, Transportation Research Board, Washington, D.C., 86–101.

Kamal, M. A., Dawson, A. R., Farouki, O. T., Hughes, D. A. B., and Sha'at, A. A. (1993). "Field and laboratory evaluation of the mechanical behaviour of unbound granular materials in pavements." Transportation Research Record, 1406, Transportation Research Board, Washington, D.C., 88–97.

Kim, D., and Kim, J. R. (2007). "Resilient behavior of compacted subgrade soils under the repeated triaxial test." Construction and Building Materials, 21(7), 1470–1479.

Kolisoja, P. (1997). "Resilient Deformation Characteristics of Granular Materials." PhD dissertation, Tampere University of Technology, Finland.

Lackenby, J. (2006). "Triaxial behaviour of ballast and the role of confining pressure under cyclic loading." PhD dissertation, University of Wollongong.

Lekarp, F., Isacsson, U., and Dawson, A. (2000). "State of the art. I: Resilient response of unbound aggregates." Journal of transportation engineering, 126(1), 66–75.

Li, D., and Selig, E. (1998). "Method for railroad track foundation design. I. Development." Journal of Geotechnical and Geoenvironmental Engineering, 124(4), 316–322.

Lim, W. L. (2004). "Mechanics of railway ballast behaviour." PhD dissertation, University of Nottingham.

Radampola, S. (2006). "Evaluation and modelling performance of capping layer in rail track substructure." Thesis dissertation, Central Queensland University.

Selig, E. T., and Waters, J. M. (1994). "Track geotechnology and substructure management." Thomas Telford.

SNCF. (2009). "R2520-2009-01 - Sollicitations mécaniques dans la plate-forme: Mesures d'accélérations verticales dans la plate-forme." Technical report (In French).

Stewart, H. E. (1982). "The prediction of track performance under dynamic traffic loading." PhD Dissertation, University of Massachusetts.

Thom, N. H., and Brown, S. F. (1987). "Effect of moisture on the structural performance of a crushed-limestone road base." Transportation Research Record, 1121, Transportation Research Board, Washington, D.C., 50–56.

Trinh, V. N. (2011). "Comportement hydromécanique des matériaux constitutifs de plateformes ferroviaires anciennes." PhD Dissertation, Ecole Nationales des Ponts et Chaussées - Université Paris – Est, France (In French).

Trinh, V. N., Tang, A. M., Cui, Y. J., Canou, J., Dupla, J., Calon, N., Lambert, L., Robinet, A., and Schoen O. (2011). "Caractérisation des matériaux constitutifs de plate-forme ferroviaire ancienne." Revue Française de Géotechnique, (134-135), 65–74 (In French).

Trinh, V. N., Tang, A. M., Cui, Y. J., Canou, J., Dupla, J., Calon, N., Lambert, L., Robinet, A., and Schoen O. (2012). "Mechanical characterisation of the fouled ballast in ancient railway track sub-structure by large-scale triaxial tests." Soils and Foundations, 52(3), 511-523.

Uthus, L., Hoff, I., and Horvli, I. (2005). "A study on the influence of water and fines on the deformation properties of unbound aggregates." In Proceedings, 7th Internacional Conference on the Bearing Capacity of Roads, Railways and Airfields, Trondheim, Norway.

Uthus, L. (2007). "Deformation Properties of Unbound Granular Aggregate." PhD dissertation, Norwegian University of Science and Technology.

Werkmeister, S. (2003). "Permanent deformation behaviour of unbound granular materials in pavement constructions." Thesis dissertation, Fakultät Bauingenieurweser der Technischen Universität Dresden.

Werkmeister, S., Dawson, A., and Wellner, F. (2004). "Pavement design model for unbound granular materials." Journal of Transportation Engineering, 130(5), 665-674.

Yang, L., Powrie, W., and Priest, J. (2009). "Dynamic stress analysis of a ballasted railway track bed during train passage." Journal of Geotechnical and Geoenvironmental Engineering, 135(5), 680–689.

CHAPTER III

Hydraulic behavior of interlayer soil

This chapter presents the mechanical behavior of interlayer soil under the effects of a number of parameters such as fine particles content, water content, stress and number of cycles. The results showed that the effects of water content and fines content are linked. On one hand, the interlayer was naturally created, and it can present a large variability in terms of fine contents. On the other hand, it is well known that the mechanical properties of fine particles and thus the interlayer, vary with changes in water content. In order to avoid any negative effect due to the increase of water content, the interlayer must be protected and the good drainage must be ensured. Because the water content change is governed by the hydraulic properties of soil, it appears important to investigate the hydraulic behavior of interlayer soil.

To this end, the hydraulic tests were performed using two infiltration columns: a large-scale one (H = 600 mm, D = 300 mm) and a small-scale one (H = 200 mm and D = 50 mm). The hydraulic behavior of interlayer soil and the effect of fine particles contents were studied through 2 comparisons: between interlayer soils with different fines contents and between an interlayer soil and its fines fraction (< 2 mm). Drying/wetting cycles were also applied. The results of the water retention curves and the hydraulic conductivities were analyzed.

This chapter consists of two papers. The first paper, published in ***Geotechnical Testing Journal***, presents the development of the large-scale infiltration column and the hydraulic behavior of natural interlayer soil from the site of Sénissiat. The second paper, under the second review in ***Canadian Geotechnical Journal***, depicts the effect of fine particles on the hydraulic behavior of interlayer soils.

Development of a Large-Scale Infiltration Column for Studying the Hydraulic Conductivity of Unsaturated Fouled Ballast

Trong Vinh Duong[1], Viet Nam Trinh[1], Yu-Jun Cui[1], Anh Minh Tang[1], Nicolas Calon[2]

Abstract: In order to study the hydraulic behavior of fouled ballast, an infiltration column of 600 mm high and 300 mm in diameter was developed. Five TDR sensors and five tensiometers were installed at various levels, allowing the measurement of volumetric water content and matric suction, respectively. The material studied was fouled ballast that was formed in the railway track-bed by penetration of fine-grained soil into the ballast. This material is characterized by a high contrast of size between the largest and the smallest particles. During the test, three stages were followed: saturation, drainage, and evaporation. Based on the test results, the water retention curve and the unsaturated hydraulic conductivity were determined. The quality of the results shows the capacity of this large-scale infiltration column in studying the unsaturated hydraulic properties of such fouled ballast.

Keywords: Infiltration column; fouled ballast; TDR; tensiometer; water retention curve; hydraulic conductivity.

Introduction

Coarse elements like ballast particles and fine-grained soils co-exist in many geotechnical problems, for instance, in road pavement or railway structures. This is particularly the case for the old railway structures which were initially built by direct emplacement of ballast on sub-soil without separation layer as for the new high-speed lines. After several years of rail traffic, a new layer was developed through the penetration of fine grain soil into the ballast. Sources of fine particles can be train-borne materials (coal, grain, etc), windborne sediments, pumping of subgrade soils, or ballast particle crushing under repeated loading. The phenomenon of filling voids in the ballast layer by fine particles is commonly termed as fouling (Selig and Waters 1994; Indraratna et al. 2011*a*). Indraratna et al. (2011*b*) indicated that highly fouled ballast loses its functions related to water drainage: the permeability of fouled ballast lower than 10^{-4} m/s is considered unacceptable following Selig and Waters (1994). Robinet (2008) investigated the French railway network and observed that 92% of stability problems have been related to insufficient drainage of the platforms. This shows the importance of a good understanding of the hydraulic behavior of soils involved in the platforms, especially fouled ballast.

---

[1] Ecole des Ponts Paris Tech (ENPC), Laboratoire Navier/CERMES
[2] French Railway Company (SNCF)

Up to now, there has been quite limited knowledge on the hydro-mechanical behavior of these kinds of soils, even though it is well recognized that these soils can play an important role in the overall behavior of railway platforms. This is probably due to the difficulty of experimentally working on these coarse-grained soils: common experimental devices for soils can no longer be used and large scale columns are needed. The difficulties are obviously much higher when these soils are unsaturated and their densities are high.

The hydraulic conductivity of saturated soils is mainly a function of their void ratio, while the hydraulic conductivity of unsaturated soils is not only dependent on the void ratio, but also the degree of saturation (or volumetric water content). Nowadays, there are various methods in the literature allowing the determination of unsaturated hydraulic conductivity. Tarantino et al. (2008) described several field techniques to measure suction, volumetric water content and hydraulic conductivity. In the laboratory condition, according to Masrouri et al. (2008), the hydraulic conductivity of an unsaturated soil can be determined using either direct or indirect techniques, based on Darcy's law. According to the flow mode, direct techniques can be divided into steady and unsteady state methods. In the steady state methods, a constant flow rate is needed under a specified average water pressure head. The steady state methods may be costly, tedious and lengthy for low permeability materials. The unsteady state methods are usually divided into two groups: outflow-inflow methods and instantaneous profile methods. In the first group, it is assumed that during the flow process, the hydraulic conductivity is constant and the relationship between water content and matrix suction is linear. The instantaneous profile methods consist of inducing transient flow in a soil specimen and monitoring the water content and suction profiles changes (Wind 1966; Daniel 1982; Delage and Cui 2001; Cui et al. 2008; Ye et al. 2009). When applying this method, very often, only the suction profile is monitored and the water content profile is obtained indirectly based on the water retention curve that is determined separately. Peters et al. (2011) used a fused quartz (transparent soil) with digital image analysis to monitor the degree of saturation during the test, but this method is not suitable for the fouled ballast studied.

Infiltration column is usually used to determine the unsaturated hydraulic conductivity of soils following the instantaneous profile method. In most cases, fine-grained soils are studied and the infiltration columns used were of small diameter: for instance, 150 mm by Bruckler et al. (2002), 103 mm by Chapuis et al. (2006). Some authors presented larger infiltration columns allowing embedding volumetric water content sensors in addition to suction sensors (Nützmann et al., 1998; Stormont and Anderson, 1999; Choo and Yanful, 2000; Yang et al., 2004; McCartney and

Zornberg, 2007; McCartney and Zornberg, 2010). In spite of their larger size (diameter around 200 mm), the columns mentioned above are not adapted to coarse-grained soils or fine-coarse grained soil mixtures where the dimension of the largest particles can reach 60 mm. For these soils, larger infiltration columns are needed. In this regard, Trani and Indraratna (2010) developed a percolation column of 240 mm in diameter and 150 mm in height to investigate the hydraulic behavior of saturated sub-ballast under cyclic loading. The use of large-sized specimens is also specified in the French standard AFNOR (2004): the diameter (D) of the soil specimen for triaxial tests must exceed 5 times the maximum diameter (d_{max}) of soil grains. This size ratio was more or less respected in various works found in literature: Yasuda et al. (1997) conducted triaxial tests with a D/d_{max} equal to 4.7 (D = 300 mm). A ratio of 5.7 was adopted by Lackenby et al. (2007) in their tests on soil specimen of 300 mm in diameter. The same ratio of 5.7 was adopted by Ekblad (2008) with a specimen diameter D equal to 500 mm. It is obvious that the development of such large columns represents a big challenge because of the technically related difficulties. Note that Tang et al. (2009) developed an infiltration tank of rectangular section (800 mm x 1000 mm) with simultaneous suction and volumetric water content monitoring for testing compacted expansive soil. The large size allowed the free swell of soil during wetting but the volumetric sensors used (Thetaprobe) are not suited to the fine-coarse-grained soil mixtures because of the limited dimension of these sensors.

In order to investigate the hydraulic conductivity of fouled ballast in both saturated and unsaturated states, a large-sized infiltration column (300 mm in diameter and 600 mm in height) was developed. This column was equipped with both tensiometers and TDRs allowing the simultaneous monitoring of suction and volumetric water content. Note that the water retention curve can be obtained directly from the measurements, and direct application of the simultaneous method can be done for the determination of the hydraulic conductivity of unsaturated fouled ballast.

Materials

The fouled ballast studied was taken from the sub-structure of an ancient railway at Sénissiat (North West of Lyon, France) that was constructed in the 1800s. This fouled ballast mainly composed of ballast and sub-soil during the degradation of the railway structures. The sub-soil was also taken at this site. Identification tests were performed in the laboratory on these materials. The results show that the sub-soil is high-plasticity silt with a liquid limit $w_L = 57.8\%$ and a plasticity index $I_p = 24.1$. The fraction of particles smaller than 80 µm is 98% and that of particles smaller than 2 µm is 50%. The fouled ballast contains 3% to 10% of stones (50-63 mm), 42% to 48% of ballast (25-50 mm),

36 to 42% of micro-ballast, sand, degraded ballast (0.08 to 25 mm), and 16% fines (< 80 µm). It represents a mixture of fine-coarse-grained soils. Figure 1 shows the grain size distribution curves of both the sub-soil and fouled ballast.
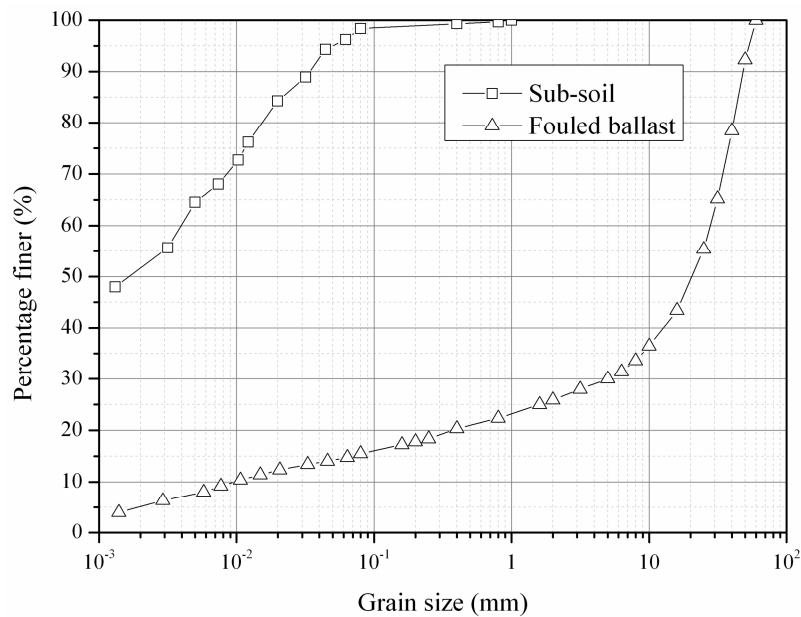

Figure 1: Grain size distributions of fouled ballast and sub-soil from the Sénissiat site

The density of particles smaller than 2 mm was determined by the pycnometer method (AFNOR 1991) and a value of $\rho_s = 2.67$ Mg/m^3 was found. The density of particles larger than 2 mm and those greater than 20 mm was determined using the same method but with a device of larger size (AFNOR 2001): $\rho_s = 2.68$ Mg/m^3 for both sizes. More details about this fouled ballast can be found in Trinh et al. (2011). The mechanical behavior of this fouled ballast under cyclic loading was investigated by Trinh et al. (2012).

Experimental setup

Figure 2 shows the infiltration column developed to study the hydraulic behavior of the fouled ballast. It has an internal diameter of 300 mm, a wall thickness of 10 mm and a height of 600 mm. The column is equipped with five volumetric water content sensors (TDR1 to TDR5) and five matric suction sensors (T1 to T5) disposed at equal distance along the column (h = 100, 200, 300, 400 and 500 mm). On the top, a hole of 50 mm in diameter was drilled allowing installation of a sensor of suction if needed. A second hole in the center allows water drainage or air expulsion. Two valves are installed at the bottom, allowing water injection after expulsion of air in the ducts. Two porous stones are placed for the two valves to avoid any clogging of ducts by soil particles.

Geotextiles are placed on the top and at the bottom of the soil specimen. O-rings are used to ensure the waterproofness. A Mariotte bottle is used for water injection. As the area occupied by the sensors is just 6.8% of the total apparatus section area, the sensors installation is expected to not affect the water transfer inside the soil column.

Figure 2: Schematic view of the infiltration column
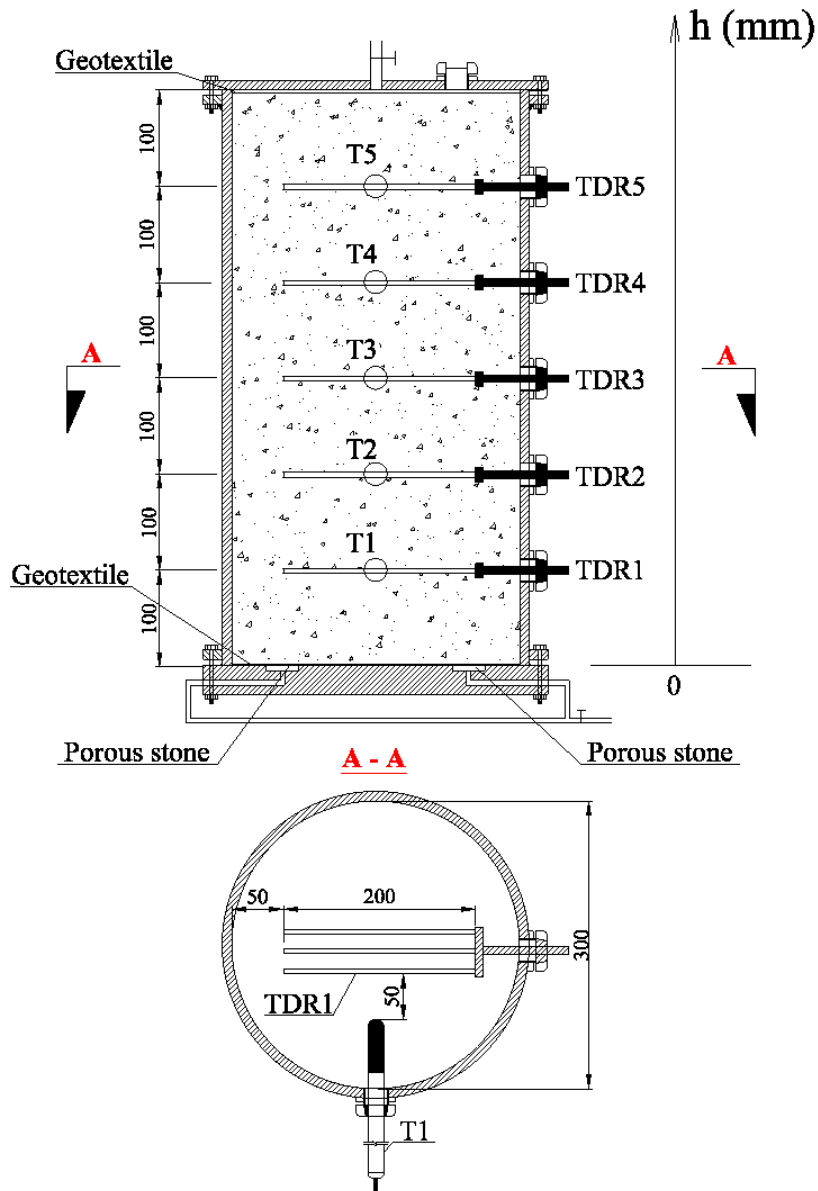
The TDR probes used are of waveguides buried (GOE) type, with 3 rods of 3.2 mm diameter and 200 mm length. According to Soilmoisture (2000), the influence zone of this TDR is 20-30 mm around the rods. The accuracy of the TDR probes is ± 2% of the measured values following the provider. The equipments used (TDR probe and Trase BE) can automatically provide the dielectric

constant K_a (which is deduced from the crossing time of electric wave within the surrounding material). Based on the calibration curve (relationship between the dielectric constant and volumetric water content) provided by the producer, the volumetric water content can be then determined. It is thereby an indirect measurement method. Several authors have shown that the calibration curve depends on the texture, density, mineralogical composition, fines content and particle size of the test material (Jacobsen and Schjønning 1993; Stolte et al. 1994; Côté and Roy 1998; Hanson and Peters 2000; Gong et al. 2003; Schneider and Fratta 2009; Ekblad and Isacsson 2007). It is therefore necessary to determine the specific calibration curve for each soil studied. Soil matric suction was measured by T8 tensiometer (UMS 2008). The working pressure range of those tensiometers is from 100 kPa to -80 kPa (they measure both positive pressure and suction), with an accuracy of ± 0.5 kPa.

Experimental procedure

The soil studied was firstly dried in an oven at 50°C for 24 h. Water was then added using a large mixer to reach the target water content. After mixing, the wet material was stored in hermetic containers for at least 24 h for moisture homogenization.

The soil specimen was then prepared by compaction in six layers of 0.10 m each in the infiltration column using a vibrating hammer. The density of each layer was controlled by fixing the soil weight and the layer height. Before compaction of the subsequent layer, a TDR probe and a metal rod of 25 mm diameter were placed on the compacted layer. Once the soil specimen was prepared, the metal rods were removed to install the tensiometers. This protocol was adopted because the tensiometers are fragile and they can't stand the compaction force without being damaged. Considering the influence zone of TDR probes, the distance between the tips of tensiometers and TDR probes was set greater than 40 mm. In order to ensure the good contact between tensiometers and soil, a paste made of sub-soil was injected in the holes before introducing the tensiometers.

The test was carried out in 3 stages: saturation, drainage and evaporation. The specimen was saturated by injecting water from the bottom. Water was observed at the outlet in less than one hour, and the soil specimen was considered saturated after one day of water flow. Saturated hydraulic conductivity was measured by applying a constant hydraulic head of 0.45 m, using the Mariotte bottle. After completion of the saturation, tensiometers were installed on the column. Note that these sensors were not installed before the saturation stage in order to avoid any cavitations due to possible high suctions in the compacted material. After the installation of tensiometer, the soil

column was re-saturated again because the soil was de-saturated when installing the tensiometers. After the saturation stage, water was allowed to flow out through the two bottom valves. After two days, when there was no more water outgoing, it was considered that the drainage stage was completed. The top cover of the column was then removed to allow evaporation. The two bottom valves were closed during this stage. The air conditions in the laboratory during this stage were: a temperature of 22°C and a relative humidity of 50±5%. The evaporation ended after about 160 h when the value given by the tensiometer T5 (h = 500mm) was -50 to -60 kPa.

Calibration of the TDR was performed within the same soil specimen. After re-saturating the soil inside the column, drainage was performed step-by-step. The drainage valve was opened to let 300 mL of water drained, and then closed again until reaching the equilibrium of the TDR measurement inside the column. This drainage was then repeated 10 times until the full drainage of pore-water inside the soil specimen. For each step, as the TDR measurement reached the equilibrium, hydrostatic water pressure distribution can be expected and the water content can then be estimated for each level of soil column based on the quantity of water drained. These values of water content were then plotted versus the value of K_a given by the TDR in order to determine the calibration curve (Figure 3). The following equation can be then used for the calibration curve of the TDR:

$$\theta_{cal} = 0.0221 \times K^2{}_a + 0.5118 \times K_a - 3.0677$$
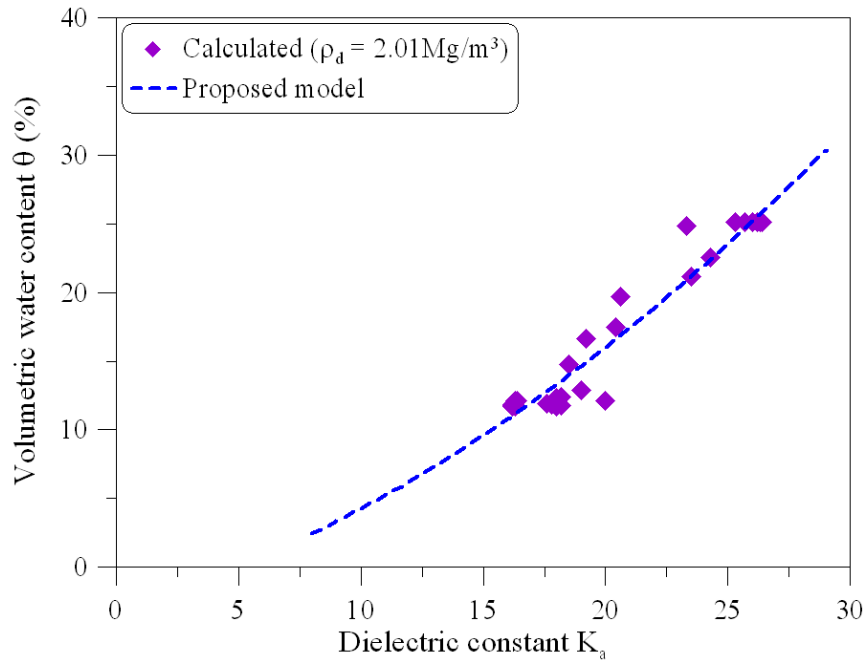
(1)

Figure 3: TDR calibration curve

Experimental results

The soil was compacted in the infiltration column at a density of 2.01 Mg/m^3 (a porosity of 0.25) and a gravimetric water content of 5.5 %, corresponding to a volumetric water content of 10%. Figure 4 shows the measured volumetric water content by TDR probes after compaction (initial state). These values are respectively 4.8, 6.0, 9.7, 8.8 and 10.1% for TDR1 to TDR5. At t = 80 h, water was injected from the base of the column to saturate the soil. It can be observed that the measured volumetric water content by TDR probes increased quickly and reached a maximum value in less than one hour. The maximum values were 23.4, 23.7, 24.4, 22.4 and 25.0% for TDR5 to TDR1, respectively. Note that at a dry density of 2.01 Mg/m^3, the volumetric water content in saturated state was 25.0%. These values corresponded to a degree of saturation of 93.6, 94.8, 97.6, 89.6 and 100%, respectively, indicating that the specimen was close to the saturated state.

The volume of water injected during the saturation stage is shown in Figure 5. In the beginning, the volume of water increased quickly and the rate decreased with time. Note that after t = 50 min, water was observed on the surface of the specimen.
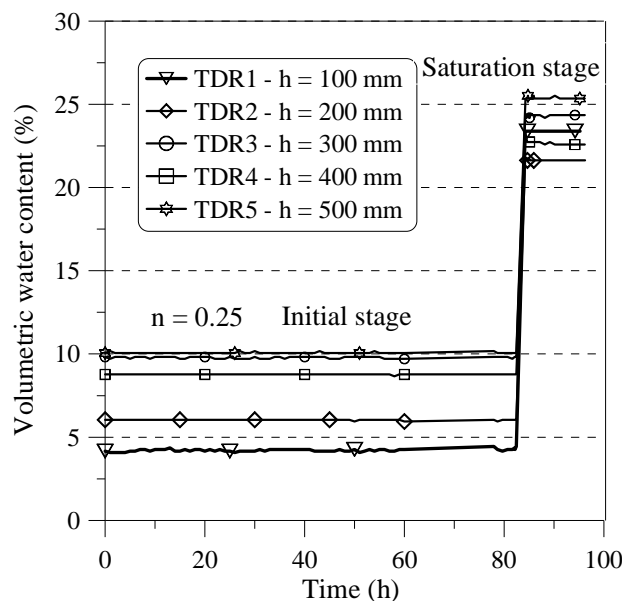
Figure 4: Volumetric water content – in the initial stage and in the saturation stage

The volume of water injected for that time was 4.000×10^{-3} m^3, while that required to saturate the specimen was 5.795×10^{-3} m^3 (calculated from the density and the initial water content of the specimen). The average degree of saturation at this time was then about 70%. From t = 50 min, the relationship between volume of water and time was almost linear. Two tests for measuring

79

hydraulic conductivity at saturated state were performed, 1 day and 3 days respectively after the saturation stage; this delay allowed improving the saturation of the soil. Figure 5 shows that the water volume rates of the two tests are similar. The average value of the hydraulic conductivity estimated is 1.75×10^{-5} m/s.
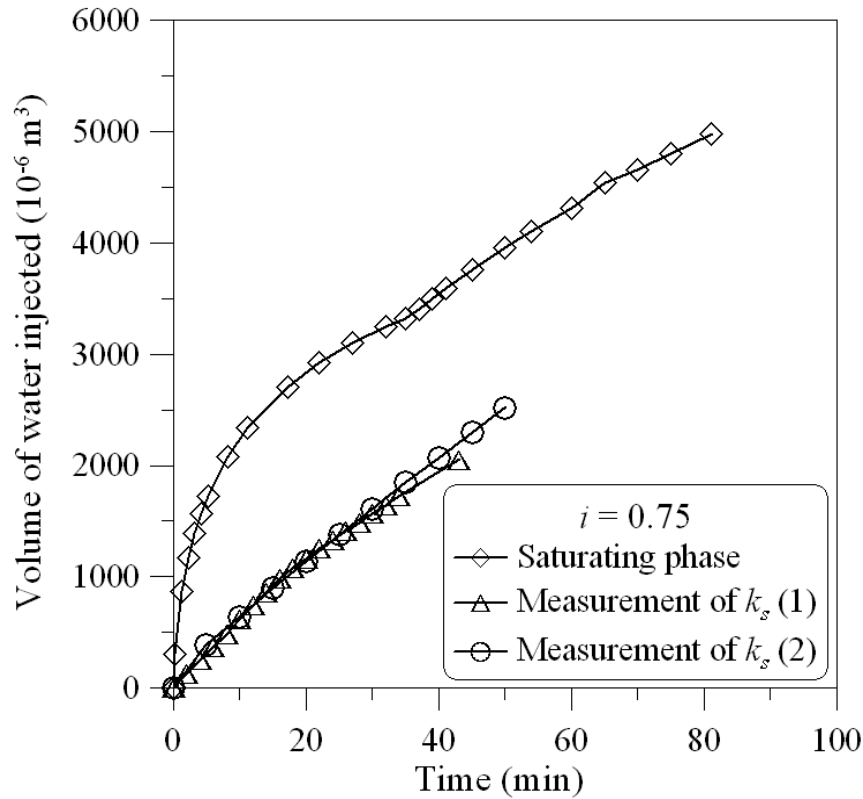
Figure 5: Water volume injected during saturation and hydraulic conductivity measurements

When the specimen was re-saturated, the level of the water surface was maintained at 10 mm above the surface of the specimen. The water pressure values of T1 to T5 were respectively 5.1, 4.1, 3.1, 2.1 and 1.2 kPa (Figure 6a) corresponding to water levels of 510, 410, 310, 210 and 120 mm, respectively. This was consistent with the positions of the tensiometers. In the drainage stage, the water pressure decreased. The values became negative five minutes after opening the valves. Then, the changes followed a constant rate for each tensiometer. All tensiometers except T2 (h = 200mm) indicated a lower pressure (higher suction) at a greater elevation (closer position to the evaporation surface).

With the same time reference, Figure 6b shows the responses of the five TDR sensors. The responses in volumetric water content were similar to that in water pressure, i.e., the volumetric

water content decreased quickly from the maximum value in 10 min. At t = 90 min, the measured volumetric water content ranged from 15 to 17% except that by TDR2 (12%).
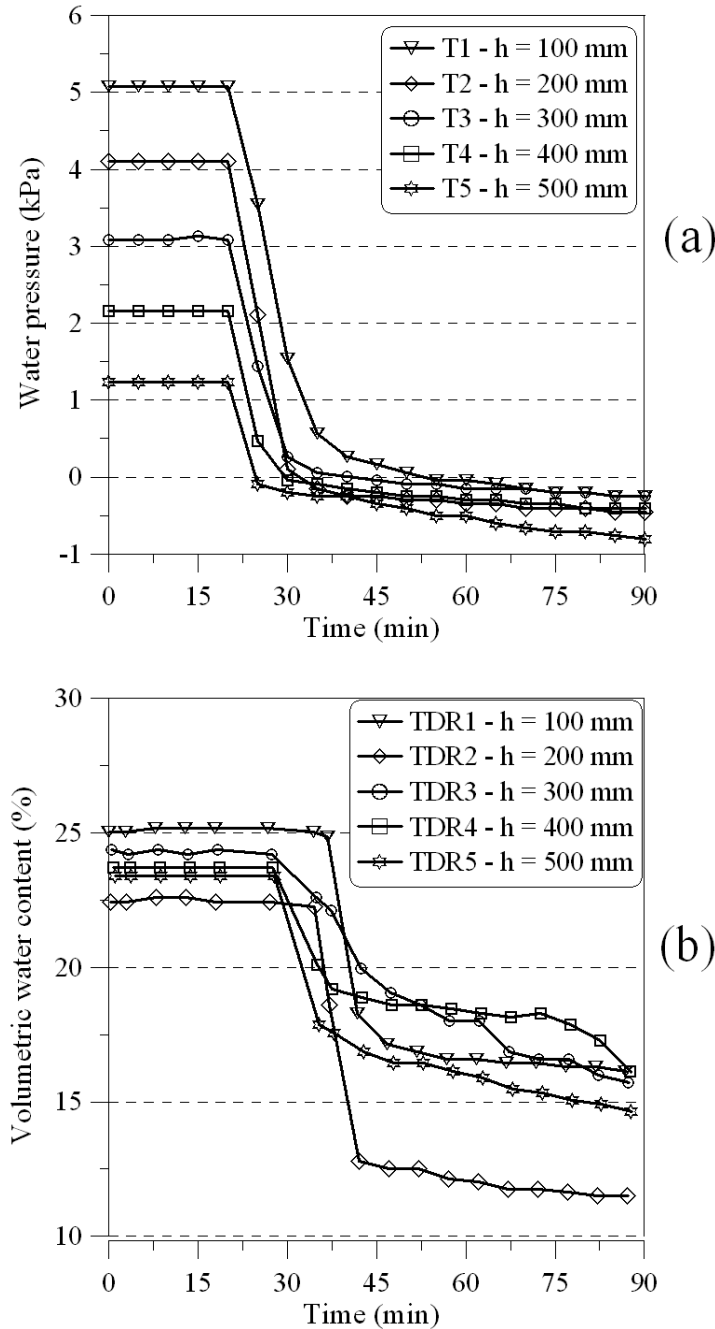
Figure 6: Water pressure (a) and volumetric water content (b) evolution from 0 to 90 min – drainage stage

The drainage stage was maintained for 54 h and the water pressure responses are shown in Figure 7a. The drainage stage stopped when no more water outflow was observed from the bottom valves (t = 54 h). The measured pressures were -2.0, -1.9, -1.6, -1.8 and -2.7 kPa for tensiometers T1 to T5, respectively. Figure 7b shows the responses of the five TDR probes. At the end of the drainage stage (t = 54 h), the volumetric water contents were 11.7, 7.9, 11.8, 10.8 and 10.9% for TDR1 to

81

TDR5, respectively. It can be seen that both the water pressure and volumetric water content did not reach equilibrium.
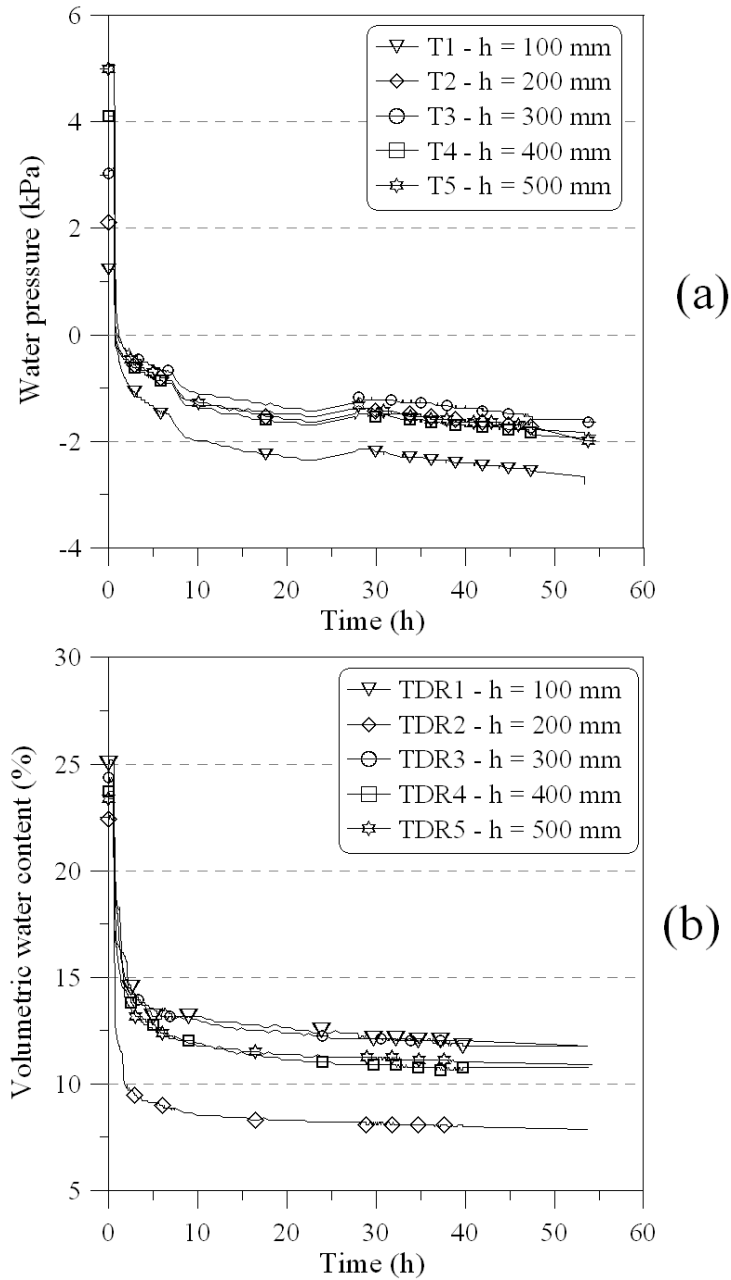
Figure 7: Water pressure (a) and volumetric water content (b) evolution – drainage stage

After the drainage stage, the bottom valves were closed, and evaporation was allowed from the top side for 160 h. Figure 8a shows the water pressure changes. The tensiometer close to the surface (T5) shows that the pressure decreased quickly from -2.7 kPa to -61.2 kPa after 160 h of evaporation, while those of other levels decreased much more slowly. The value at h = 100 mm remained almost unchanged, around -2.0 kPa.

The values of water content are shown in Figure 8b. Due to a technical problem, data are only available for t = 0 - 120 h. The same trends as for water pressure changes can be observed: the closer the tensiometer to the evaporation surface, the larger the volumetric water content changes. The value at h = 500 mm (the closest tensiometer to the evaporation surface) decreased from 11% to 7% after 120 h, while those at h = 100 mm and 200 mm remained almost constant.
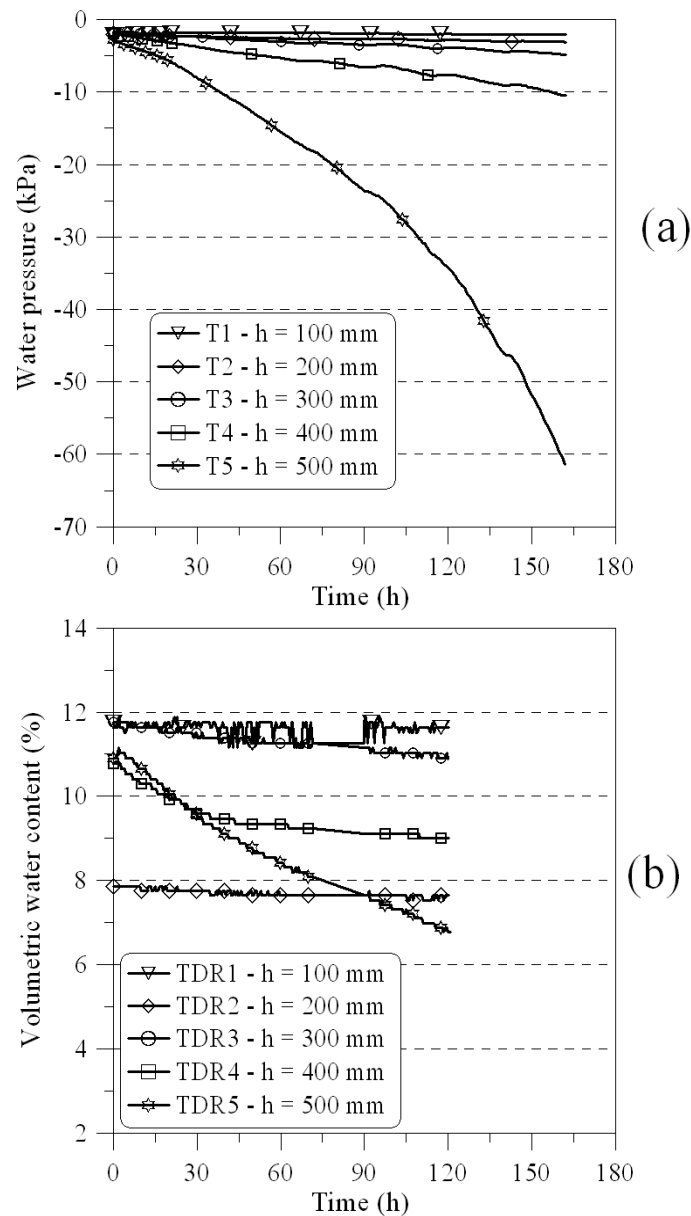

Figure 8: Water pressure (a) and volumetric water content (b) evolution – evaporation stage

Determination of the hydraulic properties in unsaturated state

As mentioned before, unlike the common infiltration column with only suction profile monitoring (Daniel 1982; Cui et al. 2008; Ye et al. 2009) or only water content monitoring, the column

developed in this study is equipped with both tensiometers and TDR sensors, allowing simultaneous measurements of suction and volumetric water content at different levels. The simultaneous profile method can be then directly applied without using the water retention curve. Before determining the unsaturated hydraulic conductivity of the soil, as one of the important hydraulic properties, the water retention curve (WRC) was determined based on the measurements of suction and volumetric water content during the test. In Figure 9 the measured volumetric water content is plotted versus the measured suction for each level. Except the data at h = 200 mm, the water retention curves obtained for various depth were similar. The best fit curves obtained from the models of van Genuchten (van Genuchten 1980) and Brooks-Corey (Brooks and Corey 1964; Stankovich and Lockington 1995) are also shown. The models formula and parameters are presented in Table 1.
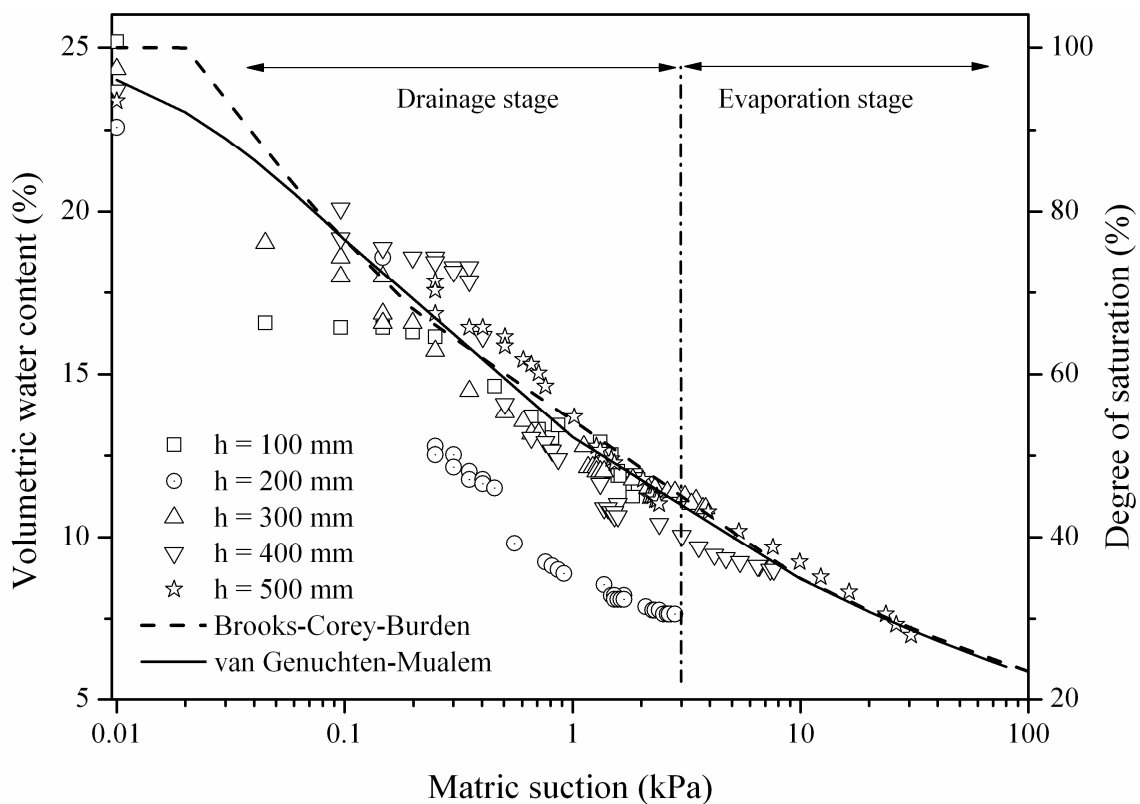
Figure 9: Measured water retention curves along with van Genuchten and Brooks-Corey water retention functions fitted to independent data

Figure 10a shows the values of suction isochrones obtained during the evaporation stage. At the beginning (t = 0), suction in the soil was similar and quite low (lower than 2 kPa), then it increased at different rates depending on the position. The closer the tensiometer to the evaporation surface the faster the suction changes. These suction isochrones were used to determine the slope of the total hydraulic head which was in turn used to calculate the hydraulic gradient ($i = \partial h/\partial z$). The

measured volumetric water content isochrones are shown in Figure 10b. The isochrones of calculated volumetric water content from the suction measured using van Genuchten's equation (Table 1) are shown in Figure 10c, together with the water content profile at the end of the saturation stage. A general decrease during the evaporation is observed: the curves are shifting leftwards especially for the upper part close to the evaporation surface.

Table 1: Model formula and parameters

(θ: volumetric water content, θ_r: residual volumetric water content; θ_s: volumetric water content at saturated state; k: hydraulic conductivity; k_s: hydraulic conductivity at saturated state; ψ: suction in kPa; ψ_a: air entry value; α, n, m, and λ are constants).

Model	Formula	Parameters for water retention curve	Parameters for hydraulic conductivity
van Genuchten	$\theta = \theta_r + \dfrac{\theta_s - \theta_r}{\left[1 + (\alpha\psi)^n\right]^m}$ $k = k_s \Theta^2 \left[1 - \left(1 - \Theta^{1/m}\right)^m\right]$ $with : \Theta = \dfrac{\theta - \theta_r}{\theta_s - \theta_r}$	$\theta_s = 25.0\%$ $\theta_r = 0\%$ $\alpha = 0.4\ \text{kPa}^{-1}$ $n = 1.17$ $m = 0.15$	$\theta_s = 25.0\ \%$ $\theta_r = 0\ \%$ $m = 0.2$
Brooks-Corey	$\theta = \theta_s \quad\quad if\ \psi < \psi_a$ $\theta = \theta_s \left(\dfrac{\psi_a}{\psi}\right)^\lambda \ if\ \psi \geq \psi_a$ $k = k_s \left(\dfrac{\psi_a}{\psi}\right)^{2+3\lambda}$	$\theta_s = 25.0\%$ $\psi_a = 0.02\ \text{kPa}$ $\lambda = 0.17$	$\psi_a = 0.1\ \text{kPa}$ $\lambda = 0.01$

McCartney et al. (2007) observed that small variations of suction or volumetric water content in experimental data can result in significant error in hydraulic conductivity. In the present study, the calculation of unsaturated hydraulic conductivity was performed using both the measured water content data (Figure 10b) and the calculated results (Figure 10c), together with the suction profiles (Figure 10a) of the evaporation state. The volume of water passing through a given height for two different times was determined based on the isochrones of volumetric water content. This volume was used to determine the flow rate q. The hydraulic conductivity was calculated using Darcy's law. In the calculation of water volume, three different heights (h = 400, 450 and 500mm) were considered. This calculation was relatively easy with the volumetric profiles shown in Figure 10c,

but a little difficult for that shown in Figure 10*b* when considering the height lower than $h = 300$ mm. Indeed, Figure 10*b* shows that negative values can be obtained when determining the water volume passing through the height h = 300 mm. This is mainly because of the little changes in this zone and the accuracy of the measurements. In the calculation, the non physical negative values were not considered for the determination of hydraulic conductivity.
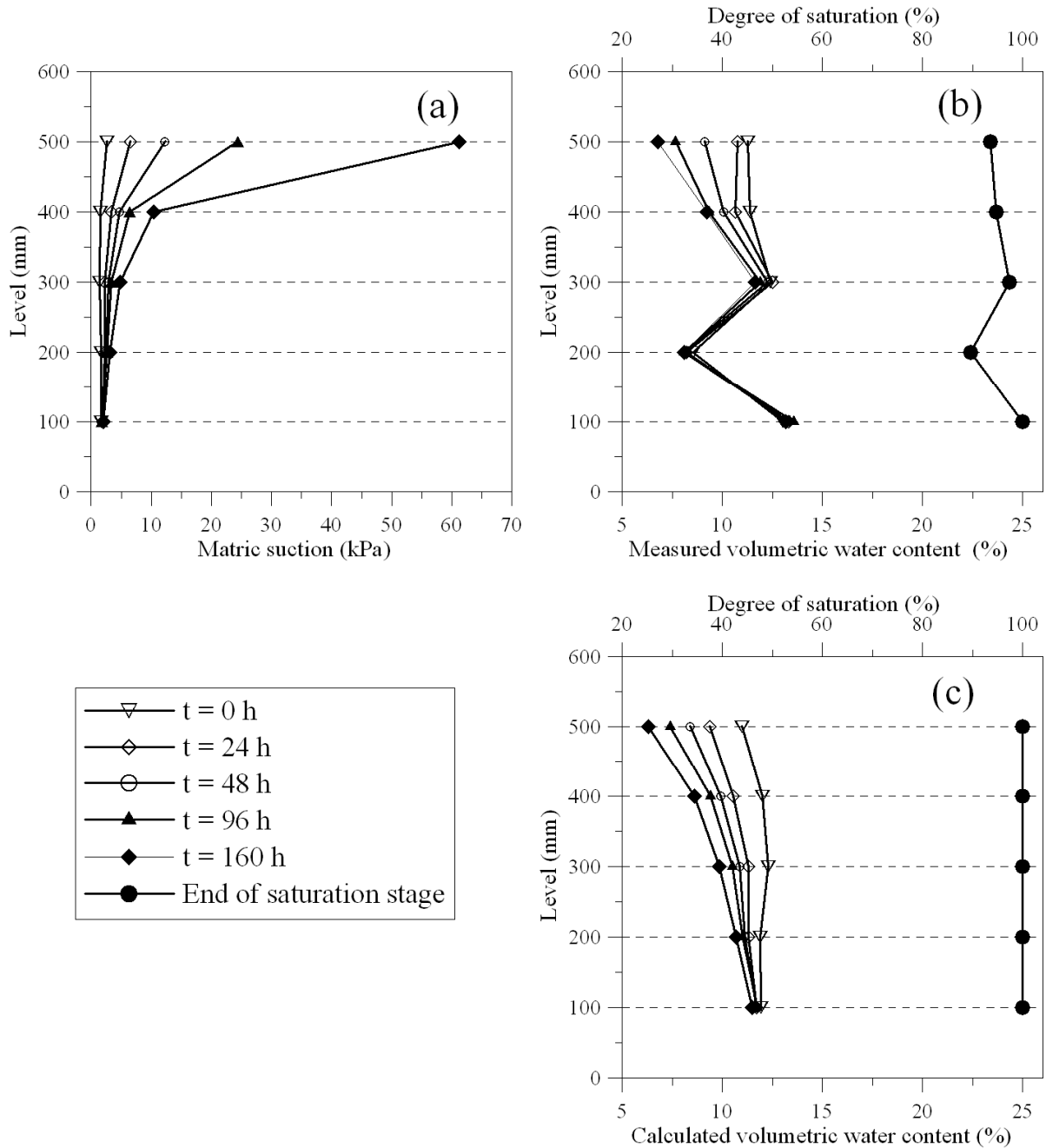
Figure 10: Evolution of profiles. (a) suction; (b) measured volumetric water content; (c) volumetric water content by van Genuchten's model

Figure 11 shows the relationship between the hydraulic conductivity of soil at a dry density ρ_d = 2.01 Mg/m^3 and suction, obtained using both Figure 10*b* and Figure 10*c*. It can be observed that the two types of volumetric water content profiles gave similar results. A general decrease with increasing suction is observed for the hydraulic conductivity. In this figure the value obtained during the saturation stage is also shown. From the saturated state to an unsaturated state at a suction of 65 kPa, the hydraulic conductivity decreased from 1.75×10^{-5} m/s to 2×10^{-10} m/s.
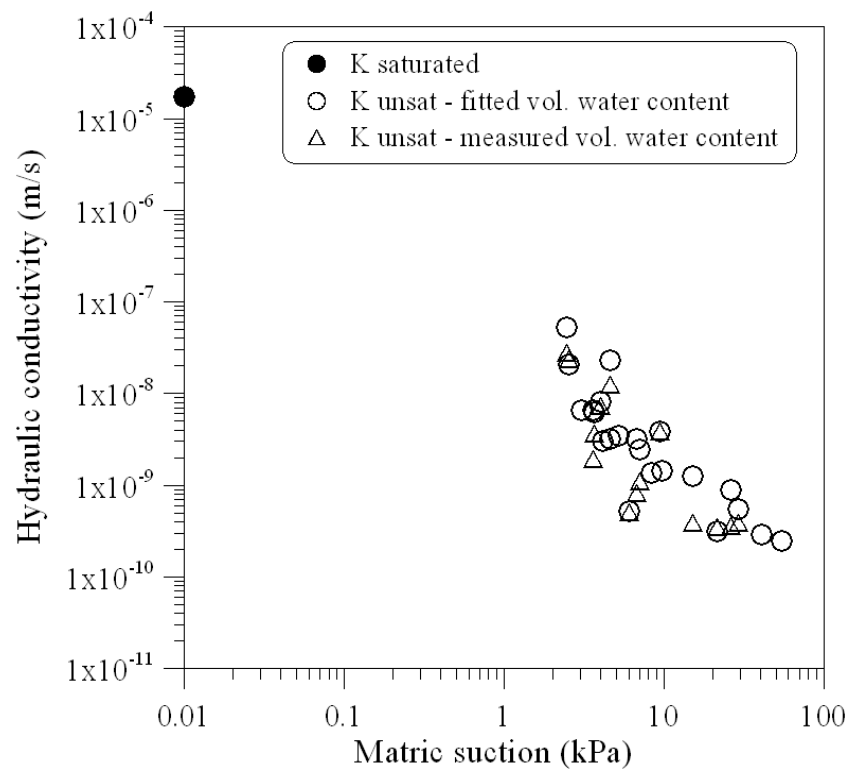
Figure 11: Unsaturated hydraulic conductivity versus suction

Figure 12*a* shows the comparison between the determined hydraulic conductivity and the values calculated from the van Genuchten's model and Brooks-Corey's model. Note that the same parameters as for the water retention curve were used when applying these two models. A general lower hydraulic conductivity was given by the models, especially by the van Genuchten's model. A better agreement between the determined and calculated values (Figure 12*b*) can be obtained using the models parameters in Table 1. Similar observation was made by Parks et al (2012): the van Genuchten's model, within parameters obtained when fitting the water retention curve, does not provide an adequate prediction of the experimental hydraulic conductivity functions of unsaturated soils in general.
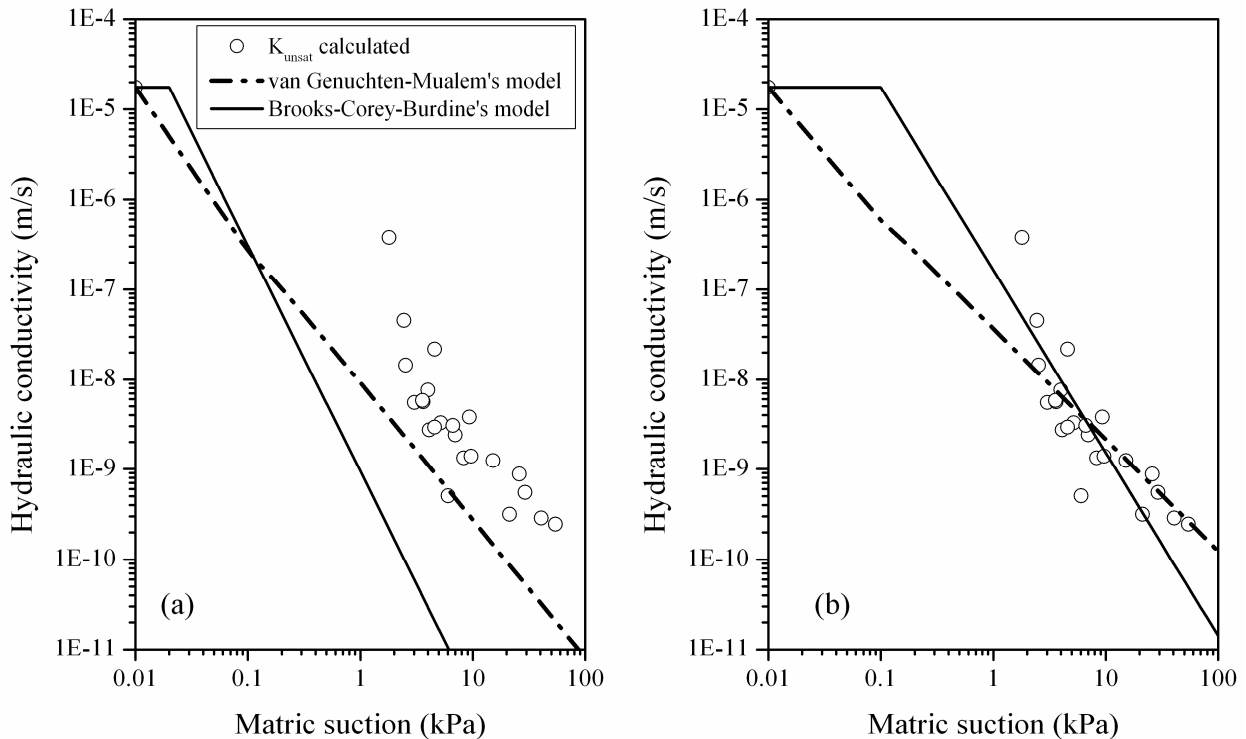
Figure 12: Comparison between calculated hydraulic conductivity values with those predicted by the van Genuchten-Mualem and Brooks-Corey-Burdine models. (a) before rectification and (b) after rectification

Discussion

The dry density of the soil studied is as high as 2.01 Mg/m^3. Heavy compaction was needed to reach it. To avoid damage of the tensiometers, metallic rods were used to prepare spaces during compaction for tensiometers installation. For TDR sensors, they were placed between different soil layers and were compacted together with the soil. The good response of these sensors during the test shows that they were not damaged by the compaction. The inconsistent data given by the TDR sensor at h = 200 mm (see Figure 4) is rather related to the soil heterogeneity. This observation confirms the difficulty of preparing large-size specimen of fined-coarse grained soils on the one hand, and on the other hand, the necessity of using representative large-size specimen for the investigation of hydraulic behavior of such materials. In figure 9, it was noted that a volumetric water content of 5% corresponds to a degree of saturation of 20%. This can be explained by the presence of the large particles of ballast in the soil.

During injection of water, there was a difference between the estimated pore volume and the volume of water injected to reach saturation (Figure 5). This can be explained by the non-uniform flow in the specimen because water flows mainly through the macro-pores. This phenomenon was also reported by Moulton (1980). This means that water outflow from the top valve is not an

indicator of full specimen saturation, and longer flow duration is needed (one day in this study). The values of degree of saturation measured by TDR sensors were in the range between 90% and 100% after this stage (see Figure 10*b*).

In the present work, the hydraulic conductivity of unsaturated fouled ballast was obtained in the infiltration column during the drainage and evaporation stages. Following ASTM (2010), the hydraulic conductivity of unsaturated soils can be estimated from infiltration column test following four methods: downward infiltration of water onto the surface of an initially unsaturated soil specimen (A1), upward imbibitions of water from the base of an initially unsaturated soil specimen (A2), downward drainage of water from an initially saturated soil specimen (A3), and evaporation of water from an initially saturated soil specimen (A4). Methods A1 and A2 can be used for fine-grained sands and for low-plasticity silts. Method A3 can be used with fine or coarse-grained sands. Method A4 can be used for any soil with the exception of clays of high plasticity. In the work of Moore (1939), unsaturated flow was induced naturally; the water rose from the water table to the surface of the soil column and was evaporated from the surface. This method allowed studying various soils ranging from fine gravel to clay.

In the saturated condition, the hydraulic conductivity obtained in the saturated condition is 1.75×10^{-5} m/s. According to the classification of Bear (1988) for railway application, the drainage is poor because this value corresponds to the hydraulic conductivity of very fine sand, silt, or loam. Note that in the material studied, there are also clay (5%), fine sand and loam. Thus, from a practical point of view, this soil cannot be used for drainage layer.

Conclusions

A large scale infiltration column was developed to study the hydraulic behavior of a fine-coarse grained mixture from the fouled ballast layer of a railway constructed in the 1800s. The column is equipped with tensiometer and TDRs to monitor the matric suction and volumetric water content, respectively. The results obtained allow the following conclusions to be drawn:

The quality of the recorded responses show that the installation protocol adopted for tensiometer probes (using metallic rod) and TDR probes (compacted together with soil) was appropriate when testing fine-coarse-grained soils such as the fouled ballast. In addition, the use of both tensiometer and TDR probes in the test enabled the direct determination of water retention curve and the direct application of the instantaneous method for determining the hydraulic conductivity of the

unsaturated soil. The results of hydraulic conductivity obtained by both the measured volumetric water content profiles and those fitted using the van Genuchten's model were found similar. This indicates that fitting curves can be used when determining the hydraulic conductivity of unsaturated fouled ballast without causing significant error.

From a practical point of views, the method developed in this study can be used in determining the hydraulic conductivity for fouled ballast in particular and for fine-coarse-grained soil mixtures in general, in both unsaturated and saturated states.

Acknowledgement

References:

ASTM, 2010, "Standard test methods for measurement of hydraulic conductivity of unsaturated soils," D7664-10.

AFNOR, 1991, "Soils : investigation and testing – Determination of particle density – Pycnometer method," *French standard,* NF P 94-054.

AFNOR, 2001, "Tests for mechanical and physical properties of aggregates. Part 6: Determination of particle density and water absorption," *French standard*, NF EN 1097-6.

AFNOR, 2004, "Unbound and hydraulically bound mixtures. Part 7: cyclic load triaxial test for unbound mixtures," *French standard,* NF EN 13286-7.

Bear, J., 1988, "Dynamic of fluids in porous media," *Dover Publications*, 781 p.

Brooks, R.H., and Corey, A.T., 1964, "Hydraulic properties of porous media", Hydro. Paper No.3, Colorado State Univ., Fort Collins, Colo.

Bruckler, L.B., Angulo-Jaramillo, P., Ruy, R., 2002, "Testing an infiltration method for estimating soil hydraulic properties in the laboratory," *Soil Science Society of America Journal*, Vol. 66, pp. 384–395.

Chapuis, R.P., Masse, I. , Madinier, B., Aubertin, M., 2006, "Essai de drainage en colonne pour obtenir les propriétés non saturées de matériaux grossiers," *Sea to Sky Geotechnique – the 59th Canadian Geotechnical Conference*, pp. 905 – 912.

Choo, L.-P., and Yanful, E.K., 2000, "Water flow through cover soils using modeling and experimental methods," *Journal of Geotechnical and Geoenvironmental Engineering*, Vol. 126, No. 4, pp. 324-334.

Côté, J., and Roy, M., 1998, "Conductivité hydraulique de matériaux de fondations de chaussées partiellement saturés," *Rapport de l'études et recherches en transports du Québec*, 177 p

Cui, Y.J., Tang, A.M., Loiseau, C., Delage, P., 2008, "Determining the unsaturated hydraulic conductivity of a compacted sand-bentonite mixture under constant-volume and free-swell conditions," *Physics and Chemistry of the Earth, Parts A/B/C*, Vol. 33, pp. S462–S471.

Daniel, D.E., 1982, "Measurement of hydraulic conductivity of unsaturated soils with thermocouple psychometers," *Soil Science Society of Americal Journal*, Vol. 46, No. 6, pp. 1125-1129.

Delage, P., and Cui, Y.J., 2001, "Comportement mécanique des sols non saturés," *Ed. Techniques Ingénieur*, Article C 302.

Ekblad, J., 2008, "Statistical evaluation of resilient models characterizing coarse granular materials," *Materials and Structures*, Vol. 41, No. 3, pp. 509–525.

Ekblad, J., and Isacsson, U., 2007, "Time-domain reflectometry measurements and soil-water characteristic curves of coarse granular materials used in road pavements," *Canadian Geotechnical Journal*, Vol. 44, No. 7, pp. 858–872.

Gong, Y., Cao, Q., and Sun, Z., 2003 "The effects of soil bulk density, clay content and temperature on soil water content measurement using time-domain reflectometry," *Hydrological Processes*, Vol. 17, No. 18, pp. 3601–3614.

Hanson, B., and Peters, D., 2000, "Soil type affects accuracy of dielectric moisture sensors," *California Agriculture*, Vol. 54, No. 3, pp. 43–47.

Indraratna, B., Su, L. and Rujikiatkamjorn, C., 2011*a*, "A new parameter for classification and evaluation of railway ballast fouling," *Canadian Geotechnical Journal,* Vol. 48, No. 2, pp. 322–326.

Indraratna, B., Salim, W. and Rujikiatkamjorn, C., 2011*b*. "Advanced Rail Geotechnology - Ballasted Track," *CRC Press.*

Jacobsen, O.H., and Schjønning, P., 1993, "A laboratory calibration of time domain reflectometry for soil water measurement including effects of bulk density and texture," *Journal of Hydrology*, Vol. 151, No. 2-4, pp.147–157.

Lackenby, J., Indraratna, B., Mcdowell, G., and Christie, D., 2007, "Effect of confining pressure on ballast degradation and deformation under cyclic triaxial loading," *Géotechnique,* Vol. 57, No. 6, pp. 527 – 536.

Masrouri, F., Bicalho, K.V., and Kawai,K., 2008, "Laboratory hydraulic testing in unsaturated soils," *Geotechnical and Geological Engineering*, Vol. 26, No. 6, pp. 691–704.

McCartney, J.S., Villar, L.F.S., and Zornberg, J.G., 2007, "Estimation of the hydraulic conductivity of unsaturated clays using infiltration column test," *Proceedings of the 6th Brazilian Symposium on Unsaturated Soils*, Vol. 1, pp. 321-328.

McCartney, J.S. and Zornberg, J.G., 2007, "Effect of wet-dry cycles on capillary break formation in geosynthetic drainage layers," *Geosynthetics 2007*, Washington, DC. January, pp. 16-19.

McCartney, J.S. and Zornberg, J.G., 2010, "Effect of infiltration and evaporation on geosynthethic capillary barrier performance," *Canadian Geotechnical Journal*, Vol. 47, No. 11, pp. 1201-1213.

Moulton, L.K., 1980, "Highway subdrainage design," *Report to the Federal Highway Administration – U.S. Departement of Transport,* FHWA-TS-80-224, 162 p.

Moore, R., 1939, "Water Conduction from Shallow Water Tables," *Hilgardia*, Vol. 12, pp. 383-426.

Nützmann, G., Thiele, M.,Maciejewski, S. and Joswig, K., 1998, "Inverse Modelling techniques for determininghydraulic properties of coarse-texturedporous media by transient outflow methods," *Advance in Water Resources. Vol. 22, No. 3, pp.273-284.*

Parks, J.M., Stewart, M.A., and McCartney, J.S., 2012, "Validation of a Centrifuge Permeameter for Investigation of Transient Infiltration and Drainage Flow Processes in Unsaturated Soils", *Geotechnical Testing Journal*, Vol. 35, No. 1. pp. 182-192.

Peters, S.B., Siemens, G., and Take, W.A., 2011, "Characterization of transparent soil for unsaturated applications," *Geotechnical Testing Journal*, Vol 34, No. 1, pp. 445-456.

Robinet, A., 2008, "Les couches de forme traitées dans les structures d'assise ferroviaires." *Mémoire de diplôme d'ingénieur du Conservatoire National des Arts et Métiers (CNAM).*

Schneider, J.M., and Fratta,D., 2009, "Time-domain reflectometry - parametric study for the evaluation of physical properties in soils," *Canadian Geotechnical Journal*, Vol. 46, pp. 753–767.

Selig, E. and Waters, J., 1994, "Track geotechnology and substructure management," Thomas Telford.

Soilmoisture, 2000, "6050X3K1 Operating Instructions", 53 p.

Stankovich, J. M., and Lockington, D. A., 1995, "Brooks-Corey and van Genuchten, soil-water-retention models" *Journal of Irrigation and Drainage Engineering*, Vol. 121, No. 1, 7 pages.

Stormont, J.C., and Anderson, C.E., 1999, "Capillary barrier effect from equilibrium technique at different temperatures and its application in determining the water retention properties of MX80 clay," *Canadian Geotechnical Journal*, Vol. 42, No. 1, pp. 287-296.

Stolte, J., Veerman, M ., Wosten, G.J., Freijer, J.H.M., Bouten, J.I ., Dirksen, W., Van Dam, C., Van den Berg, J.C., 1994, "Comparison of six methods to determine unsaturated soil hydraulic conductivity," *Soil Science Society of America Journal*, Vol. 58, No. 6, pp. 1596-1603.

Tang, A.M., Ta, A.N., Cui, Y.J., and Thiriat., J., 2009, "Development of a large scale infiltration tank for determination of the hydraulic properties of expansive clays," *Geotechnical Testing Journal*, Vol. 32, pp. 385-396.

Tarantino, A., Ridley, A.M., and Toll. D.G., 2008, "Field measurement of suction, water content, and water permeability," *Geotechnical and Geological Engineering*, Vol. 26, No. 6, pp. 751–782.

Trani, L. D. O., and Indraratna. B., 2010, "Assessment of subballast filtration under cyclic loading," *Journal of Geotechnical and Geoenvironmental Engineering*, Vol. 136, No. 11, pp. 1519–1527.

Trinh, V.N., Tang, A.M., Cui, Y.J., Dupla, J.C., Canou, J., Calon, N., Lambert, L., Robinet, A., and Schoen, O., 2011, "Caractérisation des matériaux constitutifs de plate-forme ferroviaire ancienne," *Revue Française de Géotechnique*. No. 134-135., pp. 64-75.

Trinh V.N., Tang A.M., Cui Y.J., Dupla J.C., Canou J., Calon N., Lambert L., Robinet A., Schoen O. 2012, "Mechanical characterisation of the fouled ballast in ancient railway track substructure by large-scale triaxial tests," *Soils and Foundations*. Accepted for publication.

UMS, 2008, "T8-long-term monitoring tensiometer," *User manual*, 56 pages.

van Genuchten, M.T., 1980, "A closed-form equation for predicting the hydraulic conductivity of unsaturated soils," *Soil Science Society of America Journal*, Vol. 44, No. 5, pp. 892–898.

Wind, G.P., 1966 "Capillary conductivity data estimated by a simple method," *In* "Water in the saturated zone," *Proceedings of the Wageningen symposium,* Wageningen, the Netherlands, 19–23 June 1966, pp. 181 – 191.

Yang, H., Rahardjo, H., Wibawa, B., and Leong, E.C., 2004, "A soil column apparatus for laboratory infiltration study," *Geotechnical Testing Journal*, Vol. 27, pp. 347-355.

Yasuda, N., Matsumoto, N., Yoshioka, R., and Takahashi, M., 1997, "Undrained monotonic and cyclic strength of compacted rockfill material from triaxial and torsional simple shear tests," *Canadian Geotechnical Journal*, Vol. 34, No. 3, pp. 357-367.

Ye W.M., Cui Y.J., Qian L.X., Chen B. 2009. "An experimental study of the water transfer through compacted GMZ bentonite," *Engineering Geology,* Vol. 108, pp.169- 176.

Effect of fine particles on the hydraulic behavior of interlayer soil in railway sub-structure

Trong Vinh Duong[1], Yu-Jun Cui[1], Anh Minh Tang[1], Jean-Claude Dupla[1], Nicolas Calon[2]

Abstract: The ancient railway substructure in France was built by emplacing ballast directly on sub-grade. Over years of operation, the inter-penetration of ballast and sub-grade created a soil layer between them. Under different conditions, this naturally formed layer, namely interlayer, can contain different quantities of fine particles, becoming more or less sensitive to changes in water content. As the water content changes are governed by the hydraulic behavior of interlayer soil, assessing the influence of fine particles content on the hydraulic behavior of interlayer soil is important. To this end, the hydraulic behavior of an interlayer soil taken from Sénissiat (near Lyon, France) was investigated using two infiltration columns, a large-scale column equipped with tensiometers and TDR for suction and volumetric water content measurements, respectively, and a smaller column equipped with high capacity tensiometers only. Different fines contents were considered and wetting-drying cycles were applied to the soil specimens. The hydraulic conductivity was determined by applying the instantaneous profile method. The results obtained showed that i) hysteresis exists for both the soil water retention curve and the hydraulic conductivity changes with suction; ii) the effect of wetting-drying cycles is insignificant; iii) adding 10% of fine particles to the natural interlayer soil changes the soil water retention curve but does not induce significant changes in hydraulic conductivity; iv) the hydraulic conductivity of interlayer soil with 10% of fine particles added is close to that of soil sieved at 2 mm, suggesting that the hydraulic conductivity of interlayer soil is mainly governed by fine particles through suction effect.

Keywords: railway substructure; interlayer soil; fines content; instantaneous profiles method; hydraulic conductivity.

Introduction

Many railway lines over the world have been in operation for more than one hundred years. In France, the ancient lines represent 94% of the whole railway network. As opposed to the new lines, the ancient ones were constructed by direct installation of ballast onto sub-grade without any separation layer. Over years of operation and with the increasing traffic, load, and speed of train, there are more and more problems related to the stability, loss of strength of substructure. A number of studies have been conducted to assess the state of substructure and to develop adequate maintenance methods (Trinh 2011; Duong et al. 2013; Cui et al. 2013). It was found that one of the particularities of ancient substructure is the presence of a soil layer namely interlayer that has been

---

[1] Ecole des Ponts Paris Tech (ENPC), Laboratoire Navier/CERMES
[2] French Railway Company (SNCF)

created mainly by interpenetration of ballast and fine particles of sub-grade.

In France, it has been decided recently to renew the ancient railway network. During the renewal, the interlayer will be kept as part of the substructure thanks to its high mechanical resistance related to its high dry unit mass (2.4 Mg/m^3 at the Sénissiat site, according to Trinh et al. 2011) reached by natural dynamic compaction corresponding to the circulation of trains. However, the mechanical behavior of interlayer soil can show a large variability, depending on the proportion of fine particles contained in it. A number of studies (Babic et al. 2000; Pedro 2004; Naeini and Baziar 2004; Kim et al. 2005; Verdugo and Hoz 2007; Cabalar 2008; Seif El Dine et al. 2010; Ebrahimi 2011; Anbazhagan et al. 2011; Trinh et al. 2012) showed that the mechanical behavior of soil containing a large proportion of fines is strongly influenced by the water content. As the water content changes are governed by the hydraulic behavior of soil, it appears important to assess the influence of fine particles content on the hydraulic behavior of interlayer soil.

Moreover, in field conditions, the interlayer soil normally undergoes the effect of wetting/drying cycles related to climatic changes. These wetting/drying cycles may induce changes in soil micro-structure, thereby changing the soil hydraulic properties. Therefore, it appears also important to investigate the effect of wetting/drying cycles on the hydraulic conductivity.

To the authors' knowledge, the effects of fines content and wetting/drying cycles on the unsaturated interlayer soil have not been investigated yet. In the present work, laboratory tests were performed using a large-scale infiltration column (300 mm in diameter) and a small-scale infiltration column (50 mm in diameter), and the instantaneous profile method was used to determine the hydraulic conductivity of soil. Both wetting and drying paths were performed and different fines contents were considered: natural interlayer soil (*ITL_0*), natural interlayer soil with 10% of sub-grade added (*ITL_10*), fine-grained soil prepared by passing *ITL_10* through a 2 mm sieve (*Fines*). The results enable the assessment of the effects of fine particles and wetting/drying cycles.

Materials studied

The soils (both the interlayer soil and sub-grade) were taken from the railway site Sénissiat (North-West of Lyon, France). Mineralogy analysis reveals that the interlayer soil is a mixture of materials that come from the construction and maintenance (broken stones, gravel, sand, etc) of tracks, the aging process of track components and the sub-grade. It also showed that the fine particles in the interlayer soil mainly come from the sub-grade. The main geotechnical properties of interlayer soil

and sub-grade are presented in Table 1. The results show that the sub-grade is high-plasticity silt. More details about the characterization of the interlayer soil can be found in Trinh et al. (2011).

Table 1: Properties of the soil studied

Soil	Properties	Value
Interlayer soil (ITL_0)	ρ_s (particles smaller than 2 mm)	2.67 Mg/m^3
	ρ_s (particles larger than 2 mm)	2.68 Mg/m^3
	d_{10}	0.01 mm
	d_{30}	5 mm
	d_{60}	30 mm
	liquid limit w_L (smaller than 100 µm)	40.2%
	plasticity index I_p (smaller than 100 µm)	11.3%
Sub-grade (Fines to	liquid limit w_L	57.8%
create ITL_{10})	plasticity index I_p	24.1%

In order to study the effect of fines contents on the hydraulic behavior of interlayer soil, a quantity of sub-grade representing 10% of interlayer soil by dry mass was added into the interlayer soil to form a soil with a higher content of fines: ITL_{10}. The grain size distribution curves of the natural interlayer soil (ITL_0) and ITL_{10} are presented in Fig. 1.
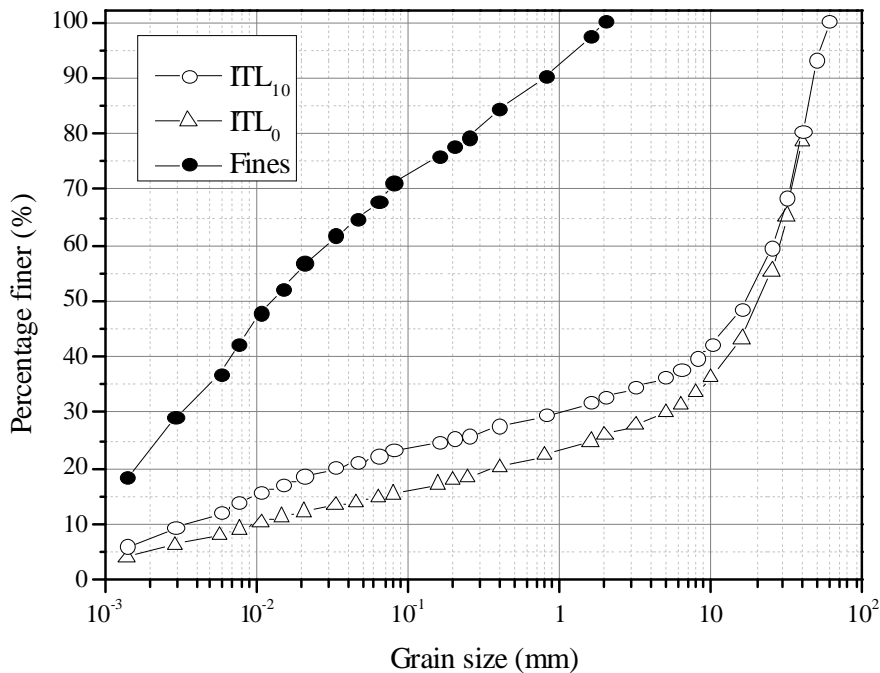

Fig. 1: Grain size distribution curves of the interlayer soil (ITL_0) and the derived ones (ITL_{10} and *Fines*)

It is worth noting that the migration of fines into ballast is recognized as one of the mechanisms for fouled ballast (Ayres 1986; Selig and Waters 1994; Alobaidi and Hoare 1996; 1998; Ghaotara et al. 2006; Mayoraz et al. 2006; Huang et al. 2009; Giannakos 2010; Fortunato et al. 2010; Indraratna et al. 2011; Ebrahimi 2011; Sussmann and Chrismer 2012). Even though the interlayer soil studied here is different from the fouled ballast by nature, in order to compare with the classification of fouled ballast, two parameters for fouled ballast are adopted here: the fouling index *FI* (Selig and Water 1994) and the relative fouling ratio R_{b-f} (Indraratna et al. 2011). *FI* is defined as:

$$FI = P_4 + P_{200} \tag{1}$$

where P_4 and P_{200} are percentages of ballast passing through sieves N° 4 (4.75 mm) and N° 200 (0.075 mm), respectively.

R_{b-f} is the weighted ratio of the dry mass of fouling particles M_f (passing through 9.5 mm sieve) to the dry mass of ballast M_b (particles retained in 9.5 mm sieve):

$$R_{b-f} = \frac{M_f \times \dfrac{G_{s-b}}{G_{s-f}}}{M_b} \times 100\% \tag{2}$$

where G_{s-f}, G_{s-b} are specific densities of fouling particles and ballast, respectively.

The values of the two indexes for ITL_0 and ITL_{10} are presented in Table 2. According to the classification, both ITL_0 and ITL_{10} are "*highly fouled*".

Table 2: Fouling state of the interlayer soil

	Fouling Index	Relative ballast fouling ratio	Fouling category
	FI (-)	R_{b-f} (%)	
ITL_0	45	56	Highly fouled
ITL_{10}	59	72	Highly fouled

To better evaluate the effect of fines on the hydraulic behavior of interlayer soil, the hydraulic conductivity of pure fine particles was also determined. For this purpose, ITL_{10} was sieved at 2 mm to obtain the fine part (namely *Fines*). The grain size distribution curve of *Fines* is also presented in Fig. 1.

Experimental methods

The interlayer soil was tested in a large-scale infiltration column (Fig. 2). The column (300 mm in diameter and 600 mm in height) is equipped with five water content sensors (TDR1 to TDR5) and five tensiometers for measuring pore-water pressure (T1 to T5) arranged at various elevations along the column (h = 100, 200, 300, 400 and 500 mm from the bottom of the soil specimen). The working pressure range of the tensiometers is from 100 kPa to -85 kPa. The accuracy of the TDR used is ± 2% and that of the tensiometer is ± 0.5 kPa. At each instrumented height, as the area occupied by the sensors is just 6.8% of the total apparatus section area, the influence of the sensors installation on water transfer is expected to be insignificant.
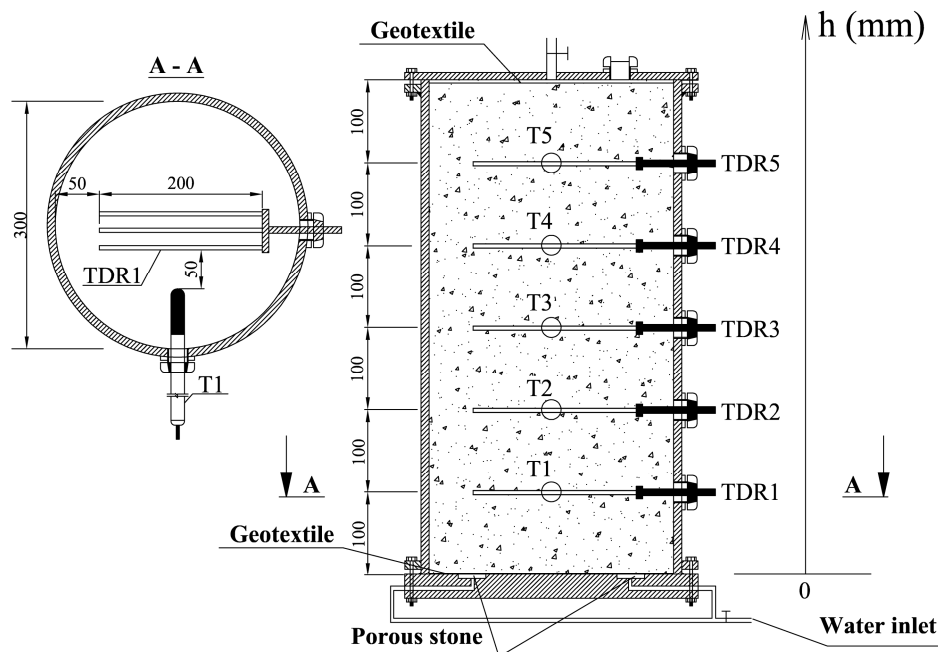
Fig. 2: Schematic view of the large-scale infiltration column

For the *ITL$_{10}$* specimen preparation, water and fine particles were added to the dry natural interlayer soil to reach the target water content and fine particles content, and a large mixer was used to homogenize the material. For the *ITL$_0$* specimen preparation, only desired quantity of water was added to the dry natural interlayer soil. After mixing, the wet materials were stored in hermetic containers for at least 24 h for moisture homogenization. Soil compaction was conducted using a vibrating hammer in six layers of 0.10 m each at a dry unit mass of 2.01 Mg/m^3. Prior to the compaction of the subsequent layer, a TDR probe and a metal rod of 25 mm diameter were placed on the compacted layer.

Once the soil specimen was prepared, water was injected from the bottom and it flowed out from the outlet after about half an hour. After saturation of the sample, the metal rods were removed and the tensiometers were installed. This protocol was adopted to avoid damaging the tensiometers during the compaction and also any cavitation due to possible high suction in the column. More details about the large-scale infiltration column can be found in Duong et al. (2013).

The TDR is an indirect measurement method and several authors reported that the calibration curve depends on the soil texture, unit mass, mineralogy, fines content and particle size (Jacobsen and Schjønning 1993; Stolte et al. 1994; Côté and Roy 1998; Gong et al. 2003; Schneider and Fratta 2009). It is therefore necessary to determine the specific calibration curve for each soil studied. For the natural interlayer soil (*ITL₀*), a relationship between volumetric water content (*θ*) and the dielectric constant K_a was established by Duong et al. (2013). As the soil composition in *ITL₁₀* is different from *ITL₀*, another relationship was needed. This was determined separately with a lower specimen of 200 mm at the same unit mass in the same column. One TDR sensor was placed in the middle of the sample. Water was added on the surface of the soil specimen to achieve the desired water content. Once the TDR gave a steady response (after about 8 hours), the water content was considered as being uniform within the sample and the value of dielectric constant K_a was recorded. This operation was repeated until the specimen reached full saturation (with 1 cm water on the soil surface). All the TDR sensors were calibrated in the same fashion. The results obtained on the five sensors are similar.
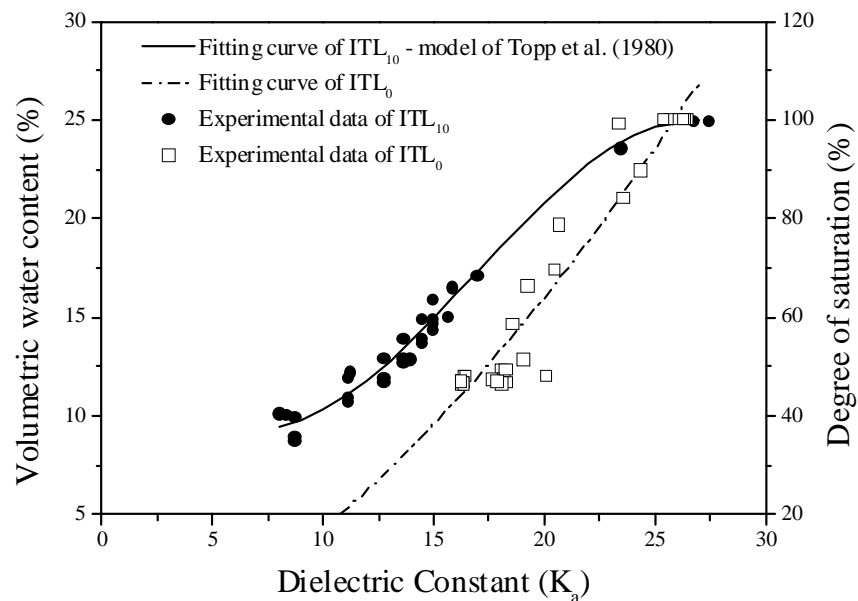

Fig. 3: Calibration curves of the TDRs used for the *ITL₁₀* and *ITL₀* specimens

Fig. 3 presents the calibration curve of TDR for ITL_{10} along with the fitting calibration curve for ITL_0 presented in Duong et al. (2013) at the same dry unit mass (2.01 Mg/m^3). It can be observed that the curve for ITL_0 lies below the curve for ITL_{10}, indicating a clear effect of soil texture. The following equation (based on the model of Topp et al. 1980) was used to fit the experimental data for ITL_{10}:

$$\theta = -4.16 \times 10^{-5} \times K_a^3 + 2.11 \times 10^{-3} \times K_a^2 - 2.36 \times 10^{-2} \times K_a + 0.17 \qquad (3)$$

The infiltration tests were conducted in two wetting/drying cycles. After installation of the tensiometers, the saturation of soil column was completed (Saturation 1). This wetting stage was followed by a draining stage (Drainage 1). Water was allowed to drain out through the bottom valves by keeping a constant water level at the bottom of soil sample using an external water source. The first wetting/drying cycle finished by a stage of evaporation (Evaporation 1) where the top cover of the column was removed to allow soil water evaporation. A fan was used to accelerate the evaporation process. The evaporation stage ended when the suction value indicated by tensiometer T5 (h = 500 mm) was about 60 kPa (higher suction would lead to cavitation). A second wetting-drying cycle was applied following the same procedure (Saturation 2, Drainage 2 and Evaporation 2). Before the second drainage, the hydraulic conductivity in saturated state was also measured by applying a constant water head of 0.61 m. This low value was adopted in order to ensure the validity of Darcy's law (Tennakoon et al. 2012). Note that the experimental procedure with saturation from the bottom and evaporation from the top is also recommended in ASTM standard (ASTM 2010).

The unsaturated hydraulic conductivity of *Fines* was determined using a small-scale infiltration column of 50 mm in diameter and 200 mm in height (Munoz et al. 2008). Its schematic view is shown in Fig. 4. Suction measurements were performed by four high-capacity tensiometers (Cui et al. 2008) installed at 40, 80, 120 and 160 mm height from the base of the sample. The accuracy of this tensiometer is ± 1 kPa. The soil was statically compacted in the column in four layers of 50 mm each. Once the compaction was completed, the tensiometers were installed. In order to ensure a good contact between the soil sample and the tensiometers, a paste of sub-grade was applied on the surface of the ceramic of tensiometers.
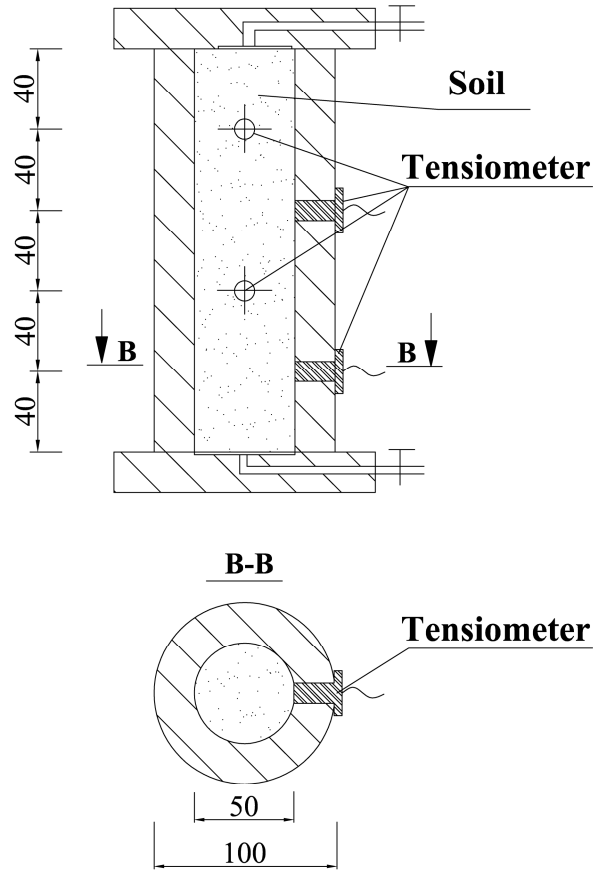
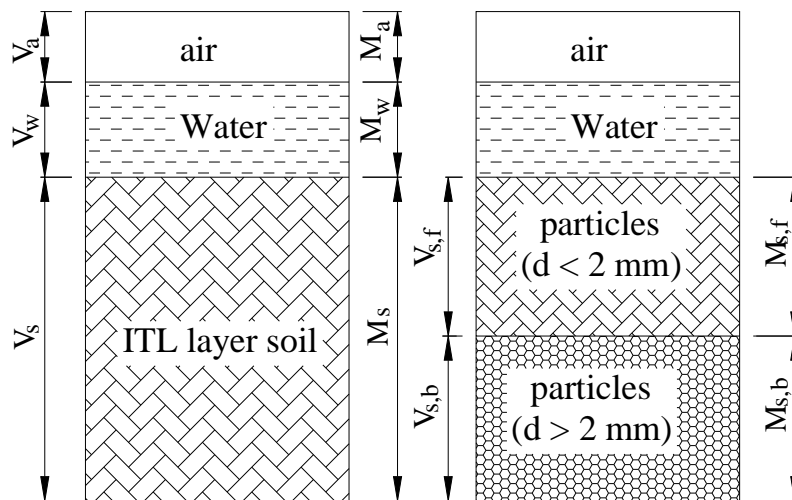**Fig. 4: Schematic view of the small-scale infiltration column**

Fig. 5: Components of the unsaturated interlayer soil

The dry unit mass and water content of *Fines* were taken equal to those of fine particles contained in the sample of interlayer soil. Using the illustration shown in Fig. 5, these two parameters can be calculated as follows:

$$\rho_{d,f} = \frac{M_{s,f}}{V_f} = \frac{M_s - M_{s,b}}{V - V_{s,b}} = \frac{(1-m)\rho_d V}{V - \dfrac{m}{\rho_{s,b}}\rho_d V} = \frac{(1-m)\rho_d \rho_{s,b}}{\rho_{s,b} - m\rho_d} \tag{4}$$

$$w_f = \frac{M_w}{M_{s,f}} = \frac{M_s w}{M_s - M_{s,b}} = \frac{w}{1-m} \tag{5}$$

where M, M_w, M_s are the total mass, mass of water and mass of solid particles, respectively; V, V_w, V_s are the total volume, volume of water and volume of solid particles respectively; ρ_d, ρ_s are the dry unit mass of the specimen and unit mass of solid particles, respectively; the subscripts f and b stand for particle smaller and larger than 2 mm, respectively; m is the percentage of particles larger than 2 mm.

Based on the grain size distribution curve, a value $m = 0.67$ was determined. From Eqs (4) and (5), a value of 1.33 Mg/m^3 was obtained for the dry unit mass of *Fines*.

The test procedure followed for the small-scale infiltration column was akin to that for the large-scale one. After the suction stabilization, the sample was saturated from the bottom (Saturation 1). After completion of saturation, an external water source was connected to the bottom in order to ensure a constant water level after the drainage. The top cover was then removed allowing water evaporation from the soil surface (Evaporation 1). When suction at 160 mm reached about 400 kPa, Evaporation 1 was stopped to avoid cavitation of the tensiometers. A second wetting-drying cycle was applied by following the same procedure as in the first cycle (Saturation 2 and Evaporation 2).

Unlike the large-scale column where both suction and water content were monitored, the small-scale column has only suction monitored. To obtain the water content changes during infiltration, the soil-water retention curve (SWRC) was needed. The water retention curve (WRC) of compacted *Fines* was determined separately using the device presented in Fig. 6. The soil was first compacted inside an oedometer cell (the dimensions of the soil specimen are 50 mm in diameter and 20 mm in height). The suction of the specimen was monitored by a high-capacity tensiometer fixed at the bottom of the cell. A light aluminum piston of 50 mm diameter was placed on the specimen to ensure the good contact between soil and tensiometer. The piston induced a vertical stress of 1.8

kPa and its influence was believed to be negligible. For the monitoring of soil water content, the whole system was placed on a balance having an accuracy of ±0.01 g. The mass change indicated the quantity of water added or evaporated. More details about this cell can be found in Le et al. (2011) and Munoz-Castelblanco et al. (2012). Wetting was conducted by adding a small quantity of water on the upper face of the sample, while drying was conducted by allowing soil water evaporation from the upper surface without the piston on it. Once the desired water content was reached, the piston was put on the soil surface and the final suction was recorded. This method was also discussed by Cunningham et al. (2003); Toker et al. (2004); Lourenço (2008); Lourenço et al. (2011); Toll et al. (2012) and Munoz-Castelblanco et al. (2012).
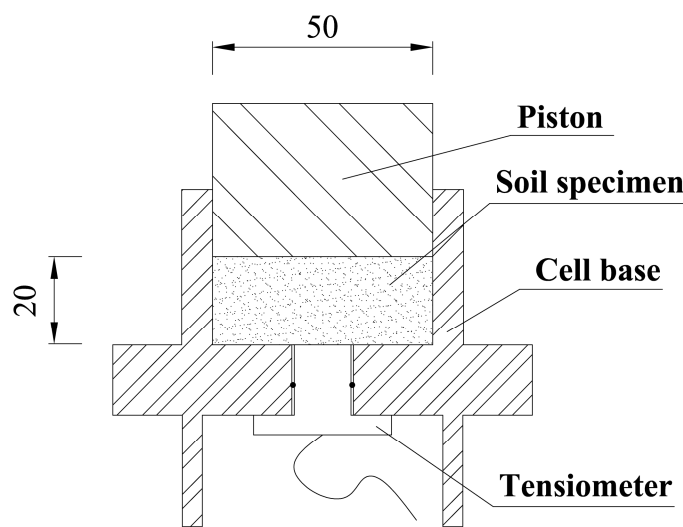
Fig. 6: Device for determining the WRC of *Fines*

For the large-scale column, both suction and water content profiles were obtained directly. For the small-scale column, the suction profiles were obtained directly while the water content profiles were determined through the SWRC. The instantaneous profile method (Daniel 1982; Delage and Cui 2001; Bruckler et al. 2002; Cui et al. 2008; Ye et al. 2009) was then applied for the determination of hydraulic conductivity for each soil. Note that this method is based on the generalized Darcy's law. The hydraulic gradient is determined by considering the slope of suction isochrones and the water volume passing through a given section between times *t* and *t+dt* is used for calculating the water flux.

Experimental results

The results of *ITL₀* were presented in Duong et al. (2013). Here only the results of *ITL₁₀* and *Fines* are presented in detail, and the results of *ITL₀* are only used for comparison.

Fig. 7 presents changes in pore water pressure and volumetric water content versus time during Drainage 1 and Evaporation 1 for *ITL₁₀*. From the saturated state where the volumetric water content reached 22 - 25%, water drained out through the bottom valves and subsequently the volumetric water content decreased to 15 - 17% at the end of the draining stage for all the TDR sensors except that at h = 200 mm (Fig. 7b). At this moment, the pore water pressure was in the range from 0 to -4 kPa (Fig. 7a). Drainage 1 finished after more than 1 day. During Evaporation 1, the pore water pressure given by the tensiometer at h = 500 mm decreased quickly while small changes were observed at other levels (Fig. 7a). This is consistent with the values of volumetric water content: the value at h = 500 m decreased significantly since the beginning of Evaporation 1 while those at other levels show slight changes (Fig. 7b).
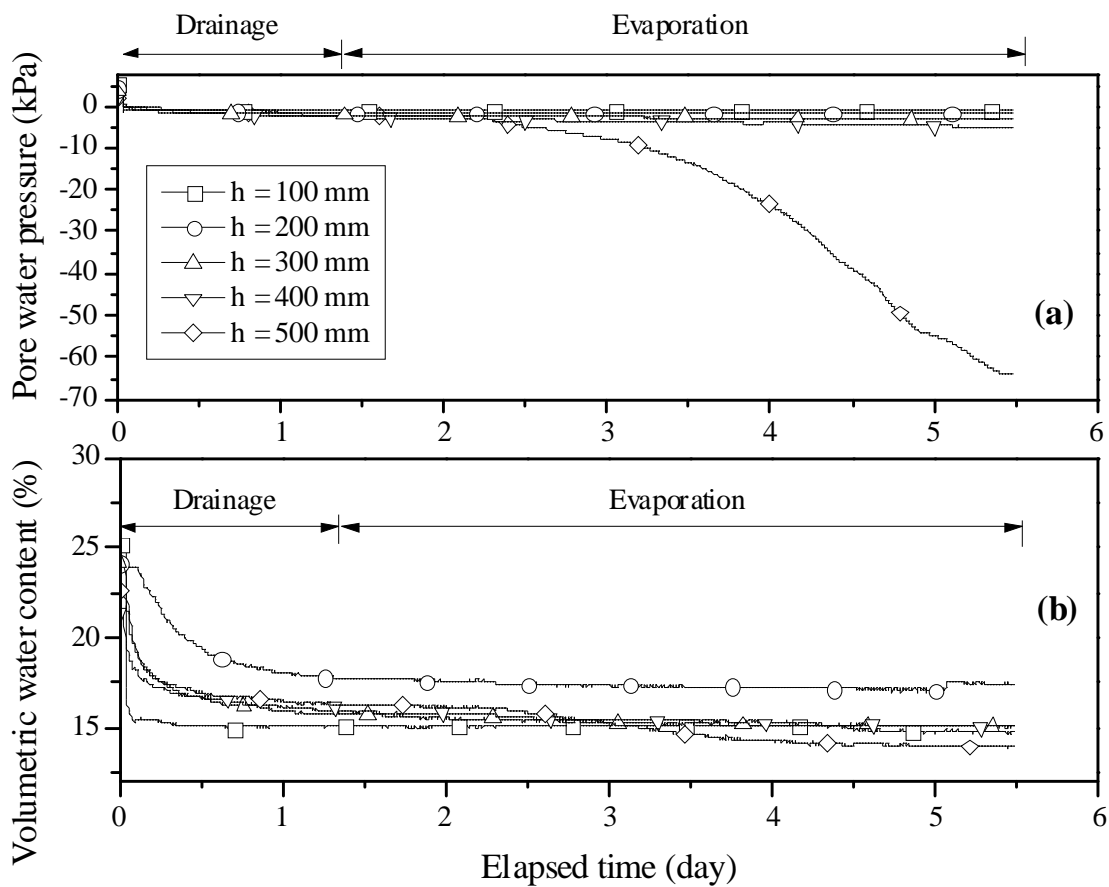

Fig. 7: Test on *ITL₁₀*: pore water pressure and volumetric water content evolutions during Drainage 1 and Evaporation 1

103

During Saturation 2, the external water source was set at a level applying a water pressure of 6.1 kPa to the bottom of sample. The results obtained show that less than one hour was needed to re-saturate the soil specimen (Fig. 8). The changes were not significant for T1 to T4 (small suction value), while those of T5 at h = 500 mm are quite significant (Fig. 8a). Furthermore, the suction changes in Fig. 8a are consistent with those of volumetric water content in Fig. 8b. At the end of this stage when the pore water pressure became positive at all levels, the 5 tensiometers indicated the values corresponding to the water head at each level (5.33 kPa, 4.36 kPa, 3.28 kPa, 2.21 kPa and 1.13 kPa for T1 to T5, respectively). The volumetric water content also reached the values of near saturated state (corresponding to the degree of saturations ranging from 87.5% to 100%).
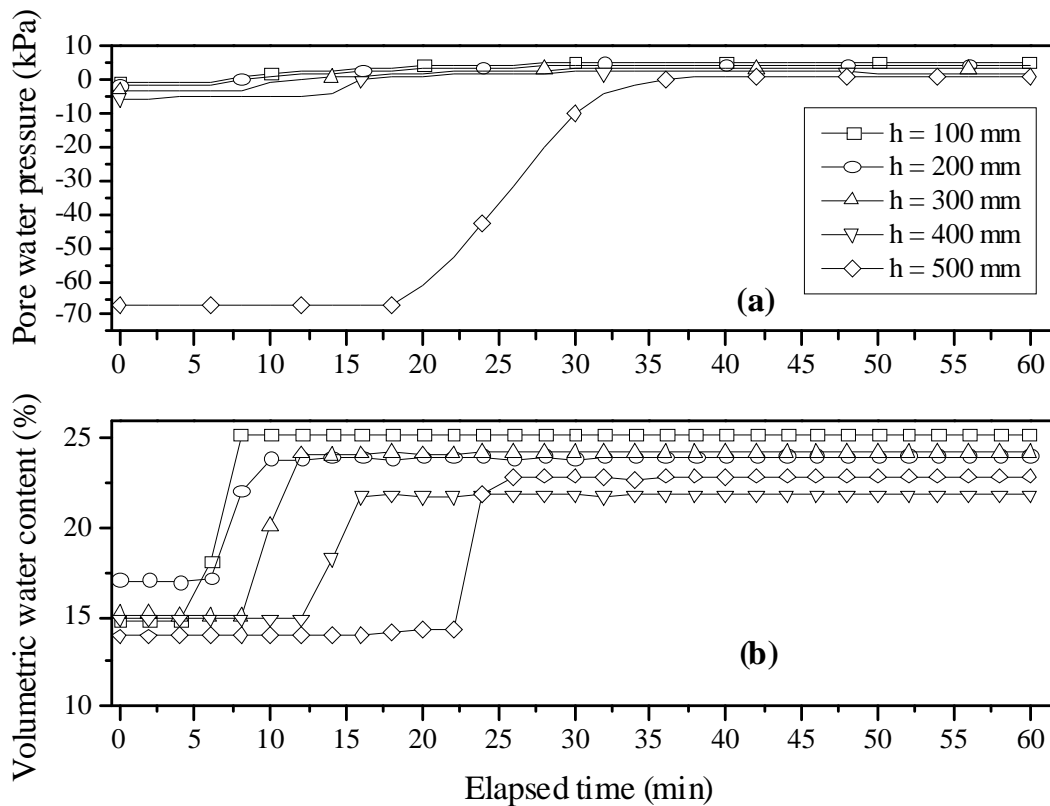
Fig. 8: Test on *ITL₁₀*: pore water pressure and volumetric water content evolutions in Saturation 2

The results obtained during Drainage 2 and Evaporation 2 are presented in Fig. 9. During the first two days, water inside the column was connected to the outside water source having a level decreased in steps of 50 mm from h = 550 to 50 mm in order to verify the response of the sensors. Each step was kept for 1 hour. At the end of Drainage 2, the outside water source was set at h = 50 mm and Evaporation 2 started. During the drainage, the volumetric water content decreased quickly while the changes of suction were much slower. As during Evaporation 1, the pore water pressure and the volumetric water content values at h = 500 mm decreased significantly while the others

remained almost constant. Once again, the changes of suction and volumetric water content are consistent for different levels: the closer to the evaporation surface, the higher the suction (Fig. 9a) and the smaller the volumetric water content (Fig. 9b) (except for h = 200 mm).

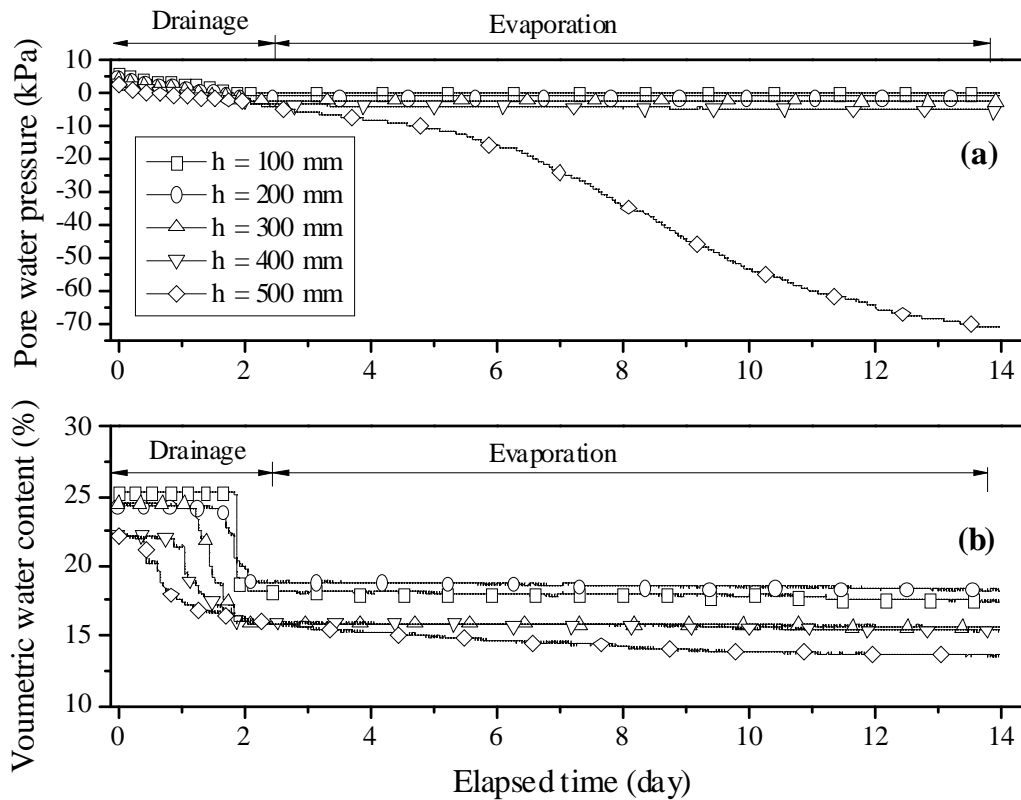**Fig. 9: Test on *ITL$_{10}$*: pore water pressure and volumetric water content evolutions during Drainage 2 and Evaporation 2**

The inconsistent data given by the TDR sensor at h = 200 mm (see Fig. 7, Fig. 8, Fig. 9) is related to the deficiency of this sensor. Indeed, some additional calibrations were conducted after the test, and the results showed some inertia of this TDR sensor: in the full range from 0 to 100%, no difference with other sensors was observed; however, in a limited range, a clear difference was identified. Thereby, the results by this sensor were not considered in further analysis.

The data of suction and volumetric water content recorded allowed the WRC of the interlayer soil to be determined. The results are presented in Fig. 10 with three paths corresponding to Drainage 1-Evaporation 1 (Drying 1), Saturation 2 (Wetting 2) and Drainage 1-Evaporation 2 (Drying 2). It can be observed that the results of two drying processes are close. In contrast, the result of wetting path lies above. Note that because the minimum recording interval of TDR was every minute and the wetting process took place very quickly; there are less data for the wetting path. The model of van Genuchten (1980) was used to fit the experimental data with the parameters presented in Table 3.

105
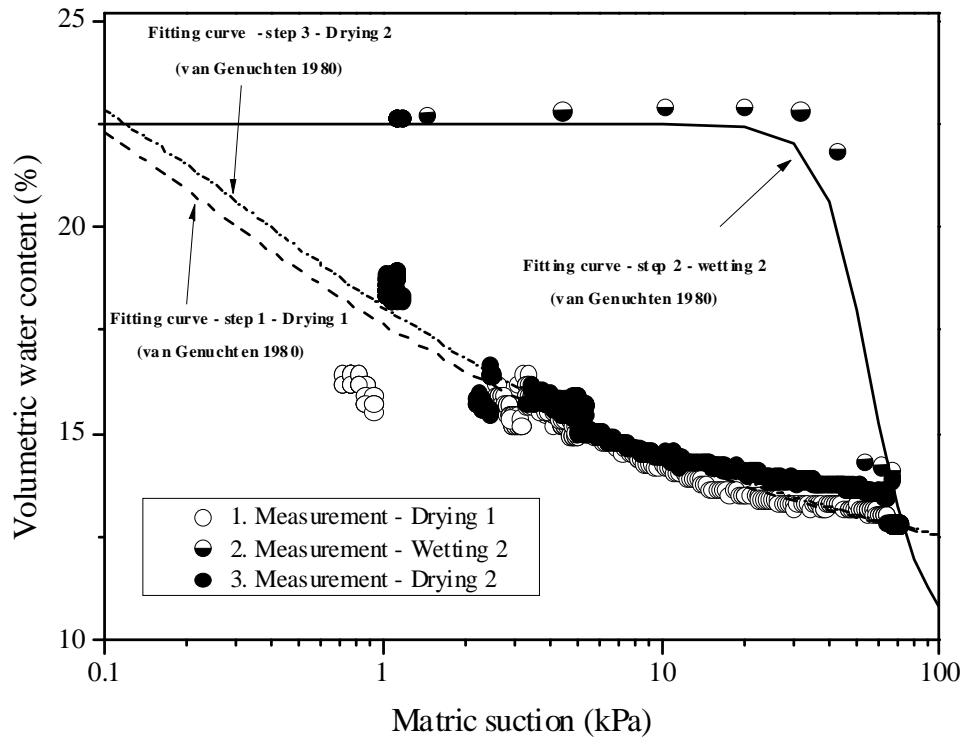
Fig. 10: WRC of *ITL₁₀* with fitting curves using the van Genuchten's model (1980)

Table 3: Parameters of the van Genuchten's model (1980) for the soil water retention curves of interlayer soil

Formula	Natural interlayer soil (*ITL₀*)	Interlayer soil with 10% sub-soil added (*ITL₁₀*)		
	Drying	Drying 1	Wetting 2	Drying 2
$\theta = \theta_r + \dfrac{\theta_s - \theta_r}{\left[1 + (\alpha h)^n\right]^m}$	$\theta_s = 25$	$\theta_s = 25$	$\theta_s = 22.5$	$\theta_s = 25$
	$\theta_r = 0$	$\theta_r = 10$	$\theta_r = 10$	$\theta_r = 10$
	$\alpha = 4$	$\alpha = 159.62$	$\alpha = 0.19$	$\alpha = 113.45$
	$n = 1.17$	$n = 1.24$	$n = 5.24$	$n = 1.25$
	$m = 0.15$	$m = 0.19$	$m = 0.81$	$m = 0.2$

Notes: θ is volumetric water content (%); θ_s is the volumetric water content at saturated state (%); θ_r is the residual volumetric water content (%); h is hydraulic head in meter; α, n, m are the model's parameters

The hydraulic conductivity versus suction is presented in Fig. 11, including the hydraulic conductivity measured at saturated state, equal to 1.67×10^{-5} m/s. It can be seen that the results for the two drying paths are similar, suggesting negligible microstructure changes. For the wetting path, all results lie above those of the drying paths, illustrating a clear phenomenon of hysteresis. The models of van Genuchten (1980) and Brooks-Corey (Brooks and Corey 1964; Stankovich and Lockington 1995) were used for fitting the data of both drying and wetting paths using the least squares method (see Fig. 11). The parameters determined are presented in Table 4.

Table 4: Parameters of the van Genuchten's model and Brooks-Corey's model for the hydraulic conductivity of *ITL$_{10}$* and *Fines*

Model	Formula	Soil	Drying path	Wetting path
van Genuchten	$k = k_s \dfrac{1 - (\alpha h)^{n-2}\left[1 + (\alpha h)^n\right]^{-m}}{\left[1 + (\alpha h)^n\right]^{2m}}$	*ITL$_{10}$*	$\alpha = 7.16$	$\alpha = 0.5$
			$n = 2.12$	$n = 2.4$
			$m = 0.06$	$m = 0.17$
		Fines	$\alpha = 2.1$	$\alpha = 0.25$
			$n = 2.06$	$n = 2.37$
			$m = 0.03$	$m = 0.15$
		For the two soils	$\alpha = 2.2$	$\alpha = 0.3$
			$n = 2.1$	$n = 2.7$
			$m = 0.05$	$m = 0.16$
Brooks-Corey	$k = k_s \left(\dfrac{s_a}{s}\right)^{2+3\lambda}$	*ITL$_{10}$*	$s_a = 0.3$	$s_a = 4$
			$\lambda = 0.05$	$\lambda = 0.1$
		Fines	$s_a = 0.7$	$s_a = 7$
			$\lambda = 0.01$	$\lambda = 0.01$
		For the two soils	$s_a = 0.74$	$s_a = 5.4$
			$\lambda = 0.03$	$\lambda = 0.02$

Notes: k is the hydraulic conductivity; k_s is the hydraulic conductivity in saturated state; h is hydraulic head in meter; s is the suction (kPa); s_a is the air-entry value (kPa); λ, α, n, m are parameters of the models.
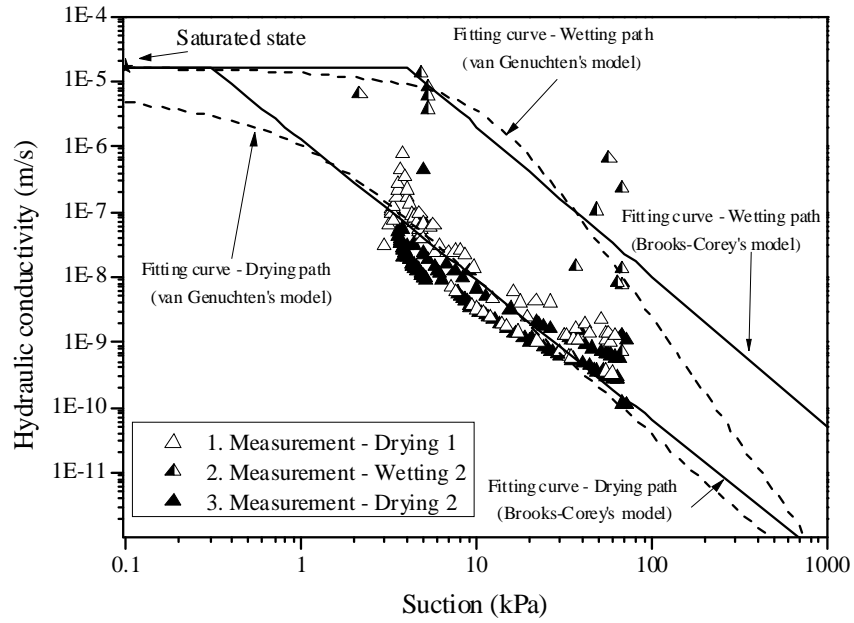
Fig. 11: Hydraulic conductivity of *ITL$_{10}$* obtained with drying-wetting cycles
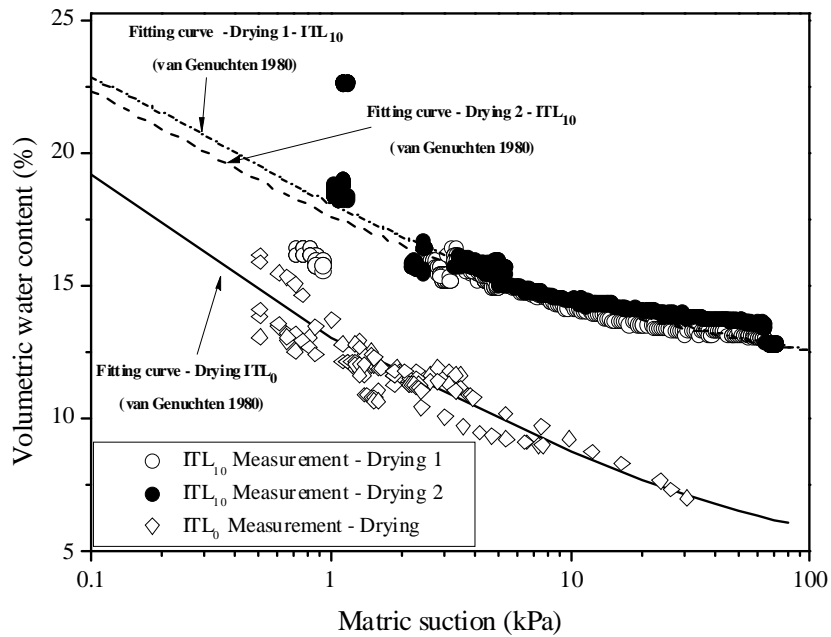
Fig. 12: Comparison of SWRC between *ITL$_0$* and *ITL$_{10}$*

Fig. 12 presents the comparison between the WRC of *ITL$_0$* and *ITL$_{10}$* for the drying path (the parameters of van Genuchten's model (1980) used for fitting the experimental data are presented in Table 3). Note that for clarity, the scattered data at low suction are not included. The WRC of *ITL$_0$* is beneath the WRC of *ITL$_{10}$*, suggesting that at a given suction, *ITL$_{10}$* has a higher water content

than ITL_0. This appears normal because with the same dry unit mass, the higher the fines content, the higher the retention capacity.

The comparison of hydraulic conductivity between ITL_0 and ITL_{10} is presented in Fig. 13. In the saturated state, the two soils have almost the same value: 1.67×10^{-5} m/s for ITL_{10} and 1.75×10^{-5} m/s for ITL_0. Both values are lower than the critical value proposed by Selig and Waters (1994) for the railway substructures. In unsaturated state, even the data are scattered for the two soils, an identical trend can be identified: the hydraulic conductivity is decreasing with the increase of suction. Moreover, the average value for ITL_{10} is slightly higher than that for ITL_0, suggesting a slightly greater hydraulic conductivity for ITL_{10}. On the whole, the difference between the hydraulic conductivity results of two soils is less evident than the difference between the SWRC results.
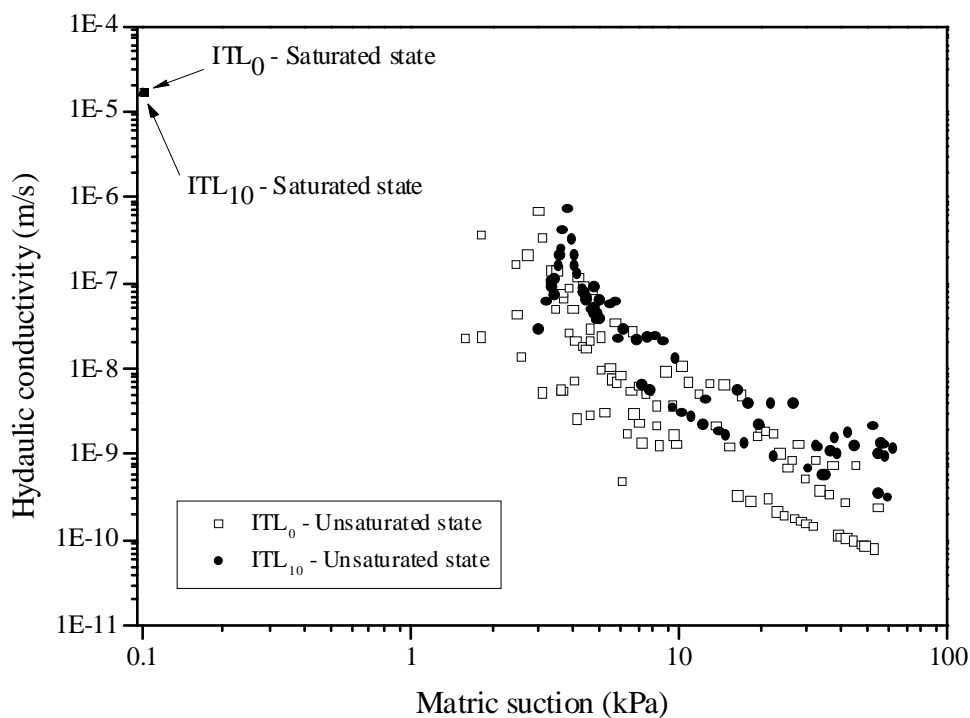
Fig. 13: Comparison of hydraulic conductivity between *ITL$_0$* and *ITL$_{10}$*

The results obtained from the small-scale infiltration test on *Fines* are shown in Fig. 14 to Fig. 18. After installation of the tensiometers, a period of 18 hours was needed to reach the suction equilibrium at 70 – 83 kPa (Fig. 14). This difference in final suctions at different levels was mainly related to the soil heterogeneity. The corresponding degree of saturation was 43%. From this initial state, the soil was first re-saturated by injecting water from the bottom with a constant water head of 0.7 kPa. The suction at the lowest level changed first, followed by the suctions at higher levels

(Fig.15). Ten minutes after the water injection, water appeared on the upper surface and suctions at all level reached zero, indicating the full saturation of the soil specimen.
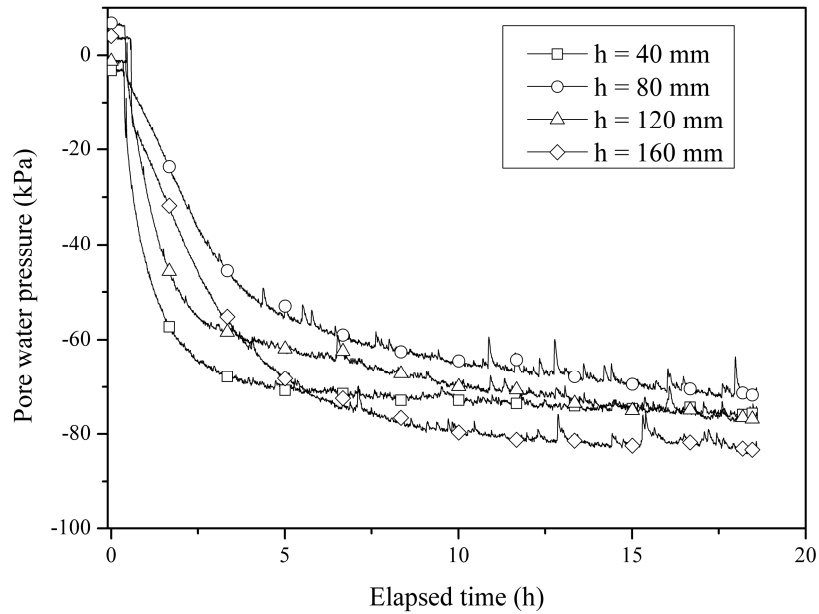
Fig. 14: Test on *Fines*: suction stabilization after the installation of tensiometers

After Saturation 1, water was drained out to an outside water source and the water level was maintained at h = 0. Afterwards, Evaporation 1 took place. The results obtained are shown in Fig. 16. Fifteen hours later, the pore water pressure measured at h = 160 mm (40 mm below the soil surface) started to decrease and reached -300 kPa at 57 hours. The changes in water pressures measured by other tensiometers were less significant.

Fig. 15: Test on *Fines*: suction evolutions during Saturation 1

110
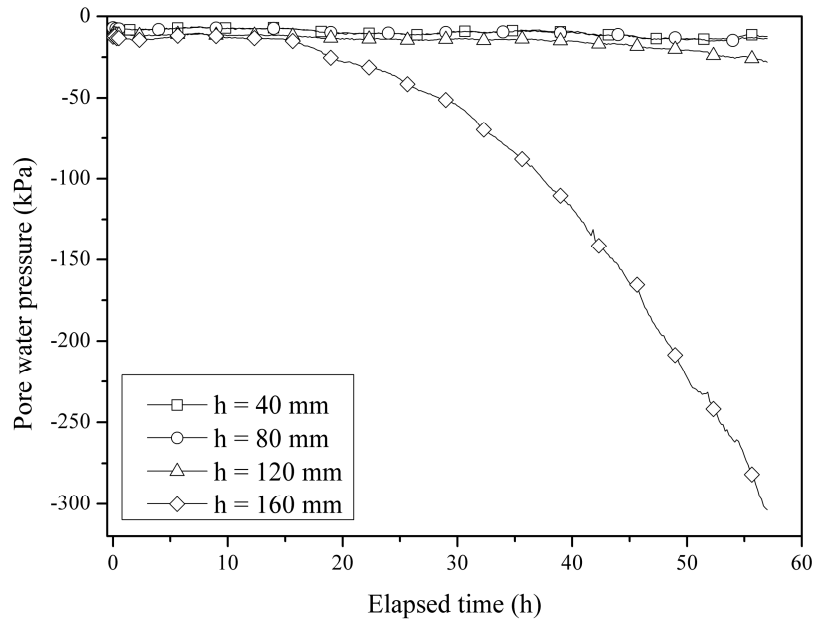
Fig. 16: Test on *Fines*: suction evolutions during Evaporation 1

Saturation 2 took place right after Evaporation 1. The results obtained during this second wetting stage are shown in Fig. 17. Less than 2 minutes was required for the pore water pressure at h = 160 mm to come back from -300 kPa to about 0. The results obtained during the subsequent drying are shown in Fig. 18 (Evaporation 2). As in the case of Evaporation 1, after 80 hours, the pore water pressure at h = 160 mm decreased to - 365 kPa while those at other levels did not change significantly.
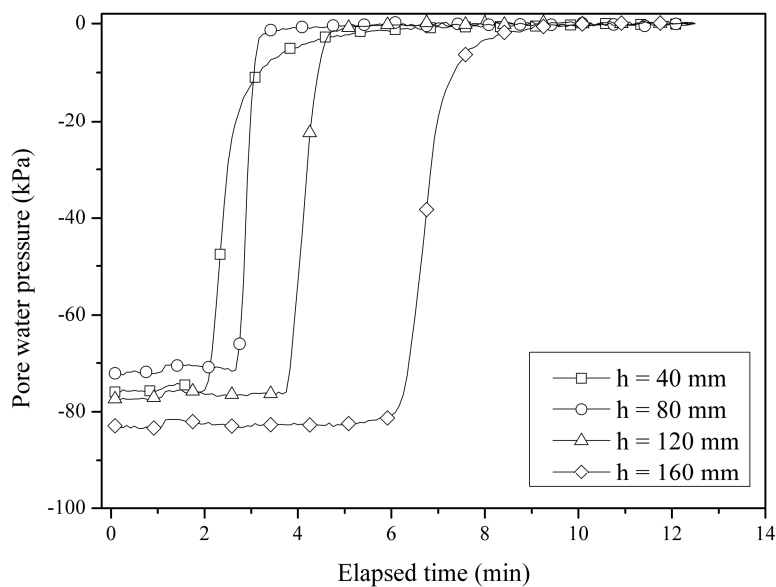

Fig. 17: Test on *Fines*: suction evolutions during Saturation 2

111

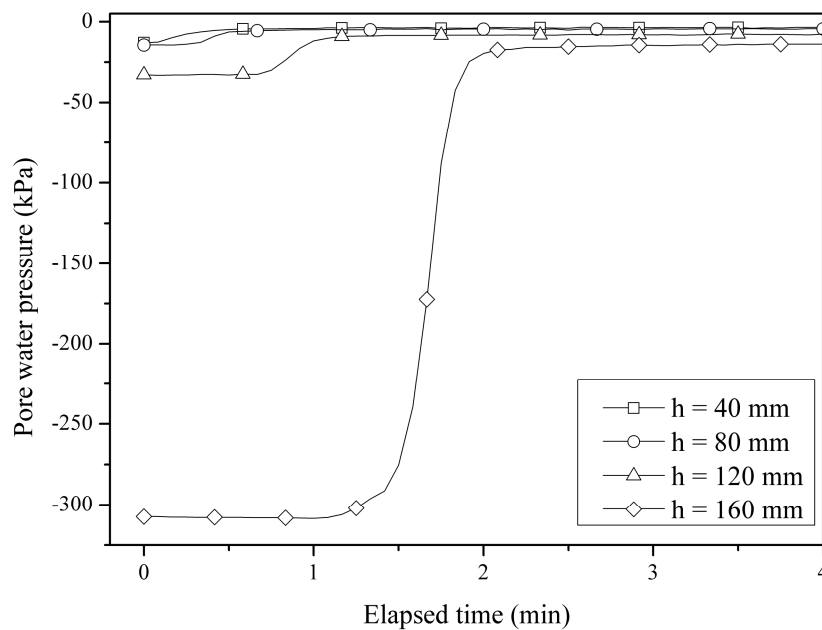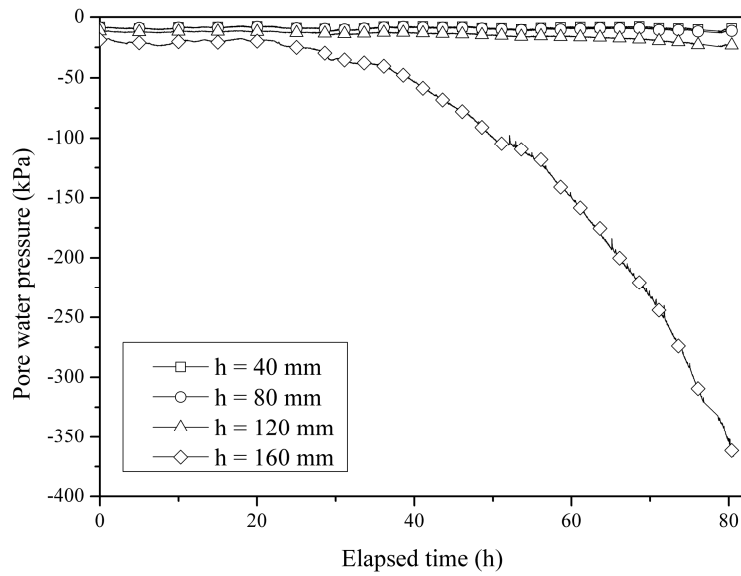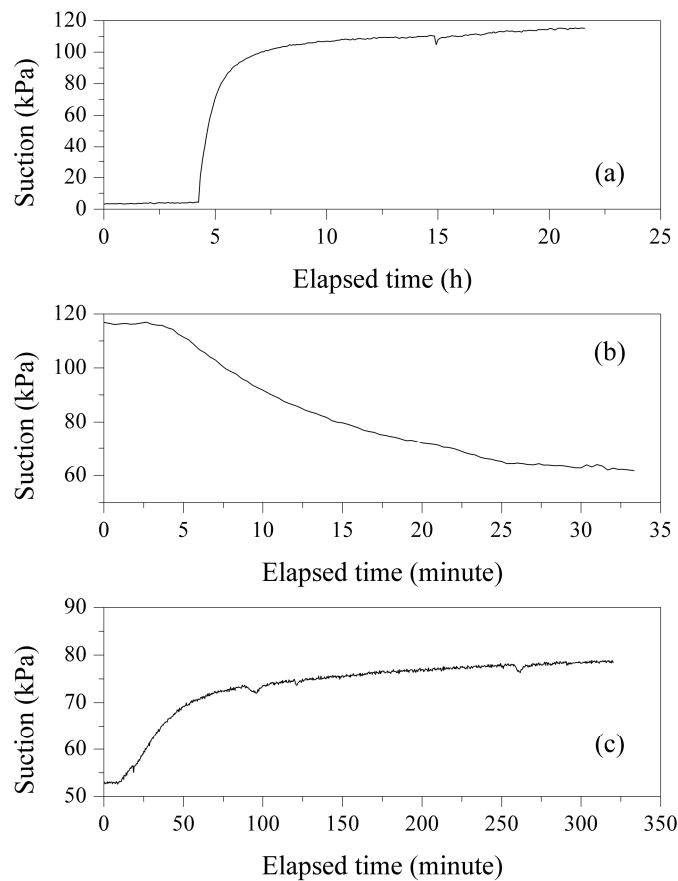**Fig. 18: Test on *Fines*: suction evolutions during Evaporation 2**

Fig. 19: Stabilization of suction during the SWRC determination. (a) initial stabilization after tensiometer installation, (b) a wetting stage, (c) a drying stage

The results from the test in the tensiometer-equipped oedometer are shown in Fig. 19. Fig. 19a depicts the suction (negative pore water pressure given by the tesiometer) evolution after the tensiometer installation. The suction increased and reached its stabilization value of 110 kPa after 17 hours. This corresponds to the initial state of the soil specimen (21.3 % volumetric water content and 42.6 % degree of saturation). Water was then added into the specimen to follow the wetting path. The variation of the first step of wetting is presented in Fig. 19b. About 35 minutes was needed for suction stabilization. The volumetric water content in this step increased from 21.3% to 21.7%. This operation was repeated until the soil reached the near saturated state. Then the drying steps started. Fig. 19c presents the suction stabilization during one drying step. An equilibrium value of 79 kPa was reached after 320 minutes. This suction increase corresponded to a decrease of volumetric water content from 22.2% to 21.6%.

The SWRC obtained for *Fines* is shown in Fig. 20. From its initial state, the soil specimen was subjected to wetting up to 70% degree of saturation, followed by drying and finally a second wetting till full saturation. It can be seen that the SWRC obtained during drying lies above that during wetting. The maximum suction value was 390 kPa corresponding to a volumetric water content of 18.9%; it was also close to the maximum suction value in the specimen during the infiltration test, indicating the compatibility of the two tests.
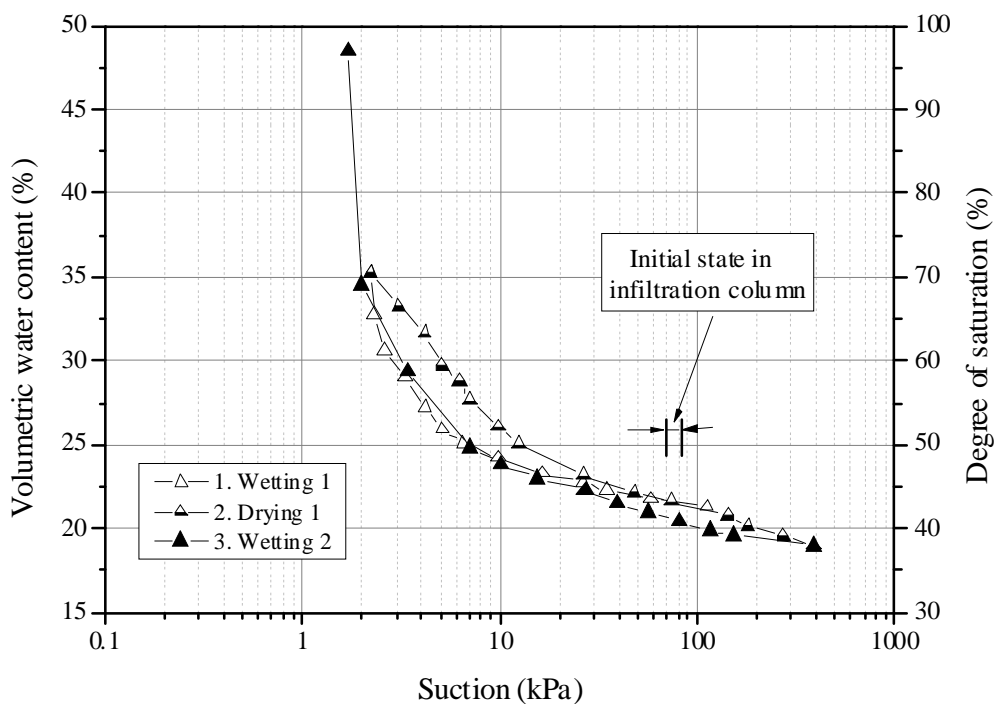
Fig. 20: WRC of *Fines*

This SWRC determined was then used to calculate the changes of volumetric water content in the small-scale infiltration column based on the suction changes presented in Fig. 15 to Fig. 18. Either the drying or the wetting path was used depending on the path followed in the infiltration test. As the second drying path of SWRC was not available, the first drying path was used for calculating the volumetric water content during the second drying path in the infiltration test. Then, based on the profiles of suction and water content, the hydraulic conductivity of compacted *Fines* was calculated. The results are shown in Fig. 21, including the hydraulic conductivity measured at saturated state by applying a constant water pressure of 0.7 kPa: 2.6×10^{-6} m/s. Albeit the large data scatter, a clear trend can be observed: as for the interlayer soil, the hydraulic conductivity increased when the suction decreased.
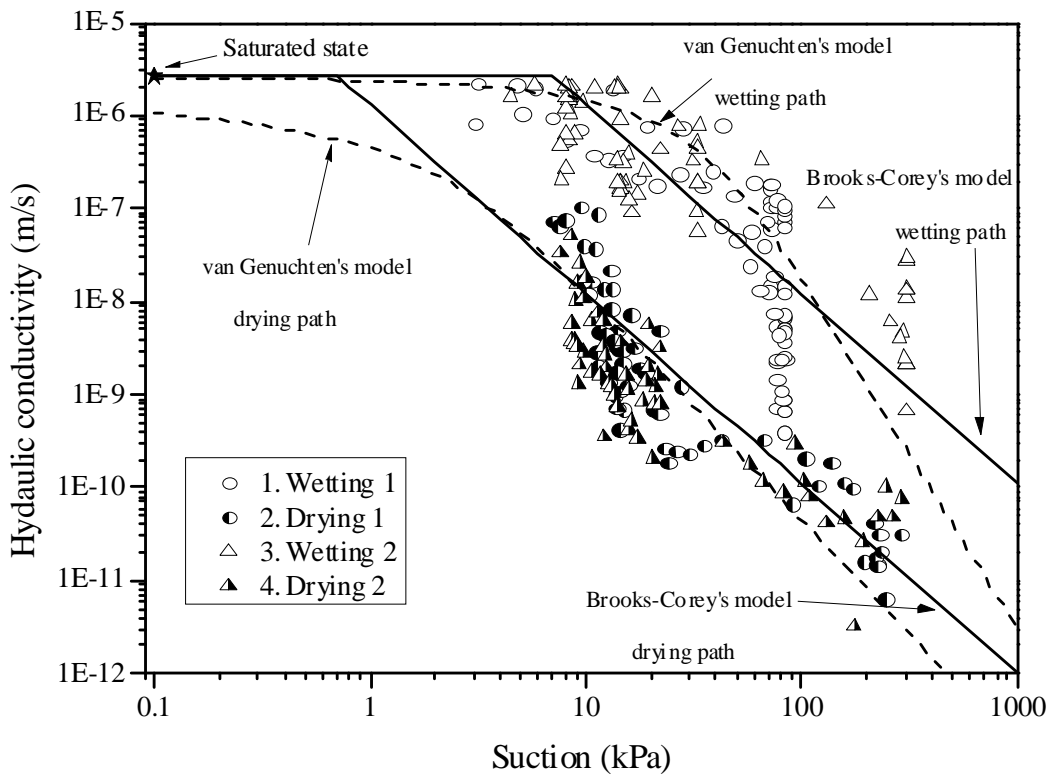
Fig. 21: Hydraulic conductivity of *Fines*, obtained with drying/wetting cycles

It is worth noting that the results obtained for the two drying paths are quite similar. The same conclusion can be drawn for the two wetting paths. The models of van Genuchten (1980) and Brooks-Corey (Brooks and Corey 1964; Stankovich and Lockington 1995) were used to fit the results (Fig. 21), and the parameters determined are presented in Table 4. Comparison between the drying and wetting curves shows that for the 2 wetting/drying cycles, the wetting curves lie always above the drying curves. It is opposed to the SWRC where the wetting curves are normally beneath

the drying ones. In addition, the curves of wetting path and drying path of the 1st cycle are close to those corresponding to the 2nd cycle, suggesting no effect of wetting/drying cycles on the hydraulic conductivity. The smallest value of hydraulic conductivity identified is 6×10^{-12} m/s corresponding to a suction value of 242 kPa, while the highest one is 2.6×10^{-6} m/s corresponding to the saturated state.
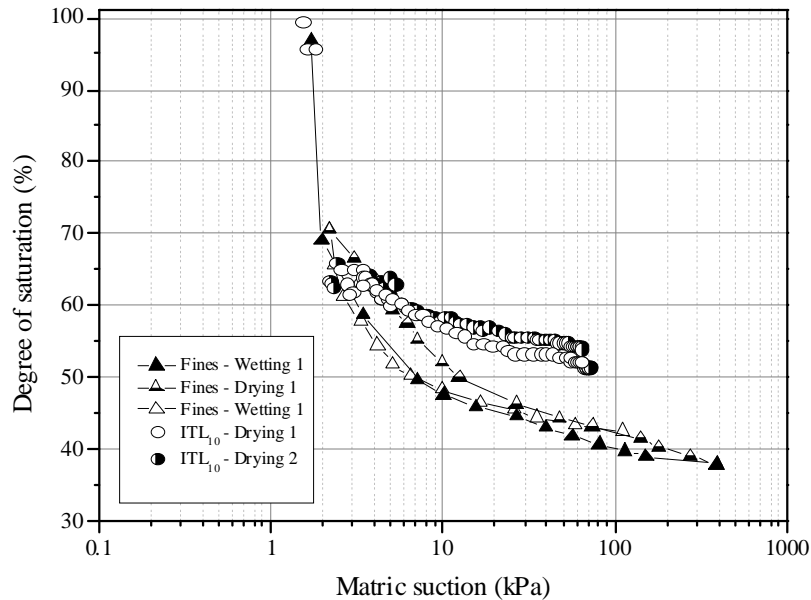
Fig. 22: Comparison of SWRC between *ITL$_{10}$* and *Fines*

Fig. 22 depicts the comparison of SWRC between *ITL$_{10}$* and *Fines* in the plane of degree of saturation versus suction. The two curves start from almost the same point - around 97% degree of saturation and 1.7 kPa suction. From 3 kPa suction, the WRC of *ITL$_{10}$* starts to separate from the WRC of *ITL$_{0}$*. The two curves are parallel (for drying path) from 10 kPa suction. The curves of *ITL$_{10}$* stop at 71 kPa while the curves of *Fines* stop at 389 kPa due to the different capacities of the tensiometers used for the two soils. The gap between two curves is about 10% of degree of saturation at the end of the curve for *ITL$_{10}$*.

In Fig. 23, the hydraulic conductivity of *ITL$_{10}$* and *Fines* is plotted versus suction. It can be observed that the wetting and drying curves of the interlayer soil are quite close to those of *Fines*, suggesting that the hydraulic conductivity of the interlayer soil is mainly governed by the hydraulic conductivity of the fines contained in it. In other words, water transfer in the interlayer soil takes place mainly through the network of pores between fine particles, coarse elements like ballast behaving as inert materials. This is confirmed by the hydraulic conductivity values at saturated state: similar values were identified - 1.67×10^{-5} m/s for *ITL$_{10}$* against 2.6×10^{-6} m/s for *Fines*.

115

From a practical point of view, Fig. 23 shows that to determine the hydraulic conductivity of interlayer soils, it is not necessary to use large-scale experimental devices to match the soil grain size; smaller devices can be used to determine their hydraulic conductivity by testing the fine particles only, provided that equivalent dry density is accounted for.
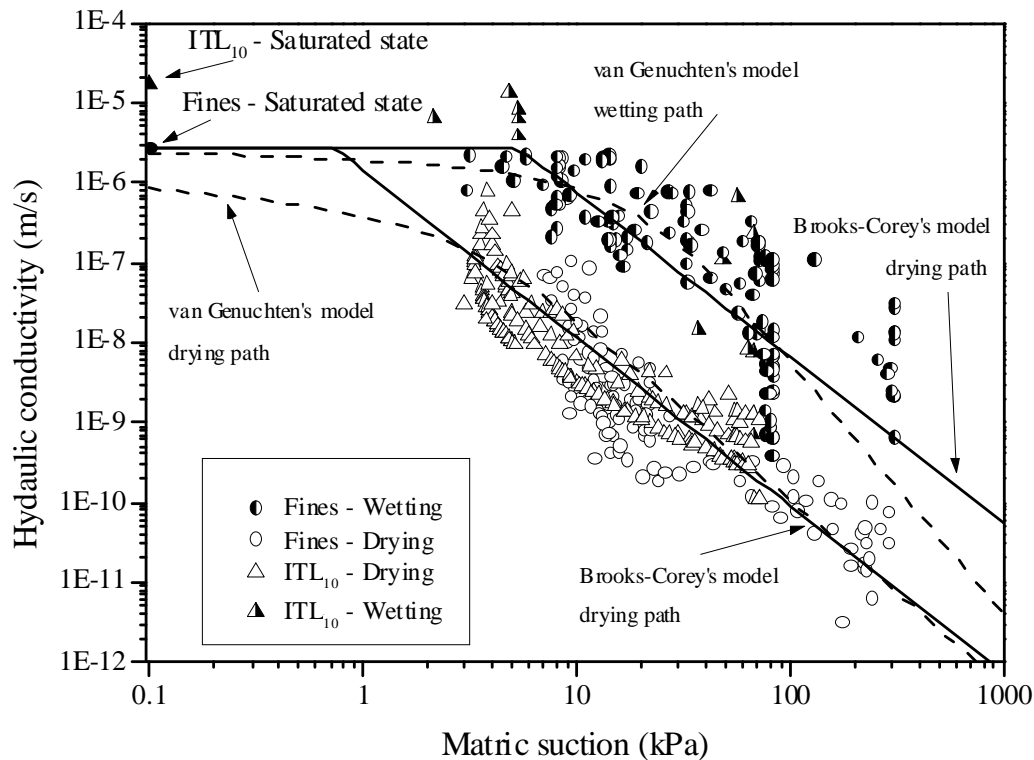
Fig. 23: Comparison of hydraulic conductivity between *ITL$_{10}$* and *Fines*

Discussions

Fig. 11 and Fig. 21 show the uncommon phenomenon of hystersis observed in hydraulic conductivity of *ITL$_{10}$* and *Fines*, respectively. The curve of wetting path lies above the curve of drying path. The same phenomenon was observed by Wayllace and Lu (2011). The following interpretations can be attempted.

Due to the different kinetic between the fast liquid transfer in wetting and the long vapor transfer in drying, the time needed for drying was much longer than that for wetting. This phenomenon was also reported by Toker et al. (2004) and discussed by Munoz-Castelblanco et al. (2012). A higher hydraulic conductivity can be expected in that case for wetting path.

In the present work, the calculation of hydraulic conductivity was performed based on the suction evolution given by tensiometers. Assuming that in the compacted soils, both macro-pores and

micro-pores existed. During wetting, the macro-pores were filled with water more quickly than micro-pores. Moreover, in the micro-pores, there were always air bubbles preventing the total saturation. In contrast, during drying, all pores (micro and macro) participated in the evaporation process. As a result, when water filled the macro-pores, the tensiometers immediately gave the suction changes corresponding to the water flow through the macro-pores, even though the suction in micro-pores would be higher. On the contrary, when water evaporates during drying, the tensiometers gave the suction changes that involve both macro and micro-pores, in a much slower fashion. In other words, the suction measured by the tensiometers was probably under-estimated for wetting paths. Côté and Roy (1998) also reported that one re-saturating stage is not enough to fully saturate a soil sample because of the air bubbles trapped in micro-pores. This can also explain the uncommon hysteresis mentioned before.

Poulovassilis (1969) (cited by Mualem 1976) considered, in a qualitative way, the influence of capillary hysteresis on the hydraulic conductivity based on the concept of independent domain theory. He defined two mechanisms related to hysteresis: (i) water fills pores of larger opening radius in a wetting process than in drying one; (ii) the pores configuration and interconnection may be different for wetting and drying. As a result, the hydraulic conductivity in wetting may be different from that in drying for the same water content. The theory about the difference between the opening radius affecting wetting process and the opening radius affecting drying process is known as the effect of ink-bottle (Bertotti and Mayergoyz 2006; Naumov 2009). According to this theory, the pores affecting the wetting curve are larger than the pores affecting the drying curve. As a result, the water transfer is faster during wetting than during drying, implying a higher hydraulic conductivity in the case of wetting.

Conclusions

Infiltration tests were performed on the interlayer soil (ITL_0) and its derived soils - adding 10% of sub-grade to form ITL_{10} and sieving ITL_{10} at 2 mm to form *Fines*. Two wetting/drying cycles were applied for each test. The obtained results allowed the effect of fine particles on the water retention capacity and hydraulic conductivity of interlayer soil to be analyzed.

The effect of wetting/drying cycles on hydraulic conductivity was found negligible - the results of the first cycle are quite similar to those of the second cycle, suggesting an insignificant microstructure change by wetting/drying cycles.

Hysteresis exists for both the soil water retention curve and the hydraulic conductivity changes with suction. The wetting process was found to be much faster than the drying process, and the hydraulic conductivity during wetting is always higher than that during drying. This can be explained by the effect of ink-bottle and the difference between the water transfer through the network of macro-pores and micro-pores.

Adding 10% fine particles to the natural interlayer soil changes the soil water retention curve but does not induce significant changes in hydraulic conductivity. In saturated state, the hydraulic conductivity of natural interlayer soil is 1.75×10^{-5} m/s, while the value of the soil with 10% fines added is 1.67×10^{-6} m/s. In unsaturated state, even though the results are little scattered, the results of ITL_{10} are within the variation range of the results of ITL_0. However, it is worth noting that the mean value of ITL_{10} is slightly greater than that of ITL_0.

The water retention curves of ITL_{10} and *Fines* are different, illustrating an obvious effect of soil texture. On the contrary, in terms of hydraulic conductivity including the values in saturated sate, a good agreement was identified between the results of two soils, regardless of the drying or wetting paths. This suggests that water transfer in the interlayer soil takes place mainly through the network of pores between fine particles, coarse elements like ballast behaving as inert materials. From a practical point of view, this finding shows that to determine the hydraulic conductivity of interlayer soils, a device as small as the small-scale infiltration cell can be employed to determine the hydraulic conductivity of interlayer soil by testing the fine particles only, provided that equivalent dry density is taken into account.

Acknowledgements

References

Alobaidi, I., and Hoare, D. 1996. The development of pore water pressure at the sub-grade-subbase interface of a highway pavement and its effect on pumping of fines. Geotextiles and geomembranes, **14**: 111-135.

Alobaidi, I., and Hoare, D. 1998. The role of geotextile reinforcement in the control of pumping at the sub-grade-subbase interface of highway pavements. Geosynthetics International, **5**(6): 619–636.

AFNOR. 2005. Identification and classification of soil- Part 2: Principles for a classification. NF EN ISO 14688.

Anbazhagan, P., Lijun, S., Buddhima, I., and Cholachat, R. 2011. Model track studies on fouled ballast using ground penetrating radar and multichannel analysis of surface wave. Journal of Applied Geophysics, **74**(4): 175–184.

ASTM 2010. Standard test method for measurement of hydraulic conductivity of unsaturated soils. D7664-10.

Ayres, D. 1986. Geotextiles or geomembranes in track? British railways' experience. Geotextiles and Geomembranes, **3**(2-3): 129–142.

Babic, B., Prager, A., and Rukavina, T. 2000. Effect of fine particles on some characteristics of granular base courses. Materials and Structures, **7**(33): 419-424.

Bertotti, G., and Mayergoyz, I. D. 2006. The science of hysteresis III. Academic Press

Brooks, R.H., and Corey, A.T., 1964. Hydraulic properties of porous media. Hydro. Paper No.3, Colorado State Univ., Fort Collins, Colo.

Bruckler, L. B., Angulo-Jaramillo, P., and Ruy, R. 2002. Testing an infiltration method for estimating soil hydraulic properties in the laboratory. Soil Science Society of America Journal, **66**: 384–395.

Cabalar, A. 2008. Effect of fines content on the behavior of mixed specimens of a sand. Electronic Journal of Geotechnical Engineering, **13**(D): 1-11.

Côté, J., and Roy, M. 1998. Conductivité hydraulique de matériaux de fondations de chaussées partiellement saturés (In French). Rapport de l'études et recherches en transports du Québec, 177p.

Cui, Y.J., Duong, T.V., Tang, A.M., Dupla, J.C., Calon, N., and Robinet, A. 2013. Investigation of the hydro-mechanical behaviour of fouled ballast. Journal of Zhejiang University-Science A (Applied Physics & Engineering), **14**(4): 244-255.

Cui, Y. J., Tang, A. M., Mantho, A., and Delaure, E. 2008. Monitoring field soil suction using a miniature tensiometer. Geotechnical Testing Journal, **31**(1) : 95-100.

Cui, Y. J., Tang, A. M., Loiseau, C., and Delage, P. 2008. Determining the unsaturated hydraulic conductivity of a compacted sand-bentonite mixture under constant-volume and free-swell conditions. Physics and Chemistry of the Earth, Parts A/B/C, 33: S462–S471.

Cunningham, M., Ridley, A., Dineen, K., and Burland, J. 2003. The mechanical behaviour of a reconstituted unsaturated silty clay. Géotechnique, **53** (2): 183-194.

Daniel, D. E. 1982. Measurement of hydraulic conductivity of unsaturated soils with thermocouple psychometers. Soil Science Society of American Journal, **46**(6): 1125–1129.

Delage, P., and Cui, Y. J. 2001. Comportement mécanique des sols non saturés. Article C302. Ed. Techniques Ingénieur.

Duong, T. V., Tang, A. M., Cui., Y. J., Trinh, V. N., and Calon, N. 2013. Development of a large-scale infiltration column for studying the hydraulic conductivity of unsaturated fouled ballast. Geotechnical Testing Journal, **36**(1): 55-63.

Ebrahimi, A. 2011. Behavior or fouled ballast. Railway Track and Structures, **107**(8): 25–31.

Fortunato, E., Pinelo, A., and Matos Fernandes, M. 2010. Characterization of the fouled ballast layer in the substructure of a 19th century railway track under renewal. Soils and Foundations, **50**(1): 55–62.

Ghataora, G., Burns, B., Burrow, M., and Evdorides, H. 2006. Development of an index test for assessing anti-pumping materials in railway track foundations. Proc.,First International Conference on Railway Foundaitons. 355–366.

Giannakos, K. 2010. Loads on track, ballast fouling, and life cycle under dynamic loading in railways. Journal of Transportation Engineering, **136**(12): 1075–1084.

Gong, Y., Cao, Q., and Sun, Z. 2003. The effects of soil bulk density, clay content and temperature on soil water content measurement using time-domain reflectometry. Hydrological Processes, **17**(18): 3601–3614.

Huang, H., Tutumluer, E., and Dombrow, W. 2009. Laboratory characterization of fouled railroad ballast behavior. Transportation Research Record: Journal of the Transportation Research Board, **2117**(1): 93–101.

Indraratna, B., Salim, W., and Rujikiatkamjorn, C. 2011. Advanced Rail Geotechnology - Ballasted Track. CRC Press.

Jacobsen, O. H., and Schjønning, P. 1993. A laboratory calibration of time domain reflectometry for soil water measurement including effects of bulk density and texture. Journal of Hydrology, **151**(2-4): 147–157.

Kim, D., Sagong, M., and Lee, Y. 2005. Effects of fine aggregate content on the mechanical properties of the compacted decomposed granitic soils. Construction and Building Materials, **19**(3): 189–196.

Le, T.T., Cui, Y.J., Muñoz, J.J., Delage, P., Tang, A.M., and Li; X.L. 2011. Studying the stress-suction coupling in soils using an oedometer equipped with a high capacity tensiometer. Frontiers of Architecture and Civil Engineering in China **5**(2): 160-170.

Lourenço, S. 2008. Suction measurements and water retention in unsaturated soils. PhD dissertation, Durham University.

Lourenço, S., Gallipoli, D., Toll, D., Augarde, C., and Evans, F. 2011. A new procedure for the determination of soil-water retention curves by continuous drying using high-suction tensiometers. Canadian Geotechnical Journal, **48**(2): 327-335

Mayoraz, F., Vulliet, L., and Laloui, L. 2006. Attrition and particle breakage under monotonic and cyclic loading. Comptes Rendus Mécanique, **334**(1): 1–7.

Mualem, Y. 1976. Hysteretical models for prediction of the hydraulic conductivity of unsaturated porous media. Water Resources Research, **12**(6): 1248-1254.

Munoz, J. J., De Gennaro, V., and Delaure, E. 2008. Experimental determination of unsaturated hydraulic conductivity in compacted silt. In Unsaturated soils: advances in geo-engineering: proceedings of the 1st European Conference on Unsaturated Soils, E-UNSAT 2008, Durham, United Kingdom, 2-4 July 2008, pp.123-127.

Munoz-Castelblanco, J. A., Pereira, J. M., Delage, P., and Cui, Y. J. 2012. The water retention properties of a natural unsaturated loess from northern France. Géotechnique, **62**(2): 95-106.

Naumov, S. 2009. Hysteresis phenomenon in Mesoporous Materials. PhD Dissertation, University of Leipzig.

Naeini, S., and Baziar, M. 2004. Effect of fines content on steady-state strength of mixed and layered specimens of a sand. Soil Dynamics and Earthquake Engineering, **24**(3): 181–187.

Pedro, L. 2004. De l'étude du comportement mécanique de sols hétérogènes modèles à son application au cas des sols naturels. PhD disertation, Ecole Nationale des Ponts et Chaussées, France. (In French).

Poulovassilis, A. 1969. The effect of hysteresis of pore water on the hydraulic conductivity. Soil Science, **20**: 52-56.

Schneider, J. M., and Fratta, D. 2009. Time-domain reflectometry - parametric study for the evaluation of physical properties in soils. Canadian Geotechnical Journal, **46**(7): 753–767.

Selig, E. T., and Waters, J. M. 1994. Track geotechnology and substructure management. Thomas Telford.

Seif El Dine, S., Dupla, J., Frank, R., Canou, J., and Kazan, Y. 2010. Mechanical characterization of matrix coarse-grained soils with a large-sized triaxial device. Canadian Geotechnical Journal, **47**(4): 425–438.

Stankovich J. M., and Lockington, D. A., 1995. Brooks-Corey and van Genuchten, soil-water-retention models. Journal of Irrigation and Drainage Engineering, 121(1): 1-7.

Stolte, J., Veerman, M ., Wosten, G. J., Freijer, J. H. M., Bouten, J. I ., Dirksen, W., Van Dam, C., and Van den Berg, J.C. 1994. Comparison of six methods to determine unsaturated soil hydraulic conductivity. Soil Science Society of America Journal, **58**(6): 1596-1603.

Sussmann, T. R., Ruel, M., and Christmer, S. 2012. Sources, influence, and criteria for ballast fouling condition assessment. Proc., 91st Annual Meeting of the Transportation Research Board. 11p.

Tennakoon, N., Indraratna, B., Rujikiatkamjorn, C., Nimbalkar, S., and Neville, T. 2012. The role of ballast-fouling characteristics on the drainage capacity of a rail substructure. Geotechnical Testing Journal, **35**(4): 1-12.

Toker, N., Germaine, J., Sjoblomt, K. and Culligan, P. 2004. A new technique for rapid measurement of continuous soil moisture characteristic curves. Géotechnique, **54**(3): 179-186.

Toll, D., Lourenço, S., and Mendes, J. 2012. Advances in suction measurements using high suction tensiometers. Engineering Geology. doi.org/10.1016/j.enggeo.2012.04.013.

Topp, G. C., Davis, J. L., and Annan, A. P. 1980. Electromagnetic determination of soil water content: measurements in coaxial transmission lines. Water Resource Research, (16): 574-582.

Trinh, V.N. 2011. Comportement hydromécanique des matériaux constitutifs de plateformes ferroviaires anciennes. (In French). PhD Dissertation, Ecole Nationales des Ponts et Chaussées - Université Paris – Est.

Trinh, V. N., Tang, A. M., Cui, Y. J., Canou, J., Dupla, J.C., Calon, N., Lambert, L., Robinet, A., and Schoen, O. 2011. Caractérisation des matériaux constitutifs de plate-forme ferroviaire ancienne. (In French). Revue Française de Géotechnique, (134-135): 65–74.

Trinh, V.N., Tang, A.M., Cui, Y.J., Dupla, J.C., Canou, J., Calon, N., Lambert, L., Robinet, A., and Schoen, O. 2012. Mechanical characterisation of the fouled ballast in ancient railway track substructure by large-scale triaxial tests. Soils and Foundations, **52**(3): 511-523.

van Genuchten, M.T. 1980. A closed-form equation for predicting the hydraulic conductivity of unsaturated soils. Soil Science Society of America Journal, **44**(5): 892–898.

Verdugo, R., and Hoz, K. 2007. Strength and stiffness of coarse granular soils. Solid Mechanics and Its Application, **146**(3): 243–252.

Wayllace, A., and Lu, N. 2011. A transient water release and imbibitions method for rapidly measuring wetting and drying soil water retention and hydraulic conductivity functions. Geotechnical Testing Journal, **35**(1): 1-15.

Ye, W. M., Cui, Y. J., Qian, L. X., and Chen, B. 2009. An experimental study of the water transfer through compacted GMZ bentonite. Engineering Geology, **108**(3): 169– 176.

CHAPTER IV

Mechanisms of the degradation of ancient railway sub-structure in France

In the three previous chapters, problems related to railway sub-structure were assessed; the hydro-mechanical behavior of interlayer soil was investigated. It remains the questions about the mechanisms of interlayer creation and mud pumping. This is dealt with in this chapter.

A physical model was developed, allowing a soil sample composed of a ballast layer overlying a sub-grade layer (representing the ancient railway sub-structure just after its construction) to be tested. The effects of loading frequency, the number of cycles and most importantly the dry unit mass and water content of sub-soil were studied. This cylindrical apparatus is equipped with several sensors allowing the water content, the pore water pressure, the load and the displacement to be monitored. The evolution of the interface between the two layers was monitored too through the transparent wall of the apparatus. The results obtained allowed the driving factors for the interlayer creation and the mud pumping to be identified.

The results are presented in two papers. The details of the physical model are presented in the first paper which was submitted to ***Geotechnical Testing Journal***. The results on the mechanisms of interlayer creation and mud pumping are presented in the second paper, accepted for a publication in ***Engineering Geology***.

A physical model for studying the migration of fine particles in railway sub-structure

Trong Vinh Duong[1], Yu-Jun Cui[1], Anh Minh Tang[1], Jean-Claude Dupla[1], Jean Canou[1], Nicolas Calon[2], Alain Robinet[2], Baptiste Chabot[1], Emanuel De Laure[1]

Abstract: In order to study the creation of interlayer and the mud pumping phenomena in the ancient French railway substructure, a physical model was developed with a 160 mm thickness ballast layer overlying a 220 mm thickness artificial silt layer (mixture of crushed sand and kaolin), both layers being compacted in a cylinder of 550 mm inner diameter. One positive pore water pressure, three tensiometers and three TDR sensors were installed around the ballast/silt interface allowing the evolution of pore water pressure (negative or positive) and volumetric water content to be monitored, respectively. A digital camera was set up for monitoring the migration of fine particles. The effects of loading (monotonic and cyclic loadings) and water content state of sub-soil ($w = 16\%$, $S_r = 55\%$ and near saturated state, $S_r = 88\%$) were investigated. It was found that the development of pore water pressure in the sub-soil is the key factor causing the migration of fine particles that results in the creation of interlayer as well as the mud pumping.

Keywords: Railway substructure; physical model; cyclic loading; pore water pressure; interlayer creation; mud pumping.

Introduction

Railway sub-structure is normally constructed with several layers (ballast, sub-ballast, sub-base, sub-grade, etc.) and the characteristics of the constitutive materials for each layer are well defined. Problems related to track settlement and stability come not only from the degradation of each layer but also from the interaction between layers. Very often, fine particles migration from sub-grade results in changes of sub-structure components, corresponding to mud pumping or creation of interlayer. Mud pumping is characterized by the migration of sub-soil fine particles in the ballast layer. It was widely recognized in both the railway context (Ayres 1986, Selig and Waters 1994, Raymond 1999, Voottipruex and Roongthanee 2003, Burns et al. 2006, Gataora et al. 2006, Aw 2004, 2007, Indraratna et al. 2011) and the pavement context (Yoder 1957, Van 1985, Alobaidi and Hoare 1994, 1996, 1998a, 1998b, 1999, Zhang 2004, Yuan et al. 2007). By contrast, the interlayer has been identified and characterized only recently (Calon et al. 2010, Trinh et al. 2011, Trinh 2011, Trinh et al. 2012, Cui et al. 2013, Duong et al. 2013). Normally, this interlayer was formed mainly

---

[1] Ecole des Ponts Paris Tech (ENPC), Laboratoire Navier/CERMES
[2] French Railway Company (SNCF)

by the interpenetration between the sub-grade soil and ballast under the effect of train action. As both mud pumping and presence of interlayer can significantly affect the track mechanical behavior, it appears important to investigate the related mechanisms in-depth.

Up to now, even migration of fine particles and its consequence have been reported in several studies, the knowledge on the driving mechanisms is still limited. Indeed, in the case of interlayer, its creation is still an open question. For the mud pumping, some different mechanisms were proposed. Takatoshi (1997, cited by Voottipruex and Roongthanee 2003) reported that pumping of fine particles is due to the effect of suction generated by the upward and downward movement of ties. Differently, Alobaidi and Hoare (1996, 1999) proposed that pumping of fine particles depends mainly on the pore water pressure developed at the interface between the sub-grade and sub-base/ballast layer.

As far as the experimental work is concerned, few studies have been undertaken in the laboratory. Alobaidi and Hoare (1996) developed an apparatus from a modified 350 mm triaxial cell. Using this apparatus, the pumping of fine particles in highway pavement was investigated under 2 Hz loading on a 32 mm diameter metallic hemisphere representing the sub-base material. However, this prototype apparatus and the adopted methodology are not suitable for the railway issue (metallic hemisphere instead of ballast, low loading frequency), and in addition, the pumping level of fine particles was only recorded at the end of the test. Burns et al. (2006) and Ghataora et al. (2006) developed a 230 mm diameter steel cylinder to test a 200 mm thick sub-grade beneath a 75 mm thick ballast layer. In this case, the diameter of the cylinder seems small when considering the ballast size (about 60 mm). Moreover, the monitoring of the intermixing of sub-soil particles and ballast particle is also not allowed.

In this study, a physical model was developed, allowing the mud pumping and the creation of interlayer to be investigated. The model had a diameter of 550 mm that is believed to be large enough to minimize any size effect. The apparatus was equipped with 3 tensiometers and 3 time domain reflectometer (TDR) allowing the monitoring of pore water pressure and volumetric water content at different positions, respectively. Moreover, a digital camera was used to monitor the evolution of the interface between ballast and sub-soil.

Materials

In order to have a quantity of homogeneous sub-soil large enough for conducting the experimental investigation planned, the sub-soil used in this study was produced artificially by mixing 30% Kaolin Speswhite clay and 70 % crushed sand C10 (by dry mass). It is named henceforth *70S30K*. Fig. 1 shows the grain size distribution curves of Kaolin Speswhite clay, of the crushed sand C10 and of the mixture *70S30K*. Note that the curve of *70S30K* is close to that of the Jossigny silt, a soil widely studied worldwide for its hydro-mechanical behavior especially in the unsaturated state (see Cui and Delage 1996 for instance). The normal proctor curve of *70S30K* is plotted in Fig. 2; its hydraulic conductivity at a dry unit mass of 1.5 Mg/m^3 is 8.4×10^{-7} m/s. Some other properties are presented in Table 1.
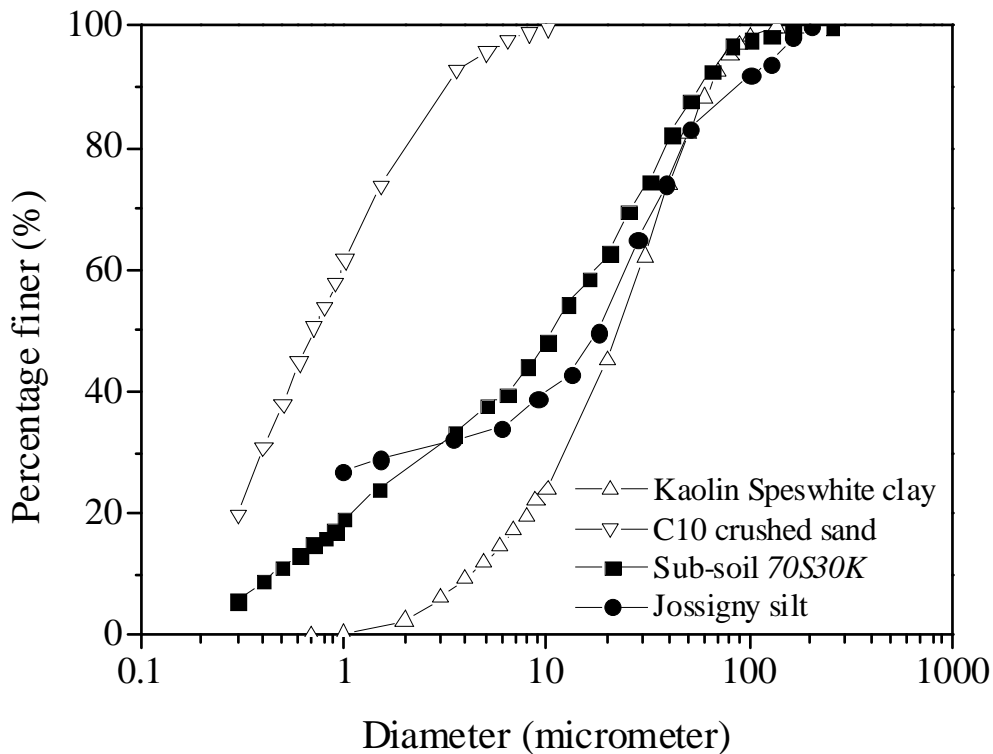

Fig. 1: Grain size distribution curve of studied material
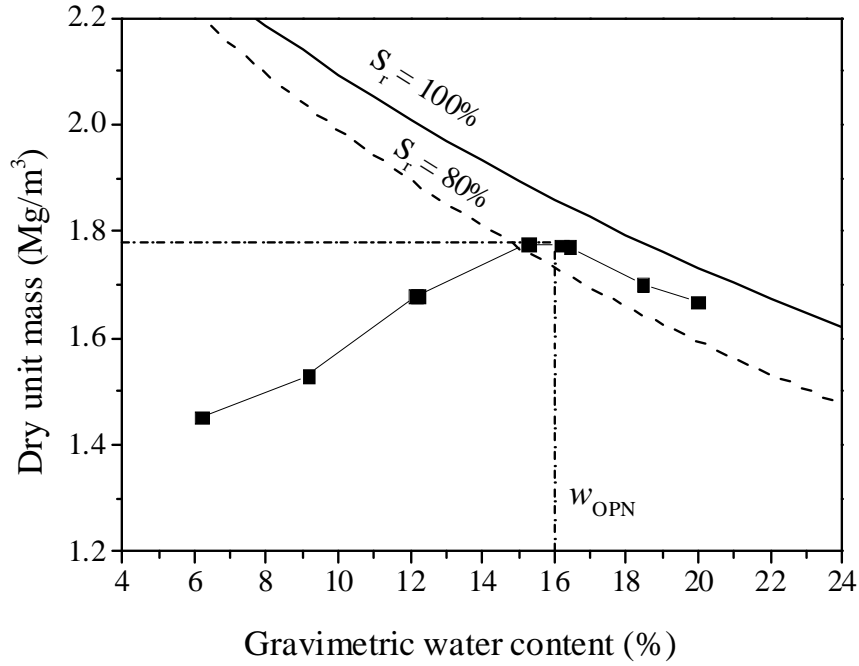
Fig. 2: Standard Proctor curve of the sub-soil

The ballast used in this study was taken from the storage of construction materials of the French Railway company (SNCF). It is a granular material with d/D = 25/50 mm. The maximum diameter of ballast is 63 mm. Detailed characteristics of the conventional ballast can be found in SNCF (1995) and Al Shaer (2005).

Table 1: Properties of sub-soil 70S30K

Parameters	Value
Specific gravity of clay G_s	2.6
Specific gravity of crushed sand G_s	2.65
Initial dry unit mass ρ_d	1.5 Mg/m^3
Porosity n	43%
Liquid Limit LL	27%
Plasticity Index IP	11%
Hydraulic conductivity K (ρ_d = 1.5 Mg/m^3)	8.4×10^{-7} m/s
Optimum water content w	16%

Experimental setup and procedures

Fig. 3 presents schematic views of the physical model including a 3D view (Fig. 3a), a side view (Fig. 3b) and a cross section (Fig. 3c). The wall was made of Poly(methyl methacrylate) (PMMA) which is a transparent thermoplastic allowing an external observation by digital camera. The transparent cell has an internal diameter of 550 mm, a wall thickness of 20 mm and a height of 600 mm. It is believed that with these dimensions, any size effect is minimized. The column has different holes that can host 10 tensiometers and 5 TDRs at different heights. These holes are divided into three groups disposed at 90°; groups 1 and 3 are for the tensiometers and group 2 is for TDRs. In this study, only three volumetric water content sensors (TDR1 to TDR3) and three tensiometers (T1 to T3) were installed along the column at different heights: h = 120, 160 and 200 mm. On the top of the PMMA wall, a LED series was installed lighting up the apparatus wall and thus improving the observation quality by the digital camera. The PMMA cylindrical wall was fixed on a metallic base plate using screws. A porous plate and a geotextile were placed at the bottom of the sample to ensure uniform water distribution and to avoid any loss of soil particles. At the bottom of apparatus (h = 0 mm), a pressure transducer was installed for measuring the positive pore water pressure in saturated case.
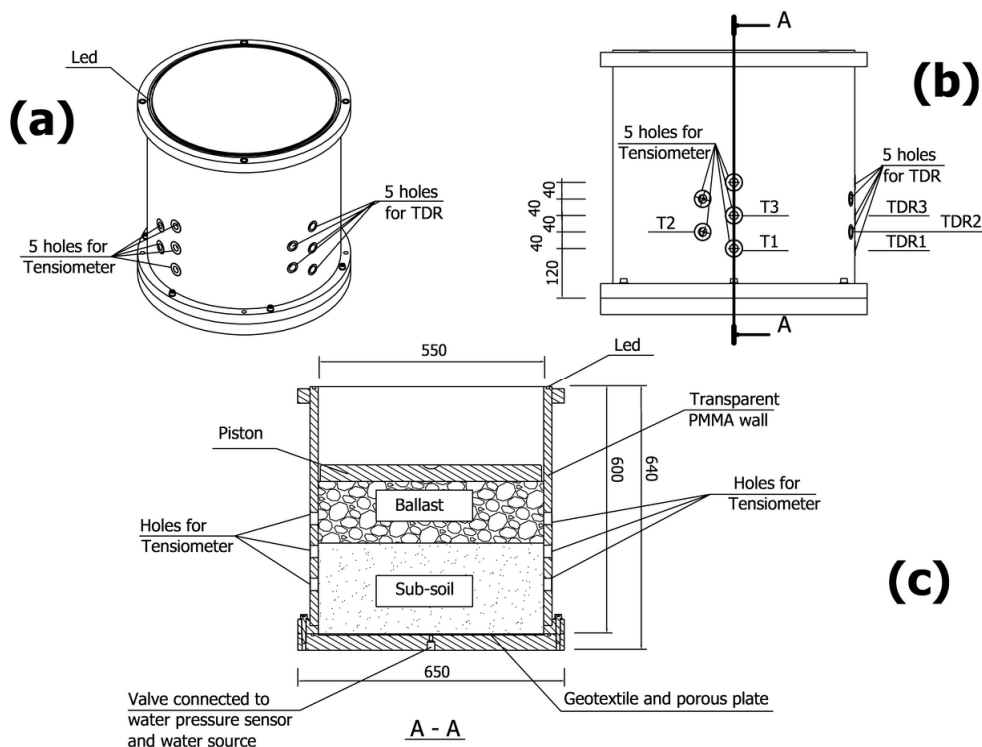

Fig. 3: Schematic view of the apparatus

Fig. 4: Photograph of the physical model

For the specimen preparation, crushed sand (C10) and clay (kaolin Speswhite) were mixed up with water to obtain the target water content - the optimum water content w = 16 % (see Fig. 2). After mixing, the wet material was stored in hermetic containers for at least 24 h for moisture homogenization. The soil specimen was prepared by manual compaction in five layers of 40 mm thick each and one layer of 20 mm thick, making a total of 220 mm thickness for the whole specimen. In the literature involving the study on the migration of fine particles, the value of dry unit mass considered is often around 1.50 Mg/m3: 1.45 Mg/m3 in Burns et al. (2006) and from 1.52 to 1.54 Mg/m3 in Alobaidi et al (1999). According to Burns et al. (2006), this value corresponds to the medium strength in field conditions. Thereby, the dry unit mass was chosen as 1.50 Mg/m3 in this study. The TDR probes were installed during the specimen compaction between the sub-layers of sub-soil at the target heights. Once the sub-soil was compacted, 160 mm ballast was placed on the sub-soil and the ballast particles were arranged in order to have a satisfactory horizontal surface between ballast and piston. After the specimen preparation, the whole column was placed under the hydraulic actuator. The tensiometers were then installed, and other operations were undertaken such

as lighting up the LED series, setting up the digital camera, preparing the loading program. Fig. 4 presents a photograph of the column with specimen.

The test was carried out in three main stages. In the first stage (namely henceforth *Unsaturated state*) where the sub-soil was in unsaturated state ($w = 16$ %; $S_r = 55$%), a pre-loading was applied in order to test the good functioning of the apparatus before applying a frequency of 5 Hz: monotonic loading from 0 to 100 kPa at a rate of 2 kN per minute or 0.14 kPa/s; low frequency cyclic loading from 30 to 100 kPa - 20 cycles at 0.1 Hz; 50 cycles at 1Hz and 100 cycles at 2 Hz. The results during this stage are shown in Fig. 5. A 5 Hz loading was applied afterwards for 500 000 cycles. Note that the choice of load amplitude and the frequency was made based on the consideration of loading conditions in the ancient sub-structure in France (see Trinh et al. 2012; Duong et al. 2013).

Basically, mud pumping is more pronounced when the sub-soil is saturated. For this reason, after the first stage – *Unsaturated sate*, a second stage namely *Saturation* followed by a third stage namely *Saturated state* was applied. In *Saturation*, the sub-soil was saturated from the bottom under a hydraulic head of 12 kPa using an external water source connected to the column. The water level was maintained at 2 cm above the ballast/sub-soil interface in order to ensure the fully saturated state of the sub-soil layer. Meanwhile, a sensor of pore water pressure was installed at $h = 0$ mm. In *Saturated state*, monotonic loading at the same increase rate as in *Unsaturated state* was applied up to 100 kPa followed by the 5 Hz cyclic loading. The test ended when fine particles were observed at the surface of ballast layer.

During the test, the variation of pore water pressure was recorded with 3 home-made tensiometers that are based on the same principle as the high capacity tensiometers developed by Mantho (2005), Cui et al. (2008), Lourenço et al. (2011) and Toll et al. (2012). The working pressure range of these tensiometers is from 700 kPa to -700 kPa (they measure both positive pressure and suction). The time domain refectory (TDR) was connected to a data logger - Trase BE allowing the dielectric constant K_a to be recorded, which is deduced from the crossing time of electromagnetic wave within the surrounding material. The accuracy of the measurement is ± 2%. The well-known model of Topp et al. (1980) was applied to calculate the volumetric water content:

$$\theta = -5.3 \times 10^{-2} + 2.92 \times 10^{-2} K_a - 5.5 \times 10^{-4} K_a^2 + 4.3 \times 10^{-6} K_a^3 \qquad (1)$$

Experimental results and discussions

Fig. 5 presents the results obtained during the pre-loading in Unsaturated state. The variation of stress applied was plotted in Fig. 5a where the stress was increased monotonically from 0 to 100 kPa and then cyclically at low frequency before the 5 Hz loading for 500 000 cycles at the end. It can be observed that during the monotonic loading, the axial displacement increased quickly and it continued to increase during the cyclic loading, to reach 7.3 mm. The displacement was decreased to 6.8 mm when the load decreased from 100 kPa to 30 kPa.
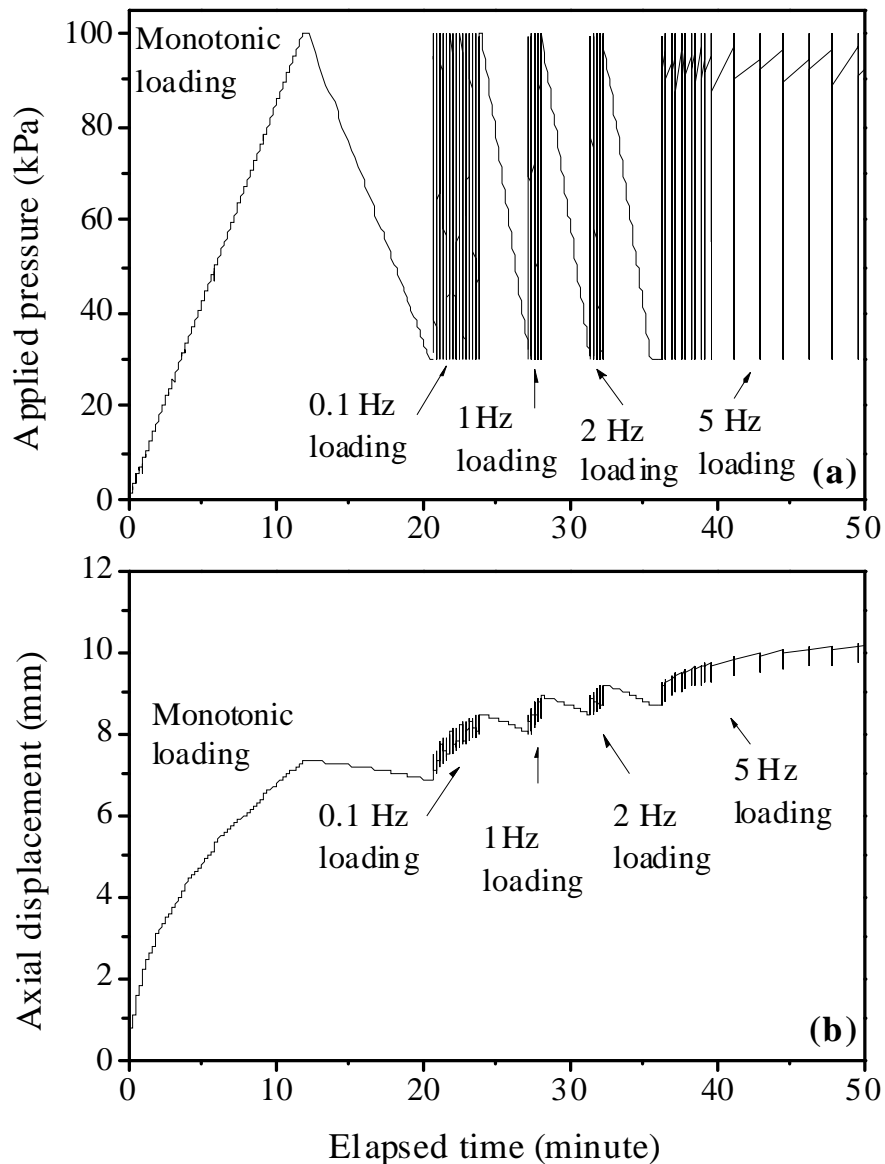

Fig. 5: Pre-loading in *Unsaturated state*

Fig. 6 shows the evolution of global displacement in *Unsaturated state* ($w = 16\%$). The displacement increased quickly during the monotonic loading, from 0 to 6.8 mm. The pre-cyclic

loading at 0.1 Hz, 1 Hz and 2 Hz increased the permanent displacement to 8.7 mm. The increasing rate of permanent displacement was also high in the first period of 5 Hz loading (from 8.7 mm to 9.9 mm for the first 10 000 cycles) and then it slowed down (it needs nearly 50 000 cycles to increase from 9.9 mm to 10.9 mm).
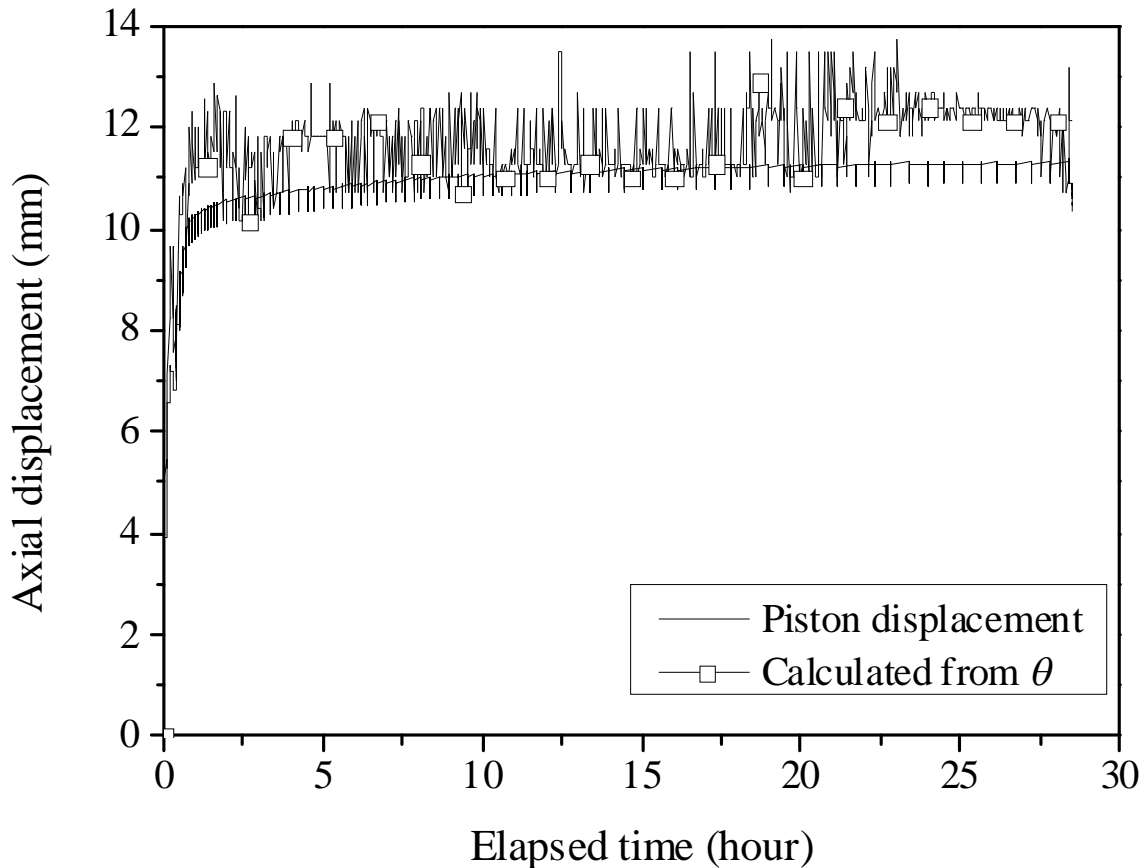
Fig. 6: Axial displacement during loading in *Unsaturated state*

Fig. 7 depicts the evolution of permanent displacement during the 5 Hz loading. It shows that the displacement tended to increase linearly with the logarithm of cycle number N when $N > 100$. This is in agreement with the results of some previous studies. Indeed, in Paute and Le Fort (1984), Hornych (1993) and AFNOR (1995) for the unbound granular materials, the permanent displacement value at 100 cycles was considered as the reference value in the modeling of ballast axial displacement after 100 cycles. In these models, the displacement evolution varies also linearly with the loading cycle number $\log N$.

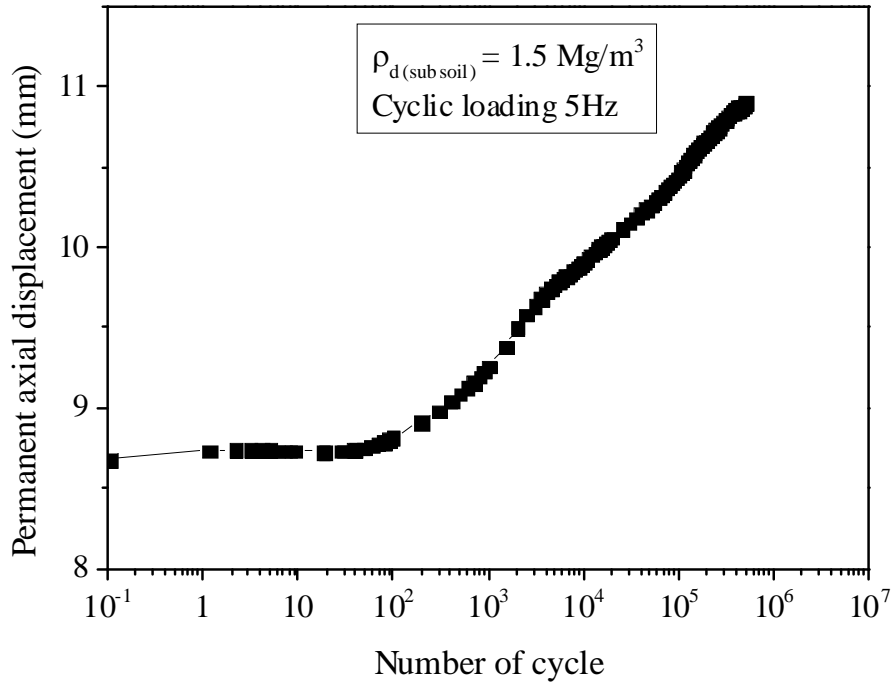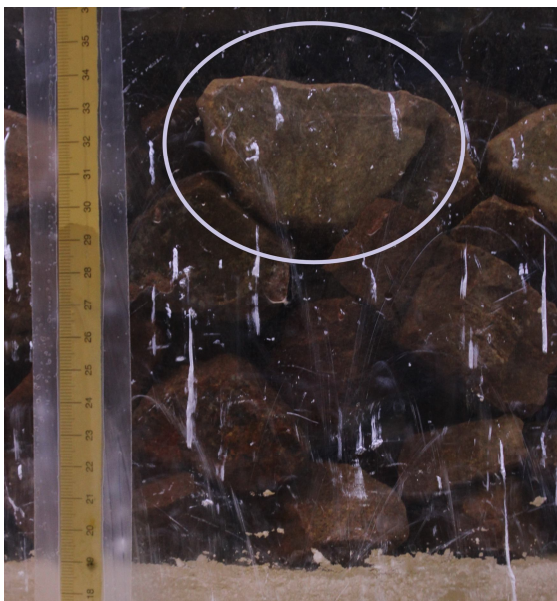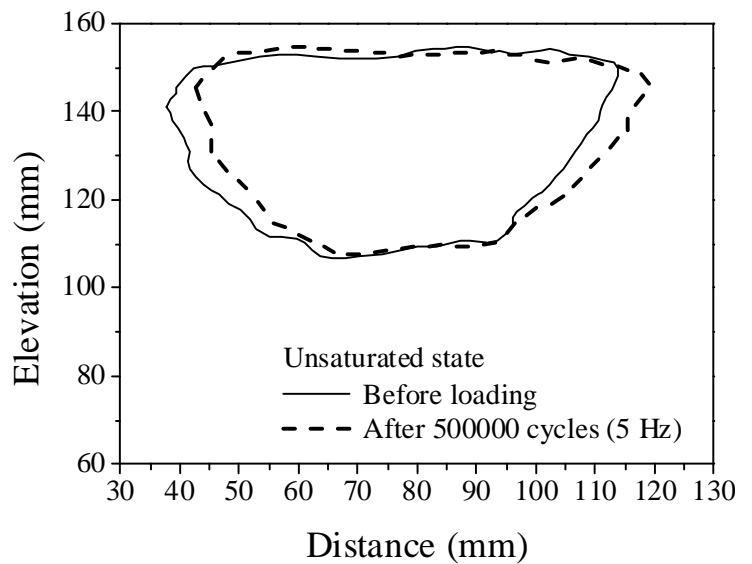**Fig. 7: Displacement during cyclic loading at 5 Hz in *Unsaturated state***

a) Reference ballast particle

b) Outline ballast change before and after loading in

Unsaturated state

Fig. 8: Monitoring of one ballast particle movement

132

From the image by the digital camera (Fig. 8a), the movement of one ballast particle was monitored. The movement during *Unsaturated state* of this ballast particle was analyzed by considering the change in its contour (Fig. 8b). It can be observed that there is not only vertical displacement but also horizontal one, indicating a rotation of the ballast particle. This suggests that ballast particles rearranged between them during the cyclic loading.

Fig. 9 presents the evolution of volumetric water content (Fig. 9a) and pore water pressure (Fig. 9b) during the *Unsaturated state*. The initial volumetric water contents are θ = 21.6 %, 22.7% and 17.9% at h = 120 mm, 160 mm and 200 mm, respectively. Note that the 200 mm level corresponds to 20 mm below the ballast/sub-soil interface. As it was the last layer for the compaction operation, its dry unit mass can be smaller than those of lower layers.
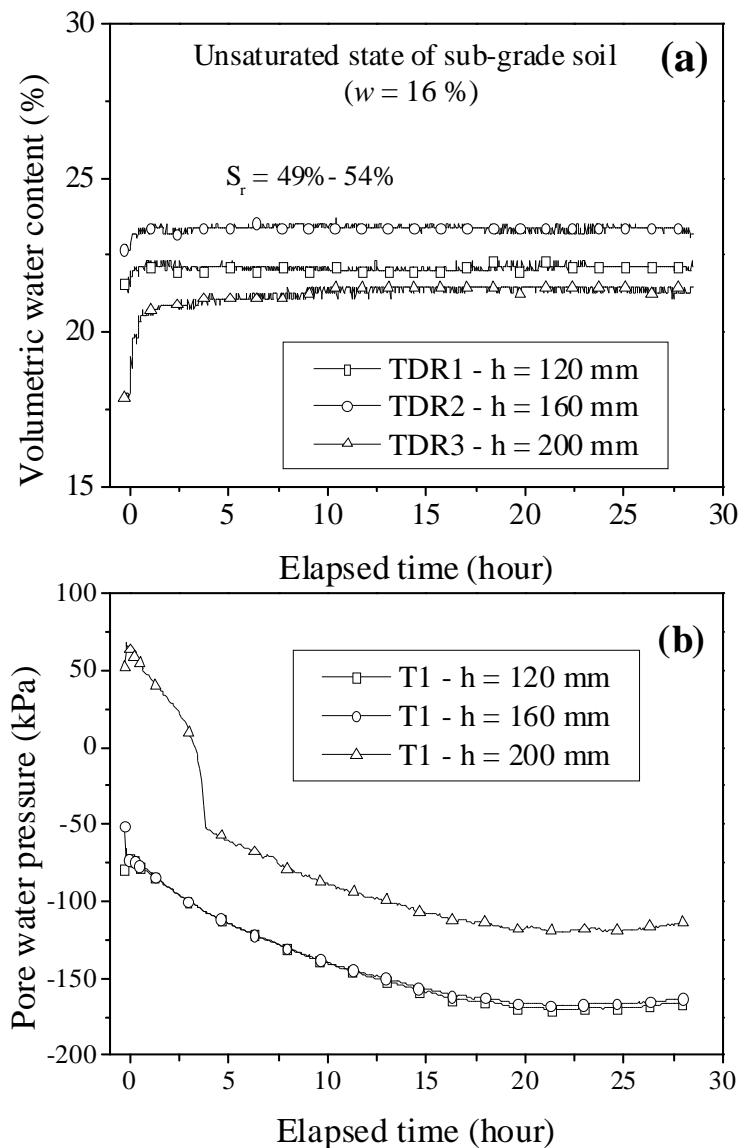

Fig. 9: Changes in volumetric water content and pore water pressure in *Unsaturated state*

As the sub-soil layer was fully saturated, the variation of volumetric water content θ can be used to estimate its settlement by assuming that soil particles and water are not compressible.

The total height is divided into three sub-layers, assuming constant volumetric water content in each sub-layer. The calculation of the settlement of each sub-layer is as follows:

$$\Delta V_{total} = h_1 \times A - \frac{Vwater}{\theta_2}$$
$$\Delta h \times A = h_1 \times A - \frac{(h_1 \times A) \times \theta_1}{\theta_2} \quad (2)$$
$$\Delta h = h_1 \times \left(1 - \frac{\theta_1}{\theta_2}\right)$$

where ΔV_{total} and Δh are the variations of total volume and settlement of the sub-layer, respectively; θ_1 and θ_2 are respectively the volumetric water contents before and after the loading; V_{water} is the volume of water in the sub-layer, A is the cross section of the specimen, h_1 is the thickness of sub-layer before loading. The final settlement is the summary of the settlements of all sub-layers:

$$\Delta h = \Delta h_{120} + \Delta h_{160} + \Delta h_{200} \quad (3)$$

The settlement result obtained is also presented in Fig. 6. It can be observed that the calculated settlement has the same trend as the displacement by external measurement but slightly larger. Note that the external displacement consists of both the displacements of ballast layer and sub-soil layer while the calculated settlement consists of only the part of sub-soil. Note also that the accuracy of TDR used is 2% that corresponds to a settlement of 4.3 mm.

During the 5 Hz loading for 500 000 cycles, the volumetric water content was almost stable with small variations (Fig. 9a). From the beginning to the end of the 5 Hz loading, the values are $22.2 \pm 0.2\%$ for TDR1 at h = 120 mm, $23.4 \pm 0.3\%$ for TDR2 at h = 160 mm and $20.9 \pm 0.5\%$ for TDR3 at h = 200 mm. On the whole, the degree of saturation of the whole sub-soil layer varied from 49% to 54%; this is quite close to the theoretical value of S_r, estimated at 55 %.

The response of tensiometers was plotted in Fig. 9b. The curves of T1 ($h = 120$) and T2 ($h = 160$) are very close while the curve of T3 ($h = 200$) is clearly above. However, the shapes of the three curves are the same. After 20 h, the pore water pressure at all three levels reached their stabilization values: -166.4 kPa at $h = 120$ mm; -163.9 kPa at $h = 160$ mm and -114.1 kPa at $h = 200$ mm.

For the visual monitoring, two photographs were taken, one before the monotonic loading and another after the 5Hz loading for 500 000 cycles, and they are presented in Fig. 10a and Fig. 10b, respectively. Referring to the level of the top surface of the sub-soil layer, these two photographs show that the level of ballast/sub-soil interface did not change. Furthermore, no migration of fine particles was observed. This suggests that the sub-soil displacement calculated from θ does not represent the global variation. Note that the local ballast/sub-soil contact was not uniform over the whole interface section because ballast particles are very angular and have different shapes. This non-uniform contact can lead to non-uniform stress, thus a larger compression in the zones just beneath ballast particles as compared to the zones among particles. The TDR whose size is 80 mm long and 25 mm large was probably situated beneath ballast particles, giving rise to a higher θ value, hence a larger estimated settlement.
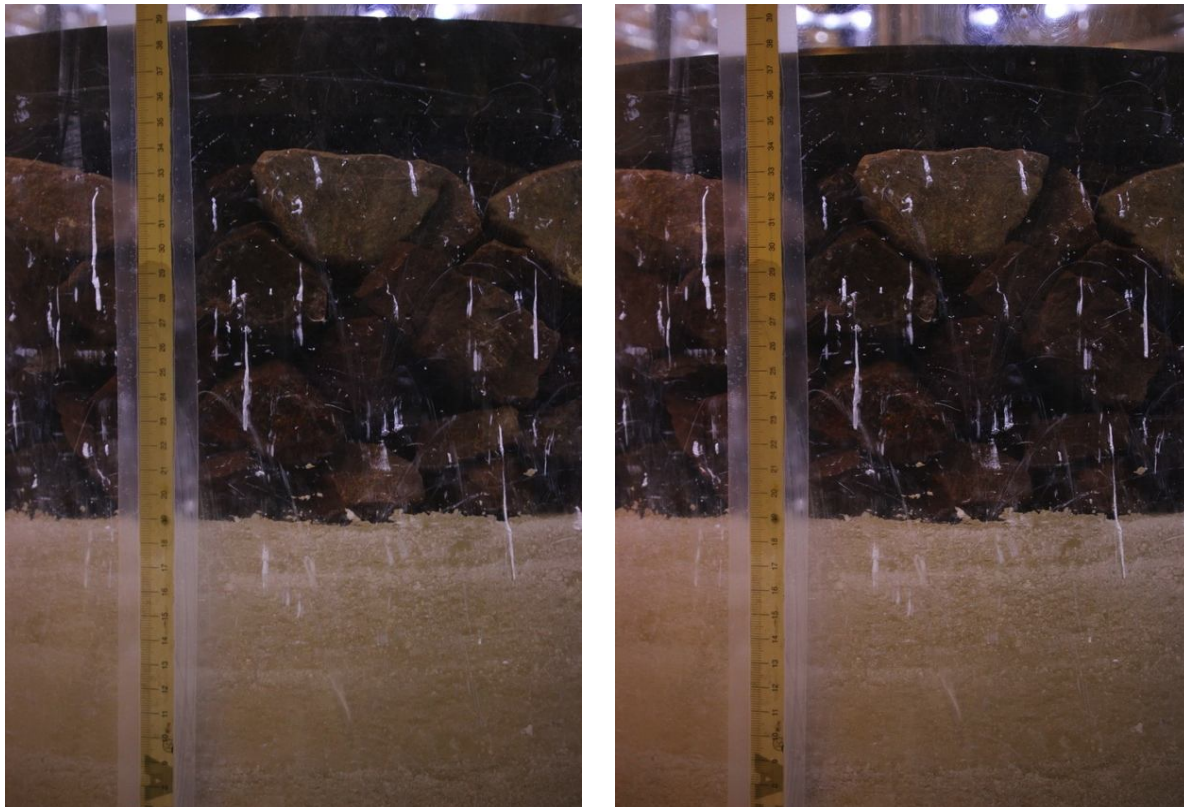
a) Before loading ($w = 16\%$)   b) After loading ($w = 16\%$)

Fig. 10: Photographs of the interface between two soils layers: a) before and b) after loading in *Unsaturated state*
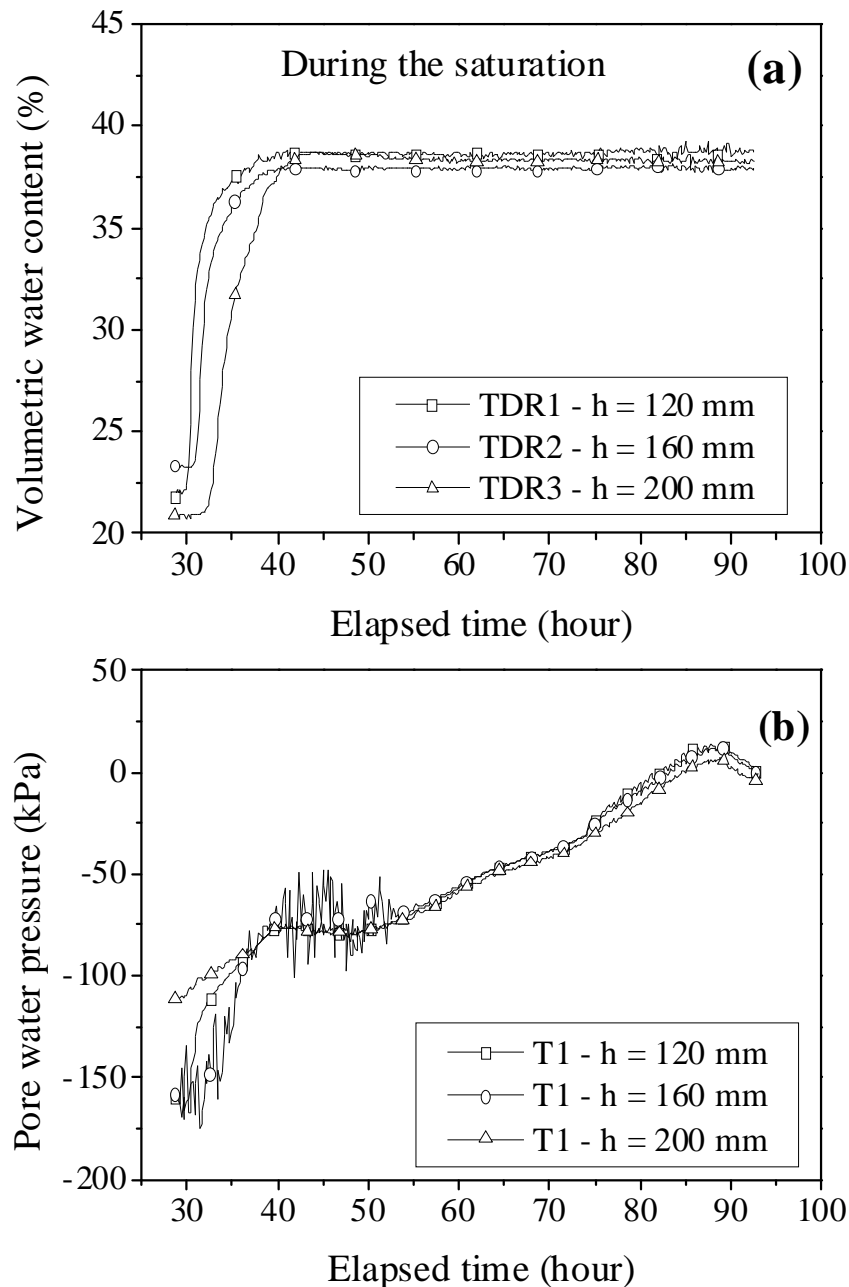
Fig. 11: Changes in volumetric water content and pore water pressure during *Saturation*

When the 5 Hz loading for 500 000 cycles ended, the sample was connected to an external water source and water was observed on the ballast/sub-soil interface after about 1 day. During this time, the volumetric water content measured by TDR increased consistently: the value at $h = 120$ mm changed firstly, then it was the turn of $h = 160$ and finally of $h = 200$ mm (Fig. 11a). At $t = 45$ h, the volumetric water contents at three levels stabilized. If one assumes that the dry unit mass of the sub-soil did not change during the test, the degree of saturation S_r was 87% to 88%. This is possible because during the saturation of very fine soil, it takes longtime to filling micro-pores. This can be observed also in Fig. 11b where the evolution of pore water pressure is depicted. Till $t = 45$ h, the

pore water pressure increased as the volumetric water content increased. Afterwards, although the volumetric water content θ became stable, the pore water pressure continued to increase up to zero. Furthermore, the three pore water pressure-time curves show the same increase trend (Fig. 11b), suggesting that the process of filling micro-pores took place continuously and uniformly within the sample.
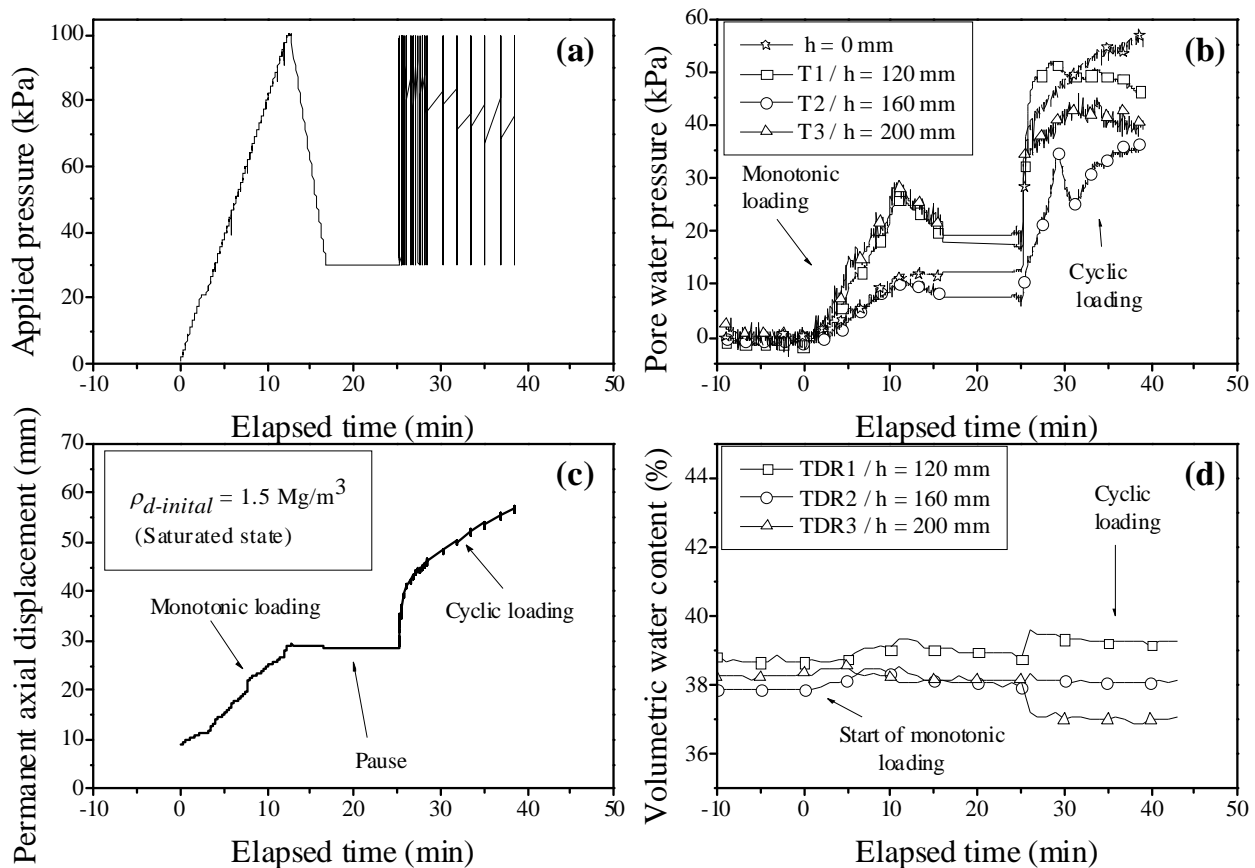
Fig. 12: Test on the sub-soil at *Saturated state*: a) applied pressure; b) permanent axial displacement; c) pore water pressure and d) volumetric water content

Once all the tensiometers gave the positive pressure values, the third stage (*Saturated state*) started with the monotonic loading followed by the 5 Hz cyclic loading. Fig. 12 shows the variations of the pressure applied (Fig. 12a), the permanent axial displacement (Fig. 12b), the pore water pressure (Fig. 12c) and the volumetric water content (Fig. 12d). When the monotonic load increased from 0 to 100 kPa, the permanent axial displacement increased from 9 mm to 28.6 mm, and the pore water pressure increased also: at $h = 120$ mm and $h = 200$ mm it increased quickly and reached around 30 kPa while at $h = 0$ mm and $h = 160$ mm it increases more gently. When the monotonic loading finished, the pore water pressure at all the three levels decreased but remained higher than zero.

This can be explained by the very low hydraulic conductivity of the sub-soil that did not allow quick water pressure dissipation.

Under the 5 Hz loading, the permanent displacement continued to increase rapidly. The pore water pressure became quickly higher than 40 kPa (except the late response at h = 160 mm, possibly due to the corresponding sensor performance). In the end, the value obtained was between 40 and 58 kPa. Note that the applied pressure varied from 30 kPa to 100 kPa. This suggests that the effective stress (total pressure minus pore pressure) became sometimes negative during the unloading (applied stress smaller than pore water pressure) and liquefaction occurred within the sub-soil. Note that the negative value of effective stress has no-physical meaning; it implies simply that during unloading there were no longer contact between soil particles. Further study is needed to verify this point.

On one hand, the sharp increase of pore water pressure weakens the sub-soil and on the other hand its dissipation brings fine particles upward. This is the key factor for the migration of fine particles. This is also consistent with the observation reported by Aw (2007) and Indraratna et al. (2011): mud pumping was identified in the zone with presence of water which softens the base layer and allows the migration of the fine particles into the void spaces between ballast particles, and also the penetration of ballast particles into the sub-grade under loading. The penetration of ballast and the migration of fine particles created a layer of mixture materials. This is probably the main mechanisms for the creation of interlayer identified in some railway sub-structures in France as mentioned before. In Fig. 12d, the change of volumetric water content is insignificant: ± 1.4% at h = 120 mm, ± 1.9% at h = 160 mm and ± 2.4% at h = 200 mm. Their variation trends are different: the volumetric water content at h = 120 mm and 160 mm increased, while the value at h = 200 mm decreased continuously. These trends can be explained as follows: assuming that the sub-soil is nearly saturated, when the soil was compressed, the pore volume decreased. As a result, the volumetric water content increased at h = 120 mm and 160 mm. At h = 200, it is not very obvious because it was just 20 mm below the ballast/sub-soil interface that underwent significant modifications.

Fig.13 shows the photographs taken just before the monotonic loading (Fig.13a), after the monotonic loading (Fig.13b) and after the cyclic loading (Fig.13c) in *Saturated state*. The movement of fine particles can be identified. The fine particles were pumped up to the surface of

ballast layer. During the monotonic loading, fine particles were also moving upwards, but not as rapidly as during the cyclic loading.
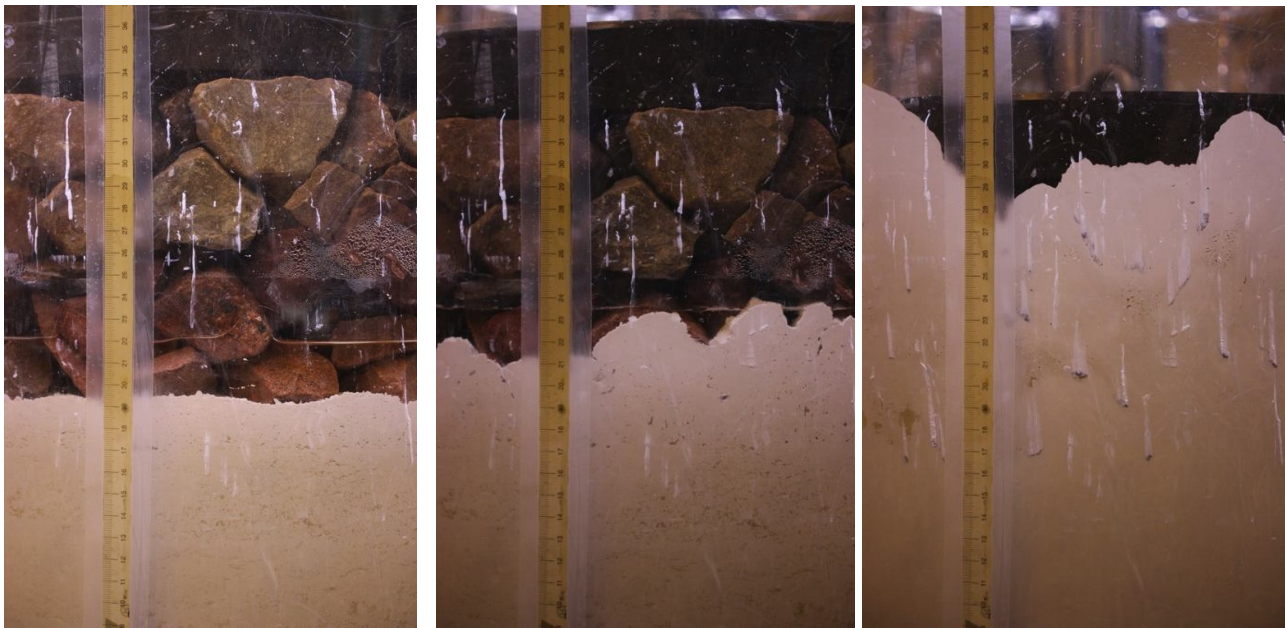
| a) after saturation and before monotonic loading | b) after monotonic loading (saturated state) | c) after cyclic loading (saturated state) |

Fig.13: Photographs showing the evolution of interface between two the soils layers: fine particles were pumped upwards

The evolution of sub-soil surface was monitored by digitization and the results are presented in Fig.14. The time interval between lines is 2 minutes. In general, the entire sub-soil surface was rising up. It is worth noting that when removing the sample at the end of the test, it was observed that the pumping up level of fine particles was uniform over the whole cross section.

In order to verify the nature of fines migration, a comparison between the volume of ballast particles in sub-soil and the volume of ballast layer voids filled by fine particles up-pumped was conducted. The volume occupied by ballast particles in sub-soil $V_{ballast}$ is calculated as follows:

$$V_{ballast} = \frac{h_{ballast} \times A}{1+e} \tag{4}$$

where $h_{ballast}$ is the settlement of ballast layer, A is the sample cross section and e is the void ratio of ballast layer.

The volume of ballast layer voids filled by fine particles of sub-soil V_{fines} can be calculated as follows:

$$V_{fines} = \frac{h_{fines} \times A}{1+e} e \qquad (5)$$

where h_{fines} is the pumping up level of fine particles in the ballast layer. Admitting that ballast particles settlement pushed the fine sub-soil particles up and these fine particles fill the voids of ballast layer, i.e., $V_{ballast} = V_{fines}$. This leads to:

$$h_{fines} = \frac{h_{ballast}}{e} \qquad (6)$$

Indraratna et al. (1997) proposed that the voids ratio of ballast e can vary from 0.74 (compacted) to 0.95 (un-compacted). In the case of the present study, as the sample was submitted to the 5 Hz loading for 500 000 cycles, the ballast layer can be considered as compacted with a void ratio equal to 0.74. As the ballast settlement under loading in *Saturated state* is 47.7 mm as presented in Fig. 12b (the ballast settlement is considered equal to the piston displacement, the most critical case), the pumping up level estimated using Eq. (6) is 64.4. This value is much less than the real pumping up level of fine particles given in Fig.14: 113.1±15 mm. This suggests that there was not only the penetration of ballast particles pushing fine particles upwards, but also the dissipation of pore water pressure bringing fine particles up into the ballast layer.
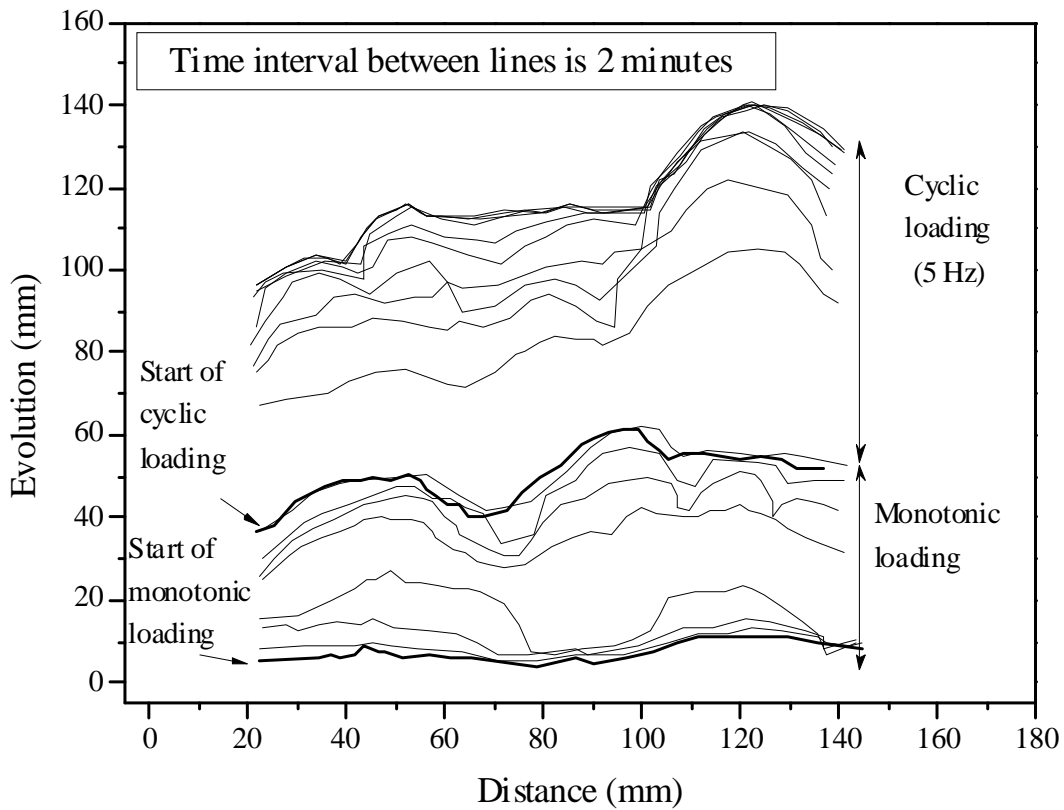
Fig.14: Sub-grade surface evolution

In order to have a better observation on the pumping up level of fine particles in the ballast layer, six reference vertical sections (30 mm, 50 mm, 70 mm, 90 mm, 110 mm and 130 mm in Fig.14) were chosen and their pumping up levels evolution over time are determined and shown in Fig. 15. On the whole, the evolutions of the ballast/sub-soil interface at these sections follow the same trend. The interface rose up immediately when loading started. From Eq. (6), the theoretical pumping level of fine particles was calculated and the result is also presented in Fig. 15. The calculated value is clearly lower than the real pumping level deduced from the photographs. This confirms that the fine particles migration was not only due to the ballast penetration but also the dissipation of excess pore water pressure.

Fig. 15: Pumping level of fine particles during the test in *Saturated state*

Conclusions

A physical model was developed to study the creation of interlayer and the mud-pumping phenomena in ancient railway sub-structure. The soil sample consisted of a ballast layer and one sub-soil layer. One por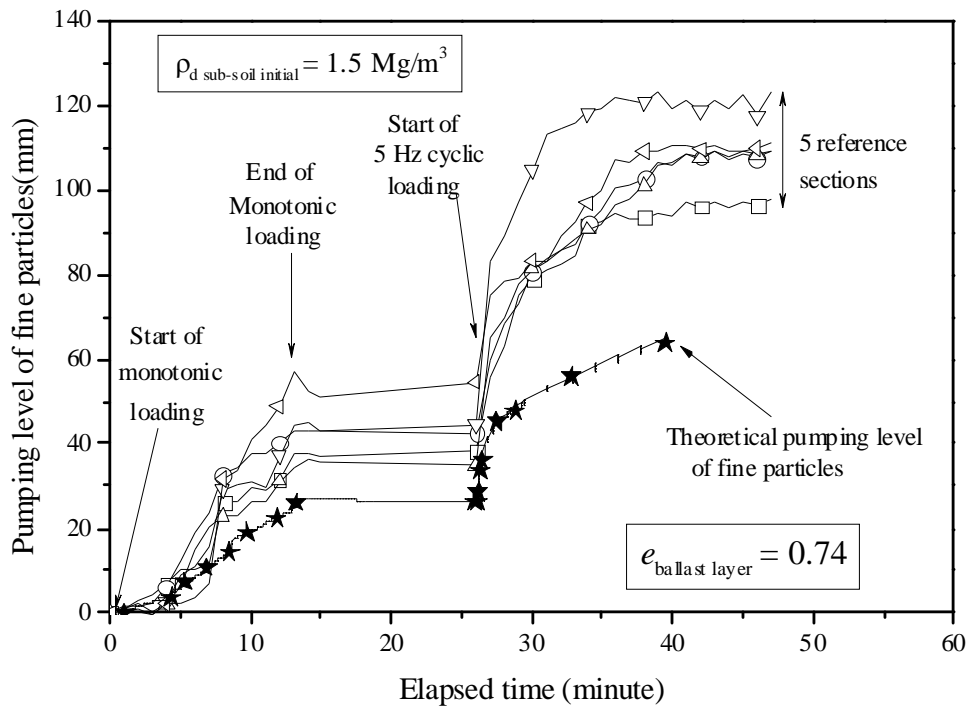e water pressure sensor, three tensiometers, three TDRs were used to monitor the variations of pore water pressure and volumetric water content. The transparent PMMA apparatus wall and a digital camera allowed direct monitoring of the different movements (ballast, ballast/sub-soil interface, etc.). A test was carried out under monotonic and cyclic loading on a sample with the sub-soil in two different states: unsaturated and saturated sates. The results obtained allowed the migration of fine particles to be investigated. The following conclusions can be drawn:

1) The quality of the recorded data showed that the physical model developed worked well and the test protocol adopted was appropriate. Moreover, it was observed that the migration of fine particles was globally the same in every points of the interface, suggesting that the soil sample was representative of the one dimensional case. The relevant results obtained proved that the experimental set up appropriate to simulate the degradation mechanism occurring in the railway substructure.

2) In the unsaturated state of sub-soil, the interface between two layers did not change even after the 5 Hz loading for 500 000 cycles. On the contrary, in the near saturated state, it rose up very fast during the very first cycles. The difference between the two cases highlights the effect of water content which softens the base layer and allows the migration of the fine particles into the void spaces between ballast particles and also the penetration of ballast particles into the sub-grade.

3) The mechanism behind the mud pumping phenomenon is the pore water pressure generation. Under cyclic loading, the pore water pressure can become higher than the total stress, giving rise to zero even negative effective stress. This is especially the case for the unloading phase. In this case, liquefaction occurs, that corresponds to the ideal condition for bring fine particles up under the effect of pore pressure dissipation. On the other hand, this is also the ideal condition for the penetration of ballast particles into the sub-soil, thus, for the interlayer creation. Note that the negative effective stress has no physical meaning. It implies simply that there were no longer any contact between soil particles and the unloading applied corresponded to a depression (suction) to water only. Further study is needed to verify this point.

Acknowledgements

References

AFNOR, 1995, "Essais Relatif aux Chaussées. Matériaux Non Traitées. Part 1 : Essai Triaxial à Chargements Répétés, NF P98-235-1", French Standard (In French).

Al Shaer, A., 2005, «Analyse des Déformations Permanentes des Voies Ferrées Ballastées – Approche Dynamique », PhD Dissertation, Ecole Nationale des Ponts et Chaussées, France (In French).

Alobaidi, I. and Hoare, D.J., 1994, "Factors Affecting the Pumping of Fines at the Subgrade-Subbase Interface of Highway Pavements: A Laboratory Study", *Geosynthetics International*, Vol. 1, No. 2, pp. 221–259.

Alobaidi, I. and Hoare, D.J., 1996, "The Development of Pore Water Pressure at the Subgrade-Subbase Interface of a Highway Pavement and its Effect on Pumping of Fines", *Geotextiles and Geomembranes*, Vol. 14, No. 2, pp. 111–135.

Alobaidi, I. and Hoare, D.J., 1998a, "Qualitative Criteria for Anti-pumping Geocomposites", *Geotextiles and Geomembranes*, Vol. 16, No. 4, pp.221–245.

Alobaidi, I. and Hoare, D.J., 1998b, "The Role of Geotextile Reinforcement in the Control of Pumping at the Subgrade-Subbase Interface of Highway Pavements", *Geosynthetics International*, Vol. 5, No. 6, pp. 619–636.

Alobaidi, I. and Hoare, D.J., 1999, "Mechanisms of Pumping at the Subgrade-Subbase Interface of Highway Pavements", *Geosynthetics International*, Vol. 6, No. 4, pp. 241–259.

Aw, E.S., 2004, "Novel Monitoring System to Diagnose Rail Track Foundation Problems", Master of Science Thesis, Massachusetts Institute of Technology, USA.

Aw, E.S., 2007, "Low Cost Monitoring System to Diagnose Problematic Rail Bed: Case Study at Mud Pumping Site", Ph.D. Dissertation, Massachusetts Institute of Technology, USA.

Ayres, D.J., 1986, "Geotextiles or Geomembranes in Track? British Railway Experience", *Geotextiles and Geomembranes*, Vol. 3, No. 2-3, pp. 129–142.

Burns, B., Ghataora, G.S. and Sharley, P., 2006, "Development and Testing of Geosand Composite Layers Using Pumps Index Test", *In: Proceedings of the First International Conference on Railway Foundations Railfound06*, University of Birmingham, UK, p. 355–366, ISBN10: 0-704426-00-5, ISBN13: 97807-04426-009.

Calon, N., Trinh, V.N., Tang, A.M., Cui, Y.J., Dupla, J.C., Canou, J., Lambert, L., Robinet, A. and Schoen O., 2010, « Caratérisation Hydraumécanique des Matériaux Constittutifs de Plateformes Ferroviaires Anciennes ». *Conférence JNGG2010,* Grenoble, France, p. 787–794 (In French).

Cui, Y. J. and Delage, P., 1996, "Yielding Behavior of an Unsaturated Compacted Silt", *Géotechnique* Vol. 46, No. 2, pp. 291-311.

Cui, Y. J., Tang, A. M., Loiseau, C., and Delage, P., 2008, "Determining the Unsaturated Hydraulic Conductivity of a Compacted Sand-Bentonite Mixture Under Constant-Volume and Free-Swell Conditions", *Physics and Chemistry of the Earth*, Parts A/B/C, Vol. 33, pp. S462–S471.

Cui, Y.J., Duong, T.V., Tang, A.M., Dupla, J.C., Calon, N. and Robinet, A., 2013, "Investigation of the Hydro-Mechanical Behaviour of Fouled Ballast", *Journal of Zhejiang University- Science A*, Vol. 14, No.4, pp.244-255.

Duong, T.V., Trinh, V.N., Cui, Y.J., Tang, A.M. and Nicolas, C., 2013, "Development of a Large-Scale Infiltration Column for Studying the Hydraulic Conductivity of Unsaturated Fouled Ballast", *Geotechnical Testing Journal,* Vol. 36, No. 1, pp. 54-63.

Ghataora, G.S., Burns, B., Burrow, M.P.N. and Evdorides, H.T., 2006, "Development of an Index Test for Assessing Anti-pumping Materials in Railway Track Foundations", *In: Proceedings of the First International Conference on Railway Foundations*, *Railfound06*, University of Birmingham, UK, p. 355–366.

Hornych, P., Corté, J.F. and Paute, J.L., 1993, « Etude des Déformations Permanents sous Chargements Répétés de Trois Graves non Traitées », *Bulletin de Liaison des Laboratoires des Ponts et Chaussees,* Vol.184, p. 77-84 (In French).

Paute, J.L. and Le Fort, R., 1984, "Determination of Untreated Gravels Mechanical Characteristics with Cyclic Loading Triaxial Apparatus", *Bullein of the International Association of Engineering Geology*, No. 29, pp. 419 – 424, (In French).

Indraratna, B., Ionescu, D., Christie, D., and Chowdhurry, R., 1997, "Compression and Degradation of Railway Ballast under One-dimensional Loading", *Australian Geomechanics Journal,* Vol 12, pp. 48 – 61.

Indraratna, B., Salim, W. and Rujikiatkamjorn. C., 2011, *Advanced Rail Geotechnology - Ballasted Track*. CRC Press.

Lourenço, S.D.N., Gallipoli, D., Toll, D.G., Augarde, C.E. and Evans, F.D., 2011, "A New Procedure for the Determination of Soil-water Retention Curves by Continuous Drying Using High-suction Tensiometers", *Canadian Geotechnical Journal*, Vol. 48, No. 2, pp. 327–335.

Mantho, A.T., 2005, « Echanges Sol-Atmosphère Application à la Sécheresse » Ph.D. Dissertation, Ecole Nationales des Ponts et Chaussées - Université Paris – Est, France (In French).

Raymond, G.P., "Railway Rehabilitation Geotextiles", *Geotextiles and Geomembranes*, Vol. 17, No. 4, pp. 213–230.

Selig, E.T. and Waters, J.M., 1994, *Track Geotechnology and Substructure Management*. Thomas Telford.

SNCF, 1995, "Specification Technique pour la Fourniture des Granulats Utilisés pour la Réalisation et l'Entretien des Voies Ferrées ST 590B", Technical guide (In French).

Toll, D.G., Lourenço, S.D.N. and Mendes, J., 2012, "Advances in Suction Measurements Using High Suction Tensiometers", *Engineering Geology*, doi:10.1016/j.enggeo.2012.04.013.

Topp, G.C., Davis, J.L. and Annan, A.P., 1980, "Electromagnetic Determination of Soil Water Content: Measurements in Coaxial Transmission Lines", *Water Resources Research*, Vol. 16, No. 3, pp. 574–582.

Trinh, V.N., 2011, « Comportement Hydromécanique des Matériaux Constittutifs de Plateformes Ferroviaires Anciennes ». Ph.D. Dissertation, Ecole Nationales des Ponts et Chaussées - Université Paris – Est, France (In French).

Trinh, V.N., Tang, A.M., Cui, Y.J., Canou, J., Dupla, J.C., Calon, N., Lambert, L., Robinet, A. and Schoen, O., 2011, « «Caractérisation des Matériaux Constitutifs de Plate-forme Ferroviaire Ancienne », *Revue Française de Géotechnique*, Vol. 134-135, pp. 65–74 (In French).

Trinh, V.N., Tang, A.M., Cui, Y.J., Dupla, J.C., Canou, J., Calon, N., Lambert, L., Robinet, A. and Schoen, O., 2012, "Mechanical Characterisation of the Fouled Ballast in Ancient Railway Track Sub-structure by Large-scale Triaxial Tests", *Soils and Foundations*, Vol. 52, No. 3, pp. 511-523.

Van, W. A., 1985, "Rigid Pavement Pumping: (1) Subbase Erosion and (2) Economic Modeling : Informational Report", *Publication FHWA/IN/JHRP-85/10. Joint Highway Research Project*, Indiana Department of Transportation and Purdue University, West Lafayette, Indiana, USA, doi:10.5703/1288284314094

Voottipruex, P. and Roongthanee, J., 2003, "Prevention of Mud Pumping in Railway Embankment a Case Study from Baeng Pra-pitsanuloke, Thailand", *The Journal of KMITB*, Vol. 13, No. 1, pp. 20–25.

Yoder, E.J., 1957, "Pumping of Highway and Airfield Pavements: Technical Paper", *Publication FHWA/IN/JHRP-57/05. Joint Highway Research Project,* Indiana Department of Transportation and Purdue University, West Lafayette, Indiana, doi: 10.5703/1288284313518.

Yuan, R., Yang, Y.S., Qiu, X. and Ma, F.S., 2007, "Environmental Hazard Analysis and Effective Remediation of Highway Seepage", *Journal of Hazardous Materials*, Vol. 142, No. 1-2, pp. 381–388.

Zhang, C., 2004, "The Effect of High Groundwater Level on Pavement Sub-grade Performance", Ph.D. Dissertation, the Florida State University - College of Engineering, USA.

Investigating the mud pumping and interlayer creation phenomena in railway sub-structure

Trong Vinh Duong[1], Anh Minh Tang[1], Yu-Jun Cui[1], Jean-Claude Dupla[1], Jean Canou[1], Nicolas Calon[2], Alain Robinet[2]

Abstract: This paper presents the driving factors for the interlayer creation and mud pumping phenomena in railway sub-structure. Tests using a physical model that consists of a ballast layer overlying a sub-soil layer were carried out under different conditions in terms of water content, loading and sub-soil dry unit mass. The physical model was equipped with various sensors and devices allowing water content, pore water pressure, axial displacement to be monitored. Visual observations were also made using a digital camera. It was observed that the ballast behavior depends on the sub-soil state. Both interlayer creation and mud pumping are related to the migration of fine particles, and water content is the most important factor for the migration of fine particles. Under unsaturated conditions, the ballast/sub-soil interface did not change. On the contrary, under the near saturated conditions, significant migration of fine particles occurred. In case of low dry unit mass, the dissipation of high pore water pressure in the sub-soil gave rise to mud pumping. In case of higher dry unit mass, the excess of pore water pressure was smaller due to the smaller volume change of sub-soil. As a result, the effect of water pressure dissipation was limited and the upward migration of fine particles was only by the penetration of ballast into the sub-soil, thereby, forming the interlayer.

Keywords: Railway sub-structure; physical model; cyclic loading; migration of fine particles; mud pumping; interlayer creation.

Introduction

Railway is nowadays one of the important transportation modes. To ensure safe and timely delivery of freight and passengers, the track must be constantly maintained (Janardhanam and Desai, 1983; Indraratna and Salim, 2005; Al-Qadi Imad, 2008; Su et al., 2010). For the economic reason, the maintenance should be optimized. In this context, a good understanding of the degradation process of railway sub-structure is essential.

In France, during the maintenance campaign of ancient tracks, a new layer namely interlayer was identified. It is suspected that this layer was formed mainly by the interpenetration between ballast

---

[1] Ecole des Ponts Paris Tech (ENPC), Laboratoire Navier/CERMES
[2] French Railway Company (SNCF)

and sub-soil. This interlayer can play an important role in the overall behavior of railway tracks (Calon et al,. 2010; Trinh et al., 2011; Trinh, 2011; Trinh et al., 2012; Cui et al., 2013; Duong et al., 2013). On the other hand, mud pumping which is characterized by the upward migration of sub-soil fine particles through the ballast voids has been known to be the worst degradation phenomenon for the railway sub-structure. This phenomenon was reported by several authors not only in the field of railway sub-structure (Ayres, 1986; Selig and Waters, 1994; Raymond, 1999; Sussmann et al., 2001; Voottipruex and Roongthanee, 2003; Burns et al., 2006; Gataora et al., 2006; Aw 2004, 2007; Indraratna et al., 2011) but also in the pavement context (Yoder, 1957; Van, 1985; Alobaidi and Hoare, 1994; 1996; 1998a; 1998b; 1999; Zhang, 2004; Yuan et al., 2007). Basically, these two phenomena (interlayer creation and mud pumping) are both related to the migration of particles and the interaction between ballast and sub-soil layers. Thus, a good knowledge on the mechanism related to the migration of fine particles is crucial for better understanding the interlayer creation and mud-pumping, and for further proposing efficient and economic methods for railway track maintenance.

To date, even though the migration of fine particles and its consequence has been reported in several studies, the knowledge on the driving mechanism of this phenomenon remains scarce. For the interlayer, as it has been recently recognized, the question about its creation is still completely open. For the mud pumping, several mechanisms were proposed but they are sometimes contradictory: Takatoshi (1997, cited by Voottipruex and Roongthanee, 2003) proposed that the mud pumping is due to the suction generated by the upward and downward moving of ties. On the contrary, Alobaidi and Hoare (1996; 1999) proposed that this phenomenon is mainly due to the water pressure developed at the interface between the sub-grade and sub-base or ballast layers. Van (1985) proposed some models for describing mud pumping in the pavement context but their application in the railway context remains to be verified based on suitable experimental data.

In the present work, using a transparent apparatus recently developed, the mechanisms of mud pumping and interlayer creation in ancient railway tracks were investigated. The ancient track was represented by a soil sample composed of a 160 mm thick ballast layer overlying a 220 mm thick sub-soil layer. The apparatus (550 mm in internal diameter and 600 mm in height) was equipped with different sensors allowing the simultaneous monitoring of pore water pressure and volumetric water content. The ballast/sub-soil interface was monitored using digital camera. Tests under both monotonic and cyclic loadings and under different conditions in terms of sub-soil saturation state,

density were conducted. The results obtained allowed the driving factors for the mud pumping interlayer creation phenomena to be analyzed.

Materials

The sub-soil used in this study was prepared from crushed sand and kaolin (70%/30% by dry mass), namely *70S30K*. The reason of using this artificial material is that it can be reproduced easily in the laboratory for having a large quantity needed for the whole test program. The material used in this study has a high percentage of fines (particles smaller than 80 µm represent 95%), similar to the sub-soils found at the sites with mud pumping identified (Alobaidi and Hoare, 1996; Aw, 2007). The mixture also has a grain size distribution curve similar to that of a widely studied soil - the Jossigny silt (Fleureau and Indarto, 1995; Cui and Delage, 1996; Bouabdallah, 1998; Delage and Cui, 2000; 2001; Colin, 2003; Le, 2008; Le Runigo et al., 2008; Masekanva, 2008). Fig. 1 shows the grain size distribution curves of the materials used, along with the curve of Jossigny silt. Some other characteristics of the studied sub-soil are presented in Table 1. The standard proctor curve of *70S30K* is plotted in Fig. 2. An optimal water content of 16% and a maximum dry unit mass of 1.78 Mg/m^3 can be identified. The hydraulic conductivities of the sub-soil mixture (*70S30K*) in function of dry unit mass are plotted in Fig. 3. A straight line was obtained in a semi-logarithmic plane. The ballast used was taken from the storage of construction materials of the French railways company (SNCF) and its characteristics meet the corresponding standard of SNCF.
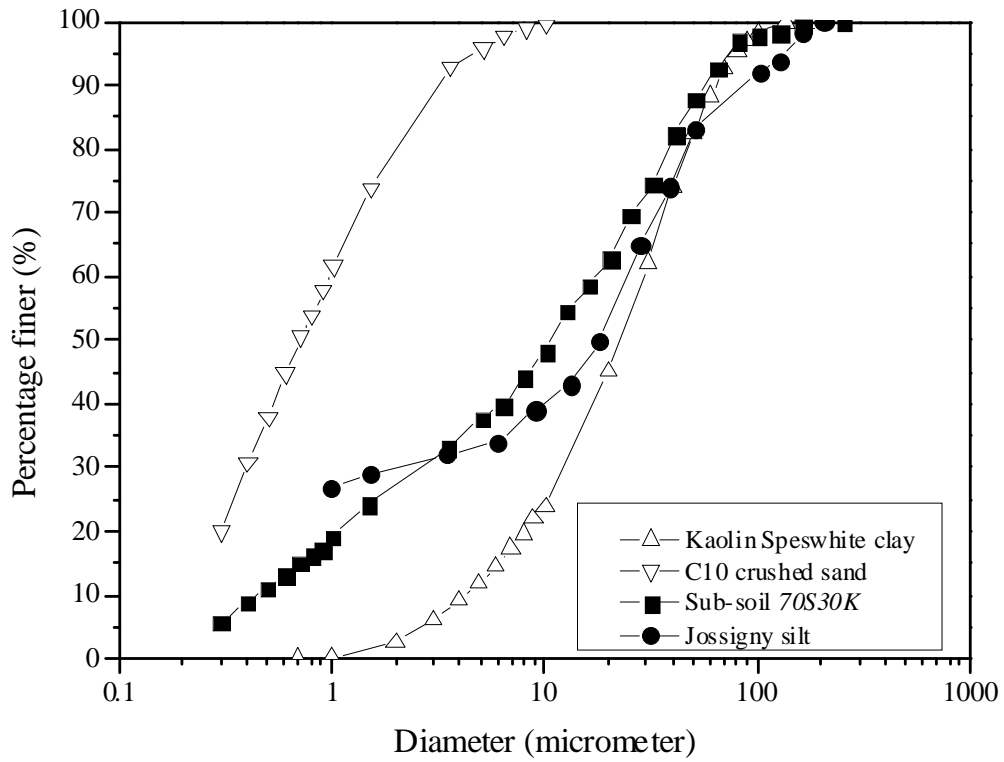
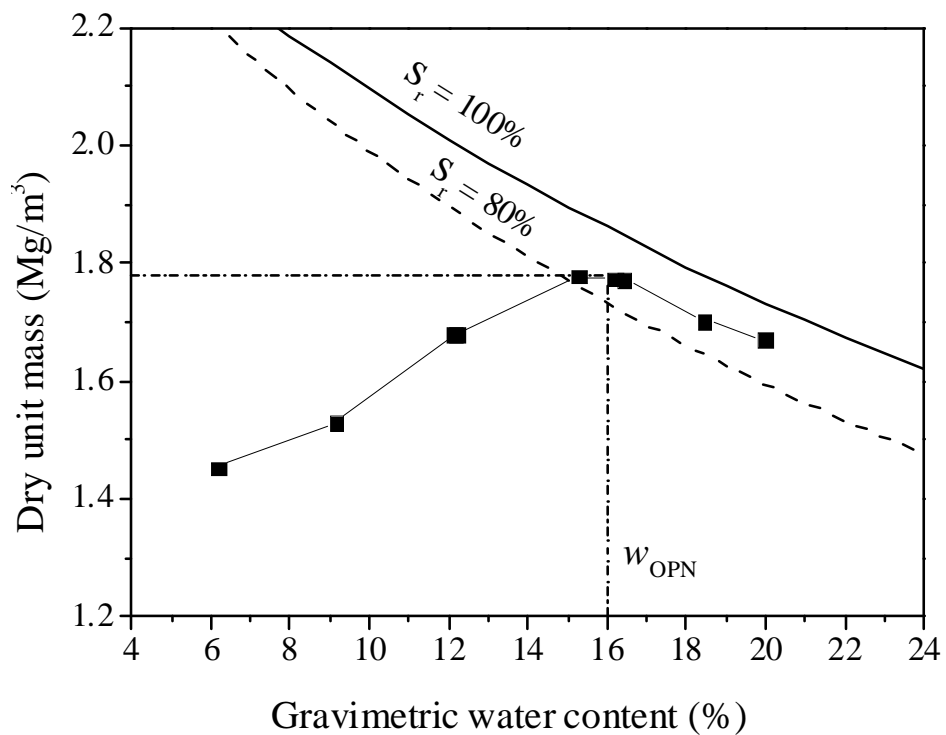**Fig. 1: Grain size distribution curve of the studied materials**

Fig. 2: Standard Proctor curve of sub-soil
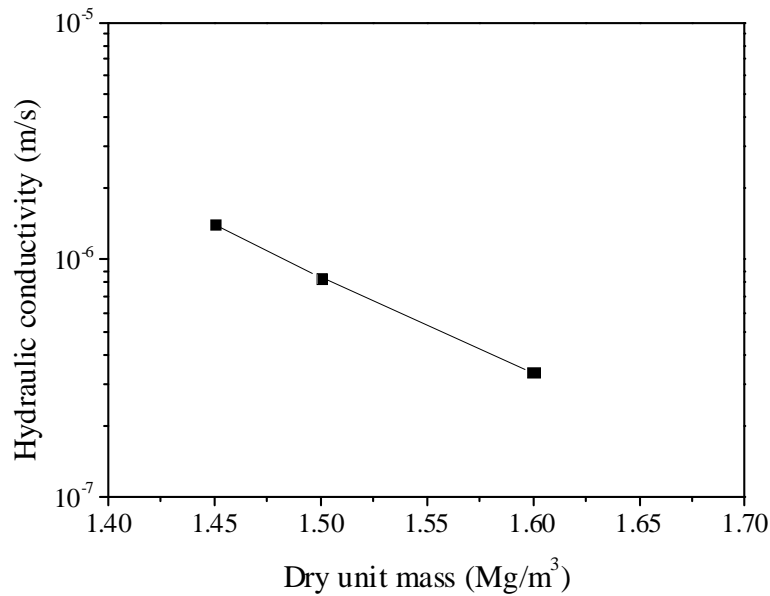
Fig. 3: Hydraulic conductivity of sub-soil

Table 1: Characteristics of sub-soil 70S30K

Parameter	Value
Specific gravity of clay ρ_s	2.60
Specific gravity of crushed sand ρ_s	2.65
Liquid Limit LL	27%
Plasticity Index IP	11%
Optimum water content w	16%

Experimental setup and procedures

Fig. 4 presents a schematic view of the physical model, with a one 3D view (Fig. 4a), one side view (Fig. 4b) and one view of cross section A-A (Fig. 4c). The cylindrical cell has an internal diameter of 550 mm, a wall thickness of 20 mm and a height of 600 mm. The wall was made of Poly(methyl methacrylate) - PMMA which is a transparent thermoplastic allowing observation of sample from outside. The following devices were installed:

- a digital camera connected to a computer, that allows the visual monitoring of the ballast/sub-soil interface;

- a LED series installed on the top of the PMMA wall, lighting up the apparatus wall and improving the visual monitoring conditions by the digital camera;

- three time-domain refectory probes (TDR1 to TDR3) embedded in the sub-soil (h = 120, 160, 200 mm), that allow the volumetric water content to be monitored. These sensors provide the dielectric constant K_a which is deduced from the crossing time of electric wave within the surrounding material. To convert K_a into volumetric water content θ, the well-known model of Topp et al. (1980) was used:

$$\theta = -5.3 \times 10^{-2} + 2.92 \times 10^{-2} K_a - 5.5 \times 10^{-4} K_a^2 + 4.3 \times 10^{-6} K_a^3 \tag{1}$$

- three tensiometers (T1 to T3) installed in couple with TDRs at different heights (h = 120, 160, 200 mm). They were home-made with the same principle as that for high capacity tensiometer (Ridley and Burland, 1993; Ridley et al., 2003; Mantho 2005, Cui et al., 2008; Toll et al., 2012; Lourenço et al., 2011).

- one pressure sensor installed at the bottom of the apparatus (h = 0 mm) for measuring positive pore water pressure under saturated conditions.

- a hydraulic actuator with integrated displacement and force sensors, that allows monotonic or cyclic loadings.
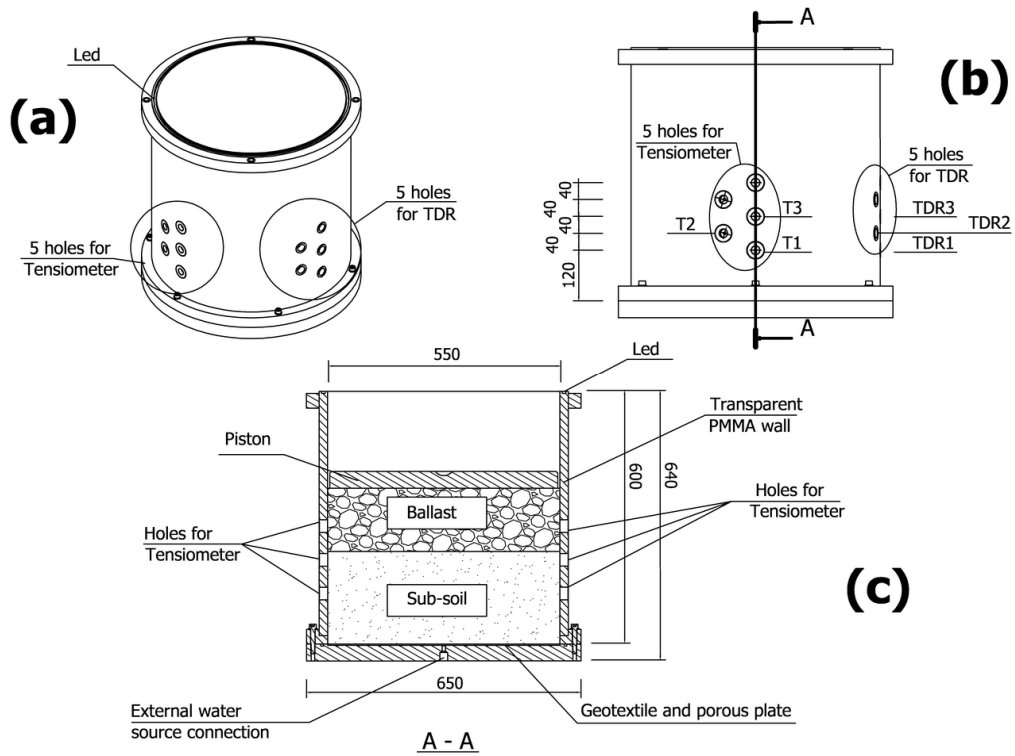
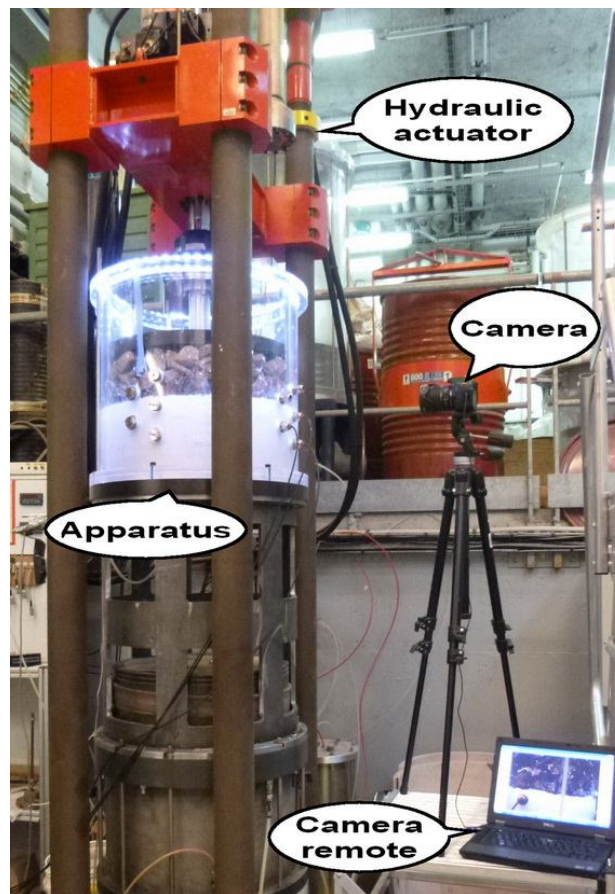**Fig. 4: Schematic view of the apparatus developed**

Fig. 5: Photograph of the experimental set up

For the soil specimen preparation, water was added to *70S30K* to reach the optimum water content $w = 16$ %. The soil specimen was then prepared by manual compaction in five layers of 40 mm thick each and one layer of 20 mm thick, making a total of 220 mm thickness for the whole specimen. For the dry unit mass, three values were considered: 1.4, 1.5 and 1.6 Mg/m^3. These values are close to those considered by other authors: 1.45 Mg/m^3 by Burns et al. (2006) and from 1.52 to 1.54 Mg/m^3 by Alobaidi et al. (1999). According to Burns et al. (2006), the values in this range correspond to the medium strength field conditions. The TDR probes were placed between the compaction layers. A 160 mm ballast layer was placed on the sub-soil and the surface of ballast layer was arranged in order to be horizontal for ensuring the good ballast/piston contact. The whole apparatus was put under the hydraulic actuator. Finally, the tensiometers were installed and other devices were set on (lighting up the LED series, setting up the camera). Fig. 5 shows a view of the whole experimental set up.

Three tests were conducted with three values of initial dry unit mass: 1.4 (E1), 1.5 (E2) and 1.6 Mg/m^3 (E3). All tests started with the sub-soil in unsaturated state ($w = 16$ %), and with application of a pre-loading stage: monotonic loading from 0 to 100 kPa (at an increase rate of 2 kN per minute); low frequency cyclic loading from 30 to 100 kPa; 0.1 Hz for 20 cycles; 1 Hz for 50 cycles and 2 Hz for 100 cycles). Afterwards, a 5 Hz loading for 500 000 cycles was applied. The value of 5 Hz frequency represents the train circulation at 100 km/h and the applied stress was chosen according to the stress distribution in the ancient railway tracks in France (Trinh, 2011; Duong et al., 2014).

In order to study the effect of water content or degree of saturation, once the 500 000 cycles ended, the sub-soil was saturated from the bottom under a hydraulic head of 12 kPa. After saturation, the water level was maintained at 20 mm above the ballast/sub-soil interface in order to ensure the saturated state of the sub-soil. Before the loading under saturated condition, a pressure sensor was installed at $h = 0$ mm. Monotonic loading at the same rate as in unsaturated case was then applied again followed by the 5 Hz cyclic loading. The test ended when fine particles were observed on the surface of ballast layer or when the number of cycles reached 500 000.

Experimental results

A typical result from test E2 under unsaturated condition ($w = 16\%$) is presented in Fig. 6 with the variations of applied pressure (Fig. 6a) and the corresponding axial displacement (Fig. 6b). The

applied stress increases monotonically from 0 to 100 kPa, and then it varied from 30 to 100 kPa representing the cyclic loadings at different frequencies. The displacement increases rapidly under monotonic loading and in the first part of the cyclic loadings. Fig. 7 shows the evolutions of global displacement (displacement of piston) in the unsaturated state ($w = 16\%$) for the three densities. The shapes of the three curves are almost the same: a quick increase followed by a steady state. Even though the pre-cyclic loading stage lasted short time, it contributed significantly to the permanent displacement. This can be explained by the re-arrangement of ballast particles and their penetration into the sub-soil. Indeed, the ballast particles being of angular shape, they can penetrate easily into the sub-soil. During the 5 Hz loading, the reversible displacement was about 0.5 mm, almost the same for three tests. However, for the global displacement, it is observed that the larger the initial dry unit mass of the sub-soil, the lower the axial displacement. This indicates clearly that the sub-soil stiffness can influence the ballast behavior.
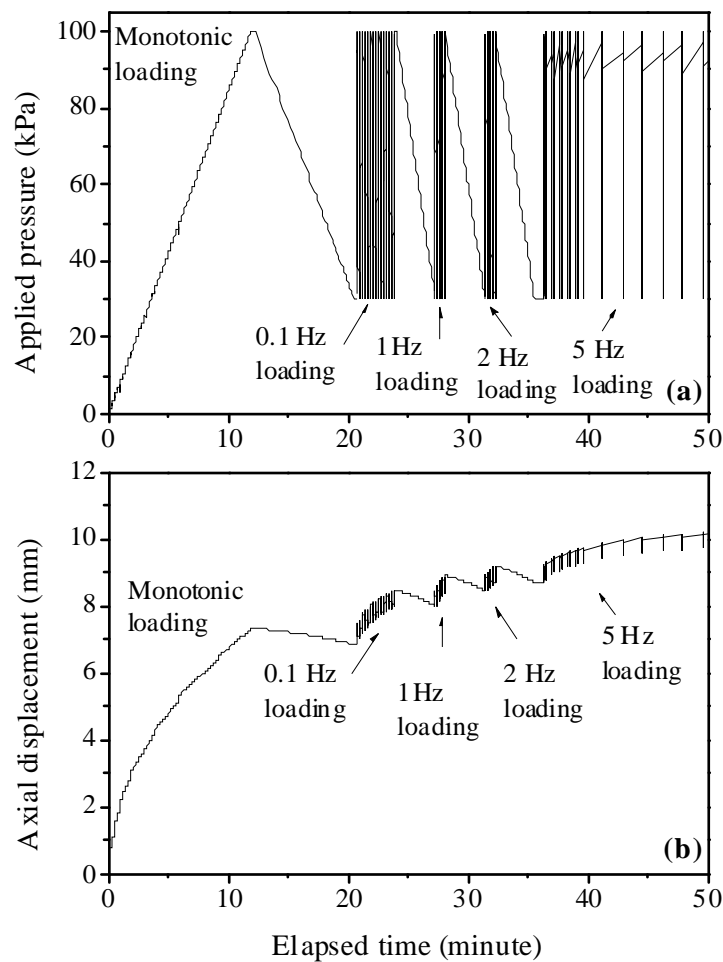

Fig. 6: Typical results ($w = 16\%$ and $\rho_{d\text{-}initial} = 1.5$ Mg/m^3) during the pre-loading

154
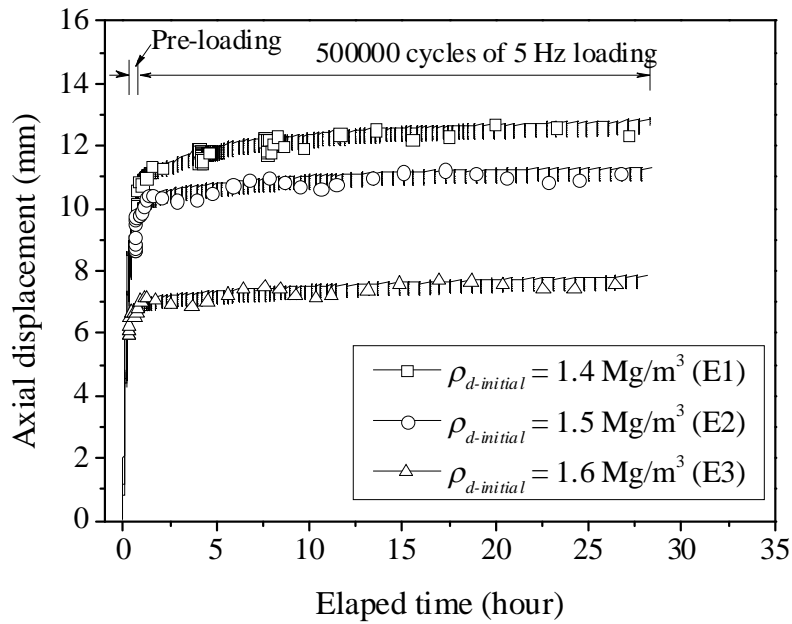
Fig. 7: Axial displacement during loading ($w = 16\%$)

Fig. 8 depicts the evolutions of permanent displacement during the 5 Hz loading under unsaturated conditions. The displacement was insignificant during the first 100 cycles. Beyond 100 cycles, it increased almost linearly with the logarithm of number of cycles. This is consistent with the constitutive models for unbound granular behavior reported in Paute and Le Fort (1984); Hornych (1993) and AFNOR (1995). Comparison of the values at the end of cyclic loading for 500 000 cycles shows that the lower the dry unit mass, the larger the permanent axial displacement. The slope change in test E1 is probably due to a problem of the horizontality of piston.

Fig. 8: Permanent displacement during 5 Hz loading ($w = 16\%$)

a) Before monotonic loading ($w = 16\%$)   b) After 500 000 cycles 5 Hz loading ($w = 16\%$)

Fig. 9: Photographs of the ballast/sub-soil interface: a) before monotonic loading and b) after 500 000 cycles 5 Hz loading ($w = 16\%$ and $\rho_{d\text{-}initial} = 1.4$ Mg/m^3).
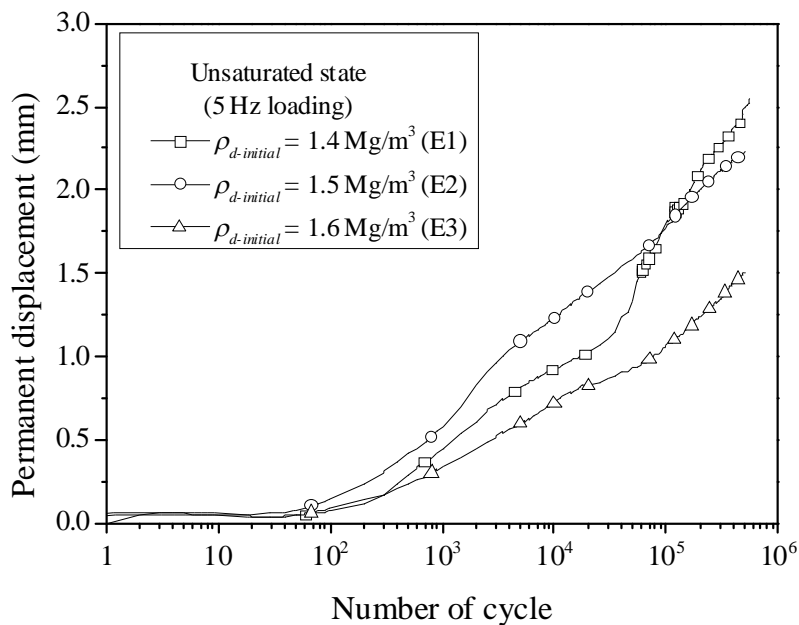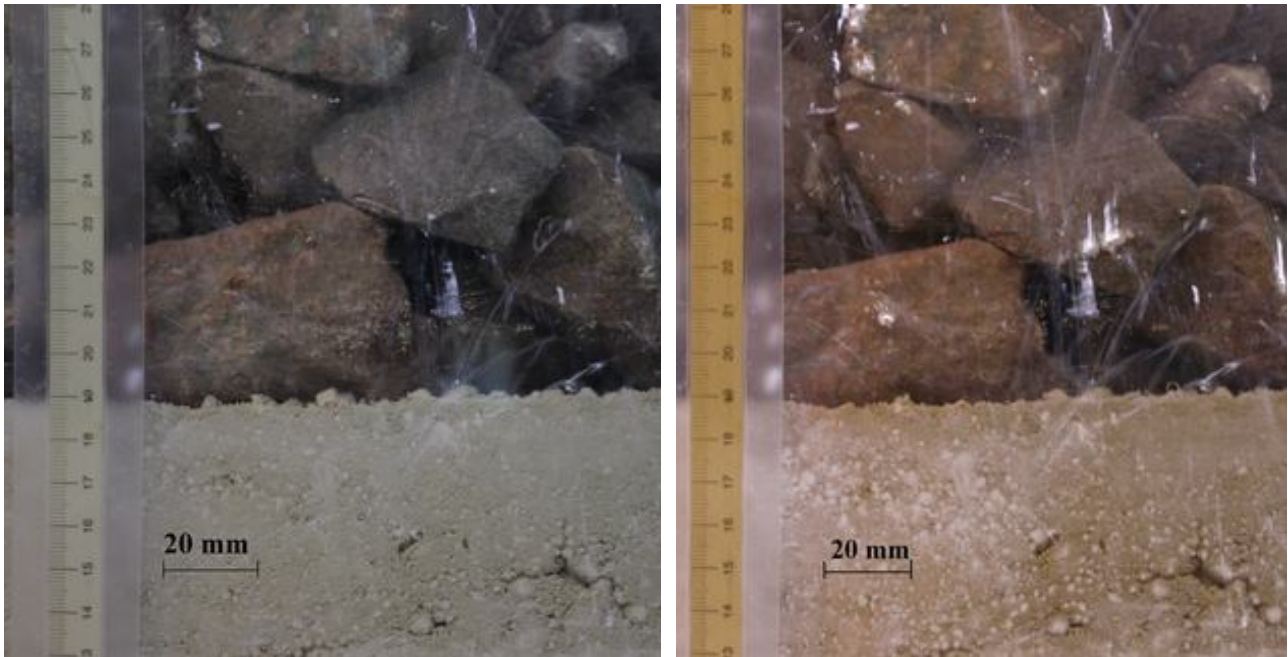
The photographs taken by the digital camera before and after loading in test E1 allowed the visualization of the movement of ballast particles and the evolution of the sub-soil surface (Fig. 9). Limited ballast movement can be seen and the ballast/sub-soil interface did not change significantly. In order to have a better comparison, based on the photographs, one ballast particle was identified in each test and its movement was analyzed. The contours of these particles at two key moments (before loading and after the 5 Hz loading for 500 000 cycles) are identified and the position changes of the ballast particles chosen are presented in Fig. 10. The reference point (zero value) corresponded to the ballast/sub-soil interface. It is observed that the difference between the positions of ballast particles is consistent with the displacement recorded: it is more pronounced at lower initial dry unit mass. Furthermore, there was not only vertical displacement but also rotation of ballast particles, indicating the re-arrangement of ballast particles.
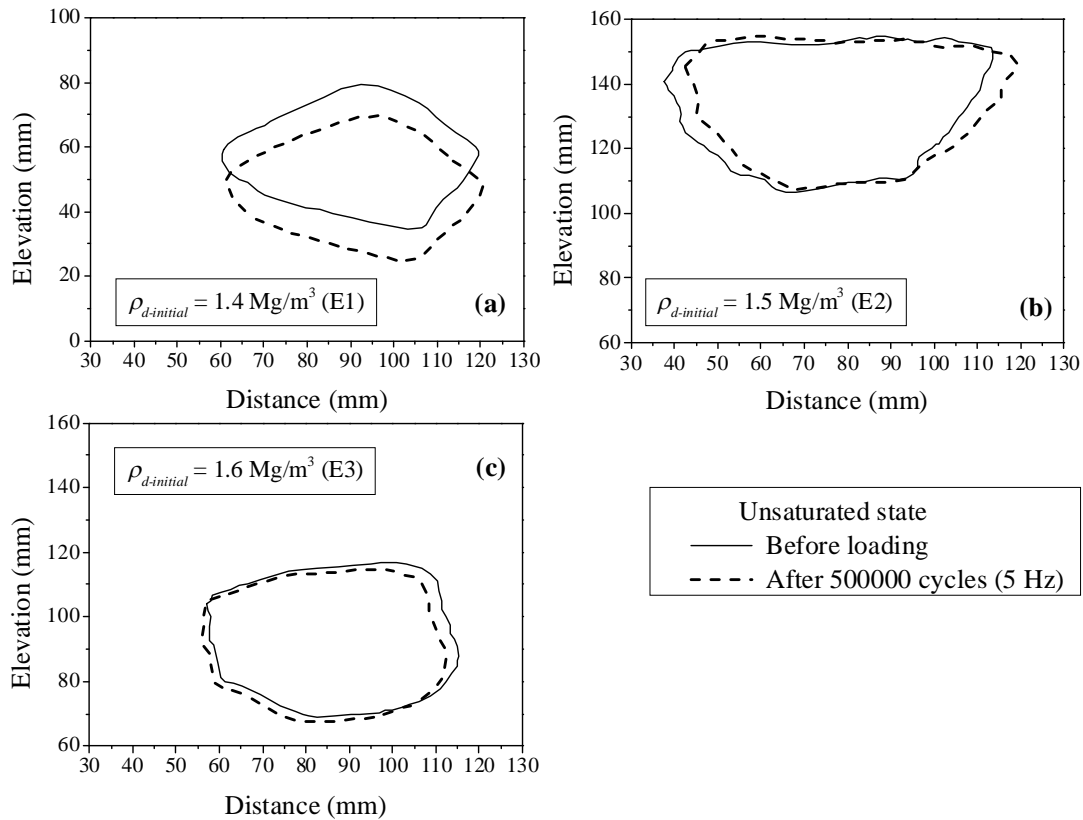
Fig. 10: Movement of ballast particles before and after the loading in unsaturated state of sub-soil.

Fig. 11 depicts the evolutions of volumetric water content of sub-soil from the beginning of the test to the end of the 5 Hz loading for 500 000 cycles. After compaction, with the same initial water content $w = 16\%$, the average volumetric water content (θ) increased with dry unit mass, as expected. During the pre-loading stage, there was an increasing trend at all levels and in all tests. The increase of θ at $h = 200$ mm (20 mm below the ballast/sub-soil surface) was the most pronounced. This can be explained by the ballast penetration into the sub-soil and the settlement of sub-soil that can results in diminution of sub-soil void, thereby increasing the volumetric water content.

Fig. 11: Evolutions of volumetric water content during the loading in saturated state

During the 5 Hz loading for 500 000 cycles, the water content was stable (Fig. 11a). The values for test E1 were 19.9 ± 0.3 % at $h = 120$ mm, 19.5 ± 0.5 % at $h = 160$ mm and 19.3 ± 0.3 % at $h = 200$ mm. The values for test E2 were 22.2 ± 0.2 % at $h = 120$ mm, 23.4 ± 0.3 % at $h = 160$ mm and 21 ± 0.5 % at $h = 200$ mm. For test E3, they were 26.6 ± 0.4 % at $h = 120$ mm, 26.7 ± 0.2 % at $h = 160$ mm and 25.9 ± 0.3 % at $h = 200$ mm. Note that the accuracy of the TDR used is 2% over the working range.
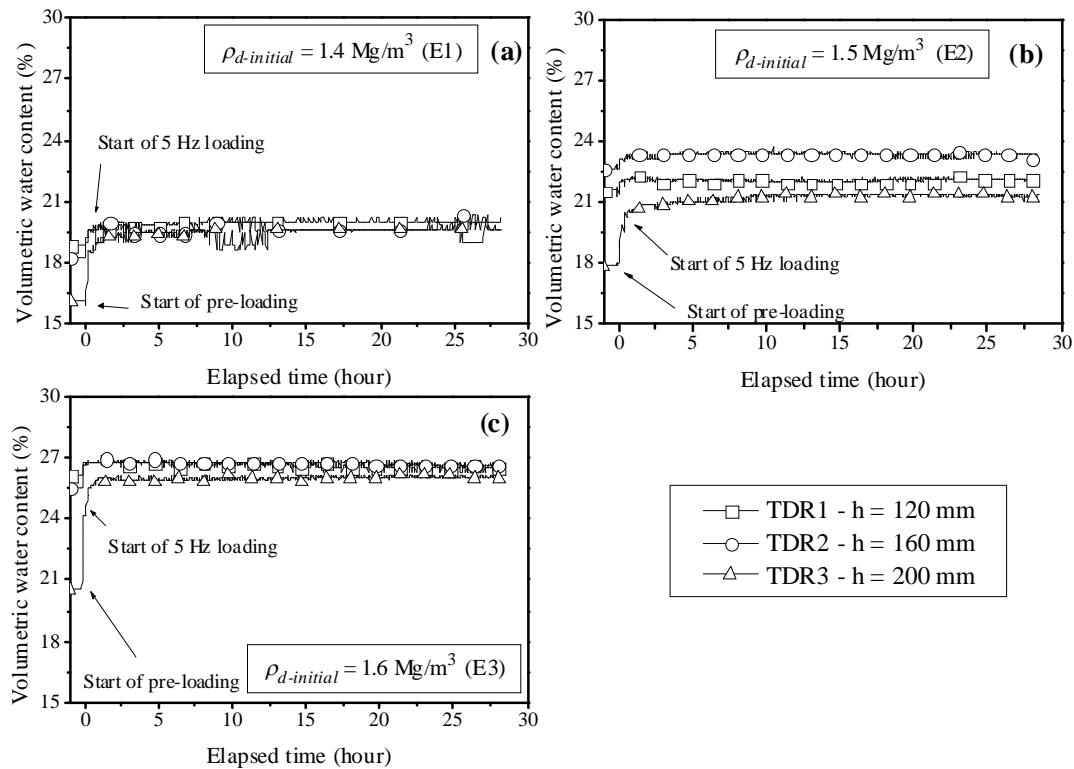
When the 5 Hz loading for 500 000 cycles in the unsaturated state ended, the sub-soil was saturated. A typical result of variations of volumetric water content from test E2 during saturation is presented in Fig. 12a. The corresponding increase of pore water pressure (or suction decrease) is presented in Fig. 12b. The three levels show the same variations, suggesting a quite fast water flow through the sample. It took about 20 hours for the volumetric water content to reach stabilization, while about 60 hour was required for the pore water pressure to reach zero. In addition, when the volumetric water content became steady, the pore pressure continued increasing. It is well known that during the saturation of very fine soil, it is very difficult to reach $S_r = 100$%. During saturation, the macro-pores are filled first, while it takes longtime for water to fill the micro-pores. This can be observed also in Fig. 12b. The fact that the evolutions of pore water pressure of all three levels are the same confirms that the micro-pores were filled quickly and the suction changes were governed mainly by

the micro-pores filling process. At the end of saturation stage where water level was fixed at 2 mm above the ballast/sub-soil interface, the water pressures given by tensiometers were consistent with the hydraulic levels: higher water pressure was obtained at lower hydraulic level. This partly indicates the good performance of the tensiometers used.
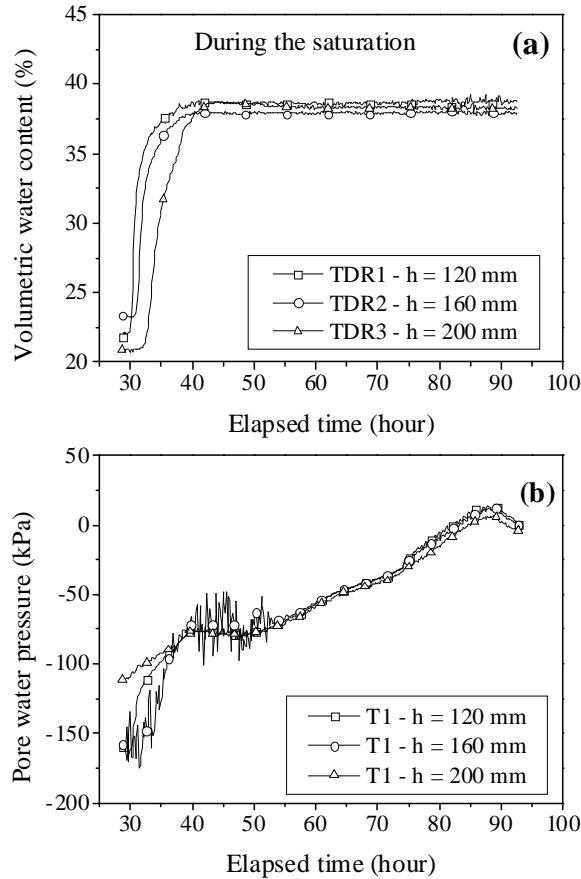
Fig. 12: Typical result of volumetric water content and pore water pressure during the saturation of sub-soil ($\rho_{d\text{-}initial}$ = 1.5 Mg/m³)

The profiles of volumetric water content are presented in Fig. 13 for the three tests at 4 key moments: before loading, after pre-loading, at the end of cyclic loading and after the saturation. It can be observed again that after preloading, the change of volumetric water content at h = 200 mm was the most pronounced for the three cases. The saturation process boosted the volumetric water content, defining well distinguished profiles. Assuming that the dry unit mass of the sub-soil did not change during the test, the degree of saturation S_r was calculated and its profiles are also presented in Fig. 13. The final degree of saturation was not the same for the three tests, depending on the initial dry unit mass.
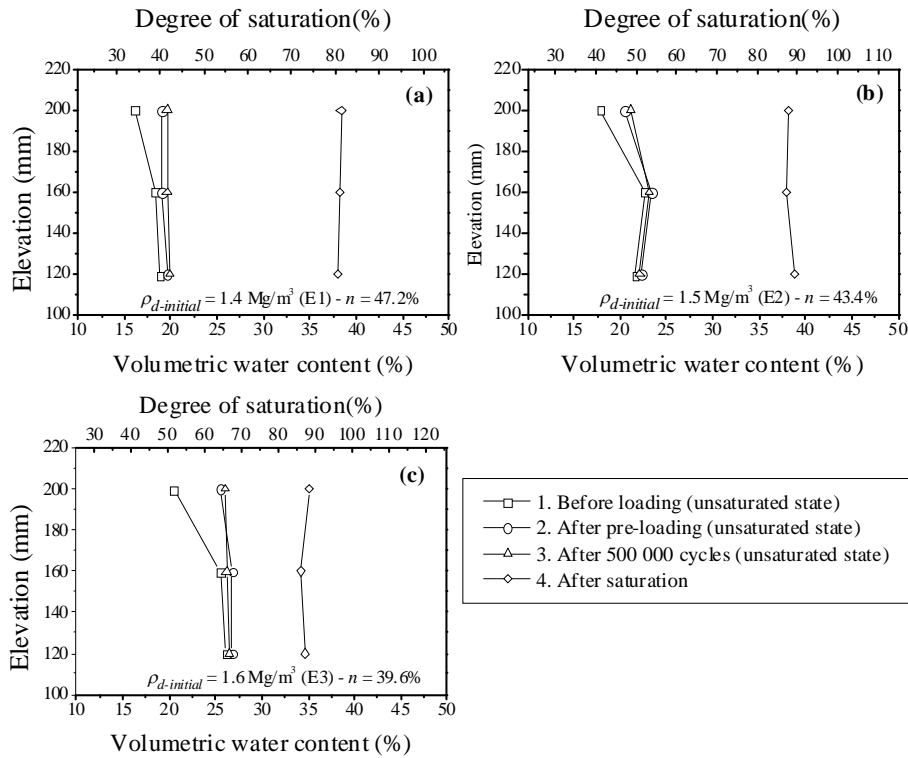
Fig. 13: Profiles of volumetric water content of degree of saturation
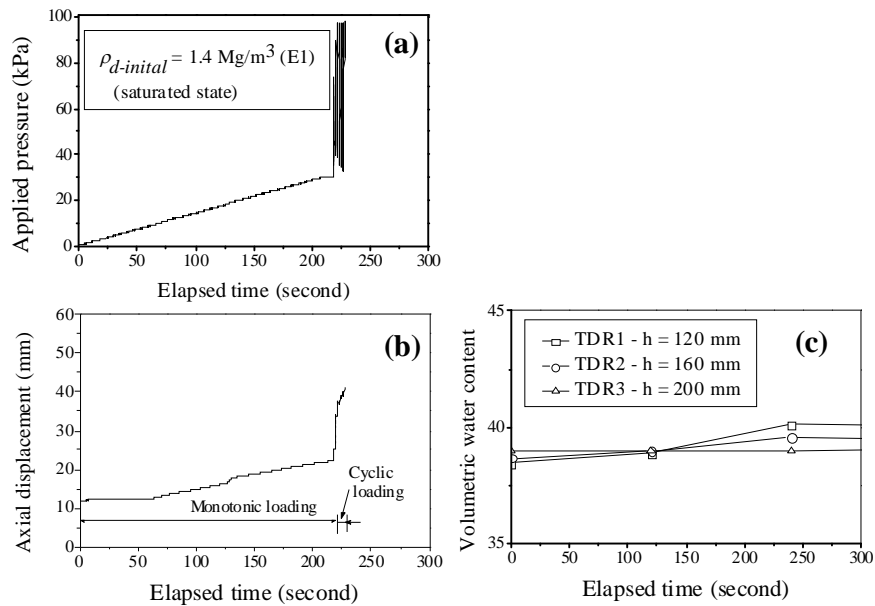
Fig. 14: Test in the case of $\rho_{d\text{-}initial}$ = 1.4 Mg/m³ under saturated conditions: a) applied pressure, b) axial displacement, c) volumetric water content

At the end of saturation stage, loadings were applied again and Fig. 14 illustrates the results from test E1, with applied pressure (Fig. 14a), permanent axial displacement (Fig. 14b) and volumetric water content (Fig. 14c) over time. It can be seen that when the applied pressure increased, the axial

160

strain increased significantly. The increase rate was sharper during the cyclic loading. Indeed, it took just 10 seconds (50 cycles) for the permanent axial displacement to increase to 40.9 mm. This significant increase in displacement was accompanied by a significant mud pumping phenomenon characterized by flow of fine particles through the ballast layer till the ballast surface. Because the mud pumping phenomenon took place much faster than expected, the pore water pressure was not recorded. The volumetric water content (Fig. 14c) seemed to change a little; but as the smallest time interval for the record of the TDR used is 1 min, the recorded data may not be representative and should not be used for further analysis.
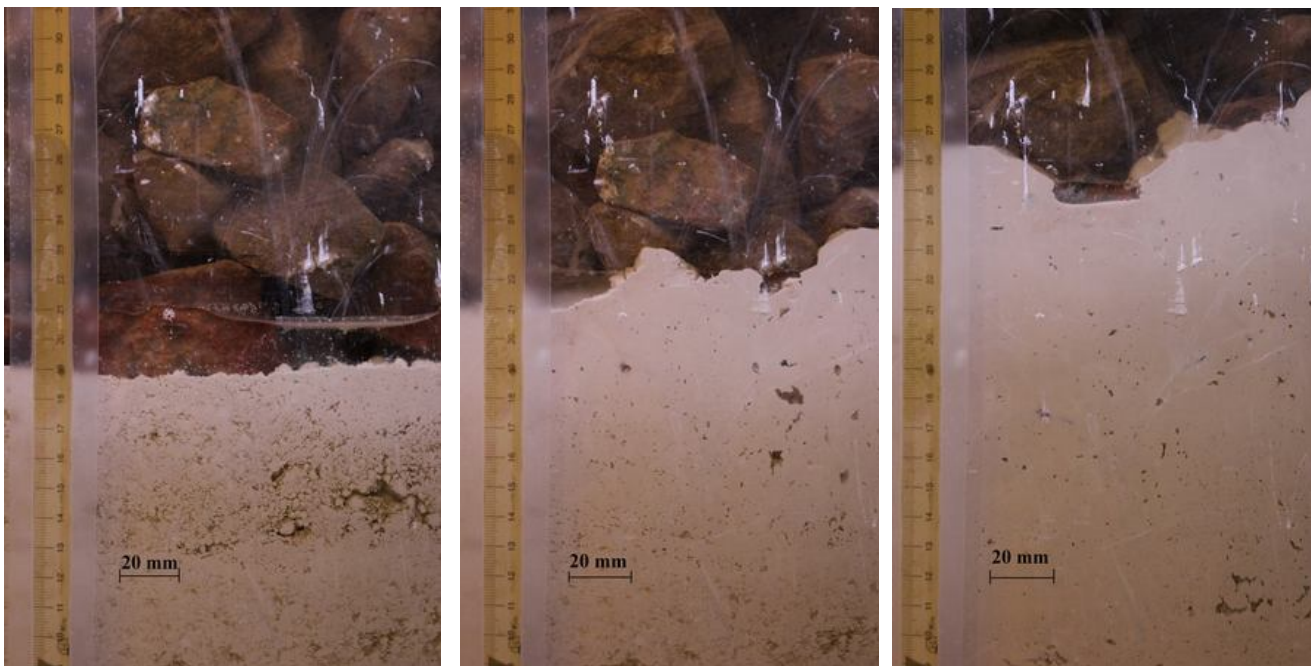
| a) After saturation and before monotonic loading | b) After monotonic loading (saturated state) | c) After cyclic loading (saturated state) |

Fig. 15: Photographs showing the evolution of the ballast/sub-soil interface ($\rho_{d\text{-}initial}$ = 1.4 Mg/m^3).

Fig. 15 shows the evolution of interface in test E1. The photographs were taken at three moments: before loading in saturated state, after monotonic loading and after cyclic loading. They are presented in Fig. 15a, b, c, respectively. It can be seen clearly that fine particles were pumped up as the loadings were applied.

Fig. 16: Test in the case of $\rho_{d\text{-}initial}$ = 1.5 Mg/m^3 under saturated conditions: a) applied pressure; b) pore water pressure, c) permanent axial displacement; and d) volumetric water content.

Fig. 16 presents the results from test E2, with applied pressure, pore water pressure, permanent axial displacement and volumetric water content (Fig. 16 a, b, c and d, respectively). During the monotonic loading (from 0 to 100 kPa), the permanent axial displacement increased from 9 mm to 29 mm. The pore water pressure at h = 120 mm and h = 200 mm increased sharply and reached 30 kPa while at h = 0 mm and h = 160 mm, the increase rate was less significant. When the monotonic loading ended, the pore water pressure at all the three levels decreased slightly but remained higher than zero. This can be explained by the low hydraulic conductivity of *70S30K* (Fig. 3) that makes long time for the dissipation of water pressure. Under the 5 Hz loading, the permanent displacement continued to increase rapidly. However, the increase of permanent axial strain was less pronounced than in test E1 at lower dry unit mass. During the cyclic loading, the pore water pressure (Fig. 16b) became quickly higher than 40 kPa (except at h = 160 mm possibly due to the lower sensor performance). In the end, the values obtained are between 40 and 58 kPa. As the applied pressure was 30-100 kPa, the effective stress (total applied stress minus pore water pressure) sometimes became zero even negative, suggesting that liquefaction occurred within the sub-soil. The volumetric water content increased slightly during the monotonic loading at all three levels (Fig.

16d). The start of cyclic loading marked an simultaneous increase at $h = 120$ and 160 mm but a decrease at h = 200 mm. Note that the level $h = 200$ mm was the closest to the ballast/sub-soil interface, and with the largest displacement as presented in Fig. 16c the position of TDR could change significantly. In addition, the evolution of the ballast/sub-soil interface could also affect the response of this TDR.

The photographs taken at the ballast/sub-soil interface at three moments (after saturation, after monotonic loading and after cyclic loading) are presented in Fig. 17. As in the previous case, the fine particles were pumped up significantly especially during the cyclic loading.

| a) After saturation and before monotonic loading | b) After monotonic loading (saturated state) | c) After cyclic loading (saturated state) |

Fig.17: Photographs showing the evolution of the ballast/sub-soil interface: ($\rho_{d\text{-}initial} = 1.5$ Mg/m^3).
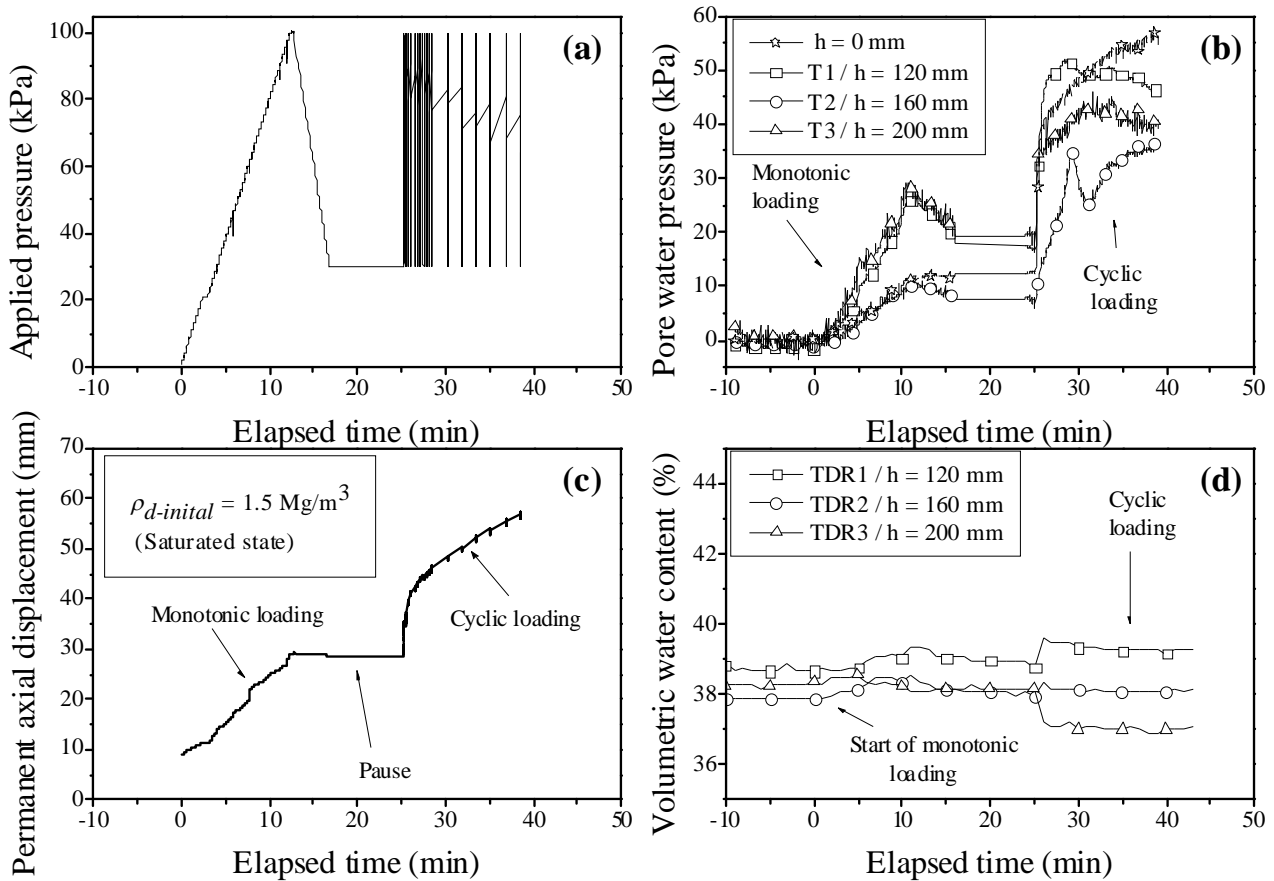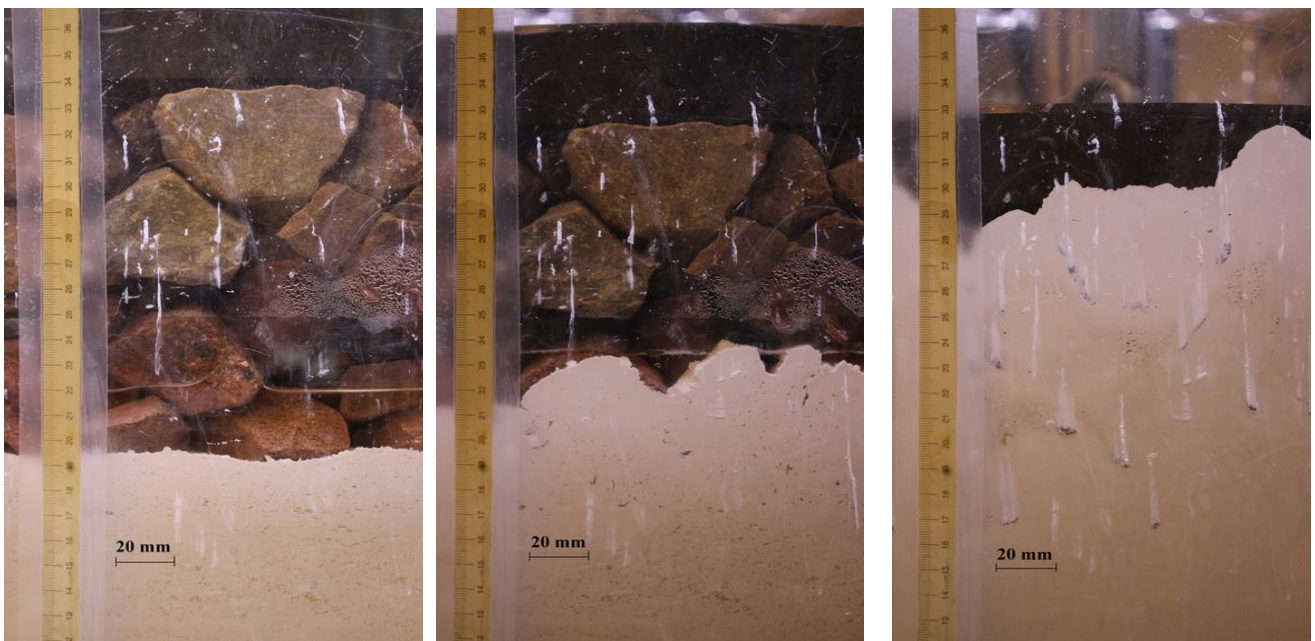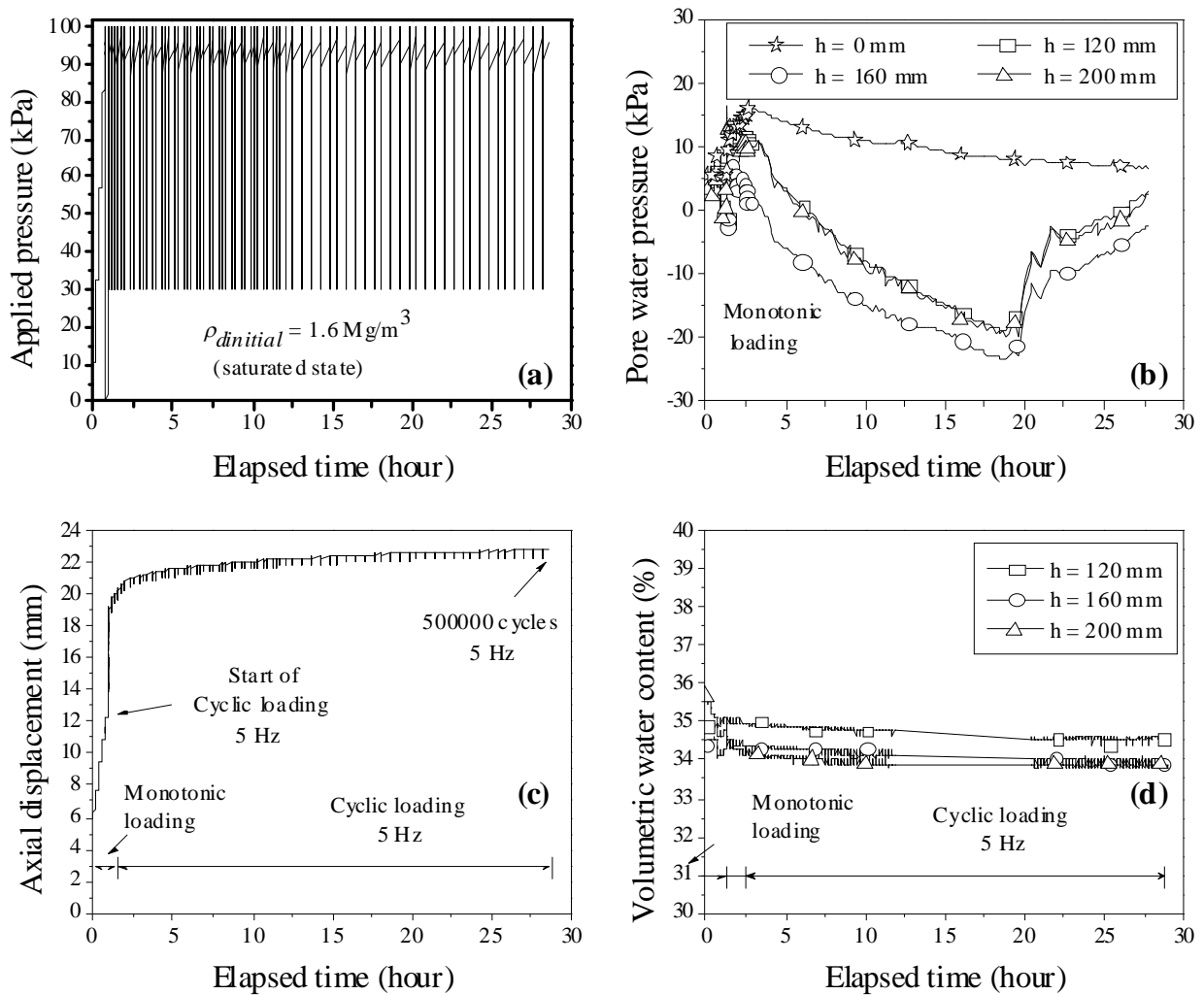
Fig 18: Test in the case of $\rho_{d\text{-}initial}$ = 1.6 Mg/m³ under saturated conditions: a) applied pressure; b) pore water pressure, c) permanent axial displacement; and d) volumetric water content.

The results from test E3 are presented in Fig. 18, in terms of applied pressure (Fig. 18a), pore water pressure (Fig. 18b), permanent axial displacement (Fig. 18c) and volumetric water content (Fig. 18c). In this test, as fine particles were not pumped up to the ballast surface, the 5 Hz cyclic loading were applied till 500 000 cycles. Monotonic loading (from 0 to 100 kPa) increased the axial displacement to 12 mm. This increase continued during the cyclic loading, especially during the first cycles of 5 Hz loading. Nevertheless, the increase rate slowed down and the axial displacement tended to be stable at around 22 mm. The pore water pressure increased during the first cycles of loading and then it decreased (Fig. 18b). If the soil is considered as unsaturated at the elevations of tensiometers, the slight decrease trend of volumetric water content comes along with the increase of suction. The sharp decrease followed by a new increase at 20 h for the pore water pressures given by the tensiometers is difficult to explain. Some technical problem might occur. For the volumetric water content, the slight decrease can be explained by the volume change of soil due to loading.

| a) After saturation and before monotonic loading | b) After monotonic loading (saturated state) | c) After cyclic loading (saturated state) |

Fig. 19: Photographs showing the evolution of the ballast/sub-soil interface ($\rho_{d\text{-}initial}$ = 1.6 Mg/m^3).
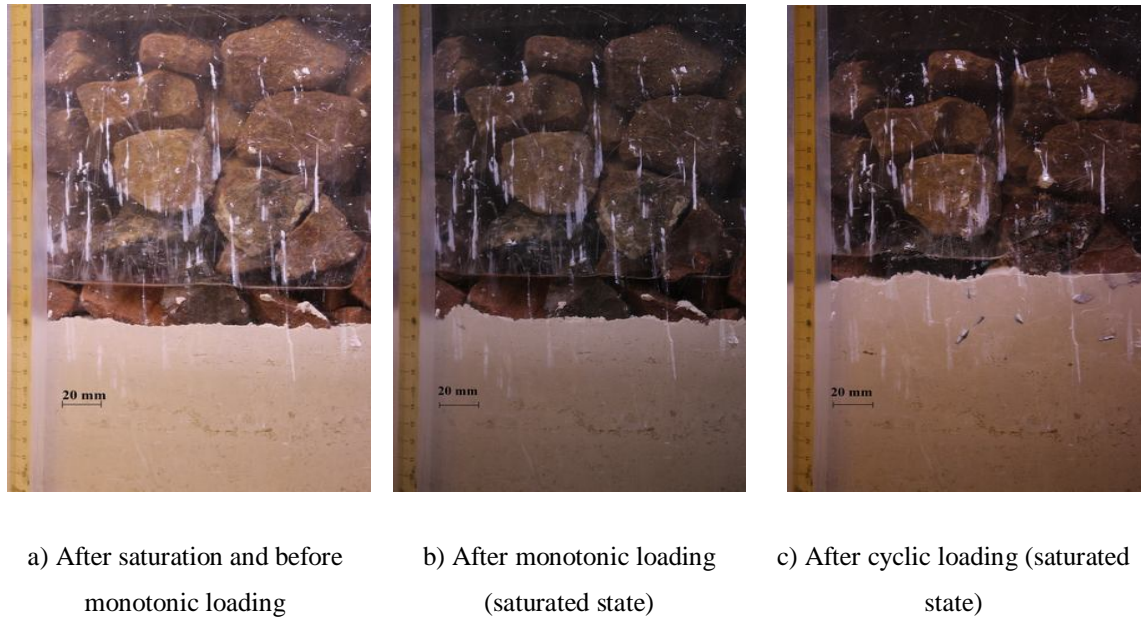
Fig. 19 shows the photographs taken in test E3 right before the monotonic loading (Fig. 19a), after the monotonic loading (Fig. 19b) and after the cyclic loading (Fig. 19c). The movement of fine particles can be also observed. During the monotonic loading, fine particles moved up, but much less than in the previous tests. Even after a large number of cycles, the sub-soil level rose up by about 20 mm, and there was no fine particles pumped up to the ballast surface.

Because when the sub-soil was in saturated state, test E1 under the 5 Hz cyclic loading ended very quickly (in 10 seconds), the tensiometers did not record the variations of pore water pressure. In order to analyze the pore water pressure changes during cyclic loading, this test was continued with 0.1 Hz loading. The results during this stage are presented in Fig. 20 with the applied stress (Fig. 20a), the pore water pressure (Fig. 20b), the piston displacement (Fig. 20c) and the volumetric water content (Fig. 20d). As expected, the axial displacement increased quickly during the cyclic loading. For the variations of pore water pressure, the values at h = 0 mm, 120 mm and 200 mm varied consistently from 40 kPa to 80 kPa while at h = 160 mm, the variation was less significant. This difference may be due to the lower tensiometer performance as mentioned previously. As the cyclic loading was at lower frequency (0.1 Hz), the variations of pore water pressure were recorded successfully. These variations are plotted together with the applied pressure in Fig. 21a (without the data at h = 160 mm for the reason mentioned previously). It can be seen that the pore water pressure followed the applied pressure. This allowed the difference between them to be calculated as presented in Fig. 21b. It is observed that the effective stress can become negative during the

unloading process. This means that the sub-soil lost totally its strength and was liquefied. Obviously, this favorites the penetration of ballast into the sub-soil, thus, increasing the axial displacement. Furthermore, the fine particles lost their cohesion and with the high pore-water pressure, they were brought up to the ballast layer by dissipation of this pressure. Deeper examination shows that the negative effective stress took place during the unloading process corresponding to the uplift of the piston. Note that the negative value for the effective stress has no physical meaning; it just indicates that there was no longer physical contact between soil particles and it corresponded to a depression or suction applied to water only. Further study is needed to verify this point.
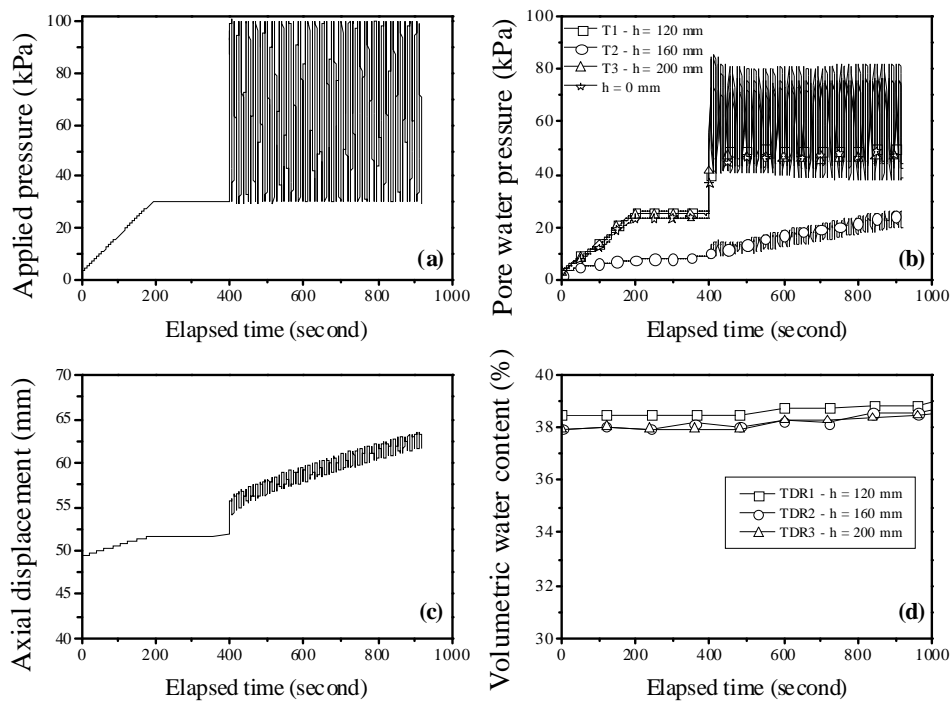
Fig. 20: Test at low frequency (0.1 Hz).
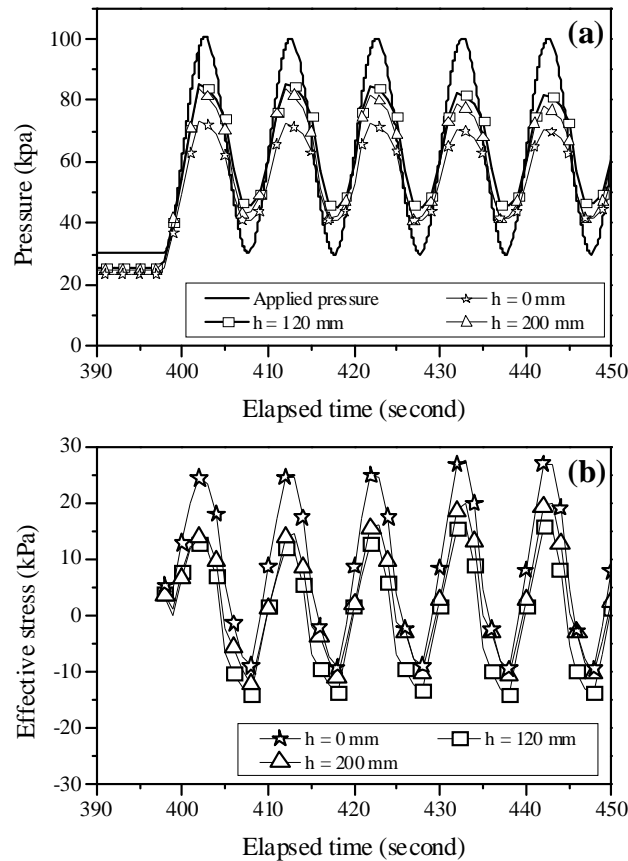
Fig. 21: Comparison between applied pressure and pore water pressure (a) and variations of effective stress.

Summarizing, in test E1 ($\rho_{d\text{-}initial}$ = 1.4 Mg/m^3), the fine particle was pumped up very quickly and it took just 10 seconds for fine particles to migrate to the ballast surface. In test E2 ($\rho_{d\text{-}initial}$ = 1.5 Mg/m^3), the time needed for fine particles to be totally pumped up to the surface was about 15 minutes, while it took 28 hours for 20 mm fines migration in test E3 ($\rho_{d\text{-}initial}$ = 1.6 Mg/m^3). This finding evidences the strong influence of the dry unit mass of sub-soil on the migration of fine particles. For further analysis, the permanent axial displacement due to the 5 Hz cyclic loading in the three tests is plotted versus number of cycles in Fig. 22. There is a clear effect of sub-soil dry unit mass: the lower the sub-soil density, the faster the development of permanent axial displacement.
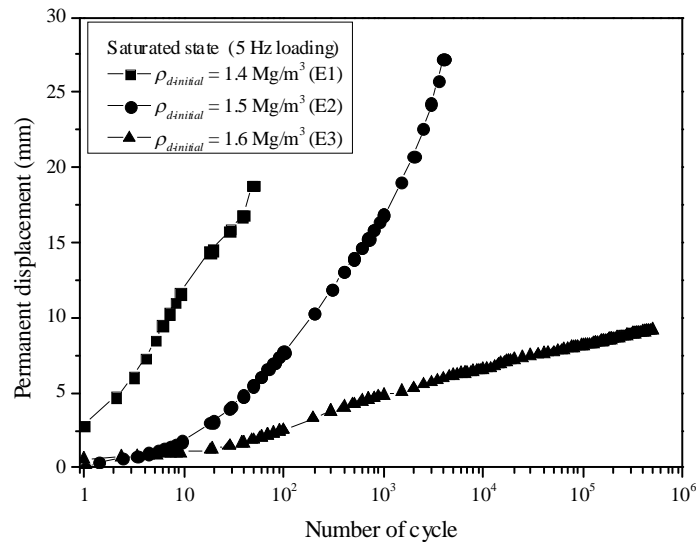
Fig. 22: Effect of number cycles - Comparison between three cases with different initial dry unit masses

Discussion

The permanent axial displacement evolutions in the tests under unsaturated conditions of sub-soil evidenced the effect of sub-soil state on the ballast behavior. During the 5 Hz loading, the water content of the sub-soil was very steady indicating an unchanged sub-soil state (Fig. 11). In this case, the axial displacement during the 5 Hz loading is mostly related to the ballast behavior. Thus, the different responses in permanent axial displacement in Fig. 8 suggest differently ballast behavior under different sub-soil dry unit masses. This statement can be confirmed by the results in Fig. 10: the displacements are different between the vertical and horizontal directions. The ballast layer can undergo a rearrangement between them under external loadings and this arrangement was not the same for different sub-soil states. This finding is useful in practice because to date, studies on ballast working together with sub-soil are scarce and in most cases, the materials are usually tested separately without considering the interaction between them; for instance testing ballast only (Indraratna et al., 1997; Indraratna and Salim, 2005; Karraz, 2008; Aursudkij et al., 2009; Indraratna et al., 2011) or testing sub-soil only (Sattler et al., 1989; Li and Selig, 1996; Miller et al., 2000; Adam et al. 2007; Liu and Xiao, 2010).

The test procedure under two water contents (or degree of saturations) of sub-soil enabled the crucial role of water to be evidenced. It was observed that the ballast/sub-soil interface did not change upon loadings in unsaturated state (Fig. 9). However, it changed significantly when the sub-soil was in saturated state. This suggests that the water content of sub-soil is a key factor for the migration of fine particles. This is consistent with the previous studies where mud pumping was

identified in the zones with presence of water. Water can soften the base layer enhancing the penetration of ballast into the sub-grade. On the other hand, the presence of water enables generation of pore-water pressure under external loading; the dissipation of this pressure brings fine particles up to the ballast layer. The ballast penetration and migrations of fine particles created a layer of mixture materials, termed as interlayer.

During the loadings under saturated conditions, five reference vertical sections were chosen and the interface evolutions at these sections were analyzed and presented in Fig. 23. In general, the interface evolutions followed the same trend and the pumping levels of fine particles are uniform across the section. This is confirmed by the visual observation after the tests. Two key moments (start of monotonic and cyclic loadings) can be clearly identified by the distinguished changes of pumping level.
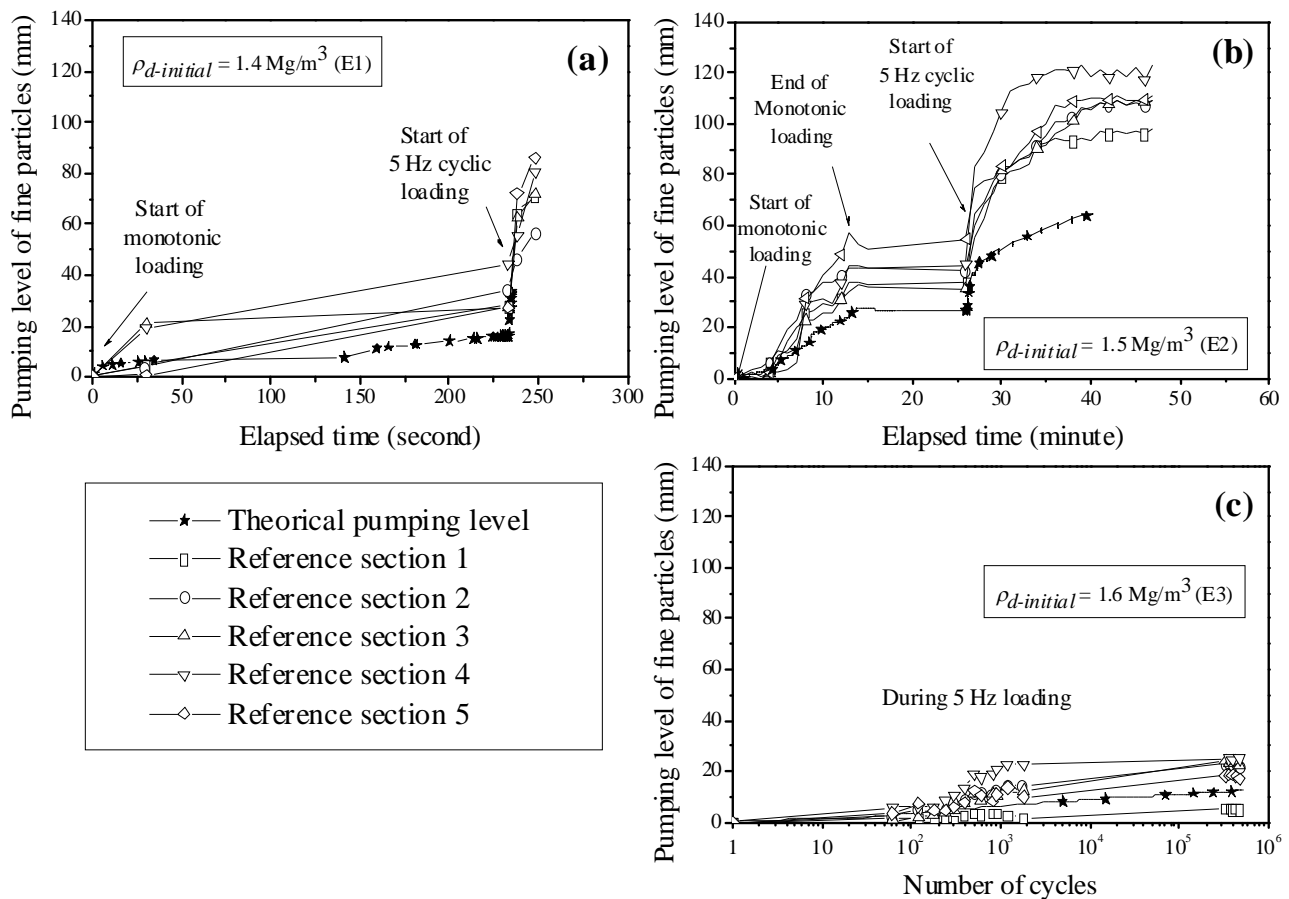

Fig. 23: Pumping level of fines particles

In order to verify the nature of the migration of fine particles, a comparison was made between the volume of ballast particles penetrated into the sub-soil V_1 and the volume of ballast layer voids filled by pumped up fine particles V_2, with

169

$$V_1 = \frac{h_1 \times A}{1 + e}$$

$$V_2 = \frac{h_2 \times A}{1 + e} e$$

(2)

where h_1 is the settlement of ballast layer, A is the sample cross section and e is the void ratio of ballast layer, h_2 is the pumping up level of fine particles in the ballast layer.

Assuming that fine particles migration related to ballast particles penetration and these fine particles fill the voids in ballast layer are equal, i.e., $V_1 = V_2$, the following expression can be obtained:

$$h_2 = \frac{h_1}{e}$$

(3)

Indraratna et al. (1997) reported that the void ratio of ballast e can vary from 0.74 (compacted) to 0.95 (un-compacted). A value of 0.75 was proposed by Tutumluer et al. (2008) and Huang et al. (2009). In the case of the present study, as the sample underwent 500 000 cycles of 5 Hz loading, the ballast layer can be considered as compacted. From Eq. 3, the theoretical pumping level of fine particles is calculated using $e = 0.74$ and plotted also in Fig. 23.It can be seen that the theoretical pumping level for tests E1 and E2 are clearly much smaller than the real pumping level deduced from photographs. This suggests that fine particles moved up not only due to ballast penetration, but also due to the dissipation of excess pore water pressure. By contrast, in the case of test E3, the theoretical curve stays in the middle of those of reference sections. This suggests that the migration of fine particles was due to the ballast penetration and not due to the dissipation of pore water pressure.

To explain the high pore water pressure in tests E1 and E2 but not in test E3, hence the mud-pumping in the first two cases and the interlayer creation in the third case, the compressibility of the sub-soil can be considered. Even though the degree of saturation after saturation in case of 1.6 Mg/m^3 is the highest values among those of the three cases; as the sub-soil was highly compacted, its compressibility is lower than in the other two cases. Thus, under cyclic loadings, the trend of volume change for the sub-soil was limited, enabling lower excess pore water pressure. On the contrary, in the two other cases, with lower dry unit mass, the soil was more compressive, enabling higher excess pore water pressure. As a result, migration of fine particles occurred by dissipation of water pressure.

In reality, most sub-soils are not always saturated. This explains why interlayer is more common than mud pumping. Water is the necessary condition, but it is the soil compressibility that governs the phenomenon to occur. In some previous studies (Wong et al., 2006; Kettil et al., 2008; Li et al., 2012), it was also reported that excess pore water pressure in sub-soil can be generated under train loading and the value depends on depth, train speed and load.

The permanent displacement curves as presented in Fig. 21 can also be used to distinguish the two phenomena (mud pumping and interlayer creation). When the curve is concave (E1 and E2) indicating a sharp increase of permanent displacement with number of cycles, mud pumping occurs; when the curve is rather convex (E3) indicating a slow increase of permanent displacement with number of cycles, interlayer creation occurs. Further study is needed to verify this statement.

Conclusions

Using a physical model developed, the mud pumping and the interlayer creation phenomena in the context of railway sub-structure were studied by investigating the driving factors. The soil sample was prepared with two layers, one ballast layer overlying one sub-soil layer, representing the ancient railway sub-structure in France. The tests were conducted at two water contents and three densities of sub-soil with monotonic and cyclic loadings. The results obtained allow the following conclusions to be drawn:

1) The analysis of the ballast settlement through the particles movement, the global displacement and the sub-soil settlement showed that the sub-soil state can strongly influence the ballast behavior: the larger the initial dry unit mass of sub-soil, the lower the permanent axial displacement. This suggests that in order to understand the overall behavior of railway sub-structure, it is important to take into account the interaction between different layers.

2) The presence of water was found to be the most crucial factor for the migration of fine particles. In unsaturated state, both ballast and sub-soil settlement occurred, but without migration of fine particles. Under near saturated state, the ballast/sub-surface interface moved up, and the pumping level depends on the sub-soil dry unit mass. In the case of $\rho_{d\text{-}initial}$ = 1.4 Mg/m^3 and 1.5 Mg/m^3, under cyclic loadings, the pore water pressure was higher than the minimum value of applied stress, resulting in sub-soil liquefaction during the unloading process. Excess pore water pressure dissipation took place, bringing fine particles upward. This corresponds to the mud pumping

phenomenon. In the case of $\rho_{d\text{-}initial} = 1.6$ Mg/m^3, there was just the interpenetration of ballast and sub-soil, resulting in a mixture layer namely interlayer.

3) The soil compressibility is a key parameter to be considered when dealing with mud pumping and interlayer creation phenomena: at high dry unit mass (as $\rho_{d\text{-}initial} = 1.6$ Mg/m^3), the compressibility is low, the generation of pore water pressure is limited, and thus only interlayer creation can take place. By contrast, at lower dry unit mass ($\rho_{d\text{-}initial} = 1.4$ and 1.5 Mg/m^3), the compressibility is higher, high pore water pressure can be built up, hence mud pumping can occur. The shape of permanent displacement curve can also be used to distinguish these two phenomena: a convex curve suggests mud pumping, while a convex curve suggests interlayer creation.

Acknowledgements

References:

Adam, D., Vogel, A., Zimmermann, A., 2007. Ground improvement techniques beneath existing rail tracks. Ground Improvement 11 (4), 229-235.

AFNOR. 1995. NF P98-235-1: Essais relatif aux chaussées. Matériaux non traitées. Part 1: Essai triaxial à chargements répétés. French Standard, (In French).

Al-Qadi Imad, L., Wei, X., Roberts, R., 2008. Scattering analysis of ground-penetrating radar data to quantify railroad ballast contamination. NDT & E International 41 (6), 441–447.

Alobaidi, I., Hoare, D.J., 1994. Factors affecting the pumping of fines at the subgrade-subbase interface of highway pavements: A laboratory study. Geosynthetics International 1 (2), 221–259.

Alobaidi, I., Hoare, D.J., 1996. The development of pore water pressure at the subgrade-subbase interface of a highway pavement and its effect on pumping of fines. Geotextiles and Geomembranes 14 (2), 111–135.

Alobaidi, I., Hoare, D.J., 1998a. Qualitative criteria for anti-pumping geocomposites. Geotextiles and Geomembranes 16 (4), 221–245.

Alobaidi, I., Hoare, D.J., 1998b. The role of geotextile reinforcement in the control of pumping at the subgrade-subbase interface of highway pavements. Geosynthetics International 5 (6), 619–636.

Alobaidi, I., Hoare, D.J., 1999. Mechanisms of pumping at the subgrade-subbase interface of highway pavements. Geosynthetics International 6 (4), 241–259.

Aursudkij, B., McDowell, G.R., Collop, A.C., 2009. Cyclic loading of railway ballast under triaxial conditions and in a railway test facility. Granular Matter 11 (6), 391-401.

Aw, E.S., 2004. Novel Monitoring system to diagnose rail track foundation problems. Master of Science Thesis, Massachusetts Institute of Technology, USA.

Aw, E.S., 2007. Low cost monitoring system to diagnose problematic rail bed: Case study at mud pumping site. PhD Dissertation, Massachusetts Institute of Technology, USA.

Ayres, D.J., 1986. Geotextiles or geomembranes in track? British railway experience. Geotextiles and Geomembranes 3 (2-3), 129–142.

Bouabdallah, A., 1998. Contribution à l'étude du comportement mécanique des sols fortement désaturés. PhD Dissertation, Ecole Centrale Paris, (In French).

Burns, B., Ghataora, G.S., Sharley, P., 2006. Development and testing of geosand composite layers using a pumping index test. In Proceedings of the First International Conference on Railway Foundations Railfound06, University of Birmingham, UK, 385–393.

Calon, N., Trinh, V.N., Tang, A.M., Cui, Y.J., Dupla, J., Canou, J., Lambert, L., Robinet, A., Schoen, O., 2010. Caractérisation hydromécanique des matériaux constitutifs de plateformes ferroviaires anciennes. In Proceeding of Conference JNGG2010, Grenoble, France, 787–794 (In French).

Colin, F., 2003. Couplages thermo-hydro-mécaniques dans les sols et les roches tendres partiellement saturés. PhD Dissertation, Université de Liège. (In French).

Cui, Y.J., Delage, P., 1996. Yielding behaviour of an unsaturated compacted silt. Géotechnique 46 (2), 291-311.

Cui, Y.J., Tang, A.M., Loiseau, C., Delage, P., 2008. Determining the unsaturated hydraulic conductivity of a compacted sand-bentonite mixture under constant-volume and free-swell conditions. Physics and Chemistry of the Earth, Parts A/B/C, 33, S462–S471.

Cui, Y.J., Duong, T.V., Tang, A.M., Dupla, J., Calon, N., Robinet, A., 2013. Investigation of the hydro-mechanical behaviour of fouled ballast. Journal of Zhejiang University- Science A 14 (4), 244-255.

Duong, T.V., Trinh, V.N., Cui, Y.J., Tang, A.M., Nicolas, C., 2013. Development of a large-scale infiltration column for studying the hydraulic conductivity of unsaturated fouled ballast. Geotechnical Testing Journal 36 (1), 54-63.

Duong, T.V., Tang, A.M., Cui, Y.J., Trinh, V.N., Dupla, J., Calon, N, Canou, J., Robinet, A., 2014. Effects of fines and water contents on the mechanical behavior of interlayer soil in ancient railway sub-structure. Soil and Foundations, accepted for publications.

Delage, P., Cui, Y.J., 2000. L'eau dans les sols non saturés. Ed. Techniques de l'Ingénieur, Article C301. (In French).

Delage, P., Cui, Y.J., 2001. Comportement mécanique des sols non saturés. Ed. Techniques de l'Ingénieur, Article C302. (In French).

Fleureau, J.M., Indarto, 1995. Comportement du limon de Jossigny remanié soumis à une pression interstitielle négative. Revue Française de Géotechnique 62, 59-66. (In French).

Ghataora, G.S., Burns, B., Burrow, M.P.N., Evdorides, H.T., 2006. Development of an index test for assessing anti-pumping materials in railway track foundations. In: Proceedings of the First International Conference on Railway Foundations, Railfound06, University of Birmingham, UK, 355–366.

Hornych, P., Corté, J.F., Paute, J.L., 1993. Etude des déformations permanentes sous chargements répétés de trois graves non traitées. Bulletin de Liaison des Laboratoires des Ponts et Chaussées 184, 77-84 (In French).

Huang, H., Tutumluer, E., Dombrow, W., 2009. Laboratory characterization of fouled railroad ballast behavior. Transportation Research Record, Journal of the Transportation Research Board 2117, 93–101. Doi: 10.3141/2117-12.

Indraratna, B., Ionescu D., Christie D., Chowdhurry, R., 1997. Compression and degradation of railway ballast under one-dimensional loading. Australian Geomechanics Journal (12), 48 – 61.

Indraratna, B., Salim, W., 2005. Mechanics of Ballasted Rail Tracks: A Geotechnical Perspective, Taylor & Francis Group, London, UK.

Indraratna, B., Salim, W., Rujikiatkamjorn, C., 2011. Advanced Rail Geotechnology - Ballasted Track, CRC Press.

Janardhanam, R., Desai, C.S., 1983. Three-dimensional testing and modelling of ballast. Journal of Geotechnical Engineering 109 (6), 783–796.

Karraz, K., 2008. Mechanical behavior of ballast under monotonic and cyclic loading. PhD Dissertation, Ecole Nationale des Ponts et Chaussées, France.

Kettil, P., Lenhof, B., Runesson, K., Wiberg, N.E., 2008. Coupled simulation of wave propagation and water flow in soil induced by high-speed train. International Journal for Numerical and Analytical Methods in Geomechanics (33) 1311-1319.

Le, T.T., 2008. Comportement thermo-hydro-mécanique de l'argile de Boom. PhD Dissertation, Ecole Nationale des Ponts et Chaussées, France. (In French).

Le Runigo, B., Cui, Y.J., Cuisinier, O., Deneele, D., Ferber, V., 2008. Durabilité du limon de Jossigny traité à la chaux et soumis à différentes sollicitations hydriques. Comportement hydraulique, microtextural et mécanique. Workshop TerdOuest I, Paris, France 13 November 2008, p. 13. (In French)

Li, D., Selig, E.T., 1996. Cumulative plastic deformation for fine-grained subgrade soils. Journal of Geotechnical Engineering December 1996: 1006-1013.

Li, S., Lai, Y., Zhang, S., Yang, Y., Yu, W., 2012. Dynamic responses of Qinghai-Tibet railway embankment subjected to train loading in different seasons. Soil Dynamics and Earthquake Engineering, (32), 1-14.

Liu, J., Xiao, J., 2010. Experimental study on the stability of railroad silt subgrade with increasing train speed. Journal of Geotechnical and Geoenvironmental Engineering 136 (6), 833-841.

Lourenço, S.D.N., Gallipoli, D. Toll, D.G., Augarde, C.E., Evans, F.D., 2011. A new procedure for the determination of soil-water retention curves by continuous drying using high-suction tensiometers. Canadian Geotechnical Journal 48 (2), 327–335.

Mantho, A.T., 2005. Echanges sol-atmosphère application à la sécheresse. PhD Dissertation, Ecole Nationales des Ponts et Chaussées - Université Paris – Est, France (In French).

Masekanya, J.P., 2008. Stabilité des pentes et saturation partielle. Etude expérimentale et modélisation numérique. PhD Dissertation, Université de Liège. (In French).

Miller, G.A., The, S.Y., Li, D., Zaman, M.M., 2000. Cyclic shear strength of soft railroad subgrade. Journal of Geotechnical and Geoenvironmental Engineering 126 (2), 139-147.

Paute, J.L., Le Fort, R., 1984. Determination of untreated gravels mechanical characteristics with cyclic loading triaxial apparatus. Bulletin of the International Association of Engineering Geology (29), 419 – 424, (In French).

Raymond, G.P., 1999. Railway rehabilitation geotextiles. Geotextiles and Geomembranes 17 (4), 213–230.

Ridley, A., Burland, J., 1993. A new instrument for the measurement of soil moisture suction. Géotechnique 43 (2), 321-324.

Ridley, A., Dineen, K., Burland, J., Vaughan, P., 2003. Soil matrix suction: some examples of its measurement and application in geotechnical engineering. Géotechnique 53 (2), 241-254.

Sattler, P., Fredlund, D.G., Klassen, M.J., Rowan, W.G., 1989. Bearing capacity approach to railway design using subgrade matric suction. Transportation Research Record 1241, 27-33.

Selig, E.T., Waters, J.M., 1994. Track Geotechnology and Substructure Management, Thomas Telford.

Su, L., Rujikiatkamjorn, C., Indraratna, B., 2010. An evaluation of fouled ballast in a laboratory model track using ground penetrating radar. Geotechnical Testing Journal 33 (5), 343-350.

Sussmann, T., Maser, K., Kutrubes, D., Heyns, F., Selig, E., 2001. Development of ground penetrating radar for railway infrastructure condition detection. Symposium on the Application of Geophysics to Engineering and Environmental Problems 2001.

Takatoshi, I., 1997. Measure for stabilization of railway earth structure. Japan Railway Technical Service, 290.

Toll, D.G., Lourenço, S.D.N., Mendes, J., 2012. Advances in suction measurements using high suction tensiometers. Engineering Geology doi:10.1016/j.enggeo.2012.04.013.

Topp, G.C., Davis, J.L., Annan, A.P., 1980. Electromagnetic determination of soil water content: measurements in coaxial transmission lines. Water Resources Research 16 (3), 574–582.

Trinh, V.N., (2011). Comportement hydromécanique des matériaux constitutifs de plateformes ferroviaires anciennes. PhD Dissertation, Ecole Nationales des Ponts et Chaussées - Université Paris – Est, France (In French).

Trinh, V.N., Tang, A.M., Cui, Y.J., Canou, J., Dupla, J., Calon, N., Lambert, L., Robinet, A., Schoen, O., 2011. Caractérisation des matériaux constitutifs de plate-forme ferroviaire ancienne. Revue Française de Géotechnique (134-135), 65–74 (In French).

Trinh, V.N., Tang, A.M., Cui, Y.J., Dupla, J., Canou, J., Calon, N., Lambert, L., Robinet, A., Schoen, O., 2012. Mechanical characterisation of the fouled ballast in ancient railway track sub-structure by large-scale triaxial tests. Soils and Foundations 52 (3), 511-523.

Tutumluer, E., Dombrow, W., Huang, H., 2008. Laboratory characterization of coal dust fouled ballast behavior. AREMA 2008 Annual Conference & Exposition September 21-24, 2008, Salt Lake City, USA.

Van, W.A., 1985. Rigid pavement pumping: (1) subbase erosion and (2) economic modeling: informational report. Publication FHWA/IN/JHRP-85/10. Joint Highway Research Project, Indiana Department of Transportation and Purdue University, West Lafayette, Indiana, USA, doi: 10.5703/1288284314094.

Voottipruex, P., Roongthanee, J., 2003. Prevention of mud pumping in railway embankment a case study from Baeng Pra-pitsanuloke, Thailand. The Journal of KMITB 13 (1), 20–25.

Wong, R.C.K., Thomson, P.R., Choi, E.S.C., 2006. In situ pore pressure responses of native peat and soil under train load: a case study. Journal of Geotechnical and Geoenvironmental Engineering 132 (10), 1360-1369.

Yoder, E.J., 1957. Pumping of highway and airfield pavements: technical paper. Publication FHWA/IN/JHRP-57/05. Joint Highway Research Project, Indiana Department of Transportation and Purdue University, West Lafayette, Indiana. Doi: 10.5703/1288284313518.

Yuan, R., Yang, Y.S., Qiu, X., Ma, F.S., 2007. Environmental hazard analysis and effective remediation of highway seepage. Journal of Hazardous Materials 142 (1-2), 381–388.

Zhang, C., 2004. The effect of high groundwater level on pavement sub-grade performance. PhD Dissertation, The Florida State Unisity - College of Engineering, USA.

CHAPTER V

Application and Recommendation

The first four chapters presented the devices specially developed for this study and the results obtained. The analysis of the results help address different questions arisen about the degradation mechanisms of the railway platforms in France.

The most important findings are: i) the combined effect of water and fines contents on the mechanical behavior of interlayer soil, ii) the important role of fines fraction in the hydraulic behavior of interlayer soil, iii) water content increase and soil compressibility are the necessary conditions for the interlayer creation and mud pumping, etc. In order to facilitate the application of the new findings to the track maintenance, it appears necessary to synthesize them and then to propose useful recommendations. The synthesis and the recommendations done are presented in this chapter

Introduction

Nowadays, the demand of faster and heavier trains or higher traffic leads to more and more maintenance and improvement activities of tracks, especially for the ancient railway lines which represent 94% of the whole railway network in France. They were constructed more than one hundred years ago with a sub-structure that was not designed to verify the new requirements as for the new lines. On the other hand, the lack of knowledge on the behavior of sub-structure and the degradation mechanism of tracks often makes the maintenance and improvement work expensive, and sometimes inefficient.

In this PhD study, problems related to the sub-structure have been addressed, by assessing the track behavior at both global scale (the whole French railway network) and local scale (one specific railway line), and by conducting laboratory tests. The laboratory tests aimed at identifying the hydro-mechanical behavior of the interlayer soil on one hand and the mechanisms of interlayer creation and mud pumping on the other hand. In this chapter, the mains results obtained are gathered in order to make recommendations for more efficient maintenance work.

Assessment of the problem recorded in ancient railway network in France

The problems preventing normal circulation in the French ancient railway system were recorded for the period from January 2010 to May 2011 (Nicolas, 2010).
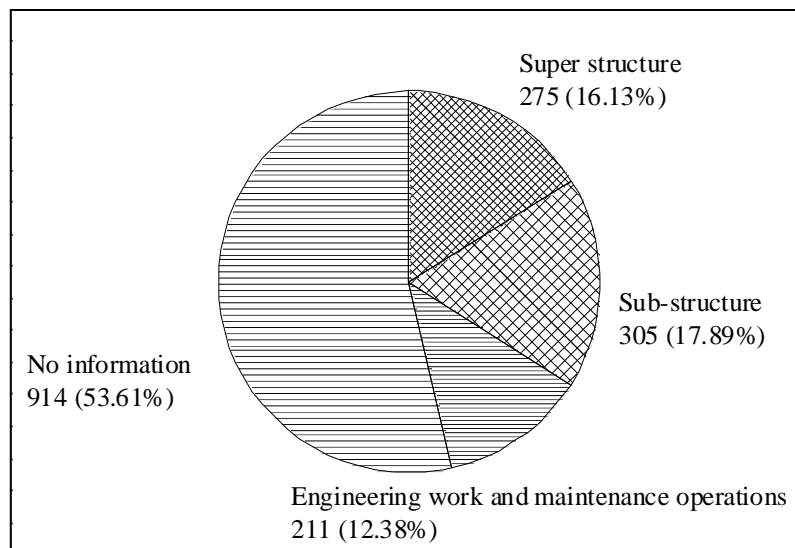

Fig. 1: Cause of the problems for the deceleration of train

178

It is showed that (Fig. 1) the number of problems related to sub-structure (17.89%) is slightly larger than the number related to upper structure (16.13%), suggesting that more attention should be paid to the sub-structure. If the maintenance policy is not appropriate, once a problem occurs to the sub-structure, it will take longtime to remediate. The complexity of the problem is that the properties of sub-structure can evolve and sometimes unexpected phenomena can occur, such as the creation of interlayer and the mud pumping. Among the sub-structure related problems, there are 186 cases where clayey sub-grade was involved and very often mud pumping was observed. It is therefore important to wee understand the behavior of sub-grades (part of the sub-structure).

The huge number of "no information" cases (53.61%) confirms that railway structures is a complex issue that needs extensive investigations in order to reveal the real mechanisms involved in the problems.
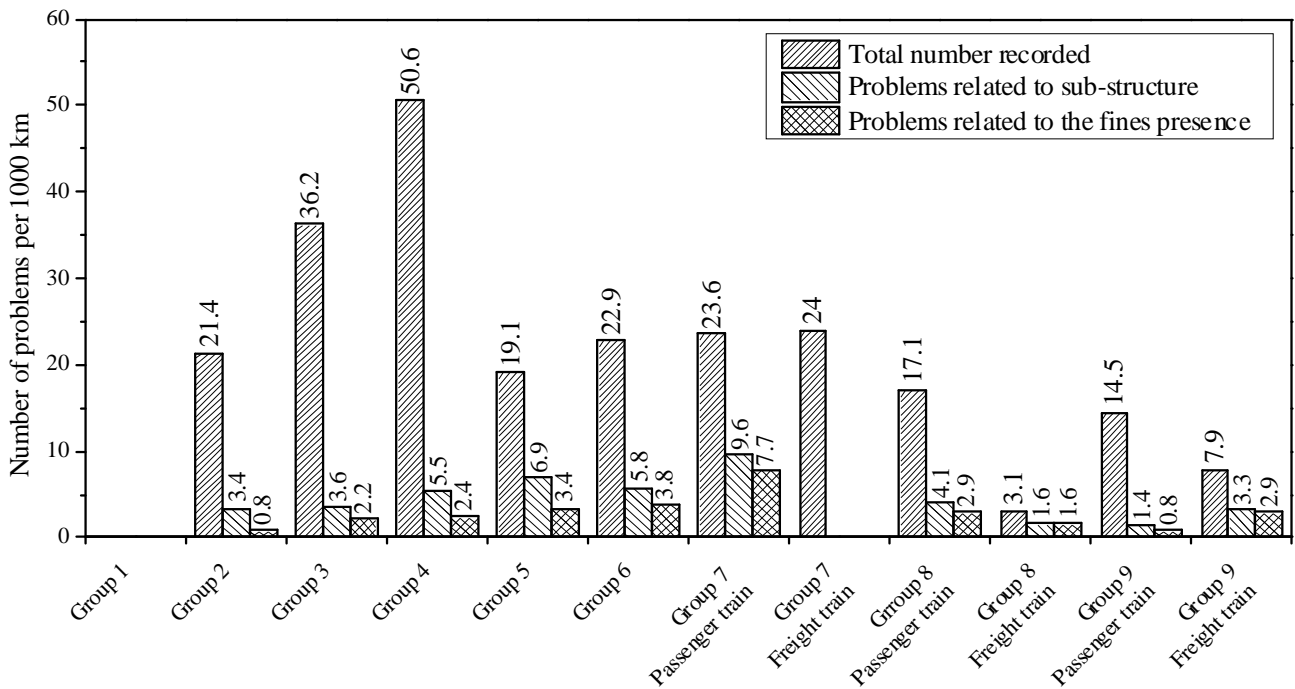
Fig. 2: Number of problems versus group UIC

The railway lines in France are divided in several groups, namely group UIC, according to the traffic and load: Group 1 includes the lines with highest load while group 9 consists of lines with lowest traffic and load. Based on this classification, the maintenance policy was logically set: maintenance is more frequently for group 2 to 6 and less for other groups (in the French railway network, there is no line in group 1). This policy is in agreement with the analysis (Fig. 2) of the data set of all problems recorded that involve both upper structure and sub-structure. The lower the group the larger the problems recorded. However, when only the data of the problems related to the

sub-structure is taken into account, the analysis showed another configuration: it is group 7 (passenger train) that has the most problems. These observations suggest that the maintenance policy should be set differently when referring to different part of railway track (upper-structure or sub-structure).

Regarding the season, it was observed that there is a peak around the months of February, March and April, while the values for other months are smaller. It is worth noting that the period from February to April corresponds to late winter and early spring. This suggests that the climatic conditions should be taken into account when assessing the sub-structure.

Among the infrapoles in France, "Ouest Parisien" (West Paris) and Poitou Charentes are the ones with the most problems. Based on this observation, one ancient line situated in the infrapole of Poitou Charentes was selected for further in-depth investigation. The geological map of this line is presented in Fig. 3.
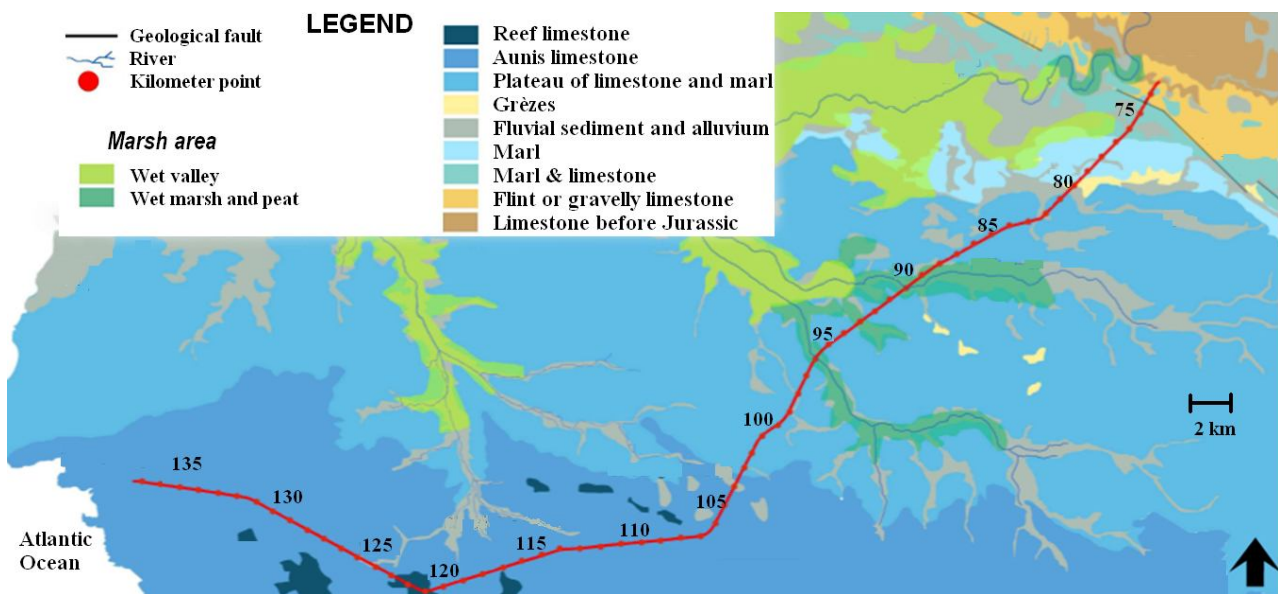
Fig. 3: Geological map of the studied line with kilometer point (PK)

The degradation speed (increase speed of NL) versus the kilometer (PK) for Track 1 and Track 2 of the line is shown in Fig. 4. Some zones with high degradation speed are identified. Referring to the geological information, it can be concluded that these kilometers correspond to the zones where sub-grades contains high fraction of fine particles: argillaceous limestone, marl or peat, sometimes colluviums. It is important to note that these soil types are sensitive to changes in water content. Furthermore, soils like peat, alluvial deposit or colluviums are very compressible and do not have the mechanical properties required for sustaining the train-induced loading. This can explains the

high increase speed of *NL* in these zones. Also, the change of sub-grade soil natures (from the first part up to PK 103) is detrimental to the performance of tracks. From PK 123 to the end of the line, with a very uniform hard limestone, the increase speed of *NL* became low, indicating a good performance of the tracks.
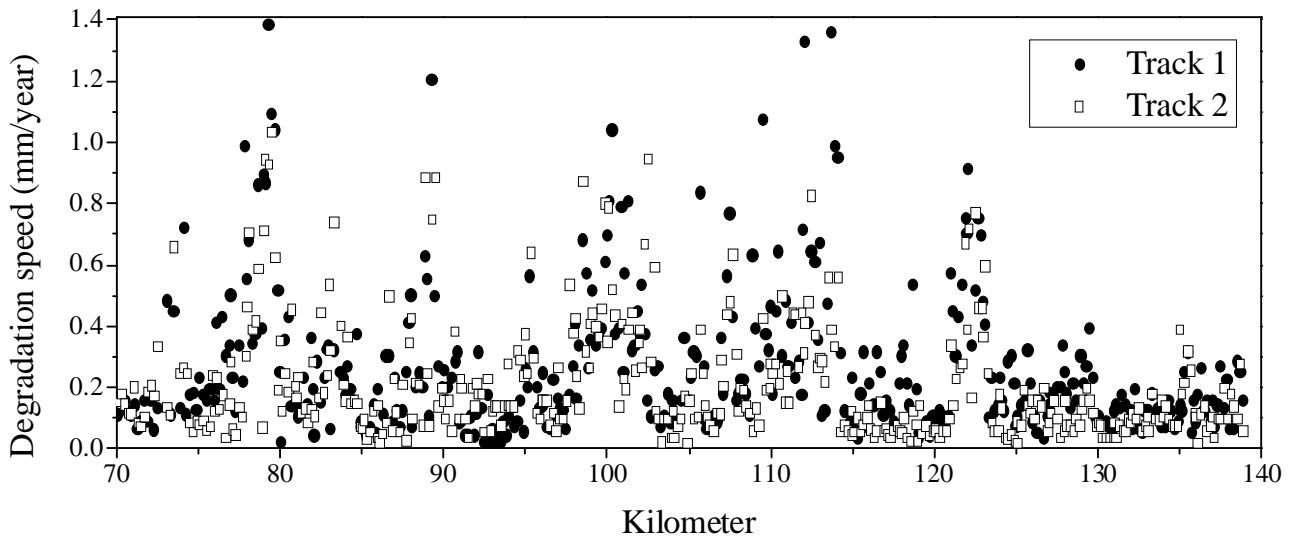
Fig. 4: Degradation speed along the studied line

During the assessment of the whole line, the zones where there are fine particles on the surface of ballast layer were identified (Fig. 5). It can be seen that most zones where there was the presence of fine particles correspond to the zones with high increase speed of *NL*. These fine particles came probably from the sub-structure when mud pumping occurred. This suggests that the sub-grade containing large fraction of fine particles is detrimental to the performance of sub-structure in the cases where the drainage system is not satisfactory. Indeed, for this kind of sub-grade soils, a decrease of mechanical performance can be expected when the water content rises.
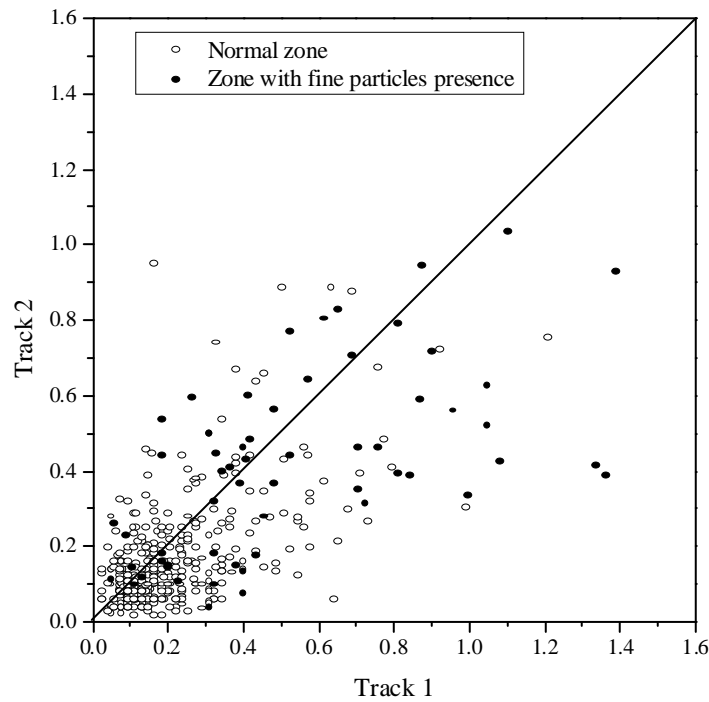
Fig. 5: Correlation of degradation speed between Track 1 and Track 2

The analysis of the rail and the sleeper type suggests that the variation of *NL* identified does not clearly depend on the rail or sleeper type. Furthermore, admitting that the traffic, train load and speed and the type of sleeper in two tracks are not necessary identical, the coincidence between the degradation speeds of Track 1 and Track 2 (Fig. 5) confirms that the general cause of the increase of *NL* came from the sub-structure.

It was found that there is a reasonable correlation between the degradation speed and the thickness of fouled ballast layer and interlayer (*e*) determined from different tests, suggesting a positive role of interlayer in reducing the degradation of tracks. The results of Panda, endoscope for Track 1 and Track 2 are presented in Fig. 6 and Fig. 7, respectively, and those of core sampler train are presented in Fig. 8. Note that the special zones refer to the zones of station, bridges, whereas normal zone refers to other zones. In general, all results show a decrease trend of degradation speed with the increase of *e*. The scatter of the data can be explained by the presence of fouled ballast which is not always evident to determine. As opposed to the sub-structure of new lines for high speed train with a number of layers protecting more or less the sub-grade, the sub-structure of ancient lines has no transition layer such; therefore, significant stress can be exerted to the sub-grade soils, leading to significant deformation of tracks or degradation of tracks. The presence of interlayer plays somehow the role of a transition layer, reducing the stress applied to the sub-grade. This explains the decrease trend of the degradation speed with the increase of *e*.
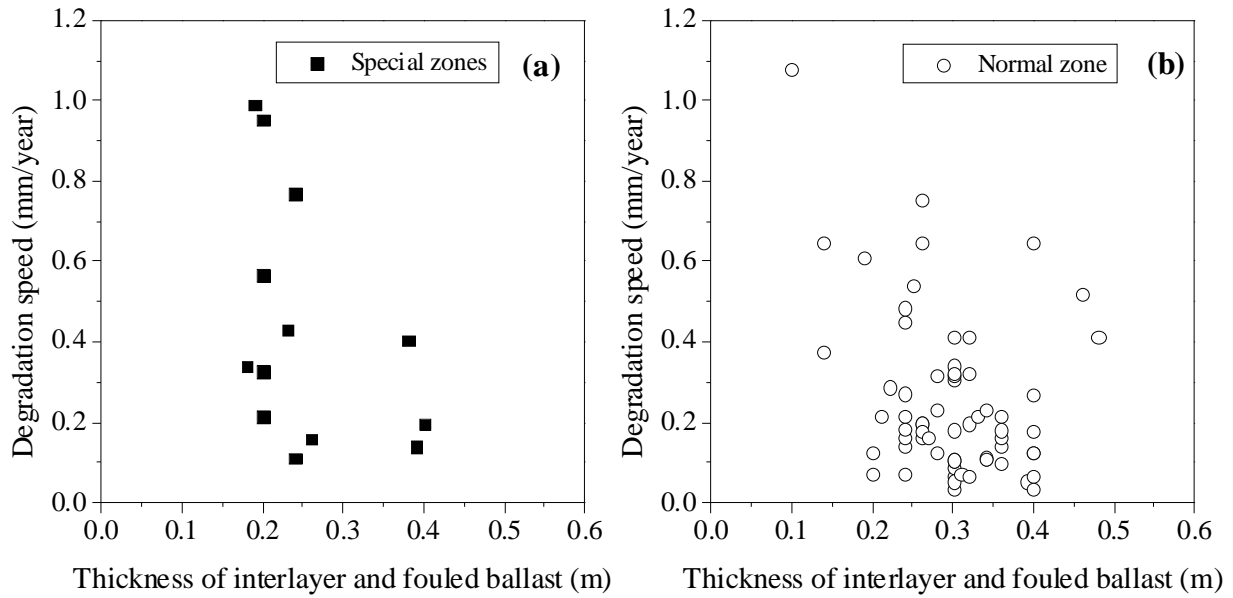
Fig. 6: Correlation of the degradation speed to the thickness of interlayer and fouled ballast for Track 1- Data from coring train. a) Special zones and b) normal zone
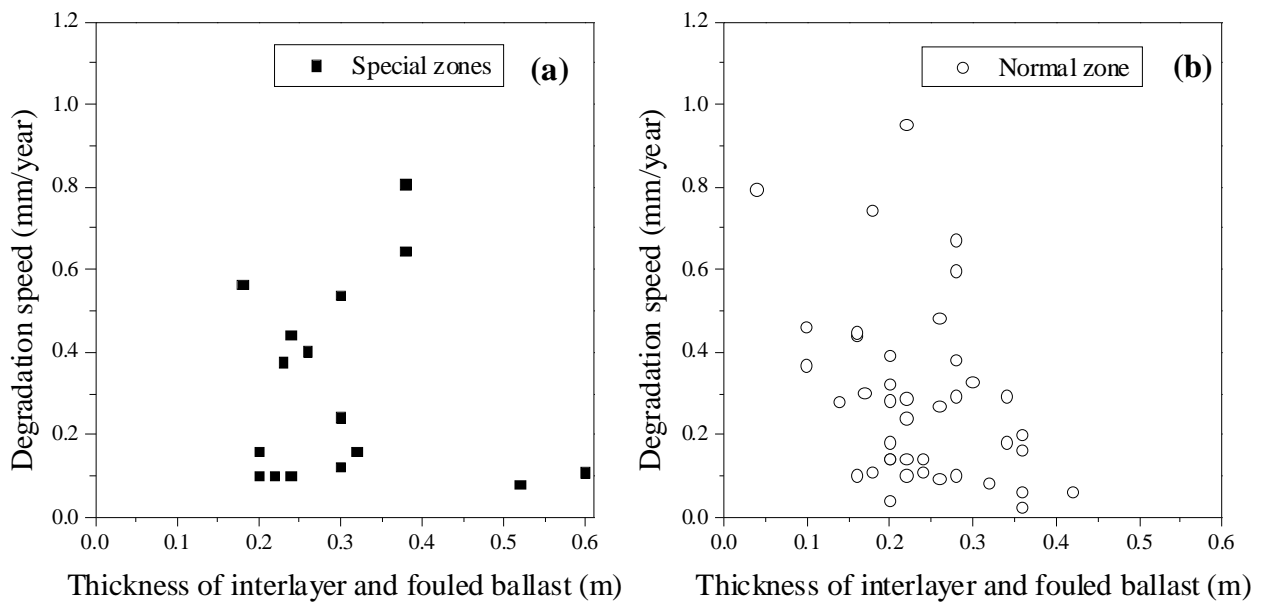
Fig. 7: Correlation of the degradation speed to the thickness of interlayer and fouled ballast for Track 2- Data from coring train. a) Special zones and b) normal zone

183
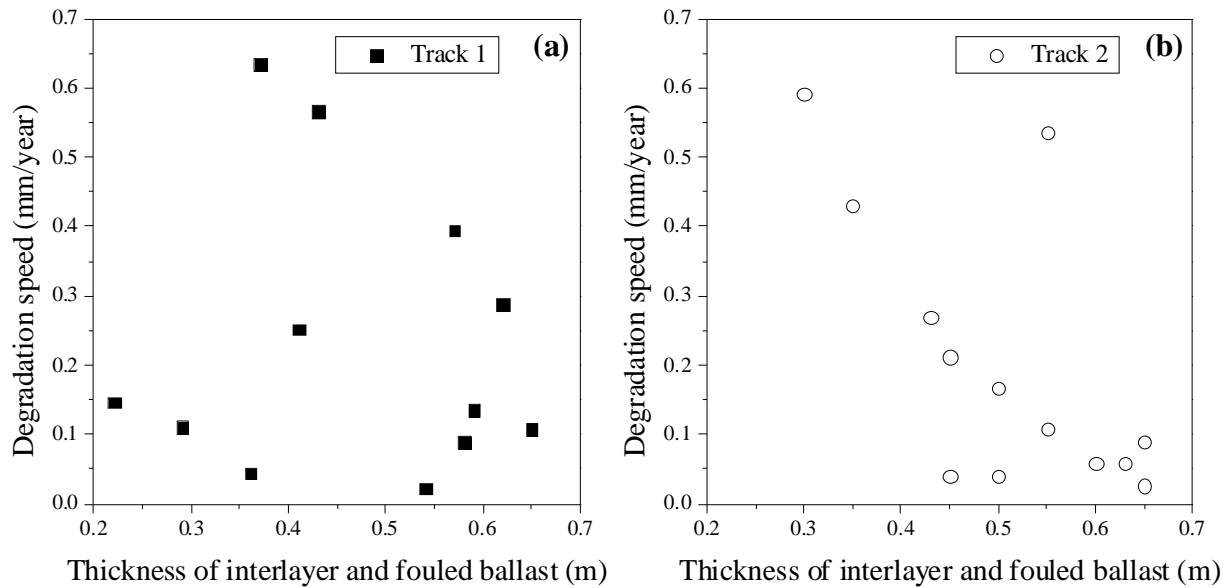
Fig. 8: Correlation of the degradation speed to the thickness of interlayer and fouled ballast - Data from Panda and endoscope. a) Track 1 and b) Track 2

Hydro-mechanical behavior of interlayer

Infiltration column tests

The case study presented previously evidenced that the interlayer can significant affect the track behavior. However, as the interlayer is "naturally" created, the fines particles of interlayer can vary from one site to another, causing a large variability of interlayer soils. In order to study the influence of fines content on the mechanical behavior of interlayer (*ITL*) soil, hydro-mechanical tests were carried out with different fines contents: -10% (*ITL$_{-10}$*), +5% (*ITL$_5$*) and +10% (*ITL$_{10}$*) by dry mass (dry mass of sub-grade/dry mass of interlayer soil). Also, the hydraulic behavior of the fine particles fraction (*Fines* smaller than 2 mm) was studied in parallel. The dry unit mass (1.33 Mg/m^3) of *Fines* considered was equal to that of fine particles contained in the sample of interlayer soil at a dry unit mass of 2.01 Mg/m^3. The grain size distribution curves of the materials are presented in Fig. 9.
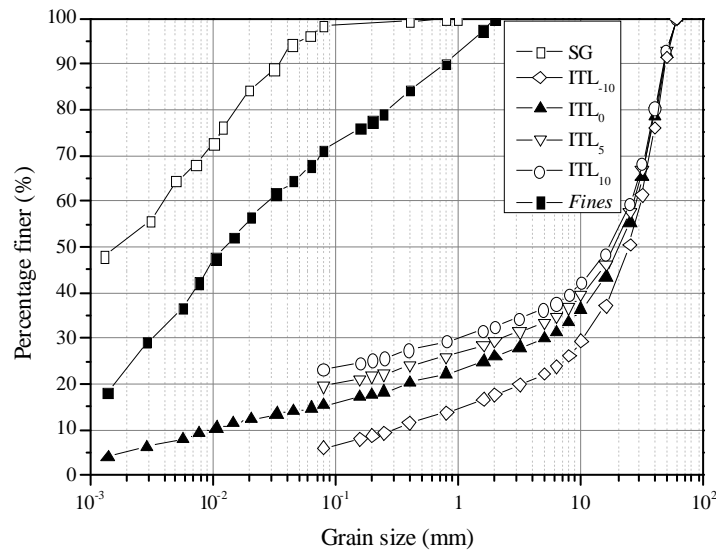
Fig. 9: Grains size distribution of the studied soils
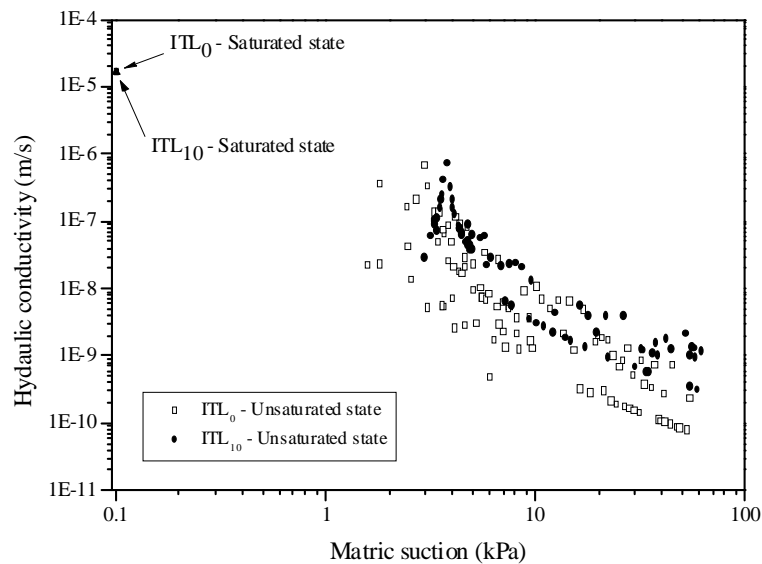
Fig. 10: Comparison of hydraulic conductivity between *ITL$_0$* and *ITL$_{10}$*

For the hydraulic behavior, adding 10% fine particles into the interlayer soil did not significantly change the hydraulic conductivity (Fig. 10). Under saturated condition, the values are 1.67×10^{-5} m/s for *ITL$_{10}$* and 1.75×10^{-5} m/s for *ITL$_0$*, respectively. However, both values are lower than the critical value (10^{-4} m/s) proposed by Selig and Waters (1994) for the railway substructures. Thereby, if the interlayer is kept, a good drainage system is required to prevent the increase of moisture content.
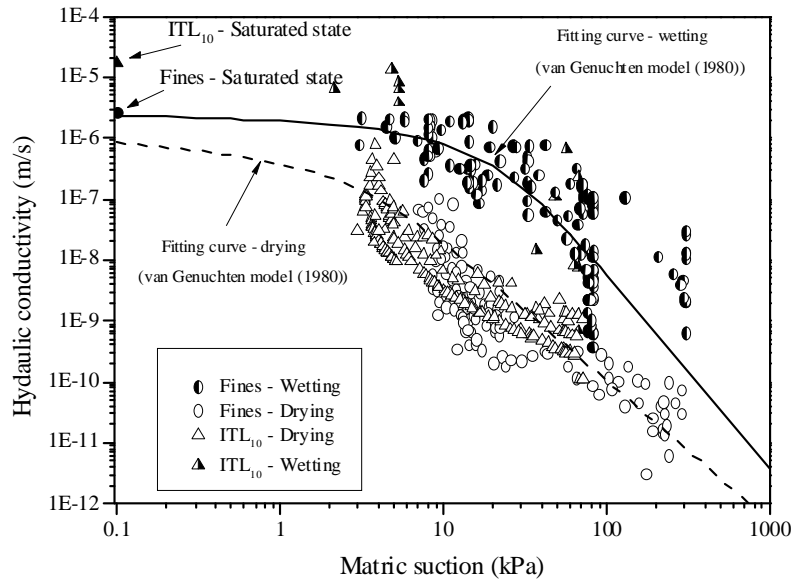
Fig. 11: Comparison of hydraulic conductivity between *ITL$_{10}$* and *Fines*

Comparison between *ITL$_{10}$* and *Fines* (Fig. 11) shows that their values of hydraulic conductivity are quite close. This suggests that the hydraulic conductivity of the interlayer soil is mainly governed by the hydraulic conductivity of the fines fraction. Thereby, to determine the hydraulic conductivity of interlayer soils, it is not necessary to use large-scale experimental devices to match the soil grain size; smaller devices can be used to determine their hydraulic conductivity by testing the fine particles only, provided that equivalent dry density is accounted for.

Monotonic triaxial tests

The results of monotonic triaxial tests allowed the internal friction angle and cohesion to be determined (Table 1).

Table 1: Friction angle and cohesion of interlayer in different conditions

Material	Friction angle φ (°)		Cohesion c (kPa)	
	$w = 4\%$	$w = 12\%$	$w = 4\%$	$w = 12\%$
ITL$_0$	39	37	42	16
ITL$_{10}$	37	29	48	21

The increase of water content causes a decrease of the friction angle and cohesion of interlayer soil. However, the effect of fines content is different depending on the saturation state of the soil. Under dry conditions ($w = 4\%$), adding 10% of fines does not significantly change the shear strength parameters, thanks to the suction effect. By contrast, in the nearly saturated state ($w = 12\%$), adding

fines decreases the internal friction angle from 37° to 29° and increases the cohesion from 16 kPa to 21 kPa. This can be explained by the fact that upon water content increase, soil suction decreases, leading to a decrease in interlayer soil strength.

Cyclic triaxial tests

During the cyclic triaxial tests, the increase of water content results in an increase in permanent axial strain. The effect of water content depends not only on the soil nature but also on the variation range of water content. These permanent axial strains are presented in Fig. 12 showing the influence of degree of saturation under difference applied deviator stresses.
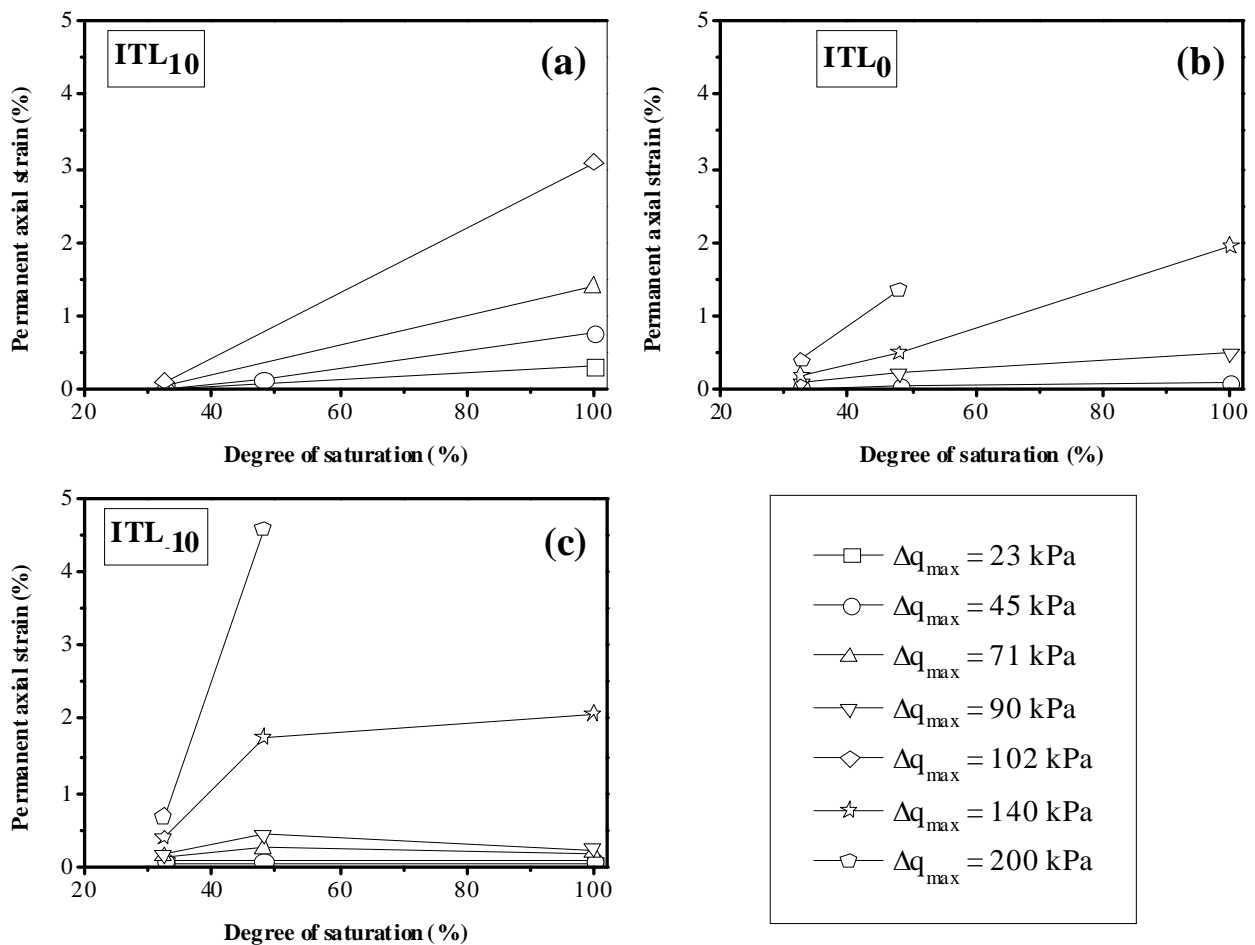
Fig. 12: Water effect on the permanent axial strain under different stresses a) *ITl₁₀*; b) *ITL₀*; c) *ITl₋₁₀*

187
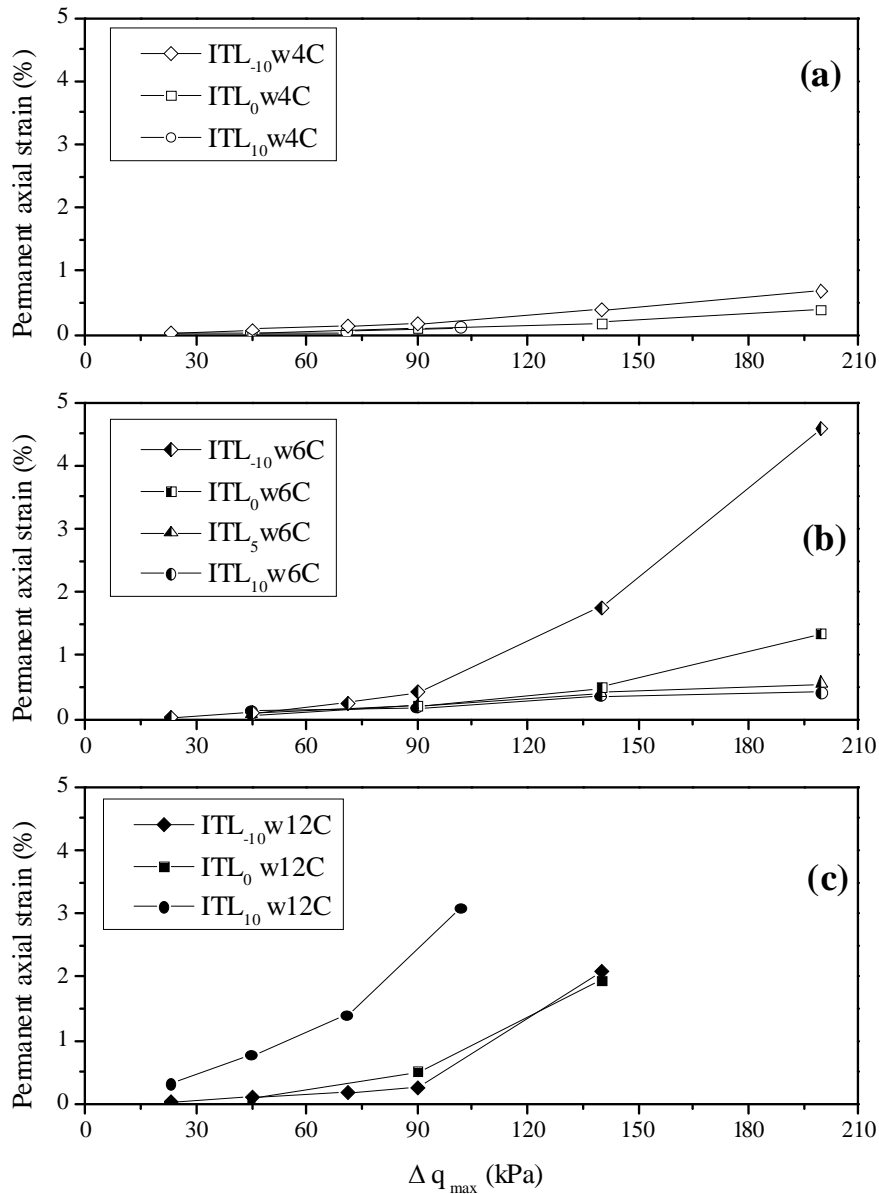
Fig. 13. Effect of fines content on the end-stage permanent axial strain at various water contents

Regarding the effect of fines content on the permanent axial strain (Fig. 13), the results showed that at a given water content in dry conditions, adding more fines has a positive effect on the mechanical behavior of interlayer soil (the permanent axial strain is reduced), while in nearly saturated conditions, adding more fines boosts the axial strain. This means that in the railway context, during the assessment and exploitation of the interlayer soil, the effect of water content and fines content must be taken into account together. The interlayer soil containing a larger quantity of fine particles have to be protected from water infiltration in order to avoid any increase of water content that would decrease its mechanical performance.

For the resilient modulus (Fig. 14), at each deviator stress level, after the first scattered results due to the plastic behavior of soil, the resilient modulus tended to stabilize with the number of cycles. It was found that the number of cycles needed to reach the stabilization depends on the material nature, water content and stress level.
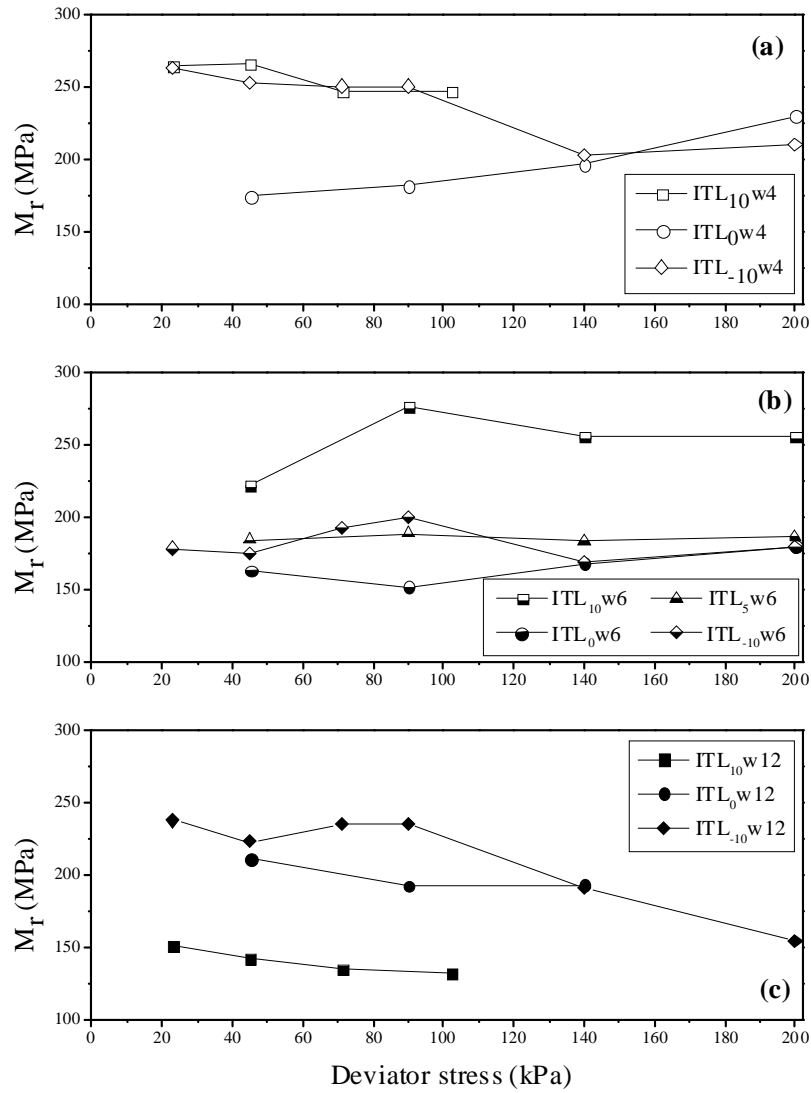
Fig. 14: End-stage resilient modulus versus deviator stress - Effect of fines content

The effects of water content and of fines content are linked, and it appeared impossible to distinguish the two effects. Indeed, in unsaturated conditions, due to the suction effect, the soil having higher fines content showed higher strength and stiffness. On the contrary, when the soil approached the saturated conditions, the fine particles provided a negative effect. This suggests that drainage measures must be taken to protect the interlayer soil when its mechanical performance appears satisfactory under unsaturated conditions but unsatisfactory under saturated conditions.

Interlayer creation/mud pumping

As presented above, the behavior of interlayer can change depending on the fines content and water content, presenting a negative or positive effect on the sub-structure. In order to avoid any negative effect and to have an appropriate maintenance method, the mechanism of the interlayer creation in general and the degradation of the sub-structure were assessed using a laboratory physical model.
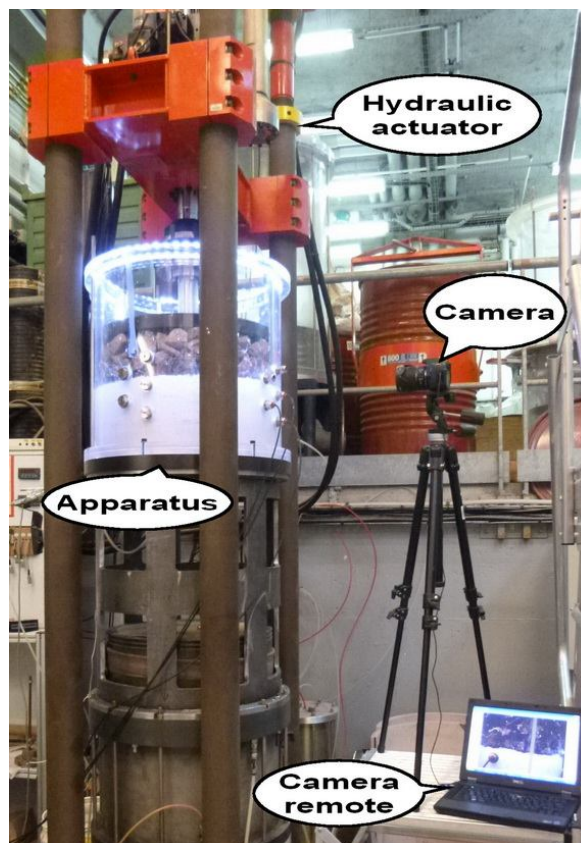
Fig. 15: Photo of the experimental set up

In the adopted physical model, the transparent cylindrical cell has an internal diameter of 550 mm and a height of 600 mm (Fig. 15). Sub-grade soil was prepared from a mixture composed of 70% sand and 30% kaolin clay (70S30K), which has a high fine particles content as shown in Fig. 16.

Three tests corresponding to three initial dry unit mass values of sub-soil were conducted with two water contents ($w = 16\%$ and near saturated state), under monotonic and cyclic loadings (5Hz).
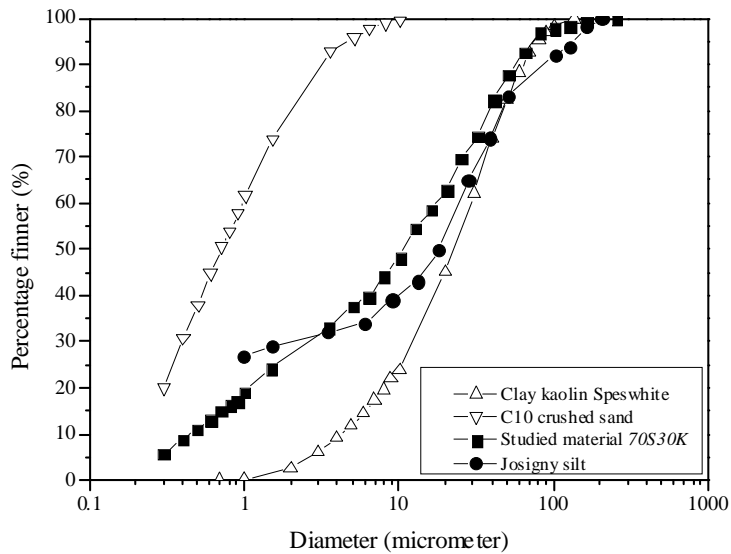
Fig. 16: Grain size distribution curve of studied material

The responses in axial displacement are shown in Fig. 17, that indicate different ballast behavior under different dry unit masses of sub-soil. This observation suggests that in the future studies on the behavior of sub-structure, it is important to study the combined effect of different layers. If the materials are tested separately, the overall behavior may be ignored.
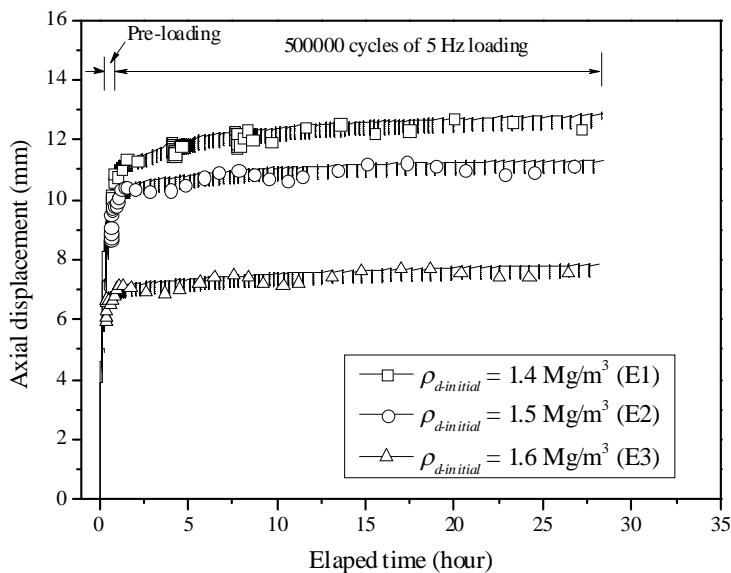
Fig. 17: Axial displacement during loading ($w = 16\%$)

Under unsaturated conditions, even after 500 000 loading cycles, the camera view (Fig. 18) showed that there is no migration of fine particles. The ballast particles rearranged among them, but at the interface between ballast and sub-soil, the level of the fine particles did not change, whatever the dry unit mass of the sub-soil. This suggests that the interlayer cannot be created under unsaturated conditions.

| a) Before loading ($w = 16\%$) | b) After loading ($w = 16\%$) |
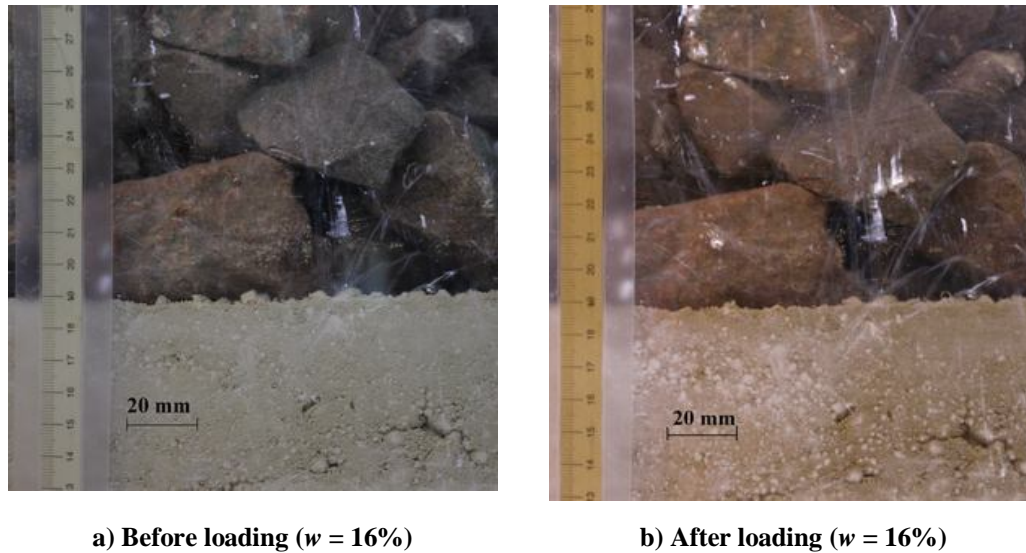
Fig. 18: Camera view of the interface between two soils: a) before and b) after loading ($w = 16\%$ and $\rho_{d\text{-}initial} = 1.4$ Mg/m^3).

Under saturated conditions (Fig. 19), the axial displacement increased rapidly and the fine particles migrated up to the ballast layer. Depending on the dry unit mass, the pumping level of fine particles is more or less significant. In case of $\rho_{d\text{-}initial} = 1.4$ Mg/m^3, it took just 10 seconds for fine particles to approach the ballast surface while in the case of $\rho_{d\text{-}initial} = 1.5$ Mg/m^3, the duration was about 15 minutes. In the case of $\rho_{d\text{-}initial} = 1.6$ Mg/m^3, it took 28 hours for 20 mm fines migration (Fig. 20). This means that the dry unit mass of sub-soil strongly influences the fine migration.

| a) after saturation and before monotonic loading | b) after monotonic loading (saturated state) | c) after cyclic loading (saturated state) |
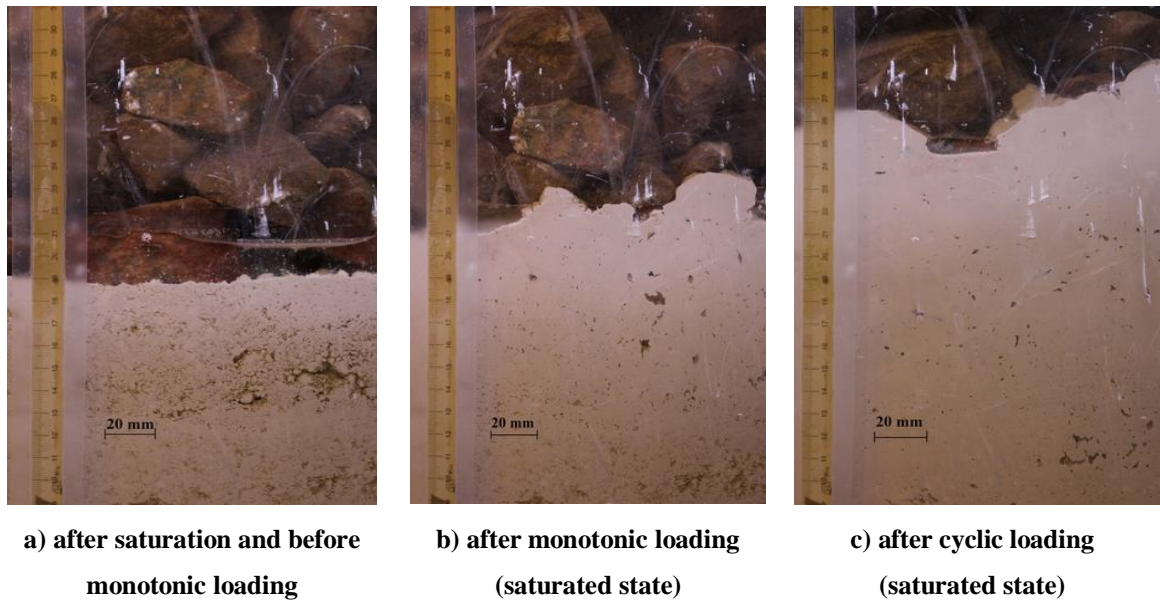
Fig. 19: Camera view of the evolution of interface between two soils layers: fine particles pumped up level ($\rho_{d\text{-}initial}$ = 1.4 Mg/m^3)

| a) after saturation and before monotonic loading | b) after monotonic loading (saturated state) | c) after cyclic loading (saturated state) |
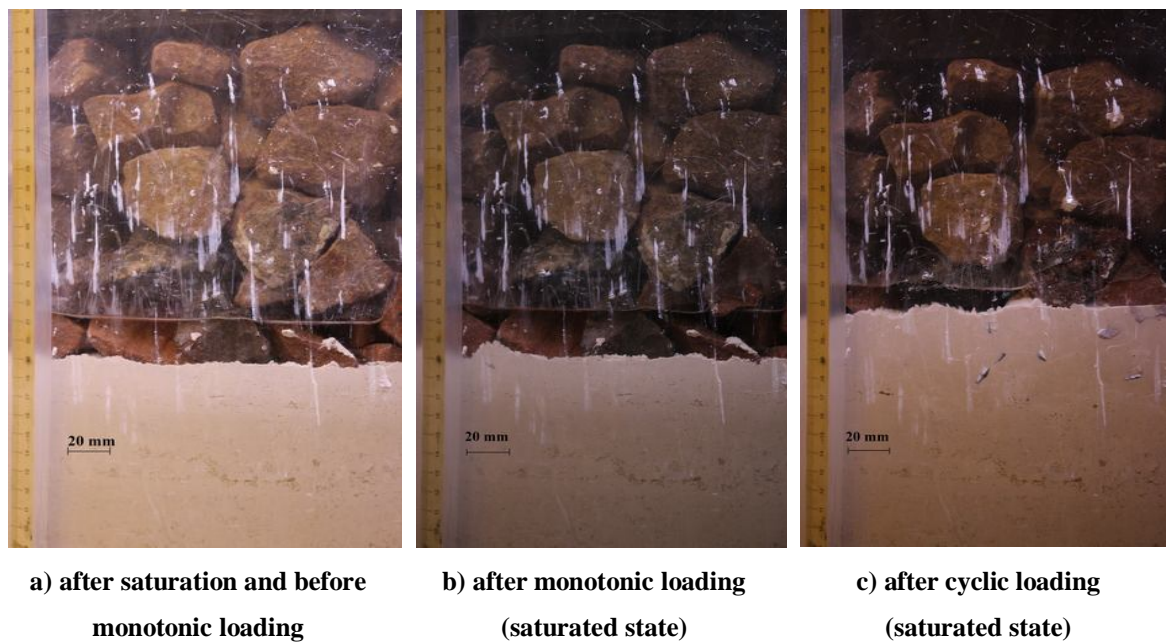
Fig. 20: Camera view of the evolution of interface between two soils layers: fine particles pumped up level ($\rho_{d\text{-}initial}$ = 1.6 Mg/m^3)

The test at $\rho_{d\text{-}initial}$ = 1.4 Mg/m^3 was continued with 0.1 Hz loading for monitoring the pore water pressure during loading cycles. It was observed that the pore water pressure followed almost immediately the variation of applied pressure. Further analysis showed that the effective stress can become negative during the unloading process (Fig. 21b). This means that the sub-soil can be liquefied and loses totally its strength. The fine particles lost their cohesion and under the effect of

dissipation of the pore water pressure, fine particles were brought up to the ballast layer, creating the mud-pumping phenomenon as in the cases of $\rho_{d\text{-}initial}$ = 1.4 or 1.5 Mg/m^3. In the case of 1.6 Mg/m^3, the pore water pressure was not high enough and fine particles were then not brought up to the ballast surface. There is only a mixture of ballast and sub-soil, corresponding to the creation of interlayer.
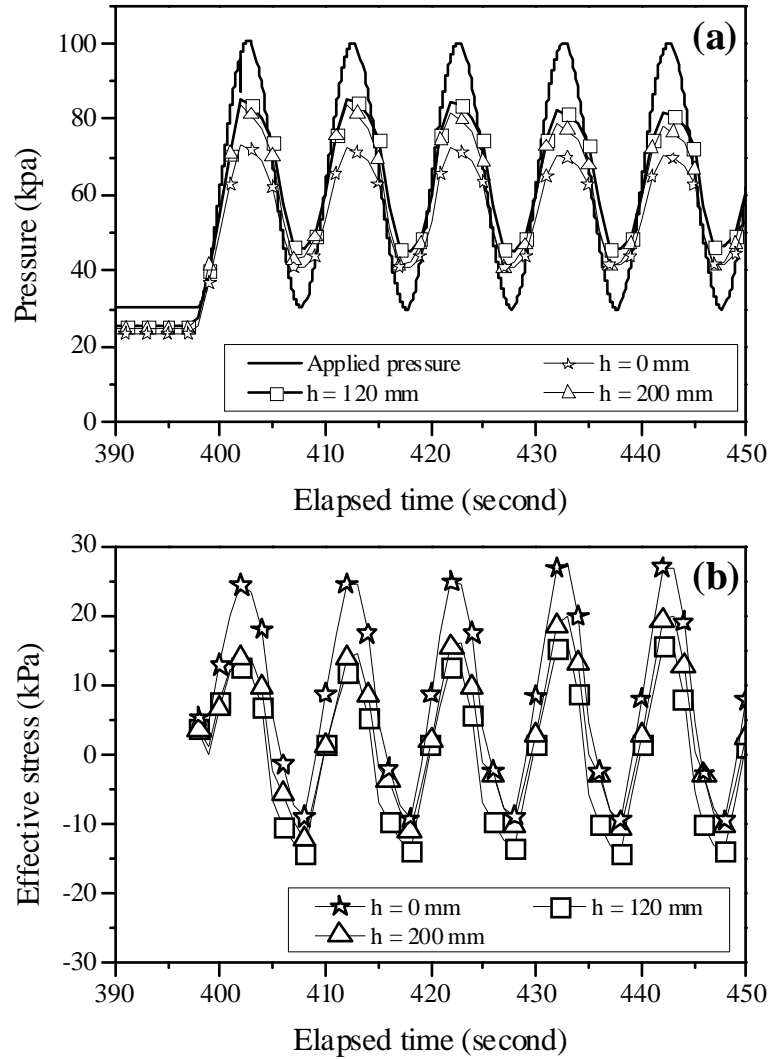
Fig. 21: Comparison between applied pressure and pore water pressure: effective stress

To distinguish the mud-pumping and interlayer creation, the displacement curve can be further analyzed. If the curve is convex (in the cases of $\rho_{d\text{-}initial}$ = 1.4 or 1.5 Mg/m^3, for instance), mud-pumping occurs. Otherwise, the creation of interlayer can be expected (Fig. 22).
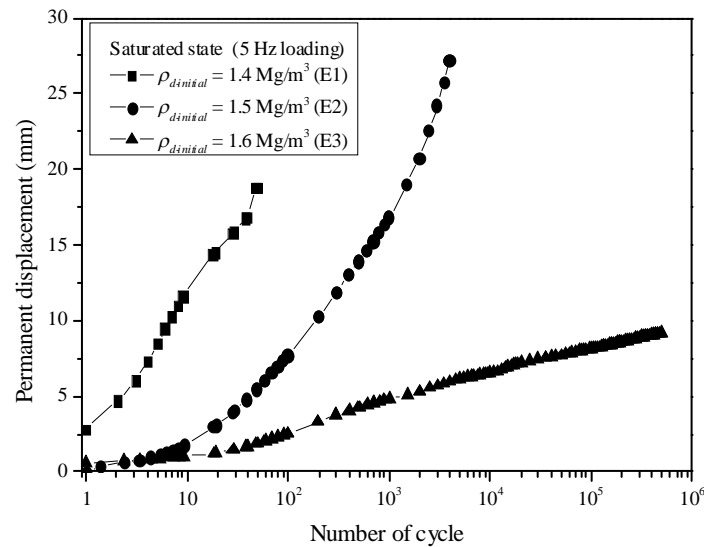
Fig. 22: Permanent displacement under saturated condition of three tests with three dry unit masses

Even the soil was not totally saturated, the pore water pressure can be developed in the case of high compressive soil ($\rho_{d\text{-}initial}$ = 1.4 or 1.5 Mg/m^3) and not in the case of low compressive soil ($\rho_{d\text{-}initial}$ = 1.6 Mg/m^3). In reality, interlayer creation is more common than mud pumping because in most cases sub-soil is in unsaturated state. Water is the necessary condition, but it is the relation between the applied stress and the soil compressibility that governs the phenomenon to be produced. However, from a practical point of view, in order to avoid any change in sub-structure component and eliminate the most driving factor, good drainage conditions must be ensured.

Conclusion

The number of sub-structure related problems without any explicit cause confirmed that the assessment of railway structure is a complex issue. From the results obtained, the following recommendations can be made for a more efficient maintenance of ancient lines:

- The sub-structure needs to be assessed at least as the upper-structure, because the upper-structure can be visually observed, but it is not the case for the sub-structure.
- The maintenance policy should be set appropriately: more attention should be paid to the sub-structure, especially for the sub-structure of group 7 (passenger train).
- The investigation by Panda and core sampler train must take place at the point where the value NL is available in order to have more correlation data.
- During the rainy period of late winter and early spring, attention should be particularly paid to the sub-structure because of the significant changes in water content in this period.

- The sub-grade has a significant influence on the performance of railway structure. The zones with a sub-grade of low mechanical properties are not apt to become the foundation of railway sub-structure. If it is inevitable, improvement must be conducted in order to meet the requirements, particularly for the zones where sub-grade soil has high fines contents and thus sensitive to changes in water content. In the investigation, the measurement of moisture content need to be performed.

- The presence of interlayer plays somehow the role of a transition layer, reducing the stress applied to the sub-grade. This explains the decrease trend of the degradation speed with the increase of interlayer thickness.

- The hydraulic conductivity of interlayer soil at the site of Sénissiat is governed by the fine fraction and does not change if more fine particles are added. These values are smaller than the critical value, suggesting that attention need to be paid to the protection of water content changes.

- Water content and fines content must be considered together in the studies of interlayer soil behavior. Appropriate drainage must be ensured to protect the interlayer soil as its mechanical performance is found satisfactory under unsaturated conditions but unsatisfactory under saturated conditions. Ground water table must be low enough (depending on the sub-soil types which is sensitive to the water change or not) to avoid the water impact on interlayer soil.

- Under unsaturated conditions, whatever the dry unit mass of sub-soil, the interlayer creation cannot occur.

- The creation of interlayer soil and the mud pumping are both related to the fine particles migration which is governed by the pore water pressure development. Water is the necessary condition, but this is the relation between applied stress and soil compressibility that governs the phenomenon (interlayer or mud pumping) to be produced.

- The sub-soil state can strongly influence the ballast behavior. This suggests that in order to understand the overall behavior of railway sub-structure, it is important to take into account the interaction between different layers.

- In order to improve the track quality by preventing the mud pumping phenomenon or the interlayer creation, the density of the underlying layers must be high enough. If it is not the case, soil improvement need to be performed to increase its stiffness.

GENERAL CONCLUSION

A study on the hydro-mechanical behavior of ancient railway platform in France has been presented. Most results obtained correspond to original findings useful for the engineering design and maintenance works for SNCF. The answers to different questions on the degradation of the railway sub-structure were found out. The study conducted covers a large area, from a statistical analysis on the whole French railway network, through an in-depth analysis of one ancient line, to the investigation of the degradation mechanisms of railway tracks (effects of water content and fines content on the hydro-mechanical behavior of interlayer soil; mud pumping, interlayer creation). The study started by an assessment of the problems related to the train circulation, followed by a case study on an ancient railway line in the West of France. Afterwards, the hydro-mechanical behavior of interlayer soil was investigated under different conditions in terms of water content, fines content, loading, number of cycles etc. Monotonic and cyclic triaxial tests were performed to investigate the shear strength properties of interlayer soil while infiltration column tests were conducted to examine the effect of fines content on the hydraulic behavior of interlayer soil. Finally, a physical model was developed, allowing the mechanisms of mud pumping and interlayer creation to be investigated. Soil samples composed of a ballast layer overlying a sub-grade layer were tested under different conditions in terms of loading frequency, number of cycles, dry unit mass and water content of sub-soil. The results allow the following conclusions to be drawn.

Railway sub-structure assessment

The assessment conducted showed that the railway sub-structure represents a complex issue since the real cause of more than half of the track-related problems were not explicitly revealed. More in-depth studies are then needed.

The sub-structure was found as important as the upper structure because the numbers of problems coming from the two parts are almost the same. As problems related to sub-structure cannot be identified as quickly as those related to upper structure, more attention should be paid to the sub-structure part. Monthly recorded problems and the number of problems for each UIC group can provide indicators for optimizing the maintenance policy.

The analysis on the state of one representative ancient line evidenced the importance of sub-grade quality for the degradation speed of tracks. The zones without mechanically stable sub-grade (soils with large fraction of fine particles) are areas where peak values of degradation speed were reported. Moreover, frequent changes of sub-grade nature along the line are also detrimental to the track performance.

The presence of interlayer turns out to be positive for the track geometry quality since a reasonable correlation between the degradation speed and layer thickness was figured out. Interlayer can reduce the train-induced stress applied to the sub-grade, hence helping decrease the degradation speed of the tracks.

Mechanical behavior of interlayer soil

The shear strength properties (internal friction angle and cohesion) of interlayer soil decreased with the increase of water content whatever the fines content. However, this effect was found more pronounced in the case of higher fines content. This is because fine particles are relatively more sensitive to water content changes.

As far as the effect of fines content is concerned, at $w = 4\%$, adding more fine particles did not result in a clear change in friction angle and cohesion. However, under nearly saturated condition ($w = 12\%$) a significant decrease was recorded with addition of fine particles. Also, thanks to the suction effect in unsaturated state ($w = 4\%$ and 6%), the permanent axial strain in cyclic triaxial tests decreased when adding more fine particles. However, in nearly saturated condition ($w = 12\%$), interlayer soil having higher fines content showed a larger axial permanent strain.

For the resilient modulus of interlayer soil, at each deviator stress level, after the first scattered results due to the plastic behavior of soil, a stabilization trend was recorded after a certain number of cycles. It was found that the number of cycles needed to reach the stabilization depends on the material nature, water content and stress level.

The effects of water content and fines content are linked. This suggests that water content and fines content need to be taken into account together in the studies of hydro-mechanical behavior of interlayer soil. From a practical point of view, drainage measures must be taken to protect the interlayer soil since its mechanical performance can be satisfactory under unsaturated conditions but unsatisfactory under saturated conditions.

These findings are important in the case of reinforcement of subgrade by soil mixing with the interlayer as the stress transmission layer. Obviously, under unsaturated conditions, thanks to the suction effect, the mechanical properties (friction angle and cohesion) of the interlayer are good enough to ensure its transmission function, in particular when the fines content is high. However, under the saturated conditions, the mechanical properties of the interlayer are less good especially in the case of high fines content. This suggests that when the drainage system is set up and it can ensure the unsaturated state of interlayer soil, the suction improved mechanical properties of interlayer can be considered in the design of the interlayer/soil-mixing columns system. On the contrary, when the unsaturated state cannot be ensured, it is necessary to consider the lowest mechanical performance of interlayer soil (in saturated state) in the design.

Hydraulic behavior of interlayer soil

The hydraulic conductivity of interlayer soil under saturated condition was found about 10^{-5} m/s, lower than the critical value (10^{-4} m/s) proposed by Selig and Waters (1994) for the railway sub-structures. This suggests that good drainage conditions must be ensured to protect interlayer from water infiltration.

During the tests on the hydraulic behavior of interlayer soil, wetting/drying cycles were applied, and it appeared that the effect of these cycles on the hydraulic conductivity was negligible, suggesting an insignificant microstructure change by wetting/drying cycles. More interestingly, hysteresis existed in the hydraulic conductivity changes with suction. The wetting process was found much faster than the drying process, with a higher hydraulic conductivity during wetting path. This phenomenon can be explained by the effect of ink-bottle and the difference between the water transfers through the network of macro- and micro-pores.

Adding 10% fine particles (*ITL$_{10}$*) to the natural interlayer soil (*ITL$_0$*) changed the soil water retention curve. Also, the water retention curves of *ITL$_{10}$* and *Fines* are different, illustrating an obvious effect of soil texture. The hydraulic conductivity of interlayer soil is governed by fines fraction. Comparisons of hydraulic conductivity between *ITL$_0$* and *ITL$_{10}$* and between *ITL$_{10}$* and its fines fraction confirmed this statement: good agreements were obtained in the comparisons. This suggests that water transfer in the interlayer soil takes place mainly through the network of pores between fine particles, coarse elements like ballast behaving as inert materials.

Mechanisms of track degradation

A physical model of 550 mm diameter was developed in order to study the interlayer creation and mud pumping. Samples composed of a ballast layer overlying sub-soil layer were tested under different conditions in terms of loading and water content.

The results showed that the sub-soil state can strongly influence the ballast behavior. Larger permanent axial displacement and more pronounced ballast movement were recorded in the case of lower initial dry unit mass of sub-soil. Thus, it is important of take into account the interaction between different layers when assessing the performance of railway sub-structures.

In the unsaturated state of sub-soil, the ballast/sub soil interface did not change even after the 5 Hz loading for 500 000 cycles. Nevertheless, it rose up sharply in the saturated state. This difference highlights the significant effect of water content on the migration of fine particles and the penetration of ballast particles into the sub-grade. Water or more exactly the pore water pressure is the driving factor for the migration of fine particles. Under cyclic loadings, the pore water pressure was higher than the minimum value of applied stress, resulting in sub-soil liquefaction during the unloading process. Excess pore water pressure dissipation took place, bringing fine particles upwards as observed in the case of $\rho_{d-initial} = 1.4$ Mg/m^3 and 1.5 Mg/m^3. This corresponded to the mud pumping phenomenon. In the case of $\rho_{d-initial} = 1.6$ Mg/m^3, there was just the interpenetration of ballast and sub-soil, resulting in a mixture layer namely interlayer.

Water and soil compressibility are combined to be the key parameters deciding which phenomenon to occur. At high dry unit mass ($\rho_{d-initial} = 1.6$ Mg/m^3), low compressibility limited the generation of pore water pressure and thus only interlayer creation took place. By contrast, at lower dry unit mass ($\rho_{d-initial} = 1.4$ and 1.5 Mg/m^3) higher compressibility built up high pore water pressure resulting in mud pumping.

PERSPECTIVES

The present study allows better understanding of the state of railway network in France and the degradation mechanisms of the track sub-structure. In light of the findings obtained, various research axes can be proposed:

- The dynamic behavior of the railway sub-structure in general and interlayer soil in particular should be investigated.

- Base on the experimental data of triaxial tests, a constitutive model for the hydro-mechanical behavior of interlayer soil can be established, taking into account the effects of fines content, water content, load level, etc.

- The study can be extended to the mud pumping phenomenon in the sub-structure composed of several layers, as in the case of high speed lines, in order to evidence the role of sub-ballast and interlayer in preventing the mud pumping phenomenon.

- It appears also interesting to investigate the behavior of interlayer in case of track improvement by soil mixing.

- Using the physical model developed, the interaction between the ballast layer and other underlying layers are to be further studied in order to evidence the effect of the stiffness of underlying layers on the behavior of ballast layer.

REFERENCES

Adam D., Vogel A., Zimmermann A. 2007. Ground improvement techniques beneath existing rail tracks. Ground Improvement 11(4): 229-235.

AFNOR, NF P 94-054. 1991. Soils : investigation and testing – Determination of particle density – Pycnometer method. French standard.

AFNOR, NF P 98-235-1. 1995. Essais Relatif aux Chaussées. Matériaux Non Traitées. Part 1: Essai Triaxial à Chargements Répétés. French Standard. (In French).

AFNOR, NF EN 1097-6. 2001. Tests for mechanical and physical properties of aggregates. Part 6: Determination of particle density and water absorption. French standard.

AFNOR, NF EN 13286-7. 2004. Unbound and hydraulically bound mixtures. Part 7: cyclic load triaxial test for unbound mixtures. French standard.

AFNOR, EN ISO 14688. 2005. Identification and classification of soil- Part 2: Principles for a classification. French standard.

AFNOR, XP CEN ISO/TS 17892-9. 2005. Geotechnical investigation and testing, Laboratory testing of soil – Part 9: Consolidated triaxial compression tests on water-saturated soils. French standard.

Alias J. 1984. La voie ferrée. Techniques de construction et d'entretien. 2nd Ed., Eyrolles. (In French).

Allen J.J., Thompson M.R. 1974. Resilient response of granular materials subjected to time dependent lateral stresses. Transportation Research Record 510: 1-13.

Al-Qadi Imad L., Wei X., Roberts R. 2008. Scattering analysis of ground-penetrating radar data to quantify railroad ballast contamination. NDT & E International 41(6): 441–447.

Al Shaer A. 2005. Analyse des Déformations Permanentes des Voies Ferrées Ballastées – Approche Dynamique. PhD Dissertation, Ecole Nationale des Ponts et Chaussées, France. (In French).

Alobaidi I., Hoare D.J. 1994. Factors Affecting the Pumping of Fines at the Subgrade- Subbase Interface of Highway Pavements: A Laboratory Study. Geosynthetics International 1(2): 221–259.

Alobaidi I., Hoare D.J. 1996. The Development of Pore Water Pressure at the Subgrade-Subbase Interface of a Highway Pavement and its Effect on Pumping of Fines. Geotextiles and Geomembranes 14(2): 111–135.

Alobaidi I., Hoare D.J. 1998. Qualitative Criteria for Anti-pumping Geocomposites. Geotextiles and Geomembranes 16(4): 221–245.

Alobaidi I., Hoare D.J. 1998. The Role of Geotextile Reinforcement in the Control of Pumping at the Subgrade-Subbase Interface of Highway Pavements. Geosynthetics International 5(6): 619–636.

Alobaidi I., Hoare D.J. 1999. Mechanisms of Pumping at the Subgrade-Subbase Interface of Highway Pavements. Geosynthetics International 6(4): 241–259.

Anbazhagan P., Lijun S., Buddhima I., Cholachat R. 2011. Model track studies on fouled ballast using ground penetrating radar and multichannel analysis of surface wave. Journal of Applied Geophysics 74(4): 175–184.

Aursudkij B., McDowell G.R., Collop A.C. 2009. Cyclic loading of railway ballast under triaxial conditions and in a railway test facility. Granular Matter 11(6): 391-401.

ASTM, D7664-10. 2010. Standard test method for measurement of hydraulic conductivity of unsaturated soils.

ASSHTO. 1993. Guide for design of pavement structures.

Aw E.S. 2004. Novel Monitoring System to Diagnose Rail Track Foundation Problems. Master of Science Thesis, Massachusetts Institute of Technology, USA.

Aw E.S. 2007. Low Cost Monitoring System to Diagnose Problematic Rail Bed: Case Study at Mud Pumping Site. Ph.D. Dissertation, Massachusetts Institute of Technology, USA.

Ayres D.J. 1986. Geotextiles or Geomembranes in Track? British Railway Experience. Geotextiles and Geomembranes 3(2-3): 129–142.

Babic B., Prager A., Rukavina, T. 2000. Effect of fine particles on some characteristics of granular base courses. Materials and Structures 7(33): 419-424.

Bailey B., Hutchinson D., Gordon D., Siemens G., Ruel M. 2011. Field and laboratory procedures for investigating the fouling process within railway track ballast. Proceeding of the 2011 Pan-Am CGS Geotechnical Conference, 8p.

Basudhar P.K., Ghosh P., Dey A., Valsa S., Nainegali L.S. 2010. Reinforced earth design of embankment and cuts in railway. Research Designs and Standards Organization, Department of Civil Engineering, Indian Institute of Technology Kanpur.

Bear J. 1988. Dynamic of fluids in porous media. Dover Publications, 781p.

Bednarik M., Magulová B., Matys M., Marschalko M. 2010. Landslide susceptibility assessment of the kralovany–liptovsky mikuláš railway case study. Physics and Chemistry of the Earth 35: 162–171.

Bertotti G., Mayergoyz I. D. 2006. The science of hysteresis III. Academic Press.

Bouabdallah A. 1998. Contribution à l'étude du comportement mécanique des sols fortement désaturés. PhD Dissertation, Ecole Centrale Paris. (In French).

Brooks R.H., Corey A.T. 1964. Hydraulic properties of porous media. Hydro. Paper No.3, Colorado State Univ., Fort Collins, Colo.

Brough M., Ghataora G., Stirling A., Madelin K., Rogers C., Chapman D. 2003. Investigation of railway track subgrade. Part 1: In-situ assessment. Proceedings of the Institution of Civil Engineers - Transport 156(3): 145–154.

Brough M., Ghataora G., Stirling A., Madelin K., Rogers C., Chapman D. 2006. Investigation of railway track subgrade. Part 2: Case study. Proceedings of the Institution of Civil Engineers - Transport 159(2):83–92.

Bruckler L.B., Angulo-Jaramillo P., Ruy R. 2002. Testing an infiltration method for estimating soil hydraulic properties in the laborator. Soil Science Society of America Journal 66: 384–395.

Burns B., Ghataora G.S., Sharley P. 2006. Development and Testing of Geosand Composite Layers Using Pumps Index Test. In: Proceedings of the First International Conference on Railway Foundations Railfound06, University of Birmingham, UK, p. 355–366, ISBN10: 0-704426-00-5, ISBN13: 97807-04426-009.

Burrow M., Bowness D., Ghataora G. 2007. A comparison of railway track foundation design methods. Proceedings of the Institution of Mechanical Engineers, Part F: Journal of Rail and Rapid Transit 221(1):1–12.

Burrow M., Ghataora G., Evdorides H. 2011. Railway foundation design principles. Journal of Civil Engineering and Architecture 5(3): 224–232.

Cabalar A. 2008. Effect of fines content on the behavior of mixed specimens of a sand. Electronic Journal of Geotechnical Engineering 13(D): 1-11.

Cabalar A. 2011. The effects of fines on the behaviour of a sand mixture. Geotechnical and Geological Engineering 29(1): 91–100.

Calon N. 2010. Etude de recommandation en vue d'assurer de façon pérenne le RVL 220 sur *une ligne classique*. Technical report, SNCF. (In French).

Calon N., Trinh V.N., Tang A.M., Cui Y.J., Dupla J.C., Canou J., Lambert L., Robinet A., Schoen O. 2010. Caractérisation hydromécanique des matériaux constitutifs de plateformes ferroviaires anciennes. Conférence JNGG2010, Grenoble, France, pp. 787–794. (In French).

Chapuis R.P., Masse I., Madinier B., Aubertin M. 2006. Essai de drainage en colonne pour obtenir les propriétés non saturées de matériaux grossiers. Sea to Sky Geotechnique - the 59th Canadian Geotechnical Conference, pp. 905 - 912.

Choo L.P., Yanful E.K. 2000. Water flow through cover soils using modeling and experimental methods. Journal of Geotechnical and Geoenvironmental Engineering 126(4): 324-334.

Côté J., Roy M. 1998. Conductivité hydraulique de matériaux de fondations de chaussées partiellement saturés. Rapport de l'études et recherches en transports du Québec, 177p.

Colin F. 2003. Couplages thermo-hydro-mécaniques dans les sols et les roches tendres partiellement saturés. PhD Dissertation, Université de Liège. (In French).

Cui Y.J., Delage P. 1996. Yielding Behavior of an Unsaturated Compacted Silt. Géotechnique 46(2): 291-311.

Cui Y.J., Tang A.M., Mantho A., Delaure E. 2008. Monitoring field soil suction using a miniature tensiometer. Geotechnical Testing Journal 31(1): 95-100.

Cui Y.J., Tang A.M., Loiseau C., Delage P. 2008. Determining the Unsaturated Hydraulic Conductivity of a Compacted Sand-Bentonite Mixture Under Constant-Volume and Free-Swell Conditions. Physics and Chemistry of the Earth, Parts A/B/C 33: S462–S471.

Cui Y.J., Duong T.V., Tang A.M., Dupla J.C., Calon N., Robinet A. 2013. Investigation of the hydro-mechanical behavior of fouled ballast. Journal of Zhejiang University- Science A 144(4):244–255.

Cunningham M., Ridley A., Dineen K., Burland J. 2003. The mechanical behaviour of a reconstituted unsaturated silty clay. Géotechnique 53(2): 183-194.

Daniel D.E. 1982. Measurement of hydraulic conductivity of unsaturated soils with thermocouple psychometers. Soil Science Society of Americal Journal 46(6): 1125-1129.

Delage P., Cui Y.J. 2000. L'eau dans les sols non saturés. Ed. Techniques de l'Ingénieur, Article C301. (In French).

Delage P., Cui Y.J., 2001. Comportement mécanique des sols non saturés. Ed. Techniques de l'Ingénieur, Article C302. (In French).

Dupla J.C., Pedro L.S., Canou J., Dormieux L. 2007. Mechanical behaviour of coarse grained soils reference. Bulletin de Liaison des Laboratoires des Ponts et Chaussées (268-269): 31-58.

Duong T.V., Trinh V.N., Cui Y.J., Tang A.M., Nicolas C. 2013. Development of a large-scale infiltration column for studying the hydraulic conductivity of unsaturated fouled ballast. Geotechnical Testing Journal 36(1): 54–63.

Duong T.V., Tang A.M., Cui Y.J., Trinh V.N., Dupla J., Calon N., Canou J., Robinet A. 2014. Effects of fines and water contents on the mechanical behavior of interlayer soil in ancient railway sub-structure. Soil and Foundations. (Accepted for publications).

Ebrahimi A. 2011. Behavior or fouled ballast. Railway Track and Structures 107(8): 25–31.

Ekblad J. 2007. Influence of water on coarse granular road materials properties. PhD dissertation, Royal Institute of Technology KTH, Stockholm, Sweden.

Ekblad J., Isacsson U. 2007. Time-domain reflectometry measurements and soil-water characteristic curves of coarse granular materials used in road pavements. Canadian Geotechnical Journal, 44(7): 858–872.

Ekblad J. 2008. Statistical evaluation of resilient models characterizing coarse granular materials. Materials and Structures 41(3): 509–525.

Ekblad J., Isacsson U. 2008. Influence of water and mica content on resilient properties of coarse granular materials. International Journal of Pavement Engineering 9(3): 215–227.

Fortunato E., Pinelo A., Matos Fernandes M. 2010. Characterization of the fouled ballast layer in the substructure of a 19th century railway track under renewal. Soils and Foundations 50(1): 55–62.

Fleureau J.M., Indarto. 1995. Comportement du limon de Jossigny remanié soumis à une pression interstitielle négative. Revue Française de Géotechnique 62: 59-66. (In French).

Ghataora G.S., Burns B., Burrow M.P.N., Evdorides H.T. 2006. Development of an Index Test for Assessing Anti-pumping Materials in Railway Track Foundations. In: Proceedings of the First International Conference on Railway Foundations, Railfound06, University of Birmingham, UK, pp.355–366.

Giannakos K. 2010. Loads on track, ballast fouling, and life cycle under dynamic loading in railways. Journal of Transportation Engineering 136(12): 1075–1084.

Gidel G., Hornych P., Chauvin J.J., Breysse D., Denis, A. 2001. A new approach for investigating the permanent deformation behavior of unbound granular material using the Repeated Load Triaxial Apparatus. Bulletin de Liaison des Laboratoires des Ponts et Chaussées 233: 5-21.

Gong Y., Cao Q., Sun Z. 2003. The effects of soil bulk density, clay content and temperature on soil water content measurement using time-domain reflectometry. Hydrological Processes 17(18): 3601–3614.

Grabe P., Clayton C. 2009. Effects of principal stress rotation on permanent deformation in rail track foundations. Journal of Geotechnical and Geoenvironmental Engineering 135(4): 555–565.

Guerin N. 1996. Approche expérimentale et numériques du comportement du ballast des voies ferrées. PhD Dissertation, Ecole Nationale des Ponts et Chaussées. (In French).

Hanson B., Peters D. 2000. Soil type affects accuracy of dielectric moisture sensors. California Agriculture 54(3): 43–47.

Hicks R.G., Monismith C.L. 1971. Factors influencing the resilient response of granular materials. Highway Research Record 345: 15–31.

Hornych P., Corté J.F., Paute J.L. 1993. Etude des Déformations Permanents sous Chargements Répétés de Trois Graves non Traitées. Bulletin de Liaison des Laboratoires des Ponts et Chaussees 184: 77-84. (In French).

Huang H., Tutumluer E., Dombrow W. 2009. Laboratory characterization of fouled railroad ballast behavior. Transportation Research Record, Journal of the Transportation Research Board 2117: 93–101. Doi: 10.3141/2117-12.

Hveem F.N., Carmany R.M. 1948. The factors underlying the rational design of pavements. In Highway Research Board Proceedings 28: 101–136.

Hveem F.N. 1955. Pavement deflections and fatique failures. In Highway Research Board Bulletin, Highway Research Board 114: 43–87.

Inam A., Ishikawa, T., Miura, S. 2012. Effect of principal stress axis rotation on cyclic plastic deformation characteristics of unsaturated base course material. Soils and Foundations 52(3): 465-480.

Indraratna B., Ionescu D., Christie D., Chowdhurry R. 1997. Compression and degradation of railway ballast under one-dimensional loading. Australian Geomechanics Journal (12): 48 - 61.

Indraratna B., Ionescu D., Christie H.D. 1998. Shear behavior of railway ballast based on large-scale triaxial tests. Journal of Geotechnical and Geoenvironmental Engineering 124(5): 439–449.

Indraratna B., Salim W. 2002. Modelling of particles breakage of coarse aggregates incorporating strength and dilatancy. Proceedings of the ICE - Geotechnical Engineering 155(4): 243–252.

Indraratna B., Salim W. 2005. Mechanics of Ballasted Rail Tracks: A Geotechnical Perspective, Taylor & Francis Group, London, UK.

Indraratna B., Su L., Rujikiatkamjorn C. 2011. A new parameter for classification and evaluation of railway ballast fouling. Canadian Geotechnical Journal 48(2): 322–326.

Indraratna B., Salim W., Rujikiatkamjorn C. 2011. Advanced Rail Geotechnology - Ballasted Track. CRC Press.

Jacobsen O.H., Schjønning P. 1993. A laboratory calibration of time domain reflectometry for soil water measurement including effects of bulk density and texture. Journal of Hydrology 151(2-4): 147–157.

Jain V., Keshav K. 1999. Stress distribution in railway formation–a simulated study. Proceeding og the 2nd International Symposium on Pre-Failure Deformation Characteristics of Geomaterials–IS Torino. pp. 653–658.

Janardhanam R., Desai C.S. 1983. Three-dimensional testing and modelling of ballast. Journal of Geotechnical Engineering 109(6): 783–796.

Karraz K. 2008. Mechanical behavior of ballast under monotonic and cyclic loading. PhD Dissertation, Ecole Nationale des Ponts et Chaussées, France.

Kettil P., Lenhof B., Runesson K., Wiberg N.E. 2008. Coupled simulation of wave propagation and water flow in soil induced by high-speed train. International Journal for Numerical and Analytical Methods in Geomechanics (33): 1311-1319.

Kim D., Sagong M., Lee Y. 2005. Effects of fine aggregate content on the mechanical properties of the compacted decomposed granitic soils. Construction and Building Materials 19(3): 189–196.

Kim D., Kim J.R. 2007. Resilient behavior of compacted subgrade soils under the repeated triaxial test. Construction and Building Materials 21(7): 1470–1479.

Kolisoja P. 1997. Resilient Deformation Characteristics of Granular Materials. PhD dissertation, Tampere University of Technology, Finland.

Lackenby J. 2006. Triaxial behaviour of ballast and the role of confining pressure under cyclic loading. PhD dissertation, University of Wollongong.

Lackenby J., Indraratna B., Mcdowell G., Christie D. 2007. Effect of confining pressure on ballast degradation and deformation under cyclic triaxial loading. Géotechnique 57(6): 527 – 536.

Langton D.D. 1999. The panda lightweight penetrometer for soil investigation and monitoring material compaction. Ground Engineering 1999, September.

LCPC, SETRA, 2000. Technical Guidelines on Embankment and Capping Layers Construction (GTR).

Le T.T. 2008. Comportement thermo-hydro-mécanique de l'argile de Boom. PhD Dissertation, Ecole Nationale des Ponts et Chaussées, France. (In French).

Le T.T., Cui Y.J., Muñoz J.J., Delage P., Tang A.M., Li X.L. 2011. Studying the stress-suction coupling in soils using an oedometer equipped with a high capacity tensiometer. Frontiers of Architecture and Civil Engineering in China 5(2): 160-170.

Le Runigo B., Cui Y.J., Cuisinier O., Deneele D., Ferber V. 2008. Durabilité du limon de Jossigny traité à la chaux et soumis à différentes sollicitations hydriques. Comportement hydraulique, microtextural et mécanique. Workshop TerdOuest I, Paris, France 13 November 2008, p. 13. (In French).

Lekarp F., Isacsson U., Dawson A. 2000. State of the art. I: Resilient response of unbound aggregates. Journal of transportation engineering 126(1): 66–75.

Li D., Selig E.T. 1994. Resilient modulus for fine-grained subgrade soils. Journal of geotechnical engineering 120(6): 939–957.

Li D., Selig E.T. 1996. Cumulative plastic deformation for fine-grained subgrade soils. Journal of Geotechnical Engineering December 1996: 1006-1013.

Li D., Selig E.T. 1998. Method for railroad track foundation design. I: Development. Journal of Geotechnical and Geoenvironmental Engineering 124(4): 316–322.

Li D., Selig E.T. 1998. Method for railroad track foundation design. II: Applications. Journal of Geotechnical and Geoenvironmental Engineering 124(4): 323–329.

Li S., Lai Y., Zhang S., Yang Y., Yu W. 2012. Dynamic responses of Qinghai-Tibet railway embankment subjected to train loading in different seasons. Soil Dynamics and Earthquake Engineering 32: 1-14.

Lieberenz K., Piereder F., 2011. Track sub-structure improvements to increase load-bearing strength. Rail Engineering International 40(4): 6–10.

Lim W.L. 2004. Mechanics of railway ballast behaviour. PhD dissertation, University of Nottingham.

Liu J., Xiao J. 2010. Experimental study on the stability of railroad silt subgrade with increasing train speed. Journal of Geotechnical and Geoenvironmental Engineering 136(6): 833-841.

Lourenço S. 2008. Suction measurements and water retention in unsaturated soils. PhD dissertation, Durham University.

Lourenço S.D.N., Gallipoli D., Toll D.G., Augarde C.E., Evans F.D. 2011. A New Procedure for the Determination of Soil-water Retention Curves by Continuous Drying Using High-suction Tensiometers. Canadian Geotechnical Journal 48(2): 327–335.

Mantho A.T. 2005. Echanges Sol-Atmosphère Application à la Sécheresse. Ph.D. Dissertation, Ecole Nationales des Ponts et Chaussées/Université Paris - Est, France. (In French).

Masekanya J.P. 2008. Stabilité des pentes et saturation partielle. Etude expérimentale et modélisation numérique. PhD Dissertation, Université de Liège. (In French).

Masrouri F., Bicalho K.V., Kawai K. 2008. Laboratory hydraulic testing in unsaturated soils. Geotechnical and Geological Engineering 26(6): 691–704.

Mayoraz F., Vulliet L., Laloui L. 2006. Attrition and particle breakage under monotonic and cyclic loading. Comptes Rendus Mécanique 334(1): 1–7.

McCartney J.S., Villar L.F.S., Zornberg J.G. 2007. Estimation of the hydraulic conductivity of unsaturated clays using infiltration column test. Proceedings of the 6th Brazilian Symposium on Unsaturated Soils 1: 321-328.

McCartney J.S., Zornberg J.G. 2007. Effect of wet-dry cycles on capillary break formation in geosynthetic drainage layers. Geosynthetics 2007, Washington, DC. January, pp. 16-19.

McCartney J.S., Zornberg J.G. 2010. Effect of infiltration and evaporation on geosynthethic capillary barrier performance. Canadian Geotechnical Journal 47(11): 1201-1213.

Miller G.A., The S.Y., Li D., Zaman M.M. 2000. Cyclic shear strength of soft railroad sub-grade. Journal of Geotechnical and Geoenvironmental Engineering 126(2): 139-147.

Moulton L.K. 1980. Highway subdrainage design. Report to the Federal Highway Administration – U.S. Departement of Transport, FHWA-TS-80-224, 162p.

Moore R. 1939. Water Conduction from Shallow Water Tables. Hilgardia 12: 383-426.

Mualem Y. 1976. Hysteretical models for prediction of the hydraulic conductivity of unsaturated porous media. Water Resources Research 12(6): 1248-1254.

Munoz J.J., De Gennaro V., Delaure E. 2008. Experimental determination of unsaturated hydraulic conductivity in compacted silt. In Unsaturated soils: advances in geo-engineering: proceedings of the 1st European Conference on Unsaturated Soils, E-UNSAT 2008, Durham, United Kingdom, 2-4 July 2008, pp.123-127.

Munoz-Castelblanco J.A., Pereira J.M., Delage P., Cui Y. J. 2012. The water retention properties of a natural unsaturated loess from northern France. Géotechnique 62(2): 95-106.

Naumov S. 2009. Hysteresis phenomenon in Mesoporous Materials. PhD Dissertation, University of Leipzig.

Naeini S., Baziar M. 2004. Effect of fines content on steady-state strength of mixed and layered specimens of a sand. Soil Dynamics and Earthquake Engineering 24(3): 181–187.

Nützmann G., Thiele M., Maciejewski S., Joswig K. 1998. Inverse Modelling techniques for determininghydraulic properties of coarse-texturedporous media by transient outflow methods. Advance in Water Resources 22(3): 273-284.

Parks J.M., Stewart M.A., McCartney J.S. 2012. Validation of a Centrifuge Permeameter for Investigation of Transient Infiltration and Drainage Flow Processes in Unsaturated Soils. Geotechnical Testing Journal 35(1): 182-192.

Paute J.L., Le Fort R. 1984. Determination of Untreated Gravels Mechanical Characteristics with Cyclic Loading Triaxial Apparatus. Bullein of the International Association of Engineering Geology 29: 419 – 424. (In French).

Pedro L. 2004. De l'étude du comportement mécanique de sols hétérogènes modèles à son application au cas des sols naturels. PhD disertation, Ecole Nationale des Ponts et Chaussées, France. (In French).

Peters S.B., Siemens G., Take W.A. 2011. Characterization of transparent soil for unsaturated applications. Geotechnical Testing Journal 34(1): 445-456.

Poulovassilis A. 1969. The effect of hysteresis of pore water on the hydraulic conductivity. Soil Science 20: 52-56.

Quezada J.C. 2012. Mécanismes de tassement du ballast et sa variabilité. PhD dissertation, Université Montpellier 2. (In French).

Radampola S. 2006. Evaluation and modelling performance of capping layer in rail track substructure. Thesis dissertation, Central Queensland University.

Radampola S.S., Gurung N., McSweeney T., Dhanasekar M. 2008. Evaluation of the properties of railway capping layer soil. Computers and Geotechnics 35(5): 719–728.

Raymond G.P. 1999. Railway rehabilitation geotextiles. Geotextiles and Geomembranes 17(4): 213–230.

Rhayma N. 2010 Contribution à l'évolution des méthodologies de caractérisation et d'amélioration des voies ferrées. PhD Dissertation, Université Blaise Pascal - Clermont II. (In French).

Read D., Hyslip J., McDaniel J. 2011. Heavy axle load revenue service mud-fouled ballast investigation, Technical report. Federal railroad administration, U.S. Departement of Transportation.

Ridley A., Burland J. 1993. A new instrument for the measurement of soil moisture suction. Géotechnique 43(2): 321-324.

Ridley A., Dineen K., Burland J., Vaughan P. 2003. Soil matrix suction: some examples of its measurement and application in geotechnical engineering. Géotechnique 53(2): 241-254.

Robinet A. 2008. Les couches de forme traitées dans les structures d'assise ferroviaires. Mémoire de diplôme d'ingénieur du Conservatoire National des Arts et Métiers (CNAM).

Sattler P., Fredlund D.G., Klassen M.J., Rowan W.G. 1989. Bearing capacity approach to railway design using subgrade matric suction. Transportation Research Record 1241: 27-33.

Schneider J.M., Fratta D. 2009. Time-domain reflectometry - parametric study for the evaluation of physical properties in soils. Canadian Geotechnical Journal 46: 753–767.

Seif El Dine S., Dupla J., Frank R., Canou J., Kazan Y. 2010. Mechanical characterization of matrix coarse-grained soils with a large-sized triaxial device. Canadian Geotechnical Journal 47(4): 425–438.

Selig E.T., Waters J.M. 1994. Track geotechnology and substructure management. Thomas Telford.

Soilmoisture, 2000. 6050X3K1 Operating Instructions. 53p.

SNCF. 1989. Armement, ballastage et entretien de la voie généralités classement des lignes en groupes au point de vue de la maintenance de la voie- ef2a1n°1. Technical report. (In French).

SNCF. 1995. Specification Technique pour la Fourniture des Granulats Utilisés pour la Réalisation et l'Entretien des Voies Ferrées ST 590B. Technical guide. (In French).

SNCF. 2009. Sollicitations mécaniques dans la plate-forme. Mesures d'accélérations verticales dans la plate-forme. Technical report R2520-2009-01. (In French).

SNCF. 2011. Référentiel Infrastructure – Procédure IN4103. (In French).

Stankovich J. M., Lockington D. A. 1995. Brooks-Corey and van Genuchten, soil-water-retention models. Journal of Irrigation and Drainage Engineering 121(1): 1-7.

Stewart H.E. 1982. The prediction of track performance under dynamic traffic loading. PhD Dissertation, University of Massachusetts.

Stormont J.C., Anderson C.E. 1999. Capillary barrier effect from equilibrium technique at different temperatures and its application in determining the water retention properties of MX80 clay. Canadian Geotechnical Journal 42(1): 287-296.

Stolte J., Veerman M ., Wosten G.J., Freijer J.H.M., Bouten J.I ., Dirksen W., Van Dam C., Van den Berg J.C. 1994. Comparison of six methods to determine unsaturated soil hydraulic conductivity. Soil Science Society of America Journal 58(6): 1596-1603.

Su L., Rujikiatkamjorn C., Indraratna B. 2010. An evaluation of fouled ballast in a laboratory model track using ground penetrating radar. Geotechnical Testing Journal 33(5): 343-350.

Sussmann T., Maser K., Kutrubes D., Heyns F., Selig E. 2001. Development of ground penetrating radar for railway infrastructure condition detection. Symposium on the Application of Geophysics to Engineering and Environmental Problems 2001.

Sussmann T. R., Ruel M., Christmer S. 2012. Sources, influence, and criteria for ballast fouling condition assessment. Proc. of 91st Annual Meeting of the Transportation Research Board. 11p.

Taheri A., Tatsuoka F. 2012. Stress-strain relations of cement-mixed gravelly soil from multiple-step triaxial compression test results. Soils and Foundations 52(4): 748-766.

Takatoshi I. 1997. Measure for stabilization of railway earth structure. Japan Railway Technical Service, 290.

Tang A.M., Ta A.N., Cui Y.J., Thiriat J. 2009. Development of a large scale infiltration tank for determination of the hydraulic properties of expansive clays. Geotechnical Testing Journal 32(5): 385-396.

Tarantino A., Ridley A.M., Toll D.G. 2008. Field measurement of suction, water content, and water permeability. Geotechnical and Geological Engineering 26(6): 751–782.

Tennakoon N., Indraratna B., Rujikiatkamjorn C., Nimbalkar S., Neville T. 2012. The role of ballast-fouling characteristics on the drainage capacity of a rail substructure. Geotechnical Testing Journal 35(4): 1-12.

Toker N., Germaine J., Sjoblomt K., Culligan P. 2004. A new technique for rapid measurement of continuous soil moisture characteristic curves. Géotechnique 54(3): 179-186.

Toll D., Lourenço S., Mendes J. 2012. Advances in suction measurements using high suction tensiometers. Engineering Geology. doi.org/10.1016/j.enggeo.2012.04.013.

Topp G.C., Davis J.L., Annan A.P. 1980. Electromagnetic Determination of Soil Water Content: Measurements in Coaxial Transmission Lines. Water Resources Research 16(3): 574–582.

Trani L.D.O., Indraratna B. 2010. Assessment of subballast filtration under cyclic loading. Journal of Geotechnical and Geoenvironmental Engineering 136(11): 1519–1527.

Trinh V.N., Tang A.M., Cui Y.J., Dupla J.C., Canou J., Calon N., Lambert L., Robinet A., Schoen O. 2010. Calibration of smart irrigation sensor (sis-ums) for the blanket layer soil from old railway lines. Proceeding of the Conference UNSAT2010, Barcelone, Espagne, pp. 739–744.

Trinh V.N., Tang A.M., Cui Y.J., Dupla J.C., Canou J., Calon N., Lambert L., Robinet A., Schoen O. 2010. Unsaturated hydraulic properties of fines-grained soil from the blanket layer of old railway lines in France. Proceeding of the Conference UNSAT2010, Barcelone, Espagne, pp 501–507.

Trinh V.N. 2011. Comportement hydromécanique des matériaux constitutifs de plateformes ferroviaires anciennes. PhD Dissertation, Ecole Nationales des Ponts et Chaussées - Université Paris - Est. (In French).

Trinh V.N., Tang A.M., Cui Y.J., Canou J., Dupla J.C., Calon N., Lambert L., Robinet A., Schoen O. 2011. Caractérisation des matériaux constitutifs de plate-forme ferroviaire ancienne. Revue Française de Géotechnique (134-135):65–74. (In French).

Trinh V.N., Tang A.M., Cui Y.J., Dupla J.C., Canou J., Calon N., Lambert L., Robinet A., Schoen O. 2011. Caractérisation hydromécanique des mátriaux constitutifs de plateformes ferroviaires anciennes. Proceeding of the International Symposium Georail 2011, Paris, France. pp. 377–387. (In French).

Trinh V.N., Tang A.M., Cui Y.J., Dupla J.C., Canou J., Calon N., Lambert L., Robinet A., Schoen O. 2012. Mechanical characterization of the fouled ballast in ancient railway track substructure by large-scale triaxial tests. Soils and Foundations 52(3):511-523.

Tutumluer E., Dombrow W., Huang H. 2008. Laboratory characterization of coal dust fouled ballast behavior. AREMA 2008 Annual Conference & Exposition September 21-24, 2008, Salt Lake City, USA.

UMS. 2008. T8-long-term monitoring tensiometer. User manual, 56 pages.

Uthus, L., 2007. Deformation Properties of Unbound Granular Aggregat. PhD disertation, Norwegian University of Science and Technology, Norway.

Uthus L., Hoff I., Horvli I. 2005. A study on the influence of water and fines on the deformation properties of unbound aggregates. Proceeding of the 7th International Conference on the Bearing Capacity of Roads, Railways and Airfields. Trondheim, Norway, pp. 1-13.

van Genuchten M.T. 1980. A closed-form equation for predicting the hydraulic conductivity of unsaturated soils. Soil Science Society of America Journal 44(5): 892–898.

Van W.A. 1985. Rigid Pavement Pumping: (1) Subbase Erosion and (2) Economic Modeling : Informational Report. Publication FHWA/IN/JHRP-85/10. Joint Highway Research Project, Indiana Department of Transportation and Purdue University, West Lafayette, Indiana, USA, doi:10.5703/1288284314094.

Verdugo R., Hoz K. 2007. Strength and stiffness of coarse granular soils. Solid Mechanics and Its Application 146(3): 243–252.

Voottipruex P., Roongthanee J. 2003. Prevention of Mud Pumping in Railway Embankment a Case Study from Baeng Pra-pitsanuloke, Thailand. The Journal of KMITB 13(1): 20–25.

Vilhar G., Jovicic V., Coop M.R. 2013. The role of particle breakage in the mechanics of a non-plastic silty sand. Soils and Foundations 53(1): 91-104.

Wang Q., Tang A.M., Cui Y.J., Delage P., Barnichon J.D., Ye W.M. 2013. The effects of technological voids on the hydro-mechanical behaviour of compacted bentonite-sand mixture. Soils and Foundations 53(2): 232-245.

Wayllace A., Lu N. 2011. A transient water release and imbibitions method for rapidly measuring wetting and drying soil water retention and hydraulic conductivity functions. Geotechnical Testing Journal 35(1): 1-15.

Werkmeister S. 2003. Permanent deformation behaviour of unbound granular materials in pavement constructions. Thesis dissertation, Fakultät Bauingenieurweser der Technischen Universität Dresden.

Wind G.P. 1966. Capillary conductivity data estimated by a simple method. *In* Water in the saturated zone. Proceedings of the Wageningen symposium,Wageningen, the Netherlands, 19–23 June 1966, pp. 181 – 191.

Wong R.C.K., Thomson P.R., Choi E.S.C. 2006. In situ pore pressure responses of native peat and soil under train load: a case study. Journal of Geotechnical and Geoenvironmental Engineering 132(10): 1360-1369.

Yang H., Rahardjo H., Wibawa B., Leong E.C. 2004. A soil column apparatus for laboratory infiltration study. Geotechnical Testing Journal 27: 347-355.

Yang L., Powrie W., Priest J. 2009. Dynamic stress analysis of a ballasted railway track bed during train passage. Journal of Geotechnical and Geoenvironmental Engineering 135(5): 680–689.

Yasuda N., Matsumoto N., Yoshioka R., Takahashi M. 1997. Undrained monotonic and cyclic strength of compacted rockfill material from triaxial and torsional simple shear tests. Canadian Geotechnical Journal 34(3): 357-367.

Ye W.M., Cui Y.J., Qian L.X., Chen B. 2009. An experimental study of the water transfer through compacted GMZ bentonite. Engineering Geology 108: 169- 176.

Yoder E.J. 1957. Pumping of highway and airfield pavements: technical paper. Publication FHWA/IN/JHRP-57/05. Joint Highway Research Project, Indiana Department of Transportation and Purdue University, West Lafayette, Indiana. Doi: 10.5703/1288284313518.

Yuan R., Yang Y.S., Qiu X., Ma F.S. 2007. Environmental hazard analysis and effective remediation of highway seepage. Journal of Hazardous Materials 142(1-2): 381–388.

Zhang C. 2004. The effect of high groundwater level on pavement sub-grade performance. PhD Dissertation, The Florida State University - College of Engineering, USA.

Zeghal M. 2009. The impact of grain crushing on road performance. Geotechnical and Geological Engineering 27(4): 549–558.